

DOT/FAA/AR-99/XX

Office of Aviation Research
Washington, D.C. 20591

Supplemental Inspection Document Development Handbook For Commuter Aircraft

September 1999

Final Report

This document is available to the U.S. public through
the National Technical Information Service (NTIS),
Springfield, Virginia 22161



U.S. Department of Transportation
Federal Aviation Administration

NOTICE

This document is disseminated under the sponsorship of the U.S. Department of Transportation in the interest of information exchange. The United States Government assumes no liability for the contents or use thereof. The United States Government does not endorse products or manufacturers. Trade or manufacturer's names appear herein solely because they are considered essential to the objective of this report. This document does not constitute FAA certification policy. Consult your local FAA aircraft certification office as to its use.

This report is available at the Federal Aviation Administration William J. Hughes Technical Center's Full-Text Technical Reports page: www.tc.faa.gov/act141/reportpage.html in Adobe Acrobat portable document format (PDF).

TABLE OF CONTENTS

<u>SECTION</u>	<u>TITLE</u>	<u>PAGE</u>
	LIST OF FIGURES.....	xii
	LIST OF TABLES.....	xviii
	EXECUTIVE SUMMARY	xx
1.0	Introduction.....	1-1
1.1	Supplemental Inspection Document (SID) Background.....	1-1
1.2	Aging Aircraft Background.....	1-2
1.3	The Damage Tolerance Approach.....	1-4
1.4	The Supplemental Inspection Document Development Handbook.....	1-8
2.0	Aircraft Damage Tolerance Evaluation Overview.....	2-1
2.1	Phase 1 - Data Collection.....	2-1
2.2	Phase 2 - Damage Tolerance Analysis.....	2-5
2.3	Phase 3 - Inspection Requirements	2-5
3.0	PSE Identification and Classification.....	3-1
3.1	Identification of the Principal Structural Elements (PSEs) for Evaluation.....	3-1
3.1.1	Wing and Empennage.....	3-1
3.1.2	Fuselage	3-7
3.2	Select Critical Locations of PSEs for Evaluation	3-10
3.2.1	Finite Element Models	3-12
3.2.2	Fatigue and Static Test Results.....	3-18
3.2.3	Service Experience.....	3-18
3.3	Determination of the Structural Category for Each Location.....	3-21
3.3.1	Safe-Life.....	3-21
3.3.2	Damage Tolerant - Obvious Damage Evident.....	3-22
3.3.3	Damage Tolerant - By Planned Inspection.....	3-24
3.3.3.1	Single Load Path Structure	3-24
3.3.3.2	Multiple Load Path - Not Inspectable for Less than Load Path Failure.....	3-24
3.3.3.3	Multiple Load Path - Inspectable for Less than Load Path Failure.....	3-27
3.3.4	Other Structure.....	3-27
3.4	Type and Extent of Potential Damage	3-29
4.0	Material Properties	4-1
4.1	Static Material Properties	4-3
4.1.1	Yield Strength.....	4-3
4.1.2	Additional Static Properties.....	4-4
4.2	Fracture Toughness Data for Each Material and Geometry.....	4-4

TABLE OF CONTENTS (CONTINUED)

<u>SECTION</u>	<u>TITLE</u>	<u>PAGE</u>
4.2.1	Background.....	4-4
4.2.1.1	Fracture Toughness	4-5
4.2.1.2	Crack Growth Resistance Curves (R-Curves)	4-7
4.2.2	Sources for Fracture Toughness Data.....	4-8
4.2.3	Procedures for Developing Fracture Toughness Data	4-9
4.2.3.1	Plane Strain Fracture Toughness, K _{Ic}	4-9
4.2.3.2	Procedures for Determining R-Curve	4-12
4.3	Develop Crack Growth Data For Each Location.....	4-13
4.3.1	Background.....	4-13
4.3.2	Sources for Fatigue Crack Growth Data	4-14
4.3.3	Sample Fatigue Crack Growth Rate Data	4-15
4.3.4	Procedures for Developing Fatigue Crack Growth Rate Data	4-17
4.3.4.1	Specimen Configuration, Size and Preparation.....	4-17
4.3.4.2	Pre-Cracking	4-19
4.3.4.3	Equipment.....	4-19
4.3.4.4	Crack Rate Growth Testing	4-20
4.3.4.5	Data Reduction / Analysis	4-21
4.3.5	Factors Influencing Fatigue Crack Growth Rate Data.....	4-21
4.3.5.1	Stress Ratio	4-22
4.3.5.2	Material Thickness	4-22
4.3.5.3	Temperature	4-22
4.3.5.4	Humidity.....	4-23
4.3.5.5	Frequency	4-23
4.3.5.6	Crack Orientation.....	4-23
4.3.6	Load Sequence Effects.....	4-23
4.4	Stress-Life (S-N) Fatigue Testing	4-25
4.4.1	Background.....	4-25
4.4.2	Sources for S-N Data	4-26
4.4.3	Procedures for Developing S-N Data	4-26
4.4.3.1	Specimen Configuration, Size, and Preparation.....	4-27
4.4.3.2	Test Equipment	4-29
4.4.3.3	Procedure and Presentation of Results.....	4-29
5.0	Define Aircraft Utilization.....	5-1
5.1	Flight Length Definition.....	5-1
5.1.1	Typical Usage Data	5-1
5.1.2	Statistical Analysis of Data	5-3
5.2	Flight Profile Definition	5-6
5.2.1	Required Data	5-7
5.2.2	Weight Configuration Calculations	5-9
5.2.3	Flight Profile Segments	5-9

TABLE OF CONTENTS (CONTINUED)

<u>SECTION</u>	<u>TITLE</u>	<u>PAGE</u>
5.3	Mission Mix Definition.....	5-12
5.4	Alternate Approach.....	5-13
6.0	Development of Load Spectrum.....	6-1
6.1	Airframe Load Spectra.....	6-1
6.1.1	Maneuver Loads.....	6-3
6.1.2	Gust Loads.....	6-8
6.1.2.1	VGH Gust Data.....	6-8
6.1.2.2	PSD Gust Loads.....	6-13
6.1.3	Taxi Loads.....	6-17
6.1.4	Landing Impact Loads.....	6-19
6.1.5	Ground-Air-Ground Cycle.....	6-19
6.1.6	Balancing Tail Loads.....	6-21
6.1.7	Thrust Loads.....	6-24
6.1.8	Cabin Pressurization Loads.....	6-24
6.1.9	Propeller Slipstream Effects.....	6-24
6.2	Landing Gear Load Spectra.....	6-25
6.2.1	Turning Loads.....	6-25
6.2.2	Braking Loads.....	6-26
6.2.3	Towing Loads.....	6-26
6.2.4	Pivot Loads.....	6-29
7.0	Stress Spectrum Generation.....	7-1
7.1	Analytically Derived Stresses.....	7-1
7.2	Flight Strain Survey Derived Stresses.....	7-3
7.2.1	Instrumentation.....	7-6
7.2.1.1	Technical Considerations.....	7-6
7.2.1.1.1	Installation.....	7-7
7.2.1.1.2	Temperature Compensation.....	7-8
7.2.1.1.3	Frequency Response Considerations.....	7-8
7.2.1.1.4	Micro-Strain Calculation.....	7-8
7.2.1.1.5	Typical Application.....	7-8
7.2.1.2	Items to Measure.....	7-9
7.2.2	Flight Conditions.....	7-10
7.2.3	Data Regression.....	7-12
7.2.3.1	Strain Equations.....	7-17
7.2.3.2	Stress Equations.....	7-19
7.2.3.2.1	Taxi Stress Equation.....	7-20
7.2.3.2.2	Maneuver Stress Equation.....	7-20
7.2.3.2.3	Gust Stress Equation.....	7-21
7.3	Stress Spectrum Development.....	7-22

TABLE OF CONTENTS (CONTINUED)

<u>SECTION</u>	<u>TITLE</u>	<u>PAGE</u>
7.3.1	Stress Spectrum Construction For Flight Strain Equations.....	7-22
7.3.2	Stress Spectrum Construction For Analytical Stresses.....	7-24
7.3.3	Spectrum Cycle Counting.....	7-26
7.3.4	Stress Spectrum Clipping	7-28
7.3.5	Transfer Factors	7-30
8.0	Damage Tolerance Analysis.....	8-1
8.1	Initial Flaw Size	8-2
8.1.1	Primary Flaws	8-2
8.1.2	Secondary Flaws.....	8-3
8.1.3	Maximum Undetectable Flaws.....	8-6
8.2	Crack Growth Analysis	8-6
8.2.1	Basic Background.....	8-6
8.2.2	Crack Growth Models	8-10
8.2.2.1	Linear Crack Growth Models	8-11
8.2.2.1.1	Walker/Chang Material Representation	8-13
8.2.2.1.2	NASGRO Material Representation.....	8-13
8.2.2.2	Crack Growth Models with Load Interaction.....	8-14
8.2.2.2.1	Generalized Willenborg-Chang	8-15
8.2.2.2.2	Crack Closure.....	8-19
8.2.3	Crack Growth Programs.....	8-19
8.2.3.1	CRACKS98	8-20
8.2.3.2	NASGRO.....	8-20
8.2.3.3	AFGROW.....	8-21
8.2.4	Stress Intensity Factor Solution Development	8-22
8.2.5	Special Case: Pressurized Fuselage Structure	8-24
8.2.5.1	Displacement Compatibility Method for Stiffened Panels.....	8-25
8.2.5.1.1	Skin Displacement.....	8-25
8.2.5.1.2	Stiffener Displacement	8-26
8.2.5.1.3	Fastener Displacement.....	8-28
8.2.5.1.4	Displacement Compatibility.....	8-28
8.2.5.1.5	Crack Tip Stress Intensity and Beta Solution.....	8-28
8.2.5.2	Bulge Factors	8-29
8.2.6	Example Problem.....	8-29
8.3	Critical Crack Length	8-35
8.4	Inspection Threshold	8-37
8.4.1	Initial Threshold Based on Crack Growth	8-39
8.4.2	Fail-Safe Tests	8-40
8.4.2.1	Selection of Fail-Safe Test Conditions	8-40
8.4.2.2	Fail-Safe Testing	8-41
8.4.2.3	Fail-Safe Analyses.....	8-41

TABLE OF CONTENTS (CONTINUED)

<u>SECTION</u>	<u>TITLE</u>	<u>PAGE</u>
8.4.3	Initial Threshold Based on Fatigue	8-41
8.5	Repeat Inspection Intervals	8-42
8.6	Fatigue Analysis.....	8-43
8.6.1	Methodology	8-44
8.6.2	Kt Determination	8-46
8.7	Widespread Fatigue Damage (WFD) Evaluation.....	8-48
8.7.1	WFD Evaluation Flow Chart.....	8-49
8.7.2	WFD Evaluation For A Specific Location	8-51
8.7.2.1	Identifying WFD Critical Locations	8-52
8.7.2.1.1	Analysis	8-52
8.7.2.1.2	Test Evidence.....	8-52
8.7.2.1.3	In-Service Experience.....	8-53
8.7.2.2	Consider Additional Damage.....	8-54
8.7.2.2.1	Disbonds.....	8-54
8.7.2.2.2	Corrosion	8-54
8.7.2.2.3	Fretting	8-54
8.7.3	Recommended Action.....	8-55
9.0	Inspection Requirements.....	9-1
9.1	Inspection Methods and Frequencies.....	9-2
9.2	Personnel Qualifications.....	9-2
9.2.1	Levels of Certification.....	9-3
9.2.1.1	Level I.....	9-3
9.2.1.2	Level II.....	9-3
9.2.1.3	Level III.....	9-3
9.2.2	Requirements for Certification.....	9-3
9.3	Visual Inspection	9-4
9.3.1	Visual Inspection Principles	9-4
9.3.2	Borosscopes	9-4
9.3.2.1	Types.....	9-5
9.3.2.2	Additional Options.....	9-5
9.3.3	Visual Inspection Process.....	9-6
9.3.4	Visual Inspection Advantages and Disadvantages.....	9-6
9.4	Penetrant Inspection	9-7
9.4.1	Penetrant Inspection Principles	9-7
9.4.2	Penetrant Inspection Process.....	9-8
9.4.2.1	Penetrant Classification and Application	9-8
9.4.2.2	Penetrant Removal.....	9-10
9.4.2.3	Developer.....	9-10
9.4.2.4	Interpretation.....	9-10
9.4.3	Advantages and Disadvantages	9-11

TABLE OF CONTENTS (CONTINUED)

<u>SECTION</u>	<u>TITLE</u>	<u>PAGE</u>
9.5	Magnetic Particle Inspection.....	9-11
9.5.1	Magnetic Particle Inspection Principles.....	9-12
9.5.2	Magnetic Particle Inspection Process	9-14
9.5.2.1	Magnetic Particles	9-14
9.5.2.2	Equipment.....	9-15
9.5.2.3	Interpretation.....	9-15
9.5.2.4	Demagnetization.....	9-16
9.5.3	Advantages and Disadvantages	9-16
9.6	Eddy Current Inspection	9-16
9.6.1	Eddy Current Inspection Principles	9-17
9.6.2	The Eddy Current Instrument.....	9-18
9.6.3	Eddy Current Inspection Process.....	9-19
9.6.3.1	Part Influences	9-19
9.6.3.2	Probe Influences.....	9-19
9.6.3.3	Calibration.....	9-20
9.6.3.4	Interpretation.....	9-20
9.6.4	Conductivity and Thickness Testing.....	9-20
9.6.5	Advantages and Disadvantages	9-21
9.7	Ultrasonic Inspection.....	9-21
9.7.1	Ultrasonic Inspection Principles.....	9-21
9.7.2	The Ultrasonic Instrument	9-22
9.7.2.1	The Transducer.....	9-22
9.7.2.2	Video Display Basics	9-23
9.7.3	The Ultrasonic Inspection Process.....	9-24
9.7.3.1	Inspection Types.....	9-24
9.7.3.2	Operator Choices.....	9-26
9.7.3.3	Instrument Calibration.....	9-26
9.7.3.4	Inspection.....	9-27
9.7.3.5	Interpretation.....	9-27
9.7.4	Thickness Testing	9-27
9.7.5	Ultrasonic Advantages and Disadvantages.....	9-27
9.8	Bond Inspection.....	9-28
9.8.1	Bond Testing Principles	9-28
9.8.2	Bond Testing Process	9-29
9.8.3	Advantages and Disadvantages	9-29
9.9	Radiographic Inspection.....	9-30
9.9.1	Radiographic Inspection Principles	9-30
9.9.2	The X-ray Unit.....	9-31
9.9.3	Radiation Safety.....	9-32
9.9.4	Radiographic Inspection Process	9-33
9.9.4.1	The Parameters.....	9-33

TABLE OF CONTENTS (CONTINUED)

<u>SECTION</u>	<u>TITLE</u>	<u>PAGE</u>
9.9.4.2	Interpretation.....	9-33
9.9.5	Radiographic Advantages and Disadvantages.....	9-33
9.10	Determining the Minimum Detectable Discontinuity	9-34
9.10.1	Required Information.....	9-34
9.10.2	Experimentation	9-35
9.10.3	Testing	9-35
9.11	Selection of an Inspection Method	9-36
9.11.1	Surface Cracks.....	9-36
9.11.1.1	Visual Method.....	9-36
9.11.1.2	Eddy Current Method.....	9-36
9.11.1.3	Magnetic Particle Method	9-36
9.11.1.4	Penetrant Method.....	9-37
9.11.1.5	Ultrasonic Method	9-37
9.11.1.6	Radiographic Method	9-37
9.11.2	Subsurface Cracks	9-37
9.11.2.1	Eddy Current Method.....	9-38
9.11.2.2	Ultrasonic Method	9-38
9.11.2.3	Visual Method.....	9-38
9.11.2.4	Magnetic Particle Method	9-38
9.11.2.5	Radiographic Method	9-38
9.11.3	Corrosion	9-39
9.11.3.1	Visual Method.....	9-39
9.11.3.2	Penetrant Method.....	9-39
9.11.3.3	Magnetic Particle Method	9-39
9.11.3.4	Eddy Current Method.....	9-39
9.11.3.5	Ultrasonic Method	9-40
9.11.3.6	Radiographic Method	9-40
9.11.4	Disbonds and Honeycomb Discontinuities	9-40
9.11.5	Delamination.....	9-41
9.11.6	Foreign Objects.....	9-41
9.12	Detection Limits	9-42
9.12.1	Probability of Detection Plot.....	9-42
9.12.1.1	Development.....	9-42
9.12.1.2	Influences and Limitations	9-43
9.12.2	Visual Inspection	9-44
9.12.2.1	Equipment Influence.....	9-44
9.12.2.2	Part Influence	9-44
9.12.2.3	Environmental Influence	9-44
9.12.3	Penetrant Inspection	9-45
9.12.3.1	Equipment Influence.....	9-45
9.12.3.2	Part Influence	9-45

TABLE OF CONTENTS (CONTINUED)

<u>SECTION</u>	<u>TITLE</u>	<u>PAGE</u>
9.12.3.3	Environmental Influence	9-45
9.12.4	Magnetic Particle Inspection.....	9-46
9.12.4.1	Equipment Influence.....	9-46
9.12.4.2	Part Influence	9-46
9.12.4.3	Environmental Influence	9-47
9.12.5	Eddy Current Inspection	9-47
9.12.5.1	Equipment Influence.....	9-47
9.12.5.2	Part Influence	9-48
9.12.5.3	Environmental Influence	9-48
9.12.6	Ultrasonic Inspection.....	9-48
9.12.6.1	Equipment Influence.....	9-48
9.12.6.2	Part Influence	9-49
9.12.6.3	Environmental Influence	9-49
9.12.7	Bond Inspection.....	9-50
9.12.7.1	Equipment Influence.....	9-50
9.12.7.2	Part Influence	9-50
9.12.7.3	Environmental Influence	9-50
9.12.8	Radiographic Inspection.....	9-50
9.12.8.1	Equipment Influence.....	9-50
9.12.8.2	Part Influence	9-51
9.12.8.3	Environmental Influence	9-52
9.13	Accessibility.....	9-53
9.13.1	Visual Inspection	9-53
9.13.2	Penetrant Inspection	9-53
9.13.3	Magnetic Particle Inspection.....	9-53
9.13.4	Eddy Current Inspection	9-54
9.13.5	Ultrasonic Inspection.....	9-54
9.13.6	Bond Inspection.....	9-54
9.13.7	Radiographic Inspection.....	9-55
9.14	Creating a Field Inspection.....	9-55
9.14.1	Cost	9-55
9.14.2	Reference Standards.....	9-56
9.14.3	Method Availability.....	9-57
10.0	SID Development.....	10-1
10.1	Developing a SID Document	10-1
10.1.1	Intent of SID Document.....	10-2
10.1.2	Considerations in Preparing the SID Document	10-3
10.2	SID Handbook Format.....	10-8
10.2.1	Physical Requirements.....	10-8
10.2.2	Contents	10-9

TABLE OF CONTENTS (CONTINUED)

<u>SECTION</u>	<u>TITLE</u>	<u>PAGE</u>
10.2.2.1	Title Page.....	10-9
10.2.2.2	List of Effective Pages.....	10-10
10.2.2.3	Record of Revisions.....	10-10
10.2.2.4	Table of Contents.....	10-11
10.2.2.5	Applicability.....	10-11
10.2.2.6	Objectives.....	10-11
10.2.2.7	Technical Document Reference.....	10-12
10.2.2.8	Listing of Supplemental Inspection Document Inspections.....	10-13
10.2.2.9	Supplemental Inspection Document Inspections.....	10-13
10.2.2.10	Inspection Methods and Requirements.....	10-16
10.3	Sample Supplemental Inspection Document.....	10-18
11.0	References.....	11-1
Appendix A	Flight Profile Length Determination.....	A-1
A.1	Calculation of Weibull Parameters.....	A-1
A.2	Flight Length Distribution.....	A-7
Appendix B	Flight Profile Data Calculations.....	B-1
Appendix C	Empennage Spectrum Determination.....	C-1
C.1	Define Usage.....	C-2
C.2	Identify Load Spectrum Type.....	C-2
C.3	Develop Load Spectrum.....	C-4
C.4	Develop Stress Spectrum for Analysis Location.....	C-9

LIST OF FIGURES

<u>NUMBER</u>	<u>TITLE</u>	<u>PAGE</u>
1-1	ALOHA AIRLINE BOEING 737 FUSELAGE FAILURE.....	1-1
1-2	DISTRIBUTION OF CRACK INITIATION/GROWTH AND FAILURE MECHANISMS	1-2
1-3	DISTRIBUTION OF CRACKING AND FAILURE ORIGINS	1-4
1-4	SCHEMATIC CRACK GROWTH CURVE.....	1-5
1-5	SCHEMATIC DIAGRAM OF ALLOWABLE STRESS VS. CRACK LENGTH.....	1-6
1-6	RESIDUAL STRENGTH AS A FUNCTION OF APPLIED LOAD CYCLES.....	1-6
1-7	SCHEMATIC FOR DETERMINING INSPECTION INTERVALS	1-7
2-1	REQUIRED EVALUATION TASKS.....	2-2
3-1	TYPICAL EXAMPLES OF PRINCIPAL STRUCTURAL ELEMENTS (PSEs)	3-3
3-2	TYPICAL WING BOX STRUCTURE	3-4
3-3	STRESSES IN WING SPAR	3-5
3-4	AIRPLANE IN BALANCED FLIGHT	3-6
3-5	TYPICAL SEMI-MONOCOQUE FUSELAGE CONSTRUCTION.....	3-7
3-6	STRESSES ON FUSELAGE SHELL	3-8
3-7	FUSELAGE POTENTIAL FATIGUE CRITICAL AREA	3-9
3-8	FINITE ELEMENT MODEL OF WING WITH ENGINE SUPPORT.....	3-15
3-9	FINITE ELEMENT MODEL REPRESENTATION	3-16
3-10	SAMPLE DETAILED FINITE ELEMENT MODEL OF SPLICE	3-17
3-11	FORGING FINITE ELEMENT MODEL (3-D)	3-17
3-12	EXAMPLE OF FAA SERVICE DIFFICULTY RECORD	3-19
3-13	SAMPLE OPERATOR SURVEY – AIRFRAME REPAIRS	3-20
3-14	SAFE LIFE PART EXAMPLE	3-22
3-15	DAMAGE TOLERANT – OBVIOUS DAMAGE EVIDENT EXAMPLE	3-23
3-16	SINGLE LOAD PATH STRUCTURE - DAMAGE TOLERANT CATEGORY EXAMPLE.....	3-25
3-17	MULTIPLE LOAD PATH STRUCTURE – NOT INSPECTABLE FOR LESS THAN LOAD PATH FAILURE CATEGORY EXAMPLE	3-26
3-18	MULTIPLE LOAD PATH STRUCTURE – INSPECTABLE FOR LESS THAN LOAD PATH FAILURE CATEGORY EXAMPLE	3-28
3-19	DETERMINATION OF INSPECTION AREA BASED ON MULTIPLE POSSIBLE CRACK ORIGINS	3-31
4-1	GRAIN ORIENTATION DEFINITIONS.....	4-2
4-2	GENERAL RESIDUAL STRENGTH DIAGRAM	4-5
4-3	VARIATION OF FRACTURE TOUGHNESS WITH THICKNESS	4-6
4-4	EFFECT OF PANEL WIDTH ON FRACTURE TOUGHNESS.....	4-6

LIST OF FIGURES (CONTINUED)

<u>NUMBER</u>	<u>TITLE</u>	<u>PAGE</u>
4-5	SAMPLE R-CURVE FOR 0.09" THICK 2024-T3 SHEET	4-7
4-6	SCHEMATIC OF R-CURVE RESIDUAL STRENGTH ANALYSIS	4-8
4-7	COMPACT TENSION, C(T), PLANE STRAIN FRACTURE TOUGHNESS SPECIMEN PER ASTM E399	4-10
4-8	PRINCIPAL TYPES OF LOAD-DISPLACEMENT RECORDS.....	4-11
4-9	FATIGUE CRACK GROWTH DATA FOR EXTRUDED 7075-T6 FOR DIFFERENT R-RATIOS	4-15
4-10	FATIGUE CRACK GROWTH DATA FOR EXTRUDED 7075-T6 COLLAPSED AND FITTED WITH TRI-SLOPE WALKER EQUATION.....	4-16
4-11	ASTM STANDARD COMPACT TENSION (CT) SPECIMEN FOR FATIGUE CRACK GROWTH RATE TESTING.....	4-18
4-12	ASTM STANDARD MIDDLE TENSION (MT) SPECIMEN FOR FATIGUE CRACK GROWTH RATE TESTING	4-18
4-13	RETARDATION DUE TO PLASTIC ZONE FROM OVERLOAD	4-24
4-14	SAMPLE S-N DIAGRAM: 2024-T4 ALUMINUM ALLOY, SMOOTH SPECIMEN.....	4-27
4-15	STANDARD SMOOTH S-N SPECIMENS	4-28
5-1	SAMPLE OPERATOR SURVEY – AIRCRAFT USAGE	5-2
5-2	TYPICAL WEIBULL DISTRIBUTION.....	5-4
5-3	DEFINITION OF PROFILE FLIGHT LENGTH.....	5-5
5-4	FLIGHT LENGTH DISTRIBUTION.....	5-6
5-5	MISSION PROFILE AND MISSION SEGMENTS	5-7
5-6	PROFILE ALTITUDES	5-8
6-1	MANEUVER SPECTRUM TIME HISTORY	6-4
6-2	MANEUVER LOAD FACTOR SPECTRUM (CUM. EXCD/NAUT. MILE).....	6-5
6-3	MANUEVER LOAD FACTOR SPECTRUM (EXCD/1000 FLTS.) FOR THE ACME MODEL 999 AIRCRAFT	6-6
6-4	VERTICAL GUST LOADS EXCEEDANCE COMPARISON FOR THE ACME MODEL 999 AIRCRAFT.....	6-9
6-5	LATERAL GUST LOAD SPECTRUM (EXCD/1000 FLTS) FOR THE ACME MODEL 999 AIRCRAFT.....	6-12
6-6	PSD PROBABILITY DISTRIBUTIONS b1 AND b2	6-14
6-7	PSD PROBABILITY DISTRIBUTIONS P1 AND P2	6-14
6-8	GUST SPECTRUM DEVELOPMENT – PROCESS FLOW	6-15
6-9	TAXI LOAD FACTOR SPECTRUM.....	6-18
6-10	LANDING IMPACT SPECTRUM	6-20
6-11	EFFECT OF SPANWISE LOCATION ON GROUND-AIR-GROUND CYCLE	6-22

LIST OF FIGURES (CONTINUED)

<u>NUMBER</u>	<u>TITLE</u>	<u>PAGE</u>
6-12	EFFECT OF FLAP DEFLECTION ON HORIZONTAL TAIL STRESS.....	6-23
6-13	TURNING LOAD FACTOR SPECTRUM	6-27
6-14	BRAKING LOAD FACTOR SPECTRUM.....	6-28
7-1	STRESS SPECTRUM DEVELOPMENT PROCESS	7-2
7-2	ANALYTICAL STRESS SPECTRUM DEVELOPMENT	7-4
7-3	FLIGHT STRAIN SURVEY PROCESS	7-5
7-4	TYPICAL FLIGHT DATA RECORDER SCHEMATIC DIAGRAM....	7-9
7-5	TYPICAL FLIGHT STRAIN SURVEY STRESS HISTORY PLOTS.....	7-13
7-6	TYPICAL MEASURED DATA STRIP CHARTS.....	7-14
7-7	EXAMPLE REGRESSION ANALYSIS OUTPUT.....	7-16
7-8	FLIGHT STRAIN SURVEY BASED STRESS SPECTRUM FLOWCHART.....	7-23
7-9	ANALYTICALLY DERIVED STRESS SPECTRUM FLOWCHART.....	7-25
7-10	RAINFLOW CYCLE COUNTING.....	7-27
7-11	PEAK STRESS CLIPPING EXAMPLE	7-28
7-12	CLIPPING EFFECTS ON CRACK GROWTH EXAMPLE	7-29
8-1	PRIMARY FLAW SIZE ASSUMPTIONS FOR HOLE FLAW LOCATION.....	8-4
8-2	PRIMARY FLAW SIZE ASSUMPTIONS FOR EDGE FLAW LOCATION.....	8-4
8-3	PRIMARY FLAW SIZE ASSUMPTIONS FOR SURFACE FLAW LOCATION.....	8-5
8-4	SECONDARY FLAW SIZE ASSUMPTIONS	8-5
8-5	FRACTURE MODES	8-7
8-6	DEFINITION OF X-Y PLANE STRESSES NEAR CRACK TIP	8-8
8-7	SIMPLIFIED STRESS INTENSITY FACTOR SOLUTIONS	8-9
8-8	CRACK GROWTH COMPUTATION PROCEDURE FOR PROBLEMS WITHOUT LOAD INTERACTION	8-12
8-9	RETARDATION DUE TO OVERLOAD AND OVERLOAD/UNDERLOAD CYCLES	8-15
8-10	CRACK GROWTH COMPUTATION PROCEDURE FOR PROBLEMS WITH LOAD INTERACTION	8-16
8-11	GENERALIZED WILLENBORG-CHANG LOAD INTERACTION MODEL	8-17
8-12	EXAMPLE OF SUPERPOSITION	8-23
8-13	EXAMPLE OF COMPOUNDING.....	8-23
8-14	LONGITUDINAL CRACK IN PRESSURIZED FUSELAGE STRUCTURE.....	8-24
8-15	SKIN DISPLACEMENT SUPERPOSITION LOADING CASES	8-26

LIST OF FIGURES (CONTINUED)

<u>NUMBER</u>	<u>TITLE</u>	<u>PAGE</u>
8-16	IDEALIZED FRAME LOADING.....	8-27
8-17	FRAME BENDING IDEALIZATION.....	8-27
8-18	EXAMPLE CRITICAL LOCATION.....	8-31
8-19	GEOMETRY IDEALIZATION.....	8-32
8-20	EXAMPLE OF WING AND CARRY-THRU FINITE ELEMENT MESH.....	8-32
8-21	LOCAL STRESSES AND FASTENER LOADS IN SPAR CAP	8-33
8-22	STRESS INTENSITY FACTOR SOLUTION CC02	8-34
8-23	SPAR CAP SKIN FLANGE HOLE CRACK GROWTH CURVE.....	8-34
8-24	RESIDUAL STRENGTH DIAGRAM TO DETERMINE CRITICAL CRACK LENGTH.....	8-37
8-25	INITIAL INSPECTION INTERVAL.....	8-40
8-26	REPEAT INSPECTION CRITERIA	8-43
8-27	SAMPLE KT VS. LIFE CURVE	8-45
8-28	EXAMPLE OF MSD.....	8-49
8-29	EXAMPLE OF MED.....	8-49
8-30	FLOW CHART OF WFD EVALUATION PROCESS	8-50
9-1	DAMAGE TOLERANT STRUCTURE INSPECTION CRITERIA	9-1
9-2	BASIC BOROSCOPE TYPES.....	9-5
9-3	PENETRANT INSPECTION PROCESS.....	9-7
9-4	CAPILLARY ACTION.....	9-8
9-5	BAR MAGNET MAGNETIC FIELD.....	9-12
9-6	HORSESHOE MAGNET MAGNETIC FIELD.....	9-12
9-7	CIRCULAR MAGNET MAGNETIC FIELD.....	9-13
9-8	CIRCULAR MAGNET WITH A SURFACE BREAK.....	9-13
9-9	EXAMPLE OF A SURFACE CRACK INDICATION.....	9-14
9-10	EDDY CURRENT COIL ARRANGEMENT	9-17
9-11	CROSS SECTION OF AN EDDY CURRENT FIELD.....	9-18
9-12	ULTRASONIC TRANSDUCER CONSTRUCTION (SHEAR BEAM).....	9-22
9-13	ULTRASONIC A SCAN EXAMPLE	9-23
9-14	ULTRASONIC C SCAN EXAMPLE	9-24
9-15	ULTRASONIC PULSE ECHO AND THROUGH TRANSMISSION METHODS.....	9-25
9-16	EXAMPLE OF SHEAR AND SURFACE INSPECTIONS	9-25
9-17	PHOTOELECTRIC EFFECT.....	9-30
9-18	COMPTON EFFECT.....	9-31
9-19	GENERAL LAYOUT OF AN X-RAY TUBE	9-32
9-20	GENERIC EXAMPLE OF POD PLOT	9-43
10-1	SID DOCUMENT DEVELOPMENT FLOW CHART	10-1
10-2	BALANCING RISK VS. COST	10-4
10-3	SKIN WITH A TAPERED DOUBLER.....	10-6

LIST OF FIGURES (CONTINUED)

<u>NUMBER</u>	<u>TITLE</u>	<u>PAGE</u>
10-4	IMPROVEMENT OF FATIGUE LIFE AND INSPECTABILITY.....	10-7
10-5	EXAMPLE TITLE PAGE	10-19
10-6	EXAMPLE LIST OF EFFECTIVE PAGES.....	10-20
10-7	EXAMPLE REVISION PAGE	10-21
10-8	EXAMPLE TABLE OF CONTENTS.....	10-22
10-9	EXAMPLE APPLICABILITY STATEMENT.....	10-23
10-10	EXAMPLE PAGE 1 IN INTRODUCTION SECTION	10-24
10-11	EXAMPLE PAGE 2 IN INTRODUCTION SECTION	10-25
10-12	EXAMPLE PAGE 3 IN INTRODUCTION SECTION	10-26
10-13	EXAMPLE PAGE 4 IN INTRODUCTION SECTION	10-27
10-14	EXAMPLE PAGE 5 IN INTRODUCTION SECTION	10-28
10-15	EXAMPLE PAGE 6 IN INTRODUCTION SECTION	10-29
10-16	EXAMPLE PAGE 7 IN INTRODUCTION SECTION	10-30
10-17	EXAMPLE PAGE 8 IN INTRODUCTION SECTION	10-31
10-18	EXAMPLE PAGE 9 IN INTRODUCTION SECTION	10-32
10-19	EXAMPLE PAGE 10 IN INTRODUCTION SECTION.....	10-33
10-20	EXAMPLE PAGE 11 IN INTRODUCTION SECTION.....	10-34
10-21	EXAMPLE DISCREPANCY REPORT FORM (IN INTRODUCTION SECTION).....	10-35
10-22	EXAMPLE TECHNICAL DOCUMENT REFERENCE PAGE	10-36
10-23	EXAMPLE LIST OF SUPPLEMENTAL INSPECTIONS.....	10-37
10-24	EXAMPLE HOURS TO YEARS EQUIVALENCE.....	10-38
10-25	EXAMPLE LIST OF SUPPLEMENTAL INSPECTIONS (TABLE FORMAT).....	10-39
10-26	EXAMPLE SUPPLEMENTAL INSPECTIONS TEXT PAGE (WITH REPAIR).....	10-40
10-27	EXAMPLE SUPPLEMENTAL INSPECTION ILLUSTRATION PAGE (WITH REPAIR).....	10-41
10-28	EXAMPLE SUPPLEMENTAL INSPECTION TEXT PAGE.....	10-42
10-29	EXAMPLE SUPPLEMENTAL INSPECTION ILLUSTRATION PAGE	10-43
10-30	EXAMPLE NON-DESTRUCTIVE INSPECTION INTRODUCTION PAGE	10-44
10-31	EXAMPLE NON-DESTRUCTIVE INSPECTION GENERAL PROCEDURE PAGE	10-45
10-32	EXAMPLE NON-DESTRUCTIVE INSPECTION TEXT PAGE	10-46
10-33	EXAMPLE NON-DESTRUCTIVE INSPECTION ADDITIONAL TEXT PAGE	10-47
10-34	EXAMPLE NON-DESTRUCTIVE INSPECTION ILLUSTRATION PAGE	10-48
A-1	TYPICAL FLIGHT DISTRIBUTION HISTOGRAM.....	A-2
A-2	MICROSOFT EXCEL SOLVER WINDOW.....	A-6

LIST OF FIGURES (CONTINUED)

<u>NUMBER</u>	<u>TITLE</u>	<u>PAGE</u>
A-3	FLIGHT LENGTH DISTRIBUTION.....	A-9
B-1	MEAN AERODYNAMIC CHORD CONCEPT	B-3
B-2	TIME, FUEL, AND DISTANCE TO CLIMB EXAMPLE CHART	B-3
B-3	TIME, FUEL, AND DISTANCE TO DESCEND EXAMPLE CHART	B-5
C-1	EMPENNAGE FINITE ELEMENT MODEL AND ANALYSIS LOCATION.....	C-1

LIST OF TABLES

<u>NUMBER</u>	<u>TITLE</u>	<u>PAGE</u>
2-1	BASIC DEFINITIONS.....	2-3
3-1	TYPICAL EXAMPLES OF PRINCIPAL STRUCTURAL ELEMENTS (PSEs)	3-2
3-2	STRUCTURAL CATAGORIES.....	3-21
4-1	MATERIAL PROPERTIES: 2014-T6 EXTRUSION.....	4-3
4-2	SUMMARY OF SPECIMEN GEOMETRY, LOADING AND TEST CONDITIONS FOR THE EXTRUDED 7075-T6 ALUMINUM ALLOY da/dN VS ΔK DATA.....	4-16
4-3	COEFFICIENTS FOR TRI-SLOPE WALKER EQUATION FOR EXTRUDED 7075-T6 ALUMINUM ALLOY.....	4-17
4-4	EXAMPLE PARAMETERS FOR MATERIAL da/dN CHARACTERIZATION	4-20
4-5	RECOMMENDED CRACK LENGTH MEASUREMENT INTERVALS.....	4-21
5-1	PROFILE SUMMARY	5-5
5-2	EXAMPLE AIRCRAFT WEIGHT CONFIGURATION CALCULATION	5-9
5-3	EXAMPLE FLIGHT PROFILE TABLE	5-11
5-4	FLIGHT DISTRIBUTION EXAMPLE (1000 FLIGHT BLOCK).....	5-12
5-5	MISSION MIX EXAMPLE (1000 FLIGHT BLOCK).....	5-13
6-1	TYPICAL AIRFRAME LOAD SPECTRA SUMMARY.....	6-2
6-2	SAMPLE MANEUVER LOAD FACTOR OCCURRENCES	6-7
6-3	VERTICAL GUST LOAD EXCEEDANCES FOR ACME MODEL 999.....	6-11
6-4	LATERAL GUST LOAD EXCEEDANCES FOR ACME MODEL 999.....	6-11
6-5	TAXI LOAD FACTOR OCCURRENCES.....	6-19
6-6	LANDING IMPACT SINK RATE OCCURRENCES.....	6-21
6-7	BALANCING TAIL LOAD CYCLES.....	6-22
6-8	BALANCING TAIL LOAD SPECTRUM TABLE.....	6-23
6-9	CABIN PRESSURIZATION LOADS	6-25
6-10	TURNING LOAD FACTOR OCCURRENCES	6-26
6-11	BRAKING LOAD FACTOR OCCURRENCES.....	6-26
6-12	TOWING LOAD SPECTRUM.....	6-29
6-13	PIVOT LOAD SPECTRUM.....	6-29
7-1	STRAIN EQUATION PARAMETERS	7-18
8-1	PRIMARY FLAW SIZE ASSUMPTIONS	8-3
8-2	EXAMPLE MATERIAL DATA	8-30
8-3	METHOD OF INITIAL THRESHOLD DETERMINATION.....	8-38
9-1	CRACK ANGLE EFFECT ON DETECTION PROBABILITY.....	9-52
A-1	EXAMPLE FLIGHT DISTRIBUTION DATA.....	A-1
A-2	PROBABILITY OF OCCURRENCE CALCULATION	A-3

LIST OF TABLES (CONTINUED)

<u>NUMBER</u>	<u>TITLE</u>	<u>PAGE</u>
A-3	CALCULATION OF FLIGHT OCCURRENCE PROBABILITY.....	A-4
A-4	CALCULATION OF $F(\Delta T)$	A-4
A-5	CALCULATION OF LEAST SQUARES ERROR	A-5
A-6	CALCULATION OF β AND η VALUES BY ITERATION.....	A-6
A-7	CALCULATION OF MEAN PROFILE TIME AND OCCURRENCE PROBABILITY.....	A-7
A-8	FLIGHT PROFILE UTILIZATION TABLE EXAMPLE.....	A-8
B-1	EXAMPLE FLIGHT PROFILE TABLE	B-1
C-1	EXAMPLE FLIGHT PROFILE TABLE	C-2
C-2	VERTICAL GUST EXCEEDANCE DATA.....	C-3
C-3	VERTICAL GUST CYCLE ACCELERATION EXCEEDANCES AND OCCURRENCES.....	C-6
C-4	GUST VELOCITY CYCLE EXCEEDANCE/OCCURRENCE TABLE.....	C-8
C-5	VERTICAL TAIL LOAD CYCLE EXCEEDANCES/OCCURRENCES	C-10
C-6	SECOND CRUISE SEGMENT STRESS SPECTRUM FOR VERTICAL TAIL FRONT SPAR CAP ON ACME MODEL 999 AIRCRAFT	C-11

EXECUTIVE SUMMARY

This document is the final report covering the results of a one-year program. This program was funded through the Federal Aviation Administration (FAA) William J. Hughes Technical Center at Atlantic City International Airport under FAA contract number DTFA03-98-C-00032. The program focused on developing a Supplemental Inspection Document Handbook. Airframe manufacturers and other engineering organizations can use the handbook to assure the continued airworthiness of commuter aircraft.

This effort was a follow on task of a previous contract. The previous contract (FAA contract number DTFA03-95-C-00044) provided the government with a methodology document and Supplemental Inspection Document (SID) for the Cessna 402 based on damage tolerance analysis.

This document utilizes the knowledge and experience gained during the execution of the previous contract to generate a "SID Handbook." This comprehensive handbook provides a manufacturer or other engineering organization with the requirements for developing a damage tolerant SID of a commuter aircraft. This handbook contains everything, either directly or by reference, that a small commuter sized airplane company would need to develop a SID. The technical issues to be resolved, sources of critical engineering data and the procedures to develop data are described in this document.

Some of the topics addressed in this document include:

- a. Identification of the Critical Areas of Principle Structural Elements (PSE)
- b. Material Data and Material Test Procedures
- c. Stress Spectrum Development
- d. Crack Growth Analysis
- e. Initial and Repeat Inspection Intervals
- f. Widespread Fatigue Damage
- g. Inspection Techniques and Procedures
- h. Documentation of Analytical Results in a Supplemental Inspection Document (SID)

1. Report No. DOT/FAA/AR-99/XX		2. Government Accession No.		3. Recipient's Catalog No.	
4. Title and Subtitle SUPPLEMENTAL INSPECTION DOCUMENT DEVELOPMENT HANDBOOK FOR COMMUTER AIRCRAFT				5. Report Date September 1999	
				6. Performing Organization Code	
7. Author(s) Bill Baumeister, Beth Gamble, Tom Harrison, Markus Heinimann and John Miesen				8. Performing Organization Report No.	
9. Performing Organization Name and Address Cessna Aircraft Company 1 Cessna Boulevard Wichita, Kansas 67277				10. Work Unit No. (TRAIS)	
				11. Contract or Grant No. DTFA03-98-C-00032	
12. Sponsoring Agency Name and Address U.S. Department of Transportation Federal Aviation Administration Office of Aviation Research Washington, DC 20591				13. Type of Report and Period Covered Final Report, 9/98 – 9/99	
				14. Sponsoring Agency Code ACE-102	
15. Supplementary Notes Federal Aviation Administration William J. Hughes Technical Center COTR: Richard Micklos					
16. Abstract <p>This document is the final report covering the results of a one-year program. This program was funded through the Federal Aviation Administration (FAA) William J. Hughes Technical Center at Atlantic City International Airport under FAA contract number DTFA03-98-C-00032. The program focused on developing a Supplemental Inspection Document Handbook. Airframe manufacturers and other engineering organizations can use the handbook to assure the continued airworthiness of commuter aircraft.</p> <p>This effort was a follow on task of a previous contract. The previous contract (FAA contract number DTFA03-95-C-00044) provided the government with a methodology document and Supplemental Inspection Document (SID) for the Cessna 402 based on damage tolerance analysis.</p> <p>This document utilizes the knowledge and experience gained during the execution of the previous contract to generate a "SID Handbook." This comprehensive handbook provides a manufacturer or other engineering organization with the requirements for developing a damage tolerant SID handbook of a commuter aircraft. This handbook contains everything, either directly or by reference, that a small commuter sized airplane company would need to develop a SID. The technical issues to be resolved, sources of critical engineering data and the procedures to develop data are described in this document.</p> <p>Some of the topics addressed in this document include: (1) Identification of the Critical Areas of Principle Structural Elements (PSE), (2) Material Data and Material Test Procedures, (3) Stress Spectrum Development, (4) Crack Growth Analysis, (5) Initial and Repeat Inspection Intervals, (6) Widespread Fatigue Damage, (7) Inspection Techniques and Procedures, and (8) Documentation of the Analytical Results in a Supplemental Inspection Document (SID).</p>					
17. Key Words Widespread Fatigue Damage, Supplemental Inspection Document (SID), Fatigue Crack Growth, Damage Tolerance			18. Distribution Statement This document is available to the public through the National Technical Information Service (NTIS), Springfield, Virginia 22161.		
19. Security Classif. (of this report) Unclassified		20. Security Classif. (of this page) Unclassified		21. No. of Pages 362	22. Price

1.0 Introduction

1.1 Supplemental Inspection Document (SID) Background

As a result of several accidents and incidents, most notably the fatigue failure of an Aloha Airlines Boeing 737 on April 28, 1988 (Figure 1-1), Congress passed the Aviation Safety Research Act of 1988 (Public Law 100-591). In response to the Aviation Safety Research Act and concerns related to the increasing age of aircraft fleets, the Federal Aviation Administration (FAA) developed the National Aging Aircraft Research Program (NAARP) to ensure the structural integrity of high-time, high-cycle aircraft. One of the three major elements of the NAARP is the development of supplemental structural inspections for commuter aircraft. Supplemental inspection documents (SIDs) have been required for large transport aircraft since 1981 [Advisory Circular (AC) 91-56], and the resulting structural inspection programs (SIP) have proven effective in ensuring the structural integrity of the aging large transport fleet.

FIGURE 1-1

ALOHA AIRLINE BOEING 737 FUSELAGE FAILURE



The FAA proposes to extend the SIP concept to aircraft operated under 14 Code of Federal Regulations (CFR) Part 121, all U.S. registered multiengine airplanes operated under 14 CFR Part 129, and all multiengine airplanes used in scheduled operations conducted under 14 CFR Part 135. The proposed rule would require implementation of a damage tolerance based structural inspection program for all airplanes older than 14 years. Furthermore implementation of a mandatory corrosion protection and control program is also proposed.

Damage tolerance based inspections and procedures, incorporated into a SID, are the best way to assure the continued safety of the commuter fleet considering the overall costs, the impact on aircraft operators and the aviation safety requirements mandated by Congress. There are two primary benefits achieved by developing a damage tolerance based inspection program. First, the FAA and aircraft industry will be able to monitor the airworthiness of each airplane as it ages and either (1) take corrective action to maintain its continued airworthiness or (2) retire it from service before the airplane becomes unairworthy. The second benefit is that each airplane may be able to stay in service longer because its continued airworthiness would be monitored, rather than the airplane be retired at an arbitrary age.

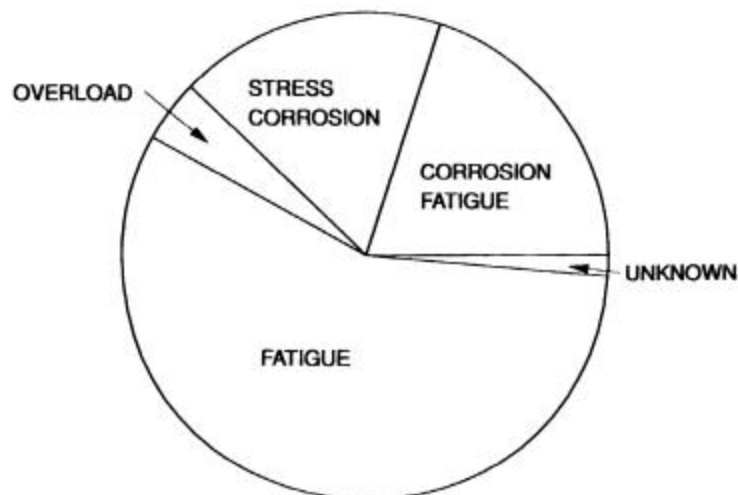
1.2 Aging Aircraft Background

As airplanes age it is common to find in service damage due to fatigue cracking, corrosion or a combination of the two. The results of two extensive studies performed by the U.S. Air Force to document the crack initiation and growth mechanisms in major cracking/failure incidents are shown in Figure 1-2 as reported in References 2 and 3.

FIGURE 1-2

DISTRIBUTION OF CRACK INITIATION/GROWTH AND FAILURE
MECHANISMS

(a) 1226 major cracking/failure incidents (21 month period)



(b) 64 major cracking/failure incidents

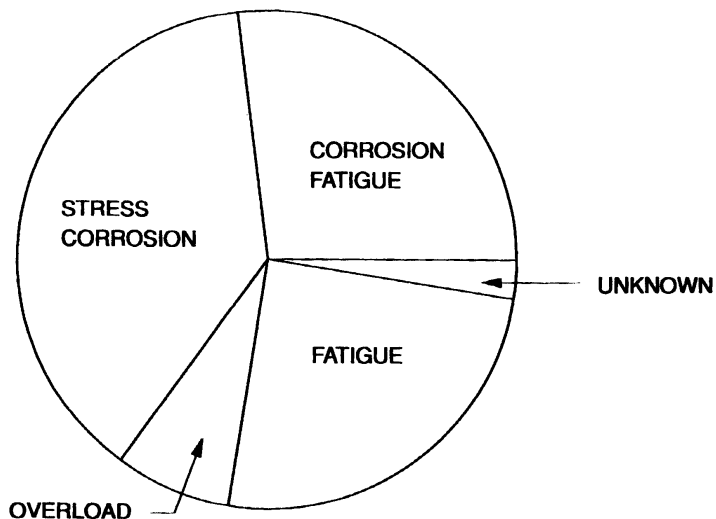


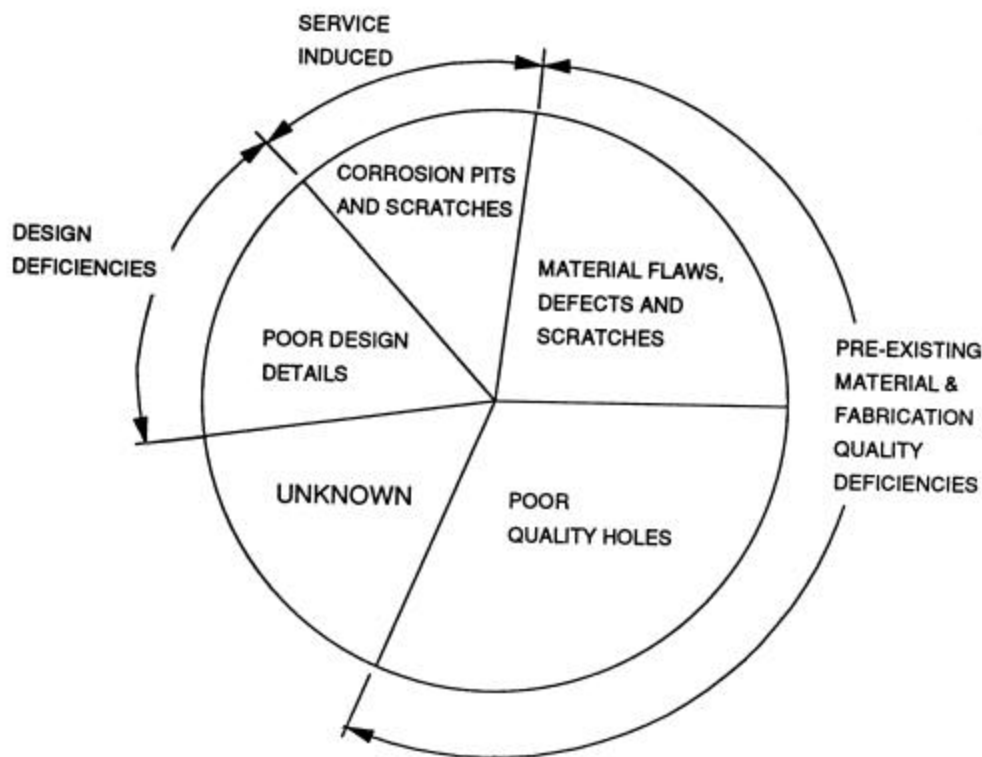
Figure 1-2 clearly shows that the vast majority of cracking cases are the result of either fatigue, corrosion fatigue or stress corrosion. The extent of the cracking and failures due to these three causes is directly related to the age of the aircraft, both in terms of total flight hours/cycles and chronological age. The older the aircraft the more likely it is that fatigue/corrosion damage will occur. Further adding to the concern about the structural integrity of aging aircraft is that typical aircraft structure contains initial “damage” due to material and manufacturing deficiencies. Figure 1-3 shows the distribution of cracking and failure origins determined in an U.S. Air Force study (Reference 3).

Deficiencies in material or manufacturing causing the majority of the crack and failure origins led to the development of the damage tolerant design philosophy, which forms the basis of current civilian and military certification requirements. The aging commuter aircraft, for which the SID requirement is being proposed, not being designed and certified to damage tolerance requirements, further increases the potential for structural failure due to fatigue and corrosion damage in the aging commuter fleet.

Aircraft developed prior to 1960 were designed and certified to static strength requirements and little if any fatigue analysis and testing was performed. Many aircraft developed in the 1960’s and 1970’s were designed to be fail-safe. The fail-safe approach required that the structure meet the residual strength requirements after the failure of a principal structural element. The United States Air Force developed the first damage tolerance requirements in the early 1970’s in response to failures of the fail-safe approach to protect the safety of their aircraft. Later, the FAA mandated the use of damage tolerance for large category transport aircraft to augment the fail-safe requirements.

FIGURE 1-3

DISTRIBUTION OF CRACKING AND FAILURE ORIGINS

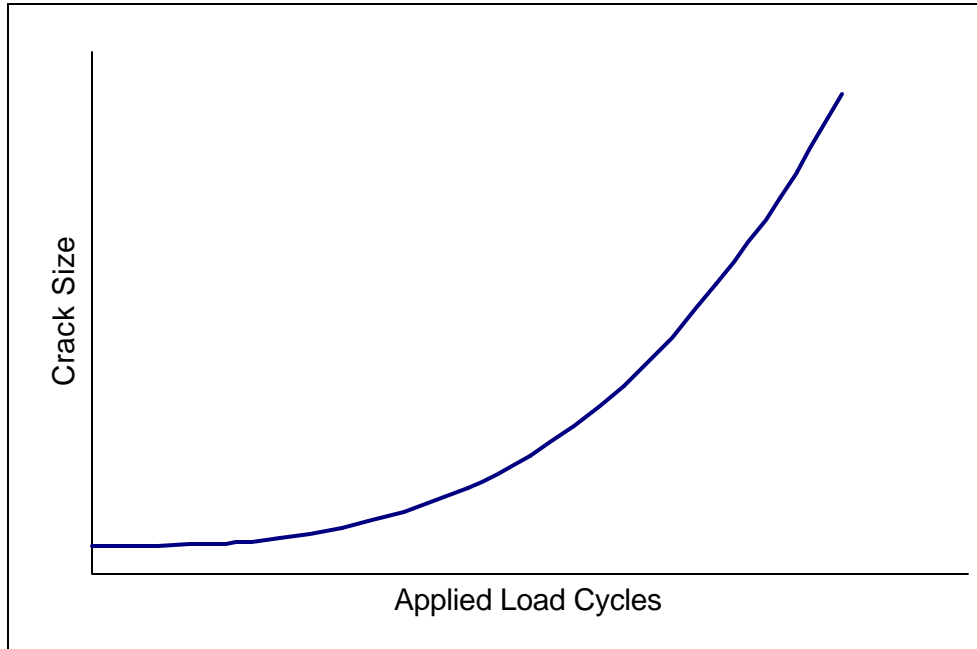


1.3 The Damage Tolerance Approach

The damage tolerance approach is based on three interconnected principles that, when combined, have proven very effective at ensuring the structural integrity of aircraft structures.

- 1) Crack Propagation: The damage tolerance approach assumes that there are pre-existing cracks in the structure. Figure 1-4 schematically shows a crack growth diagram, which shows the crack length dependency on applied load cycles. The basis for this diagram is the assumption that initial cracks, due to manufacturing or material flaws, start growing on the very first load application. Subjected to cyclic loading, the crack will grow, slowly at first and more rapidly as the crack length increases, until the critical crack length is reached, resulting in rapid propagation and fracture.

FIGURE 1-4
SCHEMATIC CRACK GROWTH CURVE



- 2) Residual Strength: When cracks are present in the structure, the maximum load, or stress, that the structure can carry is reduced. A residual strength diagram is shown schematically in Figure 1-5. This figure shows the inverse relationship between crack length and maximum load that the cracked structure can sustain prior to failure. Figure 1-5 shows that for no defects, the structure can sustain the design limit stress. However, as the crack propagates because of applied cyclic loads, the maximum stress that the structure can sustain decreases to the point where the structure can no longer carry the design limit stress. The crack length at this point is called the critical crack length. The crack growth diagram (shown in Figure 1-4) and the residual strength diagram (shown in Figure 1-5) can be combined to show the residual strength dependency on applied load cycles, as shown in Figure 1-6.

FIGURE 1-5

SCHEMATIC DIAGRAM OF ALLOWABLE STRESS VS. CRACK LENGTH

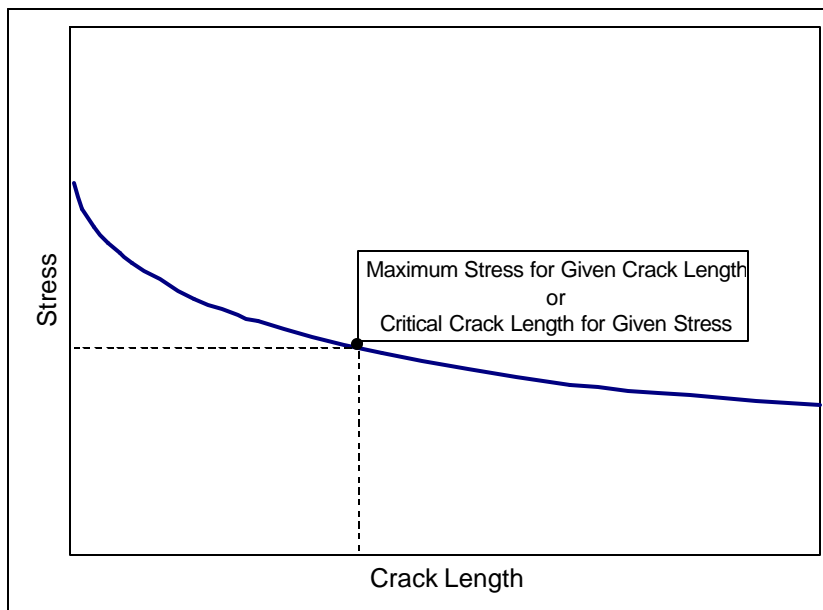
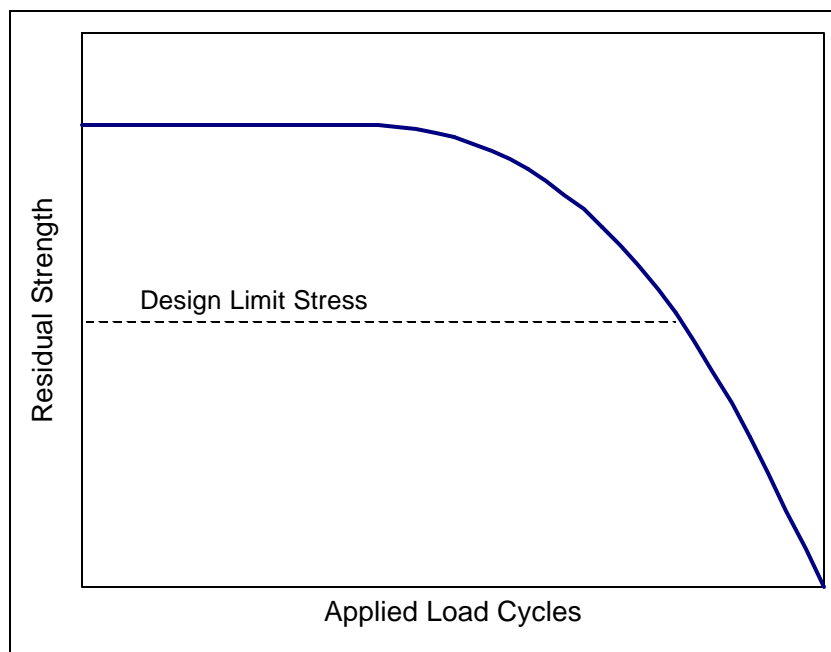


FIGURE 1-6

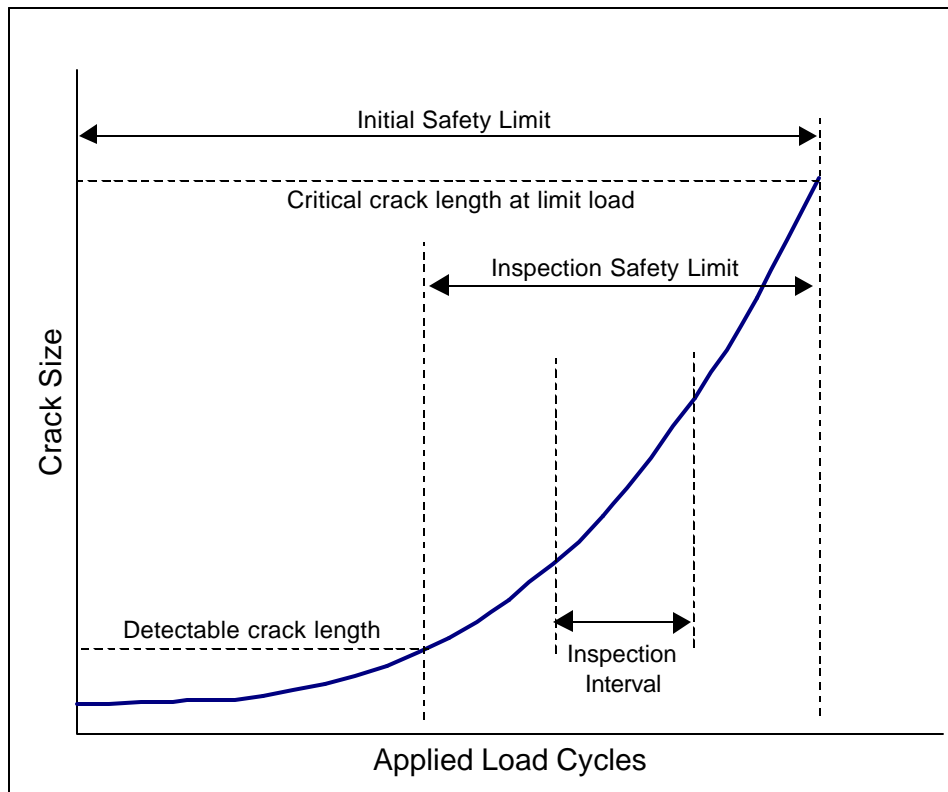
RESIDUAL STRENGTH AS A FUNCTION OF APPLIED LOAD CYCLES



3) Inspections: The information from the residual strength analysis combined with the crack growth information is used to determine the inspection program for a given structural detail. The objective of the inspection program is to detect any cracking that is occurring before the cracks reach the critical length when the structure can no longer withstand the design limit stress. The initial safety limit is the time for the initial flaw to grow to critical crack length. The initial inspection is a fraction of the initial safety limit. The inspection safety limit is the time for a nondestructive inspection detectable flaw to grow to critical crack length. The inspection intervals are chosen as fractions of the inspection safety limit. This ensures that multiple inspection opportunities exist to find the cracks before they reach critical length. Figure 1-7 schematically shows the crack growth curve with the detectable and critical crack sizes and the resulting inspection interval. The trade-off between inspection methods and intervals determines the economic feasibility of the inspection program. Using expensive nondestructive evaluation (NDE) techniques to find short cracks allows for longer inspection intervals, while the less expensive visual inspections only detect longer cracks, and therefore reduce the inspection intervals.

FIGURE 1-7

SCHEMATIC FOR DETERMINING INSPECTION INTERVALS



1.4 The Supplemental Inspection Document Development Handbook

The previous sections illustrate the need for a supplemental inspection program for aging commuter aircraft, as well as the potential for disaster if the structural integrity of aging aircraft is not assured.

The supplemental inspection document development handbook is intended to provide operators of aging commuter aircraft with guidance in the preparation of a SID. The handbook is not intended to be a stand-alone document. Numerous references are provided for detailed information on the disciplines of stress analysis, loads analysis, and fracture mechanics. To this end, this document is divided into the following sections.

- Introduction

Section 1 provides a synopsis of the aging aircraft structural integrity and damage tolerance background and the motivation for requiring supplemental inspection programs for aging commuter aircraft.

- Damage Tolerance Evaluation

Sections 2 through 9 provide the methodology for the damage tolerance evaluation. Section 2 presents an overview of the damage tolerance evaluation process. The evaluation process can be accomplished in three phases:

Phase 1 Data Collection: Gives procedures for locating required data including identification of critical areas, material properties, and defining aircraft usage.

PSE Identification and Classification Section 3

Material Properties Section 4

Define Aircraft Utilization Section 5

Phase 2 Damage Tolerance Analysis: Outlines the development of stress spectra and the various damage tolerance analyses that are to be performed (load spectra development, stress spectra development, determination of initial flaw sizes, determination of crack growth and operational limits, residual strength, fatigue, fail-safe, etc.).

Development of Load Spectrum Section 6

Stress Spectrum Generation Section 7

Damage Tolerance Analysis Section 8

Phase 3 Inspection Requirements: Section 9 provides the guidelines for determining the inspection requirements based on inspection techniques and damage tolerance analysis results.

- SID Development

Section 10 details the steps involved in preparing the supplemental inspection document based on the results of the damage tolerance evaluation.

The data collection and analysis procedures discussed in this document are based on accepted industry procedures. Guidance is provided on the effect of widespread fatigue damage (WFD) on continued operational safety.

2.0 Aircraft Damage Tolerance Evaluation Overview

Before a Supplemental Inspection Document can be written, a damage tolerance analysis of the aircraft structure must be completed. This section provides an overview of the fracture mechanics and crack propagation concepts.

The damage tolerance evaluation can be accomplished in three phases:

- | | |
|---------|---------------------------|
| Phase 1 | Data Collection |
| Phase 2 | Damage Tolerance Analysis |
| Phase 3 | Inspection Requirements |

Each of these phases can be divided into multiple tasks, as depicted in Figure 2-1. Each of these tasks must be accomplished, although not necessarily in the order depicted in the figure. Each phase is described in more detail in the following subsections.

Definitions of terms used in this handbook are presented in Table 2-1. These terms have been established in Advisory Circulars AC 91-MA and/or AC 25.571-1C and are consistently used throughout the remainder of this document.

2.1 Phase 1 - Data Collection

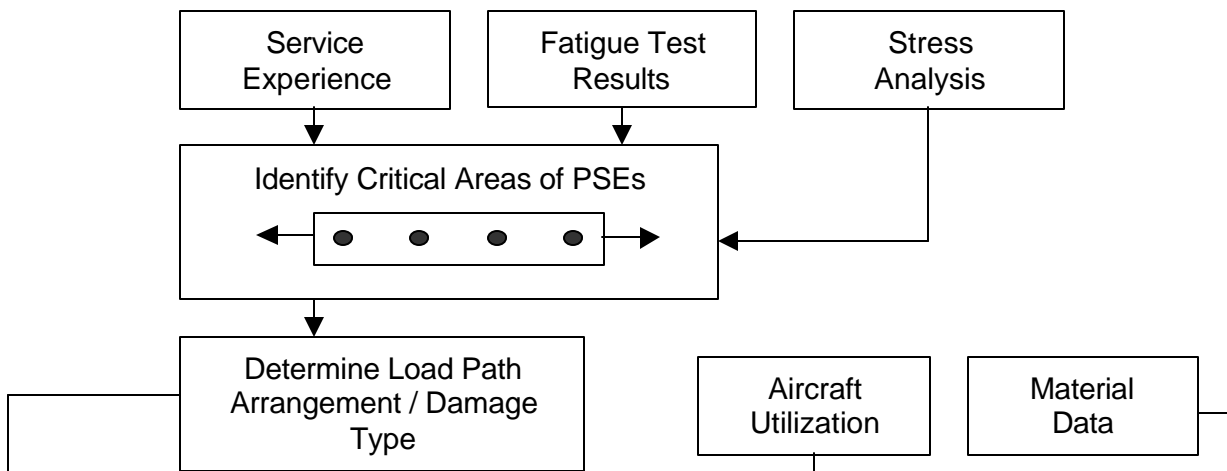
The first phase of the damage tolerance evaluation is to collect data about the aircraft structure, the type and extent of potential damage and how the aircraft is utilized in day to day operations. The steps in the data collection phase are:

- 1) Identification of the Principal Structural Elements (PSEs) for Evaluation. Damage tolerance analyses are usually practical for most of the aircraft structure. Therefore, the entire airframe needs to be examined to identify the principal structural elements (PSEs). Section 3.1 identifies what aircraft structure should be classified as PSEs.
- 2) Identification of the Critical Areas of the PSEs. Once a structural element has been classified as a PSE, the critical areas of the PSE need to be identified. The critical areas should cover the possible failure sites. For some components this may be one or two sites if the perceived risk of failure is low, or it may cover many sites if the perceived risk is high. Selecting the critical areas of the PSE is discussed in Section 3.2.

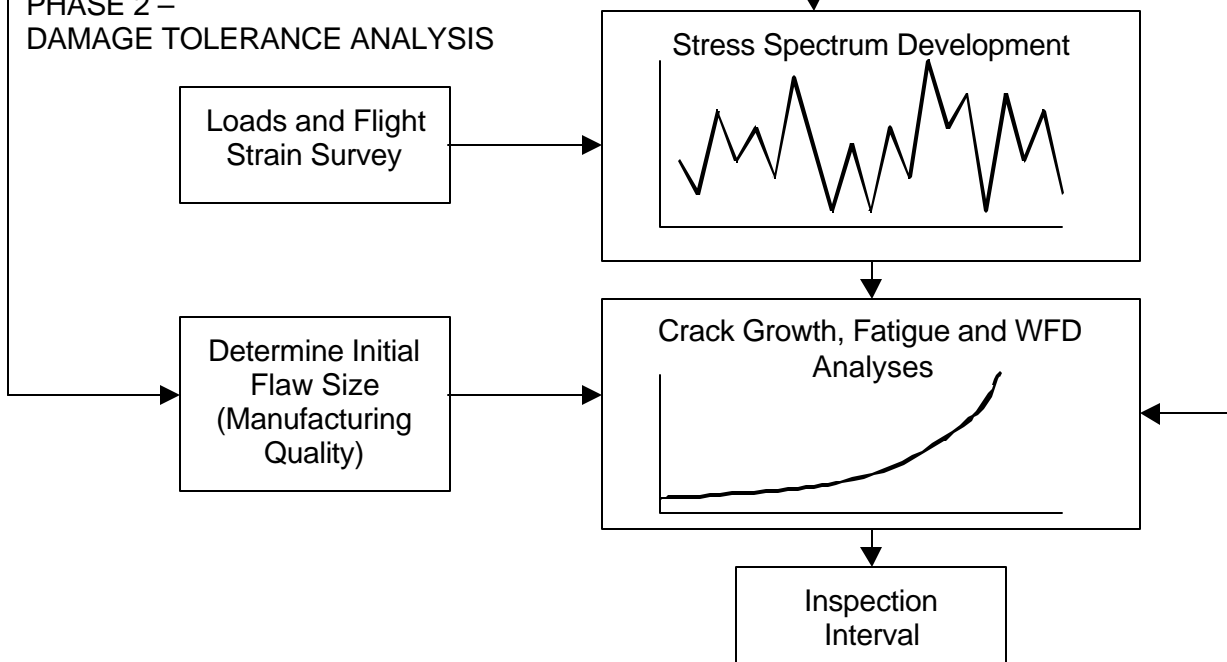
FIGURE 2-1

REQUIRED EVALUATION TASKS

PHASE 1 –
DATA COLLECTION



PHASE 2 –
DAMAGE TOLERANCE ANALYSIS



PHASE 3 –
INSPECTION REQUIREMENTS

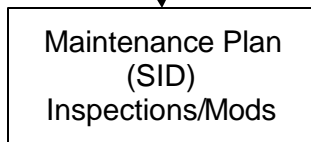


TABLE 2-1

BASIC DEFINITIONS

Damage Tolerance: Damage tolerance is the attribute of a structure that permits it to retain its required residual strength for a period of use after the structure has sustained a given level of fatigue, corrosion, accidental or discrete source damage.

Principal Structural Element (PSE): A PSE is an element that contributes significantly to carrying flight, ground or pressurization loads, and whose integrity is essential in maintaining the overall structural integrity of the airplane.

Fail-Safe: Fail-safe is the attribute of the structure that permits it to retain its required strength for a period of unrepaired usage after the failure or partial failure of a PSE.

Safe-life: Safe-life of a structure is that number of events such as flights, landings, or flight hours, during which there is a low probability that the strength will degrade below its design ultimate value due to fatigue cracking.

Single Load Path: Single load path is where the applied loads are eventually distributed through a single member, the failure of which would result in the loss of the structural capability to carry the applied loads.

Multiple Load Path: Multiple load path is identified with redundant structures in which (with the failure of individual elements) the applied loads would be safely distributed to other load carrying members.

Widespread Fatigue Damage (WFD): Widespread fatigue damage in a structure is characterized by the simultaneous presence of cracks at multiple structural details that are of sufficient size and density whereby the structure will no longer meet its damage tolerance requirement (i.e., to maintain its required residual strength after partial structural failure).

Multiple Site Damage (MSD): Multiple site damage is a source of widespread fatigue damage characterized by the simultaneous presence of fatigue cracks in the same structural element (i.e., fatigue cracks that may coalesce with or without other damage leading to a loss of required residual strength).

Multiple Element Damage (MED): Multiple element damage is a source of widespread fatigue damage characterized by the simultaneous presence of fatigue cracks in adjacent structural elements.

Scatter Factor: A life reduction factor used in the interpretation of fatigue analysis and test results.

- 3) Determination of the Structural Category for Each Location. After identifying the critical areas of each PSE, the next step is to determine the structural category of each of these areas. The structural category determines the type of analysis that must be conducted. Fatigue, damage tolerance and/or residual strength analyses must be conducted depending on the type of structure. For those structural elements requiring damage tolerance assessment, the load path structure must also be evaluated. Single load path structure poses a greater risk than does multiple load path structure. Then again, multiple load path structure has more potential sites for a failure to occur than does single load path structure. Section 3.3 discusses structural categories and load path arrangement.
- 4) Determination of the Type and Extent of Potential Damage. The fourth step is to decide the type and the extent of damage that should be considered for each location. The questions that must be asked include: Where are the most likely crack origins?, and, Should more than one crack at a time be considered? Manufacturing processes and environment as well as load path arrangement and material properties should be considered. Also routine damage such as dents and scratches occurring during routine operation of the airplane must be assessed. Section 3.4 discusses the type and extent of damage that must be considered.
- 5) Identification of Material Properties. The material that each principal structural element is made of is also an important consideration. Mechanical material properties for each PSE must be identified. In addition, some of the alloys used in aging aircraft have special problems that must be taken into account. The materials chosen to design airplanes in the 1960's and 1970's were chosen with an emphasis on static strength criteria. In order to save weight, higher static strength materials were chosen to allow for higher design stresses. However, these stronger materials are typically poorer in their resistance to both crack growth and corrosion. The material properties that must be determined and any special considerations are addressed in Section 4.
- 6) Determination of Aircraft Usage. The first five steps of the data collection phase are interrelated. The sixth and final step is independent of the previous five steps, but just as important. To conduct a damage tolerance analysis, the typical aircraft usage must be determined. Data must be collected about the length of typical flights, the environment in which the aircraft is flown and what the typical payloads are. Section 5 addresses aircraft utilization.

2.2 Phase 2 - Damage Tolerance Analysis

After the data described in Section 2.1 has been collected the damage tolerance evaluation can be conducted. The damage tolerance analysis will establish:

- 1) The time to first inspection and the repeat inspection interval (or safe crack growth life for single load path structure)
- 2) The ability of the structure to arrest isolated fractures (fail-safety)
- 3) The retention of fail-safety over the economic life of the airframe (continued airworthiness)

The best method for demonstrating compliance with the damage tolerance criteria is to conduct testing. Testing is expensive, however, and also subject to other constraints such as time and the availability of equipment. Therefore, analysis is used to cover many aspects of the damage tolerance evaluation. Analysis, though, is subject to modeling error and must be validated by comparison with test results.

The damage tolerance analysis must be completed in several steps as shown in Figure 2-1. The first step is to make a reliable estimate of the number of load cycles required to propagate a crack from the minimum detectable size to the critical size. The information about the expected service load history is available in the form of a load spectrum. Section 6 presents the development of the load spectrum.

After the load spectrum is established, the load spectrum must be converted to a stress spectrum in order to establish crack growth rates. The conversion is usually based on a stress analysis of the airframe for the straight and level flight condition or a flight strain survey. Section 7 discusses the development of the stress spectrum.

After the stress spectrum has been developed for a critical location on the PSE, various damage tolerance and fatigue analyses need to be performed. These analyses are presented in Section 8.

2.3 Phase 3 – Inspection Requirements

The final step before writing the SID document is to determine the airframe inspection requirements. Section 9 presents the inspection requirements. The objective of this section is to (1) explain the nondestructive inspection methodology, (2) provide guidance in determining the inspectable fatigue crack lengths for each actual location and (3) define the inspection technique.

3.0 PSE Identification and Classification

The first steps in the data collection phase involve identification of the principal structural elements (PSEs) and determination of the critical areas of each PSE. Once the critical areas of the PSEs have been determined, the structural category of each PSE and the type and extent of potential damage to the PSE are determined. These first four steps of the data collection phase are discussed in the following subsections.

3.1 Identification of the Principal Structural Elements (PSEs) for Evaluation

The first step in the data collection phase is to review the entire airframe to identify the principal structural elements (PSEs).

Typical examples of such elements are presented in Table 3-1, which is taken from Paragraph 6d of Advisory Circular AC 25.571-1C. Figure 3-1 shows a hypothetical example based on the table. Some of the items shown in the figure are obvious. Others are not so obvious and could be classified differently by different manufacturers depending on the flight characteristics and airframe configuration of a specific airplane. Landing gear and their attachments as well as engine support structure are PSEs. Principal structural elements in the wing and empennage are discussed in further detail in Section 3.1.1, while Section 3.1.2 addresses principal structural elements in the fuselage.

3.1.1 Wing and Empennage

It is customary to design the airplane aerodynamic surfaces (i.e., the wing, vertical stabilizer and horizontal stabilizers) using a box beam structure, which is a construction of thin skins, webs and caps/stringers. A typical wing is shown in Figure 3-2 as an example of this type of construction. These aerodynamic surfaces transmit the airload to the central attachment in the fuselage. Fittings or splices attach the wings and the stabilizers to the fuselage and therefore carry the majority of the flight loads. These attachments are critical and must be considered as PSEs.

The box beam of the wing structure bends due to the airload and twists because the center of pressure is offset from the elastic axis. Therefore, the upper portion of the wing is normally in compression, the lower wing is in tension and the skins and webs are in shear (Figure 3-3). Since the lower panel of the wing carries the tension due to bending, a failure of the panel could separate the wing from the aircraft. Thus, the lower surface of the wing is an obvious PSE.

TABLE 3-1

TYPICAL EXAMPLES OF PRINCIPAL STRUCTURAL ELEMENTS (PSEs)

WING AND EMPENNAGE:

Control surfaces, slats, flaps, and their mechanical systems and attachments (hinges, tracks and fittings);
Integrally stiffened plates;
Primary fittings;
Principal splices;
Skin or reinforcement around cutouts or discontinuities;
Skin-stringer combinations;
Spar caps; and
Spar webs.

FUSELAGE:

Circumferential frames and adjacent skin;
Door frames;
Pilot window posts;
Pressure bulkheads;
Skin and single frame or stiffener element around a cutout;
Skin and or skin splices, under circumferential loads;
Skin or skin splices, under fore and aft loads;
Skin around a cutout;
Skin and stiffener combinations under fore-and-aft loads;
Door skins, frames and latches; and
Window frames.

LANDING GEAR AND THEIR ATTACHMENTS

ENGINE SUPPORT STRUCTURE AND MOUNTS

FIGURE 3-1

TYPICAL EXAMPLES OF PRINCIPAL STRUCTURAL ELEMENTS (PSEs)

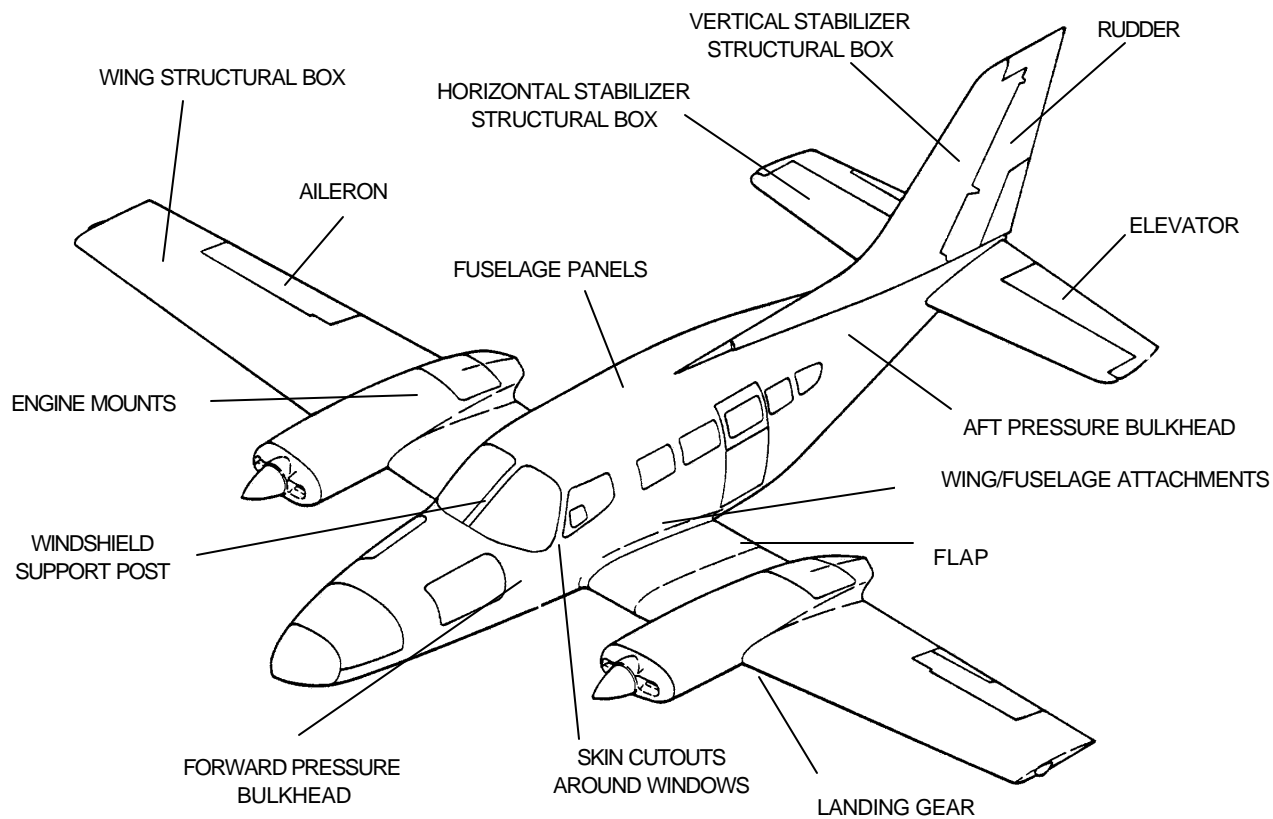


FIGURE 3-2

TYPICAL WING BOX STRUCTURE

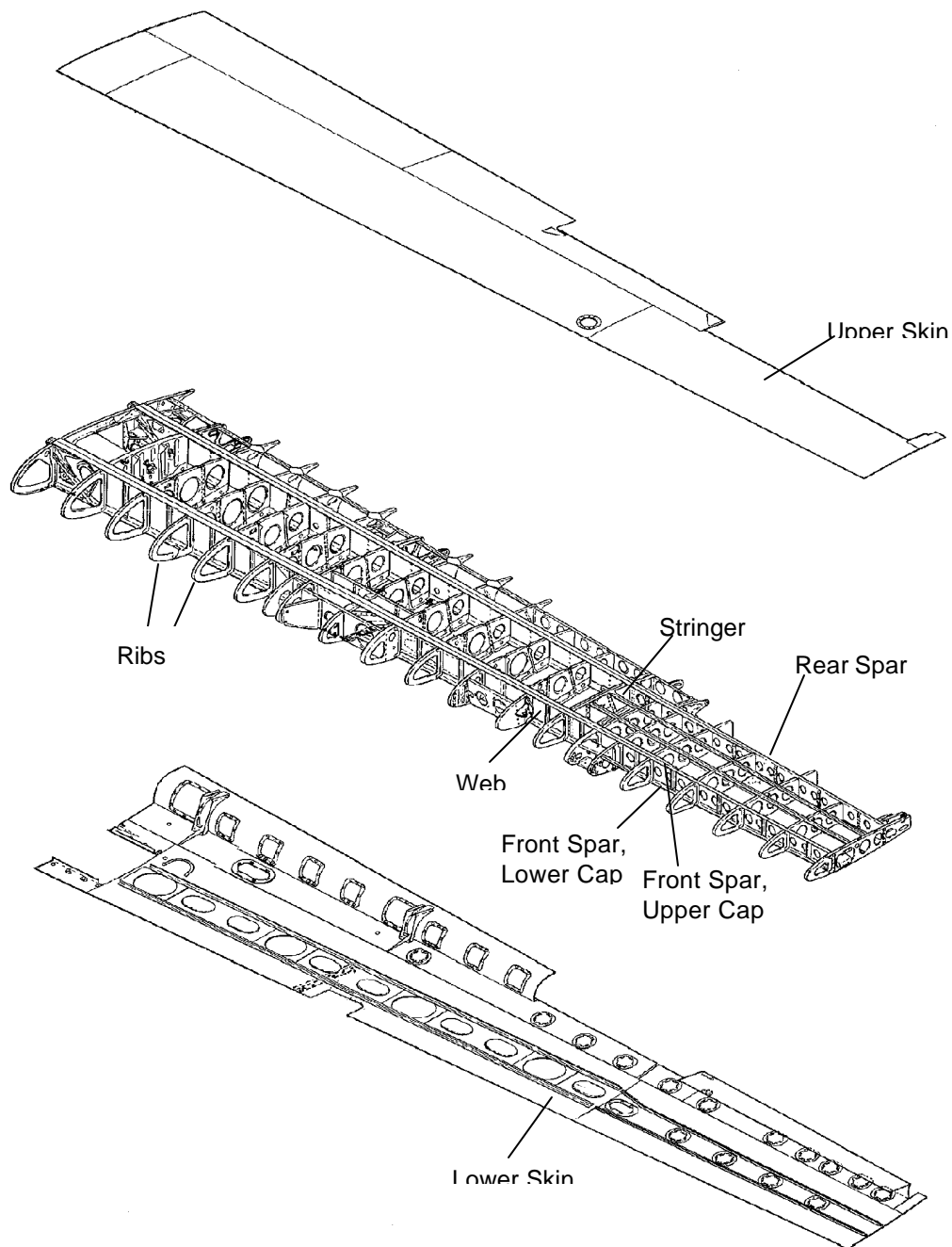
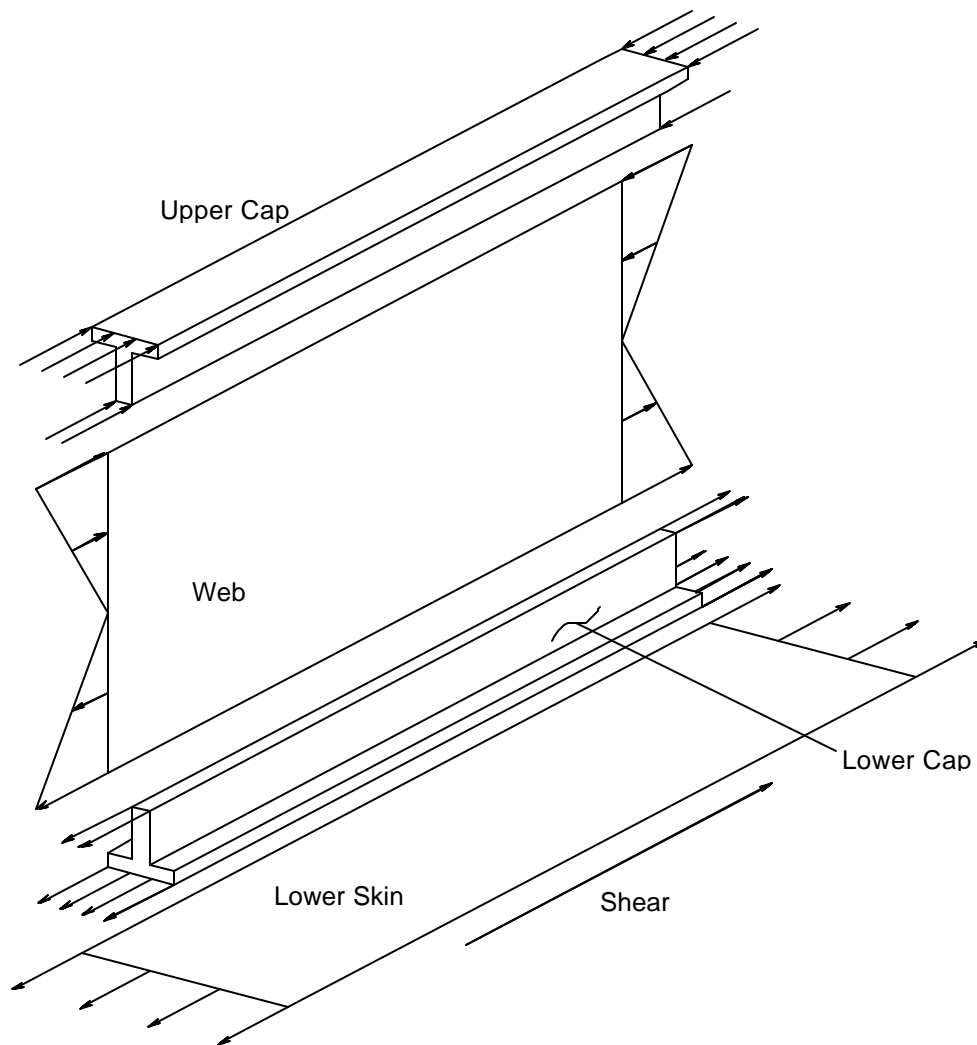


FIGURE 3-3
STRESSES IN WING SPAR

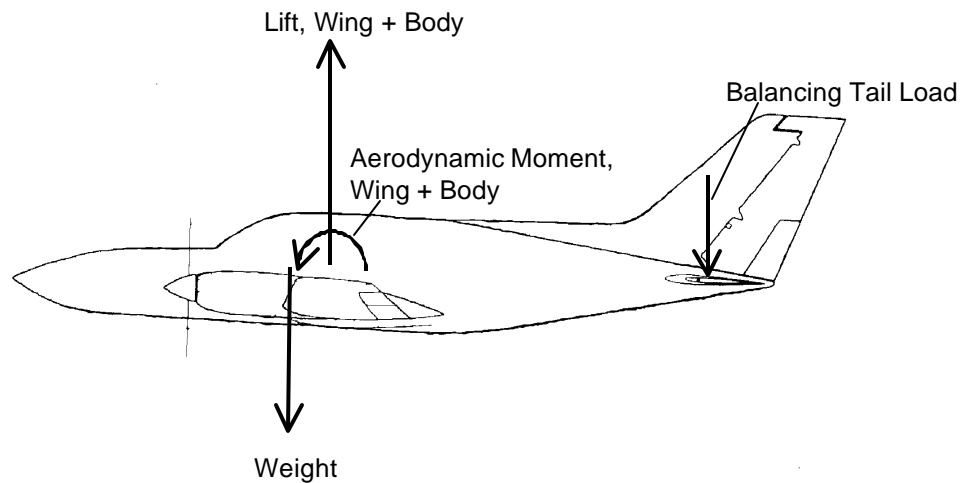


Any unique features of the wing, such as tip tanks, must also be considered. When large weights such as tip tanks are concentrated at the wing tip, the upper surface near the tip may be critical in tension. In this situation, the outboard tip of the upper wing is a PSE.

The horizontal stabilizers also sustain bending loads. In level flight, they are normally under down load to maintain pitch trim (Figure 3-4), therefore, the upper stabilizer surface may be critical. Loss of one side of the horizontal stabilizer would cause an immediate nose-down pitch and could put the aircraft into an unrecoverable dive. Thus the horizontal stabilizer is a PSE.

FIGURE 3-4

AIRPLANE IN BALANCED FLIGHT



Failure of the vertical stabilizer may or may not cause the loss of an aircraft. It depends upon the specific aircraft configuration and characteristics. Thus the vertical stabilizer needs to be investigated to determine whether it should be classified as a PSE.

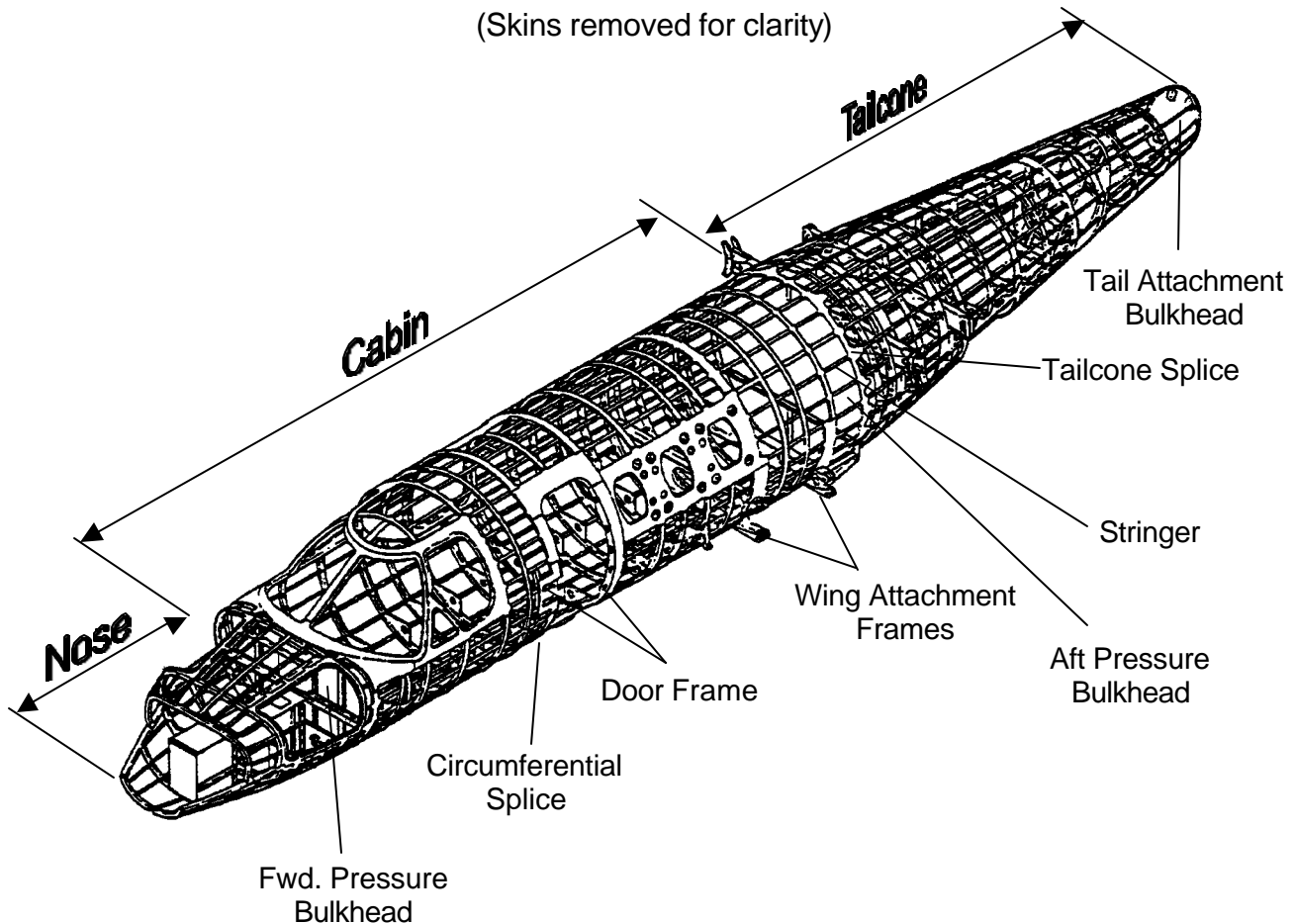
Control surfaces may be PSEs. Elevators are PSEs. Like the vertical stabilizer, the rudder may or may not be a PSE depending upon the specific aircraft configuration. Flaps, slats, spoilers and ailerons are most likely PSEs, however, the decision needs to be based on the specific type of control system. In general, if the airplane would be lost when a specific control surface fails, then that control surface must be classified as a PSE.

3.1.2 Fuselage

Typically, the fuselage of an aircraft is a stiffened shell commonly referred to as semi-monocoque construction. The fuselage is made up of longitudinal elements (longerons and stringers), transverse elements (frames and bulkheads) and skin. Figure 3-5 shows an example of this type of construction. The longerons and the stringers carry the major part of the fuselage bending moment from the applied external loads. The skin carries the shear from the external loads and cabin pressurization. Frames primarily serve to maintain the shape of the fuselage and to reduce the column length of the stringers to prevent instability. Heavier frames or bulkheads are provided at points with concentrated forces such as those from the wing, empennage, and landing gear.

FIGURE 3-5

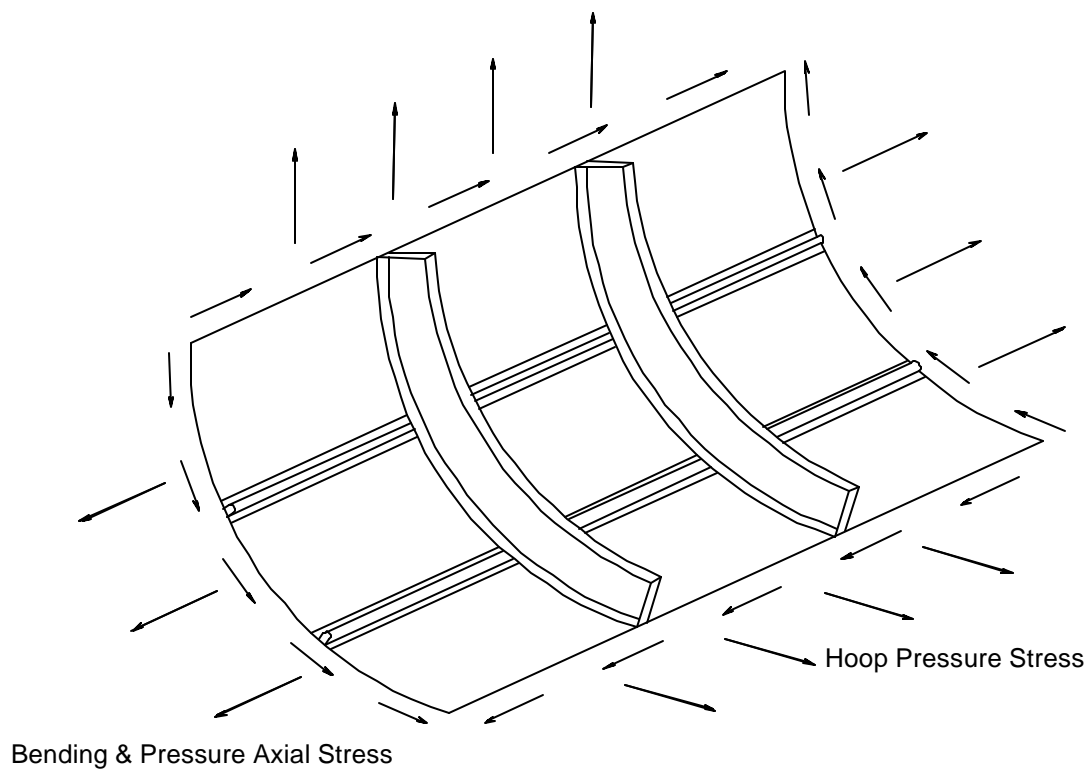
TYPICAL SEMI-MONOCOQUE FUSELAGE CONSTRUCTION



In flight, fuselages are normally subjected to down bending loads due to the combination of the horizontal stabilizer balancing tail load and the upward acting load on the wing. This combination of loads puts the upper portion of the fuselage in tension and the lower portion in compression. Also, in pressurized aircraft, the fuselage is in hoop tension due to the pressure loading. Figure 3-6 shows the stress on a typical section of the fuselage due to pressurization and bending loads.

FIGURE 3-6

STRESSES ON FUSELAGE SHELL

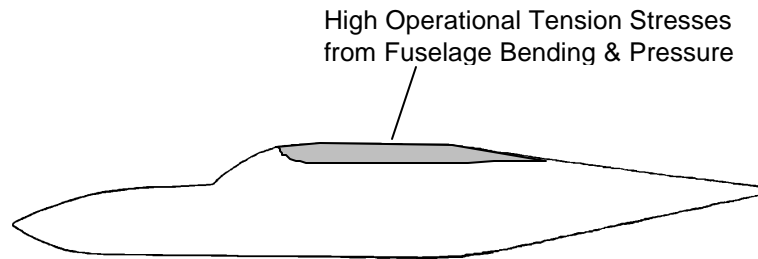


In pressurized aircraft, the hoop stress due to pressurization is usually the largest contributor to the stress on the fuselage. However, on the fuselage crown near the wing attachments, the stress due to bending can approach the magnitude of the stresses due to pressurization. This part of the crown is usually designed with some reinforcement to accommodate the transfer of loads between the wing and fuselage. At other locations along the fuselage, the stress decreases fore and aft of the wing attachments, and the tension stress caused by the downbending load decreases below the crown changing to compression in the lower half of the fuselage. Most of the pressurized fuselage structure (including skins, frames, stringers and longerons) should be classified as a PSE, with particular attention

given to the crown section, especially in the region of the wing attachments (Figure 3-7).

FIGURE 3-7

FUSELAGE POTENTIAL FATIGUE CRITICAL AREA



In non-pressurized aircraft, the longitudinal stringers and longerons that stiffen the skin of the fuselage carry the bending loads associated with flight. Since downbending is normally experienced by a fuselage during flight, the longitudinal stringers, longerons and skin in the upper portion of the fuselage are normally PSEs. In addition, each frame/bulkhead should be reviewed to determine if it should be a PSE. Most of these would not be classified as a PSE because they don't contribute significantly to carrying fuselage flight loads. However if the frames/bulkheads were subjected to additional loads (such as wing loads near the wing attachment points) these frames would require PSE designation because their failure could lead to a catastrophic failure of the airframe (Figure 3-5).

In pressurized aircraft, forward and aft pressure bulkheads exist to contain the pressurized cabin volume. These bulkheads in small transport and commuter aircraft are usually flat bulkheads stiffened by vertical and horizontal beams (Figure 3-5). All of the bulkhead structure are PSEs because of their major significance in carrying cabin pressurization loads.

Fuselage splices are also classified as PSEs for both pressurized and non-pressurized aircraft (Figure 3-5). Fuselages are designed with skin splices for ease in manufacturing. Circumferential joints are generally designed as butt splices over reinforced frames. Longitudinal joints are generally located over stringers and may be designed as either reinforced butt splices or lap splices. These fuselage splices fall under the definition of a PSE because their failure could result in catastrophic failure of the airframe.

Door, windshield, and window cutout support structure (Figure 3-5) are all PSEs in both pressurized and non-pressurized aircraft. This structure carries the loads

around the cutouts due to the bending and torsion of the fuselage. In addition, the frames, posts, lintels, and sills that make up this support structure carry bending loads due to the pressure acting on either the doors or windows. In the skin itself, the cutout acts as a stress riser. Stress concentrations at the corners of door and window cutouts have a major influence on the damage tolerance of the skin. Additional stiffeners and doublers are often placed around the cutout corner in the skin. Therefore, the corners of door and window cutouts should be included among the sites selected for evaluation of fuselage PSEs.

3.2 Select Critical Locations of PSEs for Evaluation

After determining the principal structural elements (PSEs) of the aircraft under consideration, the second step of the data collection phase is to identify the critical areas of each PSE. A critical area of a PSE is one that will require specific action such as special inspections, repair and/or modifications in order to maintain continued airworthiness during the desired operational life of the aircraft.

Several different approaches and factors should be considered when identifying the critical areas of each PSE. Detailed geometry, material information, service experience data, stress analysis, and static and fatigue test results are required to determine the critical locations. The following selection criteria, based on Reference 4, should be used to determine the critical areas for further analysis of each of the selected PSEs.

- 1) Detailed geometry. The aircraft geometry defined on drawings and/or an actual airplane should be reviewed to find:
 - Locations with high stress concentrations. Particular attention should be given to areas where several surfaces intersect such as in forgings. These areas are prone to accidental damage.
 - Locations in structural details that are prone to cracking such as fillets and fastener holes.
 - Areas that are difficult to inspect.
 - Areas that are prone to corrosion.
 - Areas that are susceptible to impact or accidental damage.
- 2) Material Information. Specific areas of concern are locations in materials where crack propagation rates are high and fracture toughness values are low. The methods to obtain the required material information are discussed in Section 4.
- 3) Service Experience Data. Locations that cracked during service operation are obvious areas for further evaluation. Areas that are subject to accidental

damage or prone to corrosion may also be identified through service experience data. Methods of obtaining service experience data are discussed in Section 3.2.3.

- 4) Stress Analysis. Finite element models should be developed (if these don't already exist) for each of the PSEs. The development of the models is discussed in Section 3.2.1. After completion of the finite element model:
 - A review of the model, and other existing stress analyses, should be made to determine areas subjected primarily to tension and shear loading, with low static margins.
 - An analysis should be conducted to determine the locations where stresses would be high in secondary members after primary member failure. This is particularly necessary for those areas not inspectable for less than primary member failure (see Section 3.3). In this case the inspection periods will depend on the life of the secondary member under redistributed loads after primary member failure.
- 5) Fatigue and Static Test Results. The results from static and fatigue tests should be reviewed. Test results are discussed in Section 3.2.2. Areas of specific concern are:
 - Locations that cracked on full-scale or component fatigue tests.
 - Locations that failed during static testing.
 - Locations of high spectrum severity. These locations should be reviewed not only for areas of high 1g stress but areas where a large number of cycles may occur each flight. For example, flap support structure is usually subjected to aerodynamic buffeting loads that may occur thousands of times per flight.

For small transport and commuter aircraft the number of candidate areas will be on the order of 40 to 70. This number is usually paired down to about 20 to 30 by similarity of elements for a more detailed analysis. This number varies depending on aircraft type but is not necessarily a function of aircraft size since all aircraft have the same major features.

To determine the critical areas of the principal structural elements the above criteria should be applied. More detailed information required by the criteria is presented in the following sections:

Section 3.2.1 Finite Element Models

Section 3.2.2 Fatigue and Static Test Results

Section 3.2.3 Service Experience

3.2.1 Finite Element Models

Finite element models (FEMs) should be developed for the aircraft under consideration. The FEM is a powerful computer tool for determining stresses and deflections in a structure that is too complex for classical analysis. These models can be used to establish internal loads and stresses in airframe components and to identify critical areas of PSEs. Finite element models should be developed for the following components:

- Wing and carry-through structure (including flaps and ailerons)
- Fuselage (including nose and tailcone)
- Engine beam and engine support fittings
- Horizontal stabilizer and elevator
- Vertical fin and rudder
- Nose and main landing gears

Finite element analysis seeks to approximate the behavior of an arbitrarily shaped structure under general loading and constraint conditions with an assembly of discrete finite elements. The first step is the construction of a structural model that breaks a structure into simple shapes or elements located in space by a common coordinate system. The coordinate points, or nodes, are locations in the model where output data are provided. For aircraft aerodynamic surfaces (wing and stabilizers), these locations are typically at the intersections of webs, ribs, skin, spars, and stringers. Basically, FEM geometrically divides a structure into small elements with easily defined stress and deflection characteristics. The behavior of the structure is obtained by analyzing the collective behavior of the small elements.

FEMs typically use the displacement method to solve for the structural response to the applied loading. Known forces are applied to the model and displacements due to the known forces are calculated. The basic stiffness equation that finite element methods use to solve for displacements is:

$$\{F\} = [k] \{u\}$$

where: $[k]$ = the elemental stiffness matrix

$\{F\}$ = vector of forces (known)

$\{u\}$ = vector of unknown displacements resulting from $\{F\}$

The individual element's stiffness matrix is usually calculated with the geometry and material properties of that element. Each type of element has its own elemental stiffness matrix. Stiffness matrices for more complex elements are determined using procedures based on energy principles.

NASTRAN is one of the finite element programs available today. It is an acronym that stands for NASA STRuctural ANalysis program. This program was developed by NASA in the mid-1960's to handle the analysis of missiles and aircraft structures. Many different vendors sell versions of NASTRAN. Some common ones include:

- MSC NASTRAN (MacNeal Schwendler Corporation)
- CSA NASTRAN (CSAR Corporation)
- Cosmic NASTRAN (Government version)
- UAI NASTRAN
- ESP NASTRAN
- NE NASTRAN

NASTRAN is available on many platforms including mainframes, UNIX based workstations and PCs. Most structural models are small enough to be efficiently run on a Pentium PC.

In addition to NASTRAN, there are many other finite element programs available for use. They fall into two basic categories: (1) conventional "H" element modelers (e.g. NASTRAN, ANSYS, ABAQUS) and (2) "P" element modelers (e.g. PolyFEM, MECHANICA, STRESSCHECK). For "H" element modelers, the stress variation within an element is fixed for a given element type selected by the analyst, and hence details with stress concentrations require the use of many small "H" elements to adequately capture the stress gradients. "P" element modelers use elements that allow the use of higher order polynomials (in some cases as high as a 9th order) to represent the stress variation within a single element. Therefore, "P" element modelers are able to capture even very steep stress gradients without highly refined meshes. The drawback is that "P" element modelers rely on iterative solutions, increasing the order of the polynomials with each pass until the solution converges. Because of their differences in modeling and solution technique, "H" and "P" element solvers are best suited to modeling different types of structural details. "H" element modelers are best suited for analyzing overall airframe structure or large components, where the main interest is obtaining load/stress distributions in the individual components, and structural details such as lightening holes, fillets, etc., are not modeled. Because of their ability to represent very steep stress gradients without relying on large numbers of small elements, "P" element modelers are

ideally suited for analysis of detail parts that have areas of high stress concentrations, such as fittings.

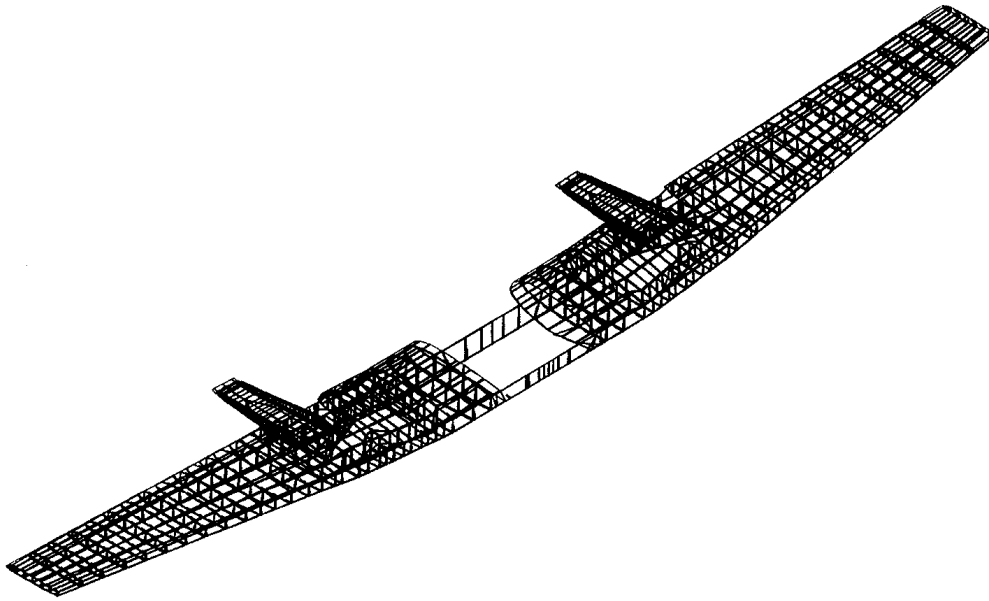
Modeling experience is invaluable to know how to simplify the structure into smaller elements. Accuracy in modeling is critical since the model will be used to establish the critical locations of the PSEs to be evaluated. Some of the things to consider include:

- If a component is modeled inadequately, the areas of maximum strain and deflection predicted by the analysis could be misleading. Modeling inadequacies include the incorrect placement of elements as well as attempting to define a structure with an insufficient number of elements.
- In most cases, the finer the grid, the more accurate the results. However, the computer capacity and time required and therefore the cost of the analysis increases with the number of elements used in the model.
- The efficiency of the analysis can be increased by concentrating elements in the interested areas of high stress while minimizing the number of elements in low stress areas.

When modeling structure, decisions have to be made as to the capabilities of the parts that are to be represented. Tension, compression, bending, membrane, shear, and torsional capabilities of the structure must be known so that the correct element type can be used in the structural model. When modeling an aircraft component like a wing or fuselage, BEAM elements are typically used to represent frames, spar caps and stringers. ROD, BAR, or BEAM elements are used for stiffeners depending on the bending and torsional capabilities of the structure. For spar webs, rib webs and skins, SHEAR elements are used for elements in compression while SHELL or PLATE elements are used for elements in tension. Figure 3-8 shows a sample finite element model of a wing with engine support structure.

FIGURE 3-8

FINITE ELEMENT MODEL OF WING WITH ENGINE SUPPORT

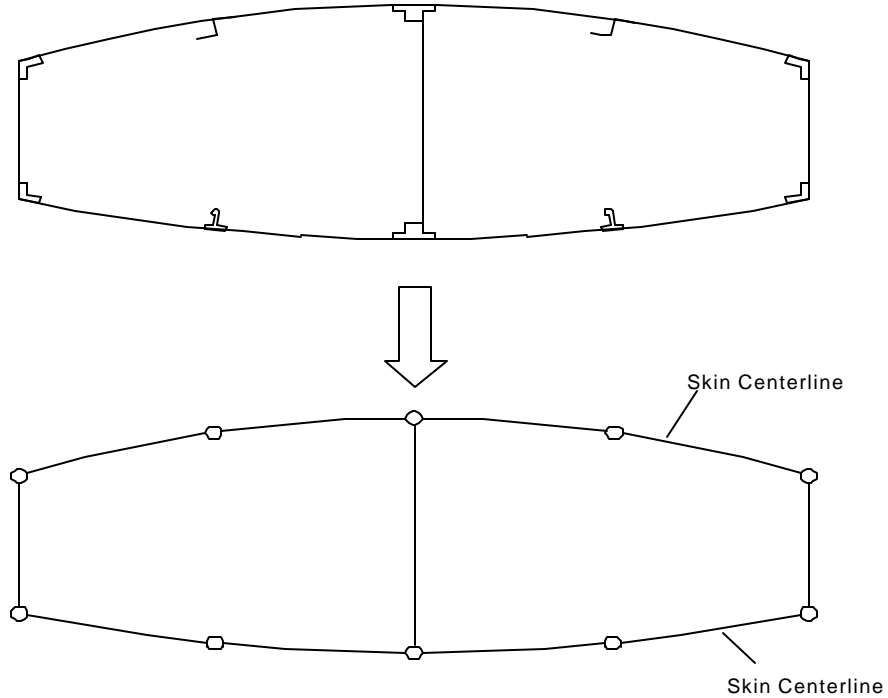


The following items, taken from Reference 5, should be considered when creating a component finite element model:

- A consistent reference system should be used for the placement of nodes, such as at the center line of the skin and web. Nodes should be placed at the intersection of each stringer/spar and rib/web/skin intersection as shown in Figure 3-9.
- Webs or skins with cutouts should be analyzed with elements of equivalent thickness. Methods of calculating equivalent thickness are presented in Reference 5.
- The unbuckled web of a beam in bending will add to the beam stiffness. This is represented by adding the equivalent web area to the area of the beam caps.
- The effective width of the buckled skin (normally $15t$ on each side of the beam cap) should be added to the cap area for members in compression. If the skin is not buckled, the full skin width should be included with the cap area in the model.
- Internal loads, should be used from the finite element model rather than the output stresses.

FIGURE 3-9

FINITE ELEMENT MODEL REPRESENTATION



In addition to models of an entire structural component, detailed models may be required of specific areas. As an example, a detailed model of a splice joint may be required to determine the load transfer at a specific fastener (Figure 3-10). The loads to be applied to the detailed model can be extracted from the internal loads output of a coarse model of the structural component. Detailed models of fittings or forgings may also be required. These models are normally made of SOLID 3-D type elements (Figure 3-11).

FIGURE 3-10

SAMPLE DETAILED FINITE ELEMENT MODEL OF SPLICE

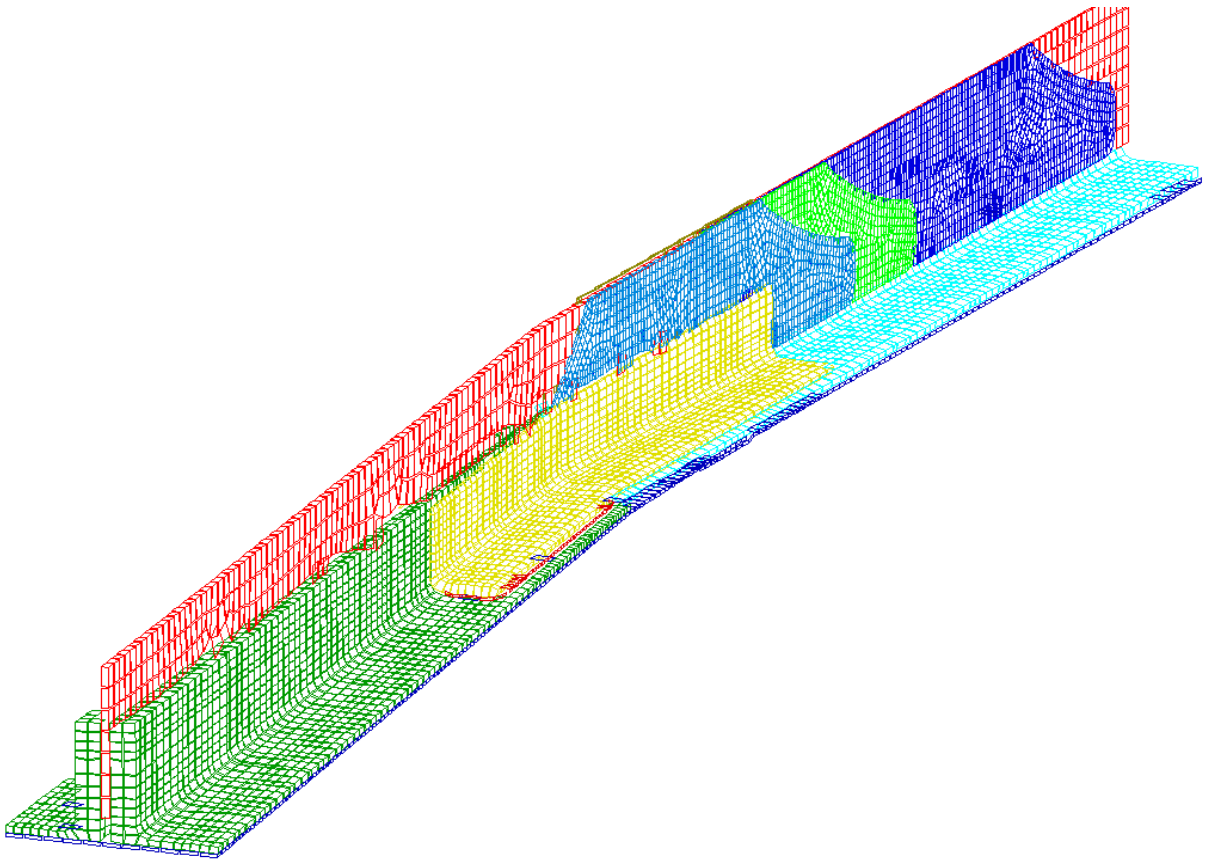
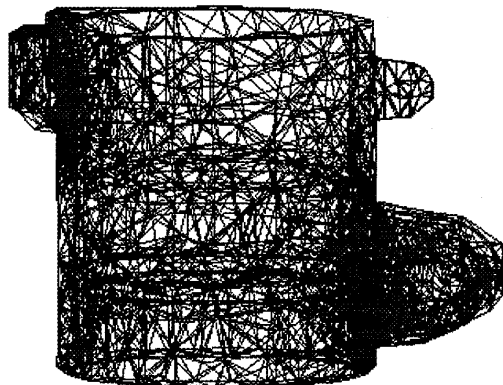


FIGURE 3-11

FORGING FINITE ELEMENT MODEL (3-D)



After completing the finite element models required for the aircraft under consideration, each model must be verified for correct structural representation by comparison with ground or flight test results. Strain gauging is the most common method of obtaining experimental data in structural tests. Bending moment and stress distribution plots are useful in determining if the finite element model truly represents the structure being modeled. If it doesn't, the model needs to be adjusted until loading and stress results reasonably match. Typically the stresses predicted by the finite element model should be within 5-10% of the measured values.

Once a finite element model has been created and verified, the model is useful in designing a structural repair or modification when a structural beef-up or change is required for continuation of safe flight.

3.2.2 Fatigue and Static Test Results

Existing fatigue test results for the aircraft under consideration may show locations that cracked during cyclic testing. This data could come from full-scale cyclic tests or from component cyclic tests. Since cyclic fatigue tests apply loading conditions that represent typical service operation, the locations where cracks developed on test articles can be expected to crack on service aircraft at some point in time.

Static test results should also be reviewed. Locations that failed during static testing are candidates for analytical evaluation. In addition, strain gage data collected during static testing is required to verify finite element models.

If strain gage data is not available from previously conducted tests, then ground testing should be conducted. A component in good condition, perhaps from a salvage yard, can be used to conduct the tests. Strain gages should be placed on the ground test article at the critical locations. The critical load condition (for example, wing maximum positive bending) for the component should be identified and applied to the ground test article. Load should be applied in increments of 20% of the maximum load and strain and load data recorded at each increment. The recorded strain data can be compared to the finite element model evaluated with the same load. The test article can also be used to evaluate the fail-safe capability of the component with a major load-carrying member severed (Section 8.4.2.2).

3.2.3 Service Experience

Service experience can be used to determine which areas of the PSEs are susceptible to fatigue cracking, corrosion, and/or accidental damage. To determine service problems that have been reported in field operations, three sources of information can be used:

- Manufacturer Service Bulletins

- FAA Service Difficulty Records
- Operator Surveys

The manufacturer issues Service Bulletins to correct common service problems discovered during normal operating service or testing. A copy of the service bulletins applicable to a specific aircraft model should be available from the aircraft manufacturer. In addition, a list of the service bulletins will be required for inclusion in the SID document.

Another method of determining structural problems that have occurred in the field is to review FAA Service Difficulty records. These records give a description of the problem, the aircraft serial number and the time in hours when the problem was found. An example of the information found in the Service Difficulty Records is shown in Figure 3-12. A copy of these records can be obtained from the FAA for a specific aircraft model. A review of these records can identify when a structural problem has been experienced by more than one aircraft.

Operator surveys asking to identify any major structural problems with the aircraft under consideration can also be used. A sample survey form that can be included with the usage survey (explained in Section 5.1.1) is shown in Figure 3-13.

FIGURE 3-12

EXAMPLE OF FAA SERVICE DIFFICULTY RECORD

```

CESSNA 402C           S/N: 402C0034      N#: 68PB  ATA: 5710  OPCD:      SEG: 1
CTRL#: 87052800013  DIFFDATE: 03/06/  FSD0: S019 TT: 10650 TSO: 10650 SUB: H
ENGINE:              S/N:              STAGE: INSP/MAINT
PROP:               S/N:              PRECAUTPROC: NONE
PARTNAME: SKIN BOND  P/N: 52220001      COND: OTHER
PART LOCATION: SPAR          PART CONDITION: CORRODED
CMPTMKE:             CMPTMDL:          S/N CMPT:
CORROSION BETWEEN BONDED SKIN AND FORWARD WING SPAR WHERE LEADING EDGE
MEETS CENTER WING PANELS.  CORROSION RUNS FROM OUTBOARD EDGE OF NACELLE TO
WING TIP, ON TOP AND BOTTOM OF WING.  FUEL LEAKS WERE NOTED ALONG LOWER
FORWARD WING SPAR CAP.  CORROSION WAS DETECTED BY EDDY CURRENT INSPECTION.
    
```


FIGURE 3-13

SAMPLE OPERATOR SURVEY - AIRFRAME REPAIRS

INFORMATION NEEDED FOR FATIGUE ANALYSIS	
<p>This form should be filled out for each aircraft in the fleet. The specific information about each individual aircraft is important in developing the history of usage of the aircraft fleet and the structural locations critical with service.</p>	
<u>Aircraft Serial No.</u>	<u>Model</u>
<u>Total Service Time Of Aircraft</u>	<u>hours</u>
	<u>landings</u>
Structural Airframe Repair Comments List the location and description of the repairs made to the primary structure of the aircraft because of longevity of service of the aircraft (not those required routinely to meet airworthiness regulations). Also note any repairs required due to corrosion. This information will be helpful in determining the locations to be included in the fatigue analysis. Please include any information that you think may be helpful to engineers in their analysis. Continue on back of the sheet if necessary.	

3.3 Determination of the Structural Category for Each Location

For determining the analysis requirements, airplane structure can be categorized into one of four different structural categories. Three of the four categories pertain to those structural elements classified as PSEs, while the fourth category applies to secondary structure. These structural categories are shown in Table 3-2. The following paragraphs define each structural category and give an example of each.

TABLE 3-2

STRUCTURAL CATEGORIES

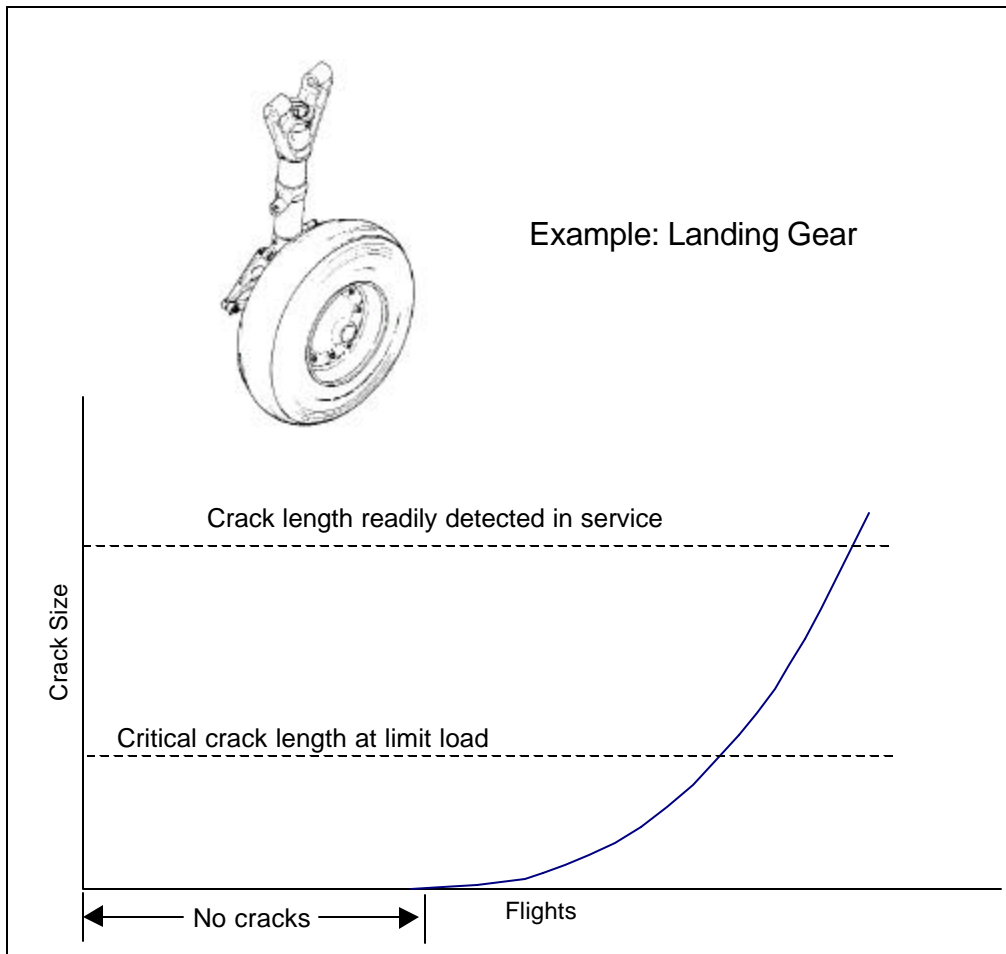
Structural Category				Technique to Ensure Safety	Analysis Requirements	Examples
1	Principal Structural Elements	Safe-Life Design	Safe-Life	Conservative fatigue life	Fatigue	Landing Gear
2		Damage Tolerant Design	Obvious damage evident	Adequate residual strength with extensive damage obvious during walkaround	Residual Strength	Stringer & Skin cracks lead to Fuel Leaks
3		Damage Tolerant Design	Damage found by planned inspection	Inspection program matched to structural characteristics	<ul style="list-style-type: none"> •Crack Growth •Residual Strength •Inspection Program 	All primary structure not included in 1 or 2
4	Other Structure	Damage Tolerant Design	Secondary Structure	Designed for loss of component or safe separation	Continued Safe Flight	Wing Speed Brake

3.3.1 Safe-Life

Safe-life (fatigue) analysis is reserved for those parts for which damage tolerance is impracticable. Engine mounts and landing gear are usually the only parts which should be analyzed as safe-life. For example, a landing gear trunnion is single load path structure that is usually made of high strength steel. High strength materials are usually brittle and have low fracture toughness values. Therefore cracks in high strength materials tend to fail at small crack lengths, many before detection is practical. Safe-life parts will need to have scatter factors applied to the analytical or test derived fatigue life of the part. The reliability goal for safe-life parts is a failure rate of 10^{-9} in a single flight. At the end of the defined safe-life (analytical or test life divided by the appropriate scatter factor) the part must be replaced. Figure 3-14 schematically shows a crack length vs. flight curve for a safe-life part example. The critical crack length is smaller than can readily be detected by inspection.

FIGURE 3-14

SAFE-LIFE PART EXAMPLE



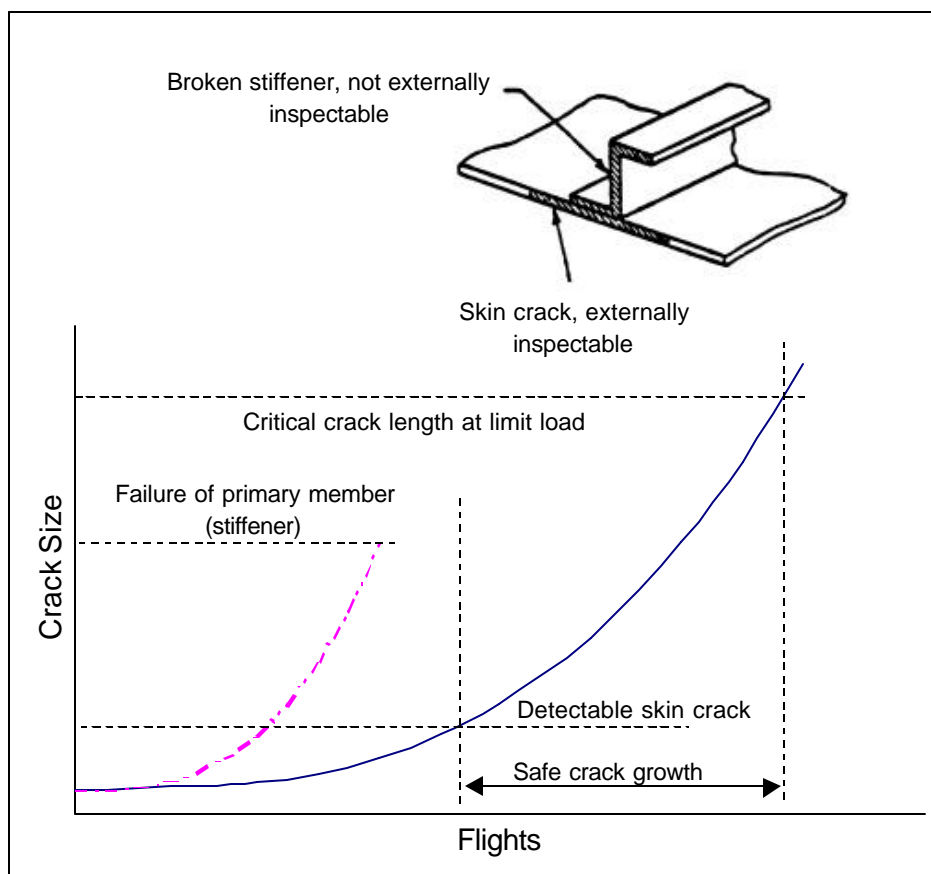
3.3.2 Damage Tolerant - Obvious Damage Evident

The second classification of structure is multiple load path structure with damage that is obvious without detailed inspection. The damage is in-flight evident or ground evident, or can be found by a walkaround inspection. This structure is designed such that a reasonable safe period for inspection is possible, considering skin crack growth after failure of an internal member. An example of this type of structure is a wing, where cracking in the skin would be detected by a fuel leak even though there was a failure of an internal stiffener. This means that a detailed inspection of the internal stiffener, which may require access into the fuel tank in the case of wing structure, or the removal of the interior in the case of the fuselage, will not be necessary. Figure 3-15, taken from Reference 4, illustrates the wing

structure example explained above. Pressure leaks in a pressurized fuselage are another example of how damage can be discovered without detailed inspection.

FIGURE 3-15

DAMAGE TOLERANT – OBVIOUS DAMAGE EVIDENT EXAMPLE



3.3.3 Damage Tolerant - By Planned Inspection

The third classification of structure is principle structural elements which are damage tolerant, and the damage must be found by planned inspection. This category of structure can be broken down into three additional categories:

1. Single load path structure
2. Multiple load path structure – not inspectable for less than load path failure
3. Multiple load path structure – inspectable for less than load path failure

Each of these structural categories are discussed in the following subsections.

3.3.3.1 Single Load Path Structure

Single load path damage tolerant structure is defined as structure with no redundant load paths. Structural safety is maintained with inspections based on a damage tolerance evaluation. Figure 3-16 shows an example of this structural category.

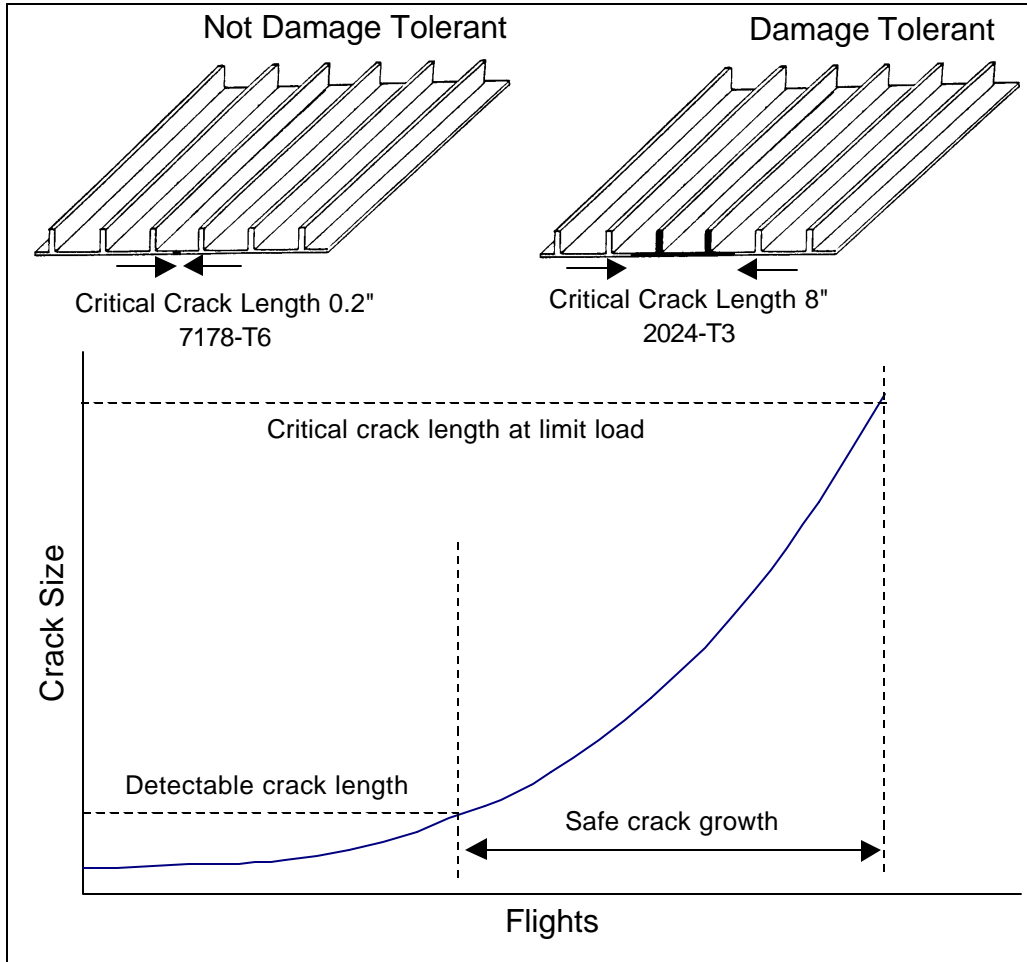
In this example, two materials are used to define single load path damage tolerant structure in an integrated lower wing plank surface. If the material is 2024-T3 aluminum the critical crack size at limit stress may be about 8 inches. It is therefore conceivable that reasonable inspection periods could be planned from a readily detectable crack size to critical crack size. This structure would be considered damage tolerant. However, if the wing plank were made of 7178-T6 aluminum the critical crack size may be only about 0.2 inches at -65° F. This crack is not considered readily inspectable, the damage most likely would not be found by inspection techniques before the critical crack length was reached. Therefore the structure cannot be considered damage tolerant.

3.3.3.2 Multiple Load Path - Not Inspectable for Less than Load Path Failure

Multiple load path structure - not inspectable for less than load path failure is defined as structure designed so that a safe period for inspection is possible after the primary member is completely failed and is detectable. This structural category is used for cases of multiple load path structure for which a crack in the primary member may be too difficult to find without disassembly. However, the structure may be inspectable for complete failure of the primary member. Figure 3-17 shows an example of this category.

FIGURE 3-16

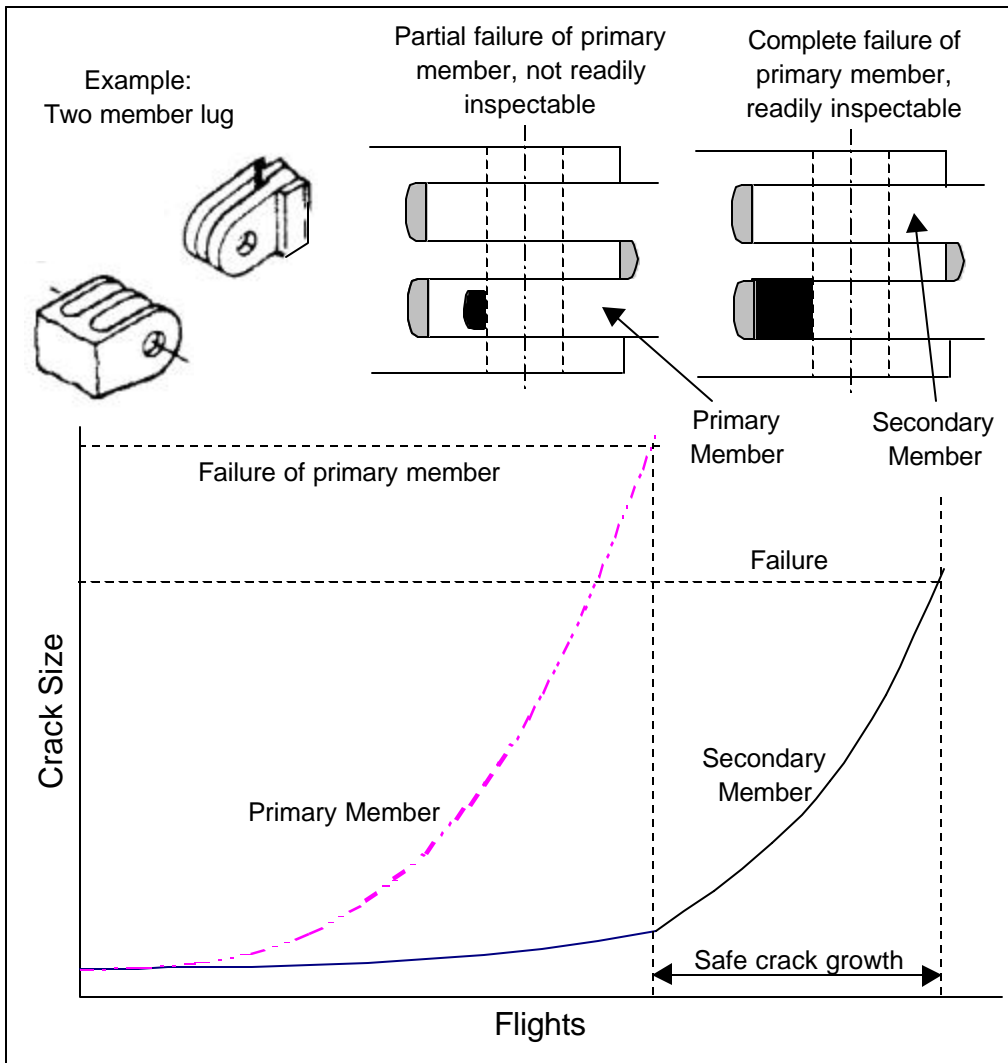
SINGLE LOAD PATH STRUCTURE - DAMAGE TOLERANT CATEGORY
EXAMPLE



In this example a loaded lug is made of two members that are side-by-side. The inspection interval would be based on the life of the secondary member, accounting for load redistribution and prior damage in the secondary member.

FIGURE 3-17

MULTIPLE LOAD PATH STRUCTURE - NOT INSPECTABLE FOR LESS THAN
LOAD PATH FAILURE CATEGORY EXAMPLE



3.3.3.3 Multiple Load Path - Inspectable for Less than Load Path Failure

Multiple load path - inspectable for less than load path failure is used for structure if partial damage in the primary member is inspectable. Damage in the secondary member prior to primary member failure must be accounted for (usually assuming a 0.005 inch crack in secondary member and a 0.05 inch crack in the primary member at time zero). Figure 3-18 shows an example of this category taken from Reference 4.

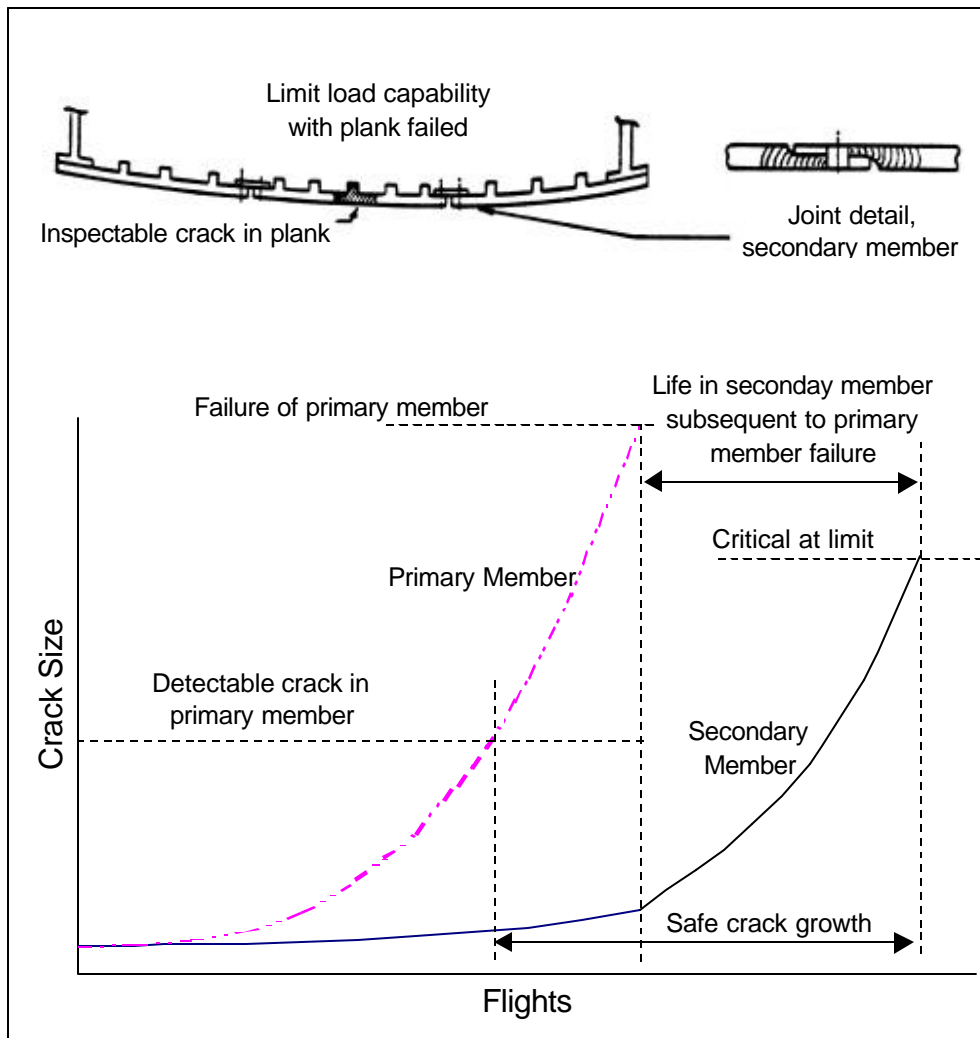
In this example a lower wing surface is made up of multiple integrally stiffened planks that are spliced together. The crack growth period starts when the crack in the primary plank (the middle plank in the figure) is readily detectable. This crack growth period extends all the way to the time at which the secondary plank (the right side plank in the figure) fails. This is different from the previous structural category in that the crack in the primary member is detectable before failure therefore, the safety limit is usually longer.

3.3.4 Other Structure

The fourth category of structure is structure that is damage tolerant but is designed for loss of the component or safe separation. The failure of this type of structure would not lead to the loss of the aircraft and would therefore be classified as secondary structure and not a PSE. Examples would be brackets, portions of the wing spoiler or a wing speed brake. Although these items may not be analyzed, they should be considered as items to be inspected in the Supplemental Inspection Document (SID) if these are not addressed in the aircraft maintenance manual.

FIGURE 3-18

MULTIPLE LOAD PATH STRUCTURE - INSPECTABLE FOR LESS THAN LOAD
PATH FAILURE CATEGORY EXAMPLE



3.4 Type and Extent of Potential Damage

The fourth step in the data collection phase is to determine the type and extent of potential damage that must be considered for each location evaluated. Questions that must be asked include:

- Where are the most likely crack origins?, and
- Should more than one crack at a time be considered?

The load path arrangement (Section 3.3) and material properties (Section 4.0) provide some of the answers to these questions. Additional factors that must be considered for all critical locations include:

- Manufacturing Process:

Cracks will initiate in the highest stressed areas of a component. Manufacturing processes play a significant role in determining the local stresses in a component. Manufacturing processes such as forming can lead to residual stresses in the finished component. The effects of residual stresses need to be considered when determining the critical area of a component. Forgings and extrusions have oriented grain directions, resulting in varying crack initiation and crack growth behavior depending on orientation. The grain orientation in forged or extruded components should be considered when selecting the extent and orientation of the assumed damage. Burrs and scratches in poorly drilled holes also act as stress risers and potential crack origins. The effect of burrs and scratches is generally accounted for in choosing an assumed damage size that correlates to the initial manufacturing quality (Section 8.1).

- Environment:

Aggressive environments that can cause corrosion in a structural component will lead to a reduction in both crack initiation and crack growth. High temperature environments can result in significant changes in fatigue and crack growth properties of commonly used materials, even though the static properties are not significantly affected. Furthermore, temperature changes can result in significant thermal stress cycles. Hence, components subjected to high (or low) temperature must also be analyzed for thermal stress in addition to the normal stress analysis.

- Possibility of Routine Damage:

Routine damage is damage such as nicks, dents and scratches that occur during routine operation and handling of the aircraft. Routine damage acts as a local stress riser, and therefore can lead to accelerated crack initiation. Of

special concern are areas where routine damage could result in a lower stressed, non-critical area becoming the highest stress (i.e. critical) area due to the presence of the stress riser. Analysis of components susceptible to routine damage should therefore consider initial damage representative of the nicks, dents and scratches expected in service, occurring at the highest stressed area.

- Possibility of Multiple Cracks Occurring:

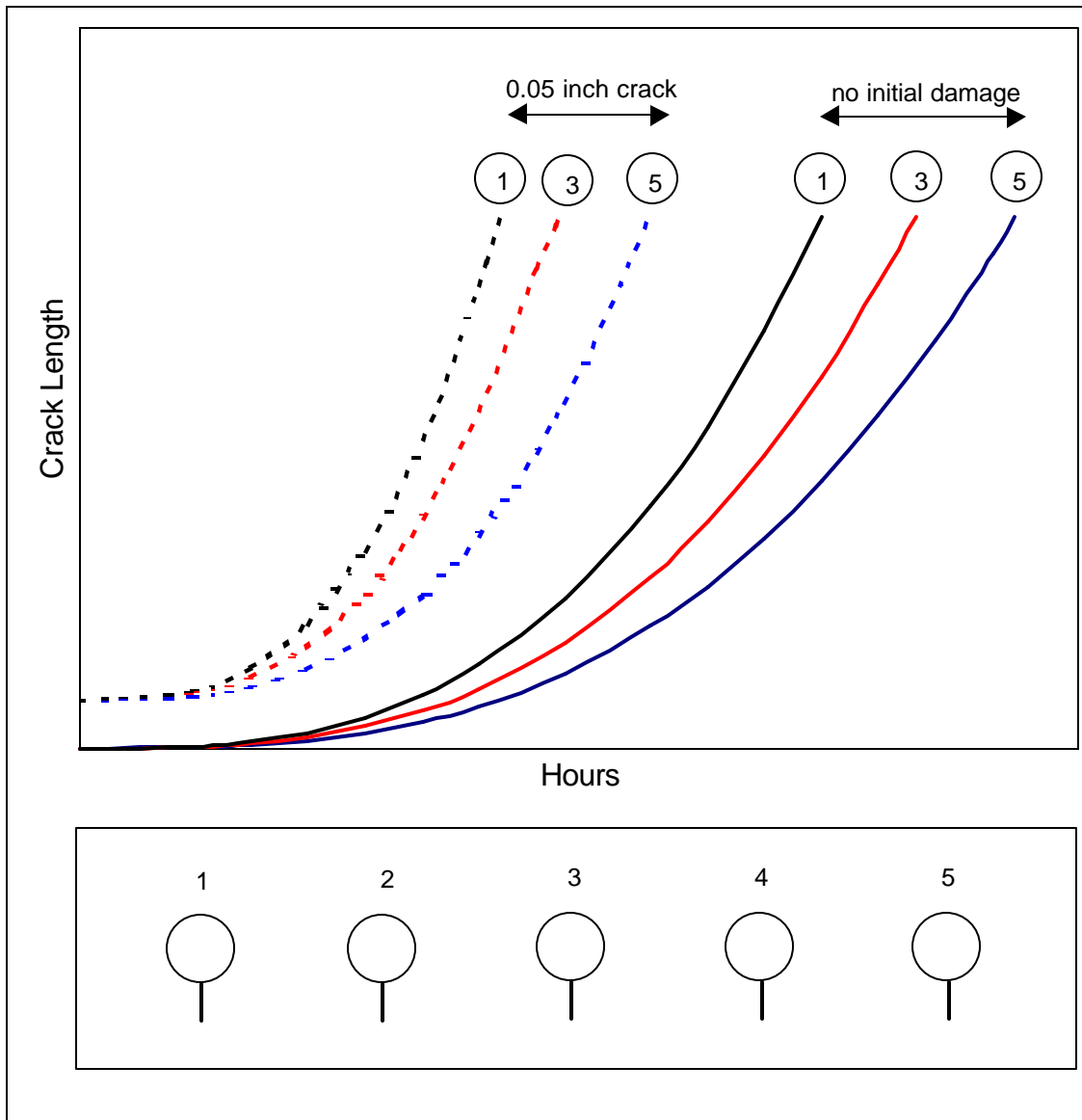
The possibility of multiple cracks occurring in the same component exists when several areas have high stresses of similar magnitudes (e.g. row of fastener holes). If the possibility of multiple cracks occurring is deemed high, the component in question may require a detailed WFD evaluation (Section 8.7).

- Inspection Area

The most critical area in a structural detail is used to set the inspection intervals for the directed inspections published in the SID document. This, however, does not mean that the directed inspection should only focus on the most critical area. While the most critical area determines the inspection intervals for the directed inspection, the inspection needs to include the structure around the critical location. This is best illustrated with an example. Consider a plate with multiple holes, each hole is subjected to slightly different loads, so that the crack growth life from a 0.05 inch flaw is shortest for Hole 1 and longest for Hole 5 (see Figure 3-19). The crack growth for Hole 1 is used to set the inspection intervals. The inspection, however, needs to include all the holes, because the assumed 0.05 inch flaw is not necessarily present at Hole 1, but might be present at one of the other holes. If this is the case, the crack growth for the undamaged Hole 1 will be longer than it is for the damaged Hole 3 or Hole 5, as illustrated in Figure 3-19. Therefore, the directed inspection will need to inspect not only the most critical hole (Hole 1), but all the other holes, since these holes are more critical than the undamaged Hole 1 when a 0.05 inch crack is present.

FIGURE 3-19

DETERMINATION OF INSPECTION AREA BASED ON MULTIPLE POSSIBLE
CRACK ORIGINS



4.0 Material Properties

The fifth step of the data collection phase is locating the material properties required for a fatigue and damage tolerance evaluation of all the various structural components to be analyzed. This is one of the essential steps in preparing a Supplemental Inspection Document. The basic properties that need to be collected for each principal structural element are listed below:

- Static Material Properties Section 4.1
- Fracture Toughness Section 4.2
- Fatigue Crack Growth Rate Section 4.3
- Stress-Life Data Section 4.4

In addition to the specific properties listed above, consideration also needs to be given to less quantifiable material characteristics. Of special importance are characteristics that tend to be detrimental to a material's static properties, fracture toughness, crack growth rate or crack initiation behavior as the material ages in service. The most important characteristics to be considered are susceptibility to corrosion, stress corrosion cracking, hydrogen embrittlement and creep. Information on the above characteristics of a given material is available from published sources, such as References 6, 7 and 8. The materials that show any of these detrimental characteristics need to be identified, so that material degradation due to these detrimental characteristics will be considered, and if necessary included, in the fatigue and damage tolerance evaluation.

Some of the aluminum alloys found on aging aircraft, have special problems that need to be considered. Examples include:

- 2024-T3: Exfoliation and multi-site corrosion fatigue damage.
- 7075-T6 series (T6, T651, T6511): Stress corrosion cracking, general corrosion, low damage tolerance.
- 7178-T6 series: Stress corrosion cracking, general corrosion, low damage tolerance, and potentially low toughness.
- 7079-T6 series: Stress corrosion cracking.
- 2014-T6 Forgings: Pitting corrosion, potential sources of multi-site damage.

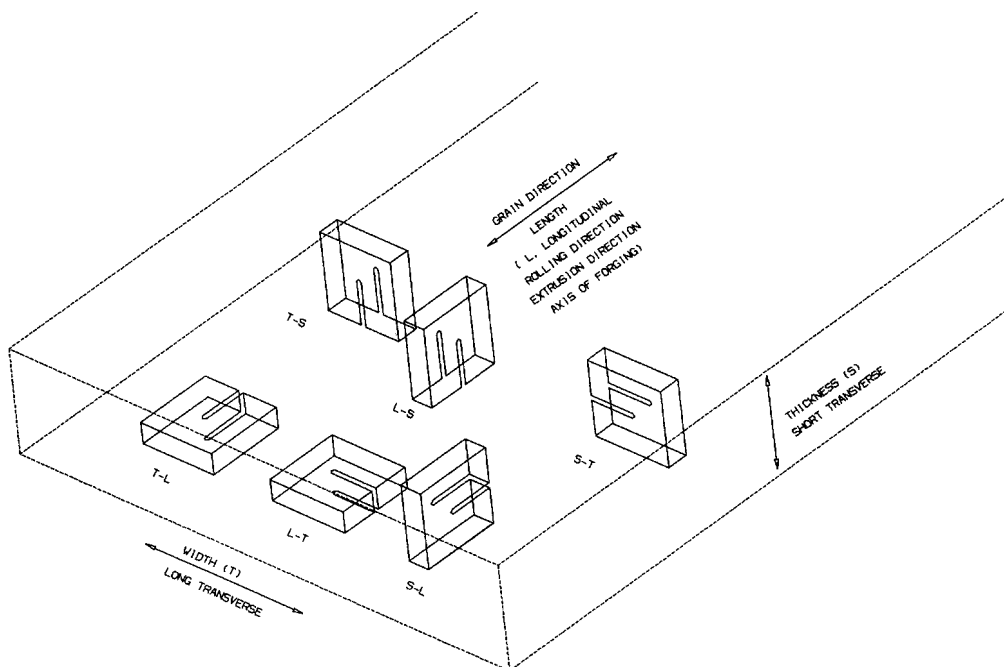
In general, the T6 series tempers in 7000 series aluminum alloys have been found to be susceptible to various forms of corrosion damage.

Other materials, in addition to some aluminum alloys, have problems. Precipitation hardened (PH) stainless steels, when aged to high strength levels, are sensitive to pitting corrosion. In addition, some of the Ti-6AL-4V titanium alloys used in the early 70's have poor stress corrosion cracking resistance.

Most of the commonly used materials in aircraft are not fully isotropic, i.e., there are some small differences in material properties based on grain orientation. This effect is especially pronounced with material forms that have a clear manufacturing direction, such as sheet, plate (rolling direction) and extrusions (see Figure 4-1). Whenever possible, the grain orientation of the material properties used in the analysis should match the actual part. For crack growth analysis in parts fabricated from sheet material, the crack growth rate data in the T-L direction should be used.

FIGURE 4-1

GRAIN ORIENTATION DEFINITIONS



All the various material properties that are required for structural analyses are usually documented in a tabular format. An example of the material properties documented in this manner are shown in Table 4-1.

TABLE 4-1

MATERIAL PROPERTIES: 2014-T6 EXTRUSION

Static Strength, ksi				
F _{TU}	60			(1)
F _{Ty}	53			(1)
Modulus of Elasticity, 10 ³ ksi				
E	10.8			(2)
Fracture Toughness, ksi√in				
K _{Ic}	27.9			(3)
K _C	65.0			(4)
Crack Growth Threshold Data				
ΔK _{th0}	2.38			(5)
A.....	0.833			(5)
Δσ _e	18			(6)
NASGRO 2.0 da/dN Equation Constants (7)				
	C	n	p	q
Single Slope	0.350E-7	2.800	0.5	1.0
da/dN is taken directly from the FLAGRO Database with R values of -1.0, -.5, 0, .3, .4, .5, .6, .7, .8, .9				
Willenborg-Chang Load Interaction Shut-off Ratio				
R _{SO}	2.30			(8)
<ol style="list-style-type: none"> 1. Mil-Hdbk-5G, Ref. 6, pg. 3-33 (L, A basis, AMS 4153 & QQ-A-200/2). 2. Mil-Hdbk-5G, Ref. 6, pg. 3-33 (tension). 3. MCIC-HB-01R, Ref. 7, assumed same as 2014-T6 forging, L-T mean value. 4. MCIC-HB-01R, Ref. 7, 2014-T6, L-T average value. 5. UDRI TR-95-93 CRACKS95 System Manual, Ref. 9, pg. 5-3. 6. American Society for Metals, Metals Reference Book, 1983, 2nd ed., Ref. 10. 7. JSC-22267A Fatigue Crack Growth Computer Program NASA/FLAGRO, Version 2.0, 1994, Ref. 11, assumed same as 2014-T6 plate, L-T value. 8. Chang, J.B., and Engle, R.M., Ref. 12. 				

4.1 Static Material Properties

Sources for the static material properties listed in Table 4-1 are given in the subsequent sections, while the fracture toughness, crack growth and fatigue material data is discussed in Sections 4.2 through 4.4, respectively.

4.1.1 Yield Strength

The material yield strength, F_{Ty}, (also referenced as σ_{ys}) is used to calculate the extent of the plastic zone at the crack tip when a load interaction model is used. The

yield strength is also the maximum allowable stress value when residual strength is calculated. The primary source for yield strength data for a wide variety of metals and alloys used in the aerospace industry is MIL-HDBK-5G (Reference 6).

Other possible sources for yield strength data include References 8 and 10. If yield strength data for the specific material, temper and product form to be analyzed are not available from any of the above references, the yield strength needs to be determined through testing. ASTM Standard E8 (Reference 13) gives the methodology and procedures to be followed to obtain the yield strength.

4.1.2 Additional Static Properties

In addition to the yield strength, additional static properties are referenced. These include the ultimate tensile strength (F_{Tu}) and the modulus of elasticity (E). MIL-HDBK-5G (Reference 6) is the primary source for these allowables.

Other possible sources for ultimate strength and modulus of elasticity data include References 8 and 10. If ultimate strength and elastic modulus data for the specific material, temper and product form to be analyzed are not available from any of the above references, technical search centers (e.g. TELTECH, etc.) may be able to find the required data in the open literature. If no data is found in the open literature, then the tensile material properties need to be determined through testing. ASTM Standards E8 (Reference 13) and E111 (Reference 14) give the methodology and procedures to be followed to obtain the yield strength, ultimate strength and the modulus of elasticity.

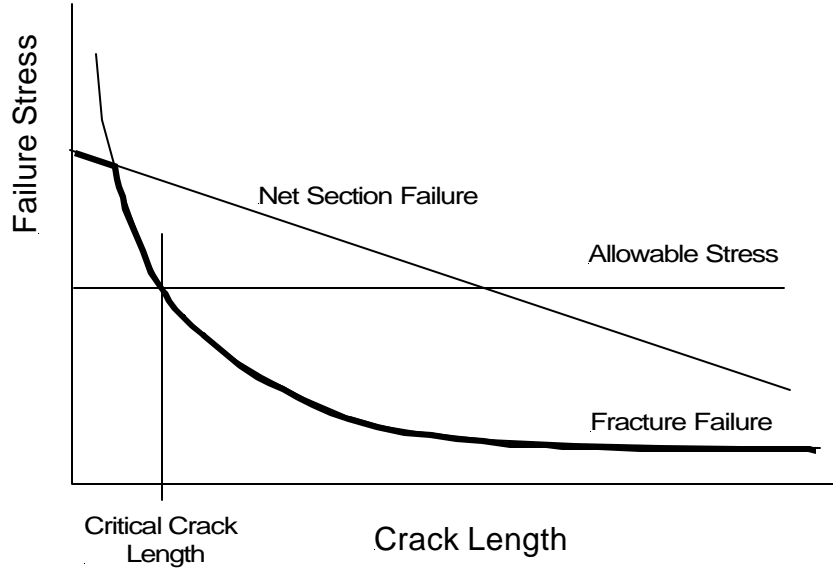
4.2 Fracture Toughness Data for Each Material and Geometry

4.2.1 Background

A cracked component will fail when the minimum of net section yield or fracture toughness is exceeded. Figure 4-2 shows a general residual strength diagram, which shows the dependency of failure stress on crack length for both net section yield and fracture toughness. Fracture toughness represents the ability of a part with a crack or defect to sustain a load without catastrophic failure (fracture). It characterizes the intensity of the stress field in the material around the crack tip when fracture (rapid unstable crack extension) takes place.

FIGURE 4-2

GENERAL RESIDUAL STRENGTH DIAGRAM



4.2.1.1 Fracture Toughness

The fracture toughness is defined as the critical stress intensity factor at the component failure stress.

$$K_{crit} = \sigma_{crit} \sqrt{\pi a \beta}$$

However, unlike the static strength limit stress values, such as ultimate and yield stress, the fracture toughness is not purely a material property. The fracture toughness is a function of both thickness and component geometry. For thick parts the fracture toughness reaches a limiting value designated as the plane strain fracture toughness, K_{Ic} . As part thickness decreases the fracture toughness increases, reaching the plane stress fracture toughness, K_{Ic} , before decreasing for very thin materials. Figure 4-3 schematically shows the effect of thickness on fracture toughness.

The plane strain fracture toughness is a basic material property. The plane stress fracture toughness, however, is geometry dependent. For sheet material of the same thickness, the fracture toughness increases with panel width for panels below a certain width (see Figure 4-4). The primary reason for this effect is that for narrower panels the net section stress at failure approaches the material yield stress.

FIGURE 4-3

VARIATION OF FRACTURE TOUGHNESS WITH THICKNESS

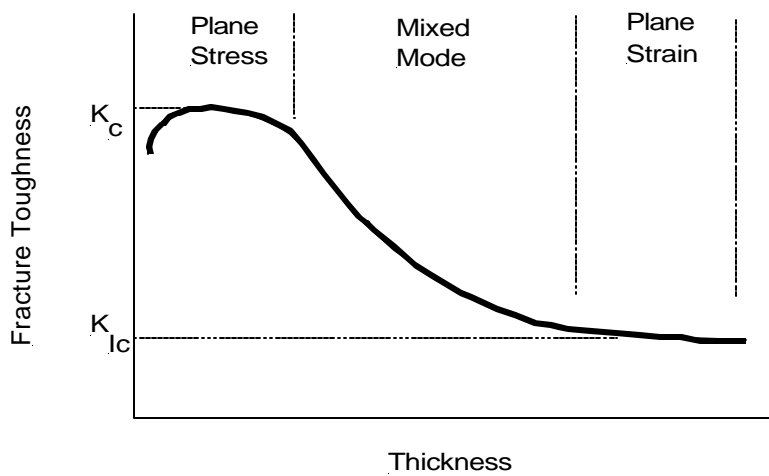
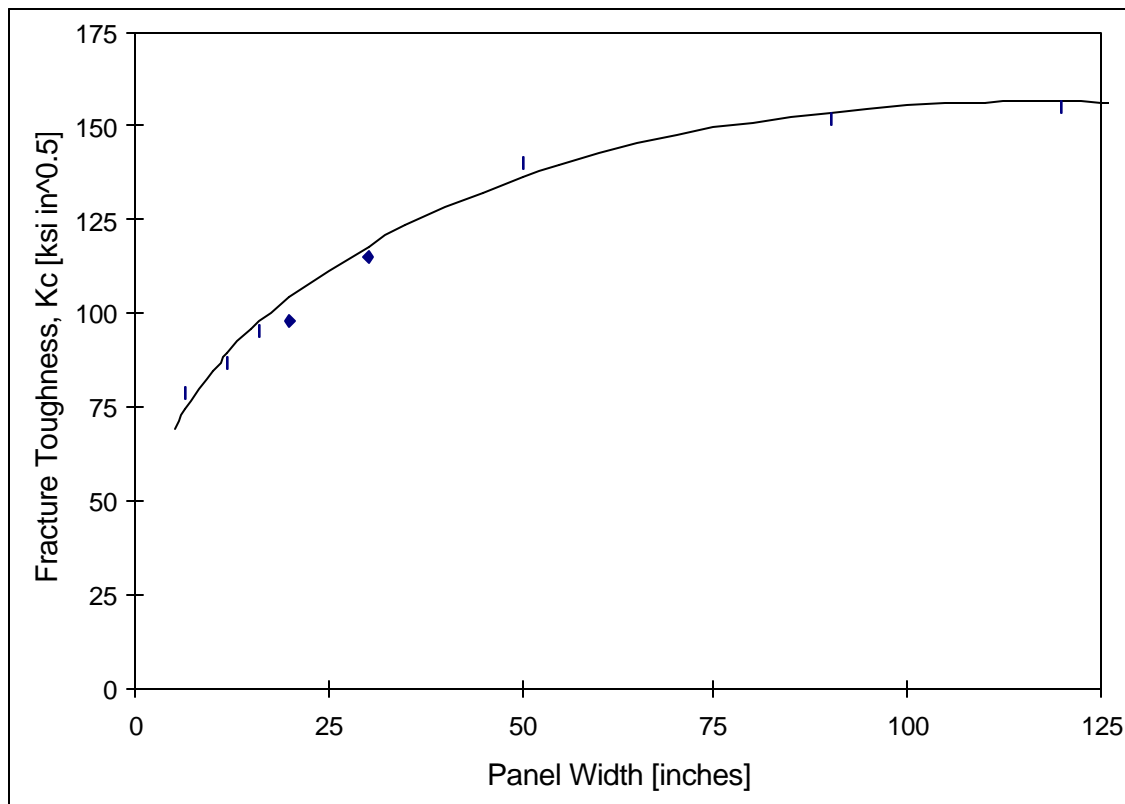


FIGURE 4-4

EFFECT OF PANEL WIDTH ON FRACTURE TOUGHNESS

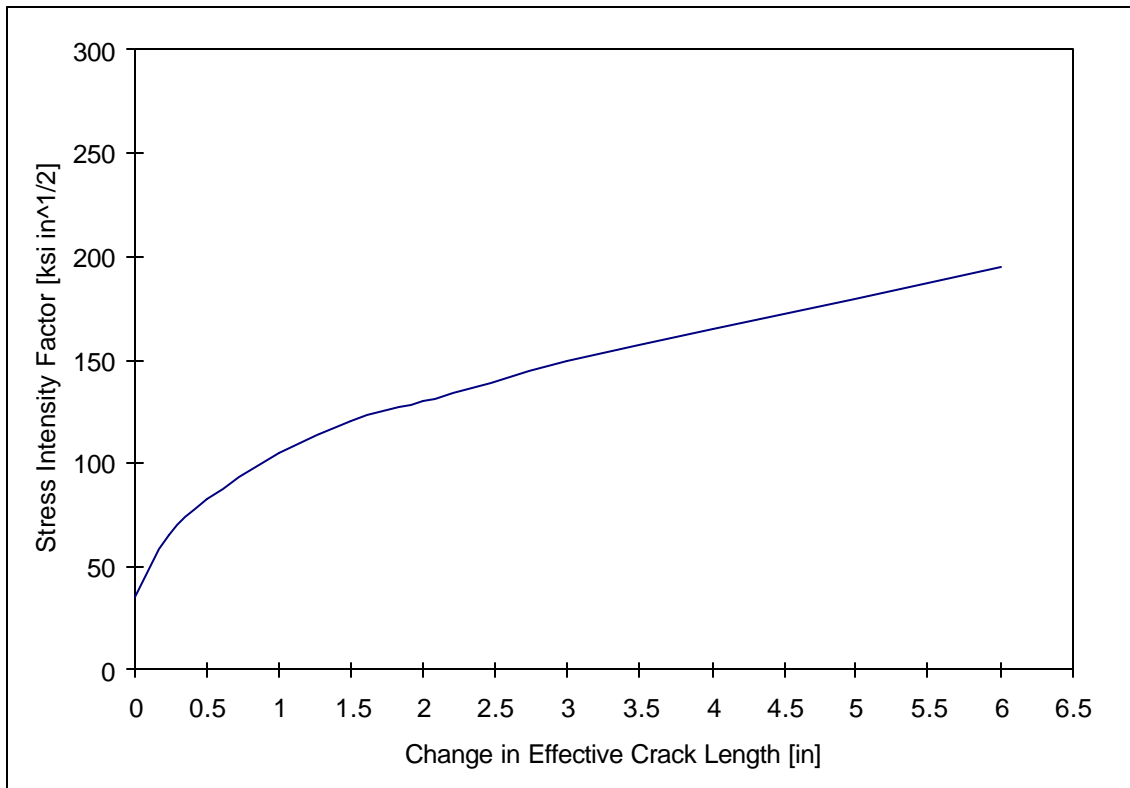


4.2.1.2 Crack Growth Resistance Curves (R-Curves)

Because the fracture toughness of wide, thin panels is not a material property, an alternate approach, which takes the stable crack extension that occurs in thin, wide sheets into account, was developed. The result is the crack resistance or R-curve, which characterizes the resistance to fracture of materials during incremental slow-stable crack extension and results from growth of the plastic zone as the crack extends. The R-curve is determined experimentally for a given material and thickness using standard specimens (see Section 4.2.3.2). Typically R-curves are presented as either stress intensity factor or crack extension energy as a function of stable crack extension. Figure 4-5 shows a sample R-Curve obtained from a 2024-T3 aluminum alloy test specimen, 24 inches wide and 0.09 inches thick (Reference 7).

FIGURE 4-5

SAMPLE R-CURVE FOR 0.09" THICK 2024-T3 SHEET

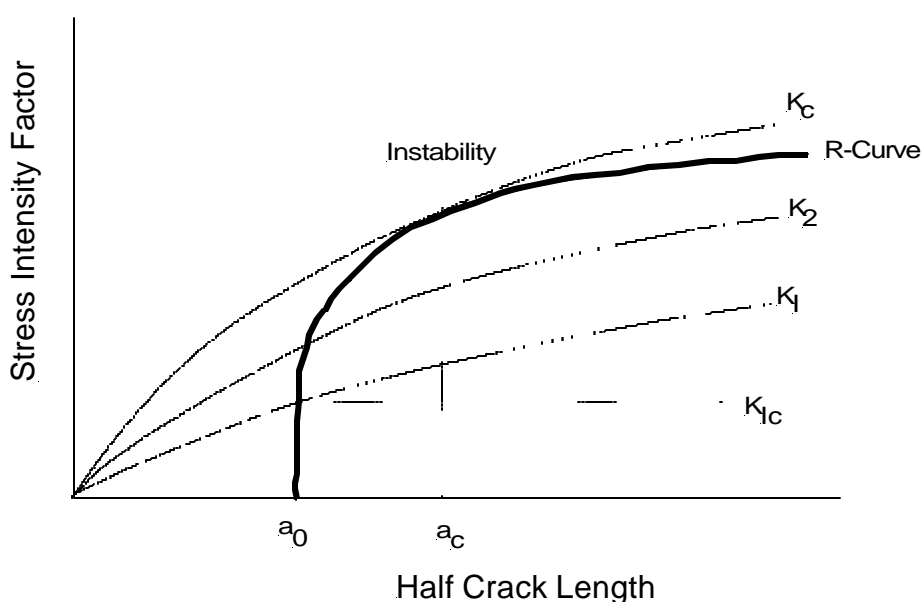


Panel failure occurs at the point where the R-curve and the stress intensity curve (K-Curve) for the geometry under consideration are tangent to each other. Any further increase in stress intensity factor will cause unstable fracture. The procedure for performing an R-curve analysis is schematically shown in Figure 4-6. To determine the critical stress for a given crack length, the R-curve is plotted starting at the initial

crack length, a_0 . The K-curve for a given stress and geometry is dependent on crack size. K-curves for low stress (K_1 , K_2) will intersect the R-curve and lie below the R-curve asymptote, indicating that the resistance to crack extension in the material (R-curve) is larger than the crack extension driving force (K_1 , K_2). As the stress level increases, a particular K-curve (K_c) will be reached that has a tangency point with the R-curve, indicating the point of instability. The stress, σ_c , corresponding to the K_c -curve is the critical stress, and the final crack length, including stable crack extension is a_c .

FIGURE 4-6

SCHEMATIC OF R-CURVE RESIDUAL STRENGTH ANALYSIS



4.2.2 Sources for Fracture Toughness Data

Since the plane strain fracture toughness is a material property, it is generally available from sources such as the MIL-HDBK-5G (Reference 6), Damage Tolerant Design Handbook (Reference 7) and the Aerospace Structural Metals Handbook (Reference 8). Some sources, like Reference 7, will also include tables of the experimentally determined K_c value for thin materials at a given panel width. Plane stress fracture toughness results from such tables can be used, if the panel used to obtain the test data had the same thickness, temper and was no wider than the structural element to be analyzed. Note that Reference 7 also gives apparent fracture toughness data, K_{app} . The difference between K_{app} and K_c is the crack length at failure used to calculate the critical fracture toughness, K_{crit} , for a given failure stress. The apparent fracture toughness, K_{app} , is the value of K_{crit} calculated based on the crack length at the start of the test (no stable crack extension), while the plane stress fracture toughness, K_c , is the value of K_{crit} based on the actual crack

length at failure, including the stable crack extension that occurred during the test. In general, using fracture toughness data from specimens that are thicker and narrower than the structural element to be analyzed is conservative.

If the required fracture toughness data is not found in References 6, 7 or 8, a technical search service (e.g. TELTECH, etc.) may be able to locate the desired data in the open literature. If data cannot be found then the fracture toughness data needs to be determined through testing.

4.2.3 Procedures for Developing Fracture Toughness Data

Procedures for developing plane strain fracture toughness data, K_{Ic} , and plane stress (R-curve determination) fracture toughness data, K_{Ic} , are given in the subsequent sections.

4.2.3.1 Plane Strain Fracture Toughness, K_{Ic}

The detailed procedures required to perform plane strain fracture toughness testing is contained in ASTM Standard E399-90 (Reference 15). This section is intended to introduce some of the essential points, but in no way is intended to replace ASTM E399.

The K_{Ic} test method involves testing notched specimens that have been pre-cracked in fatigue, followed by loading in tension until failure by separation occurs. Load versus displacement across the specimen notch is recorded.

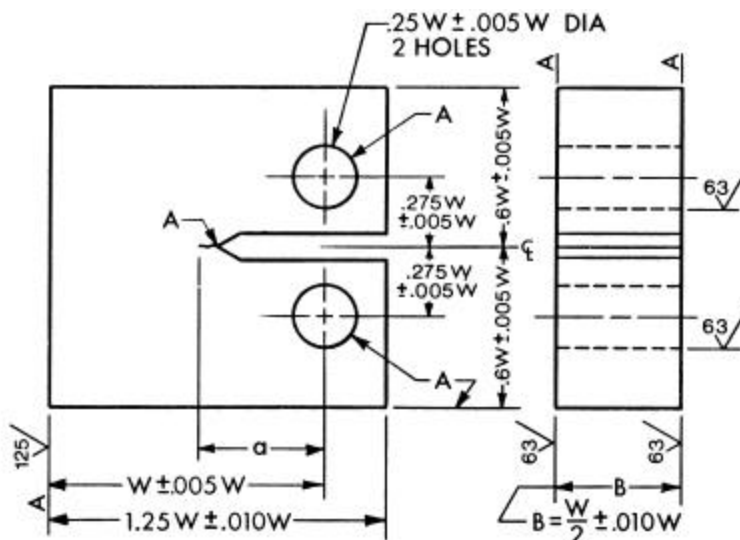
The first step in planning K_{Ic} tests is initial estimation of the specimen thickness, B . The minimum required thickness of the specimen is given by:

$$B \geq 2.5 \left(\frac{K_{Ic}}{\sigma_{ys}} \right)^2$$

An estimate of K_{Ic} is usually used along with the yield strength value. It is also recommended that K_{Ic} be initially overestimated so that a conservatively large specimen is used. The different specimen acceptable configurations for K_{Ic} tests are 1) Single Edge Bend, SE(B), 2) Compact Tension, C(T), 3) Arc-Shaped Tension, A(T), 4) Disk-Shaped Compact Tension, DC(T), and 5) Arc-Shaped Bend, A(B). A compact tension K_{Ic} specimen is shown in Figure 4-7 (taken from Reference 15).

FIGURE 4-7

COMPACT TENSION, C(T), PLANE STRAIN FRACTURE TOUGHNESS
 SPECIMEN PER ASTM E399



The K_{Ic} test procedure requires that specimen failure originates from a sharp fatigue crack, therefore fatigue precracking of the specimens will be required. To aid in precracking, the various standard K_{Ic} specimens have notches that ensure that the crack will start in the desired location and direction. Several different notch configurations are acceptable, including Chevron, straight and slots ending in drilled holes (refer to Reference 15).

The final crack length, including fatigue crack and starter notch, is required to be between 0.45 and 0.55 of the specimen width, W , and must meet the symmetry requirements given in Reference 15. The load used for fatigue precracking must be chosen so that during precracking the maximum stress intensity factor, K_{max} , meets the following requirements: 1) $K_{max}/E < 0.002$ and 2) $K_{max} < 60\%$ of the K_{Ic} estimate of the material.

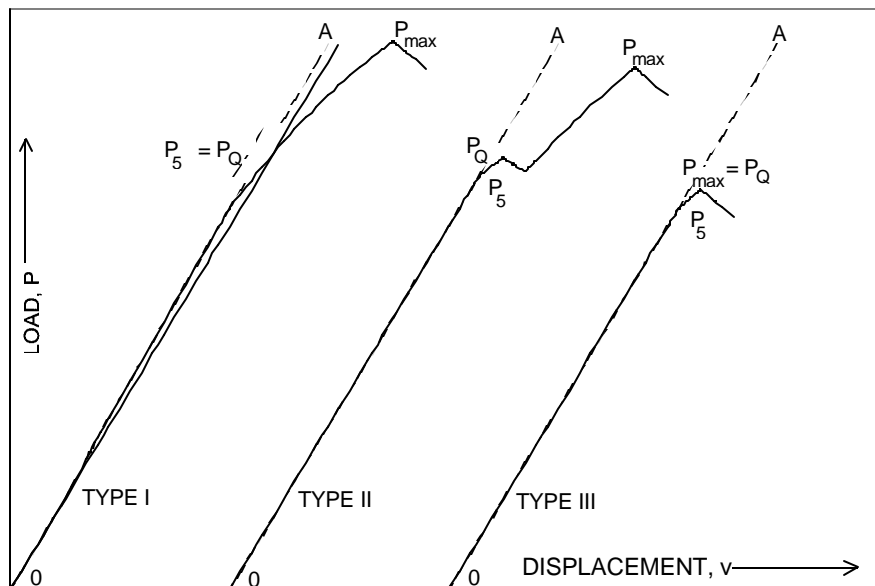
The equipment used to conduct K_{Ic} tests consists of the loading machine, specimen holding fixtures, displacement gages and the specimens, all of which need to meet the accuracy and linearity requirements specified in Reference 15. Furthermore, it is necessary to ensure that the eccentricity due to misalignment is minimized while assembling the loading train. To obtain satisfactory alignment it is recommended that the centerline of the upper and lower loading rods are coincident within 0.03 inch during the test and the specimen be centered with the clevis opening within 0.03 inch.

The completely precracked and instrumented specimens are statically loaded to failure. The load rate is chosen in order to obtain a rate of stress intensity increase, dK/dt , of 30 to 150 ksi \sqrt{in} / min. A plot of load versus the displacement of the gages

is generated as the test progresses. The principal types of load versus displacement plots are shown in Figure 4-8.

FIGURE 4-8

PRINCIPAL TYPES OF LOAD-DISPLACEMENT RECORDS



The parameters P_{max} and P_Q are determined from the load-displacement plots per ASTM E399 (Reference 15). Data obtained from the test and specimen fracture surfaces are checked to ensure that the test validity requirements from ASTM E399 (Reference 15) are met. The required constraints are listed below.

- The ratio of P_{max} / P_Q must be less than 1.1.
- Difference between maximum (a_{max}) and minimum crack length (a_{min}) must be less than 10% of the average crack length ($a_{avg.}$) as determined per ASTM E399 (Reference 15).
- Front and back surface crack lengths must be within 10% of $a_{avg.}$ to limit crack tunneling.
- Difference between front and back surface crack lengths must be less than 10% of $a_{avg.}$ to limit oblique through cracks.
- The average crack length must be within $0.45W$ and $0.55W$.

If the above requirements are met, a conditional fracture toughness, K_Q , is calculated using the value of P_Q determined from the load-displacement record and the specimen specific stress intensity factor solutions given in Reference 15. In

order for K_Q to be the plane strain fracture toughness, K_{Ic} , the following requirements must also be met.

- $B \geq 2.5 \left(\frac{K_Q}{\sigma_{ys}} \right)^2$, B is the specimen thickness.
- $a_{avg} \geq 2.5 \left(\frac{K_Q}{\sigma_{ys}} \right)^2$, a_{avg} . is the average crack length at failure.

These requirements assure that the specimen was thick enough, and the final crack length was long enough, to result in a valid plane strain fracture toughness test. The value of σ_{ys} is the value determined from tensile test on specimens from the same material and lot as the fracture toughness specimen.

If the test was determined to be valid, the parameters are repeated for the rest of the specimens to be tested. If any of the constraints are violated, appropriate parameters are changed before the next specimens are tested. A minimum of three valid tests each from 2 lots (6 total) is recommended to determine K_{Ic} .

4.2.3.2 Procedures for Determining R-Curve

Unlike the plane strain fracture toughness standard outlined in the previous section, there is no ASTM standard for plane stress fracture toughness, K_c . Section 4.2.1.1 discusses some of the factors affecting fracture toughness for thin materials and wide panels. ASTM E561 provides the standard practice for R-Curve determination. This section introduces some of the essential points, but in no way is intended to replace ASTM E561 (Reference 16).

ASTM E561 covers the determination of the resistance to fracture of metallic materials using either a center-cracked tension (M(T)), compact tension (C(T)) or crack-line-wedge-loaded (C(W)) specimen. Since the plane stress fracture toughness is a function of thickness, the R-curve specimens will need to have the same thickness as the analysis location.

The procedure consists of fatigue precracking the standard specimens to obtain a fatigue crack from initial starter notches. The fatigue crack must extend at least 0.05 inches from the end of the starter notch. Final precrack size and symmetry requirements for the standard specimen configurations are presented in Reference 16. The specimens are then incrementally loaded, time is allowed between load steps to allow the crack to stabilize, and the applied load and the crack length are measured. The crack length is measured using either COD displacement gages, traveling microscopes, or electrical resistance procedures, with a minimum accuracy of 0.01 inches. Although an R-curve can be developed with four or five points, ten or fifteen points will improve confidence in the data.

Depending on the measurement technique, either the actual or the effective crack size is obtained from the measurements. The effective crack length is typically used for the determination of the applied stress intensity factor and the amount of crack extension. The effective crack length is defined as the physical crack length plus the plastic zone adjustment, r_Y , to account for plastic crack deformation effects on the linear-elastic stress field. For Mode 1 loading, the plane stress plastic zone adjustment is:

$$r_Y = \frac{1}{2\pi} \frac{K^2}{\sigma_Y^2}$$

where K is the applied stress intensity factor, and σ_Y is the material yield strength.

At each data point the applied load and effective crack length are used to calculate the crack-extension resistance, K_R . The appropriate stress intensity factor solutions for the standard specimens are given in Reference 16. Plotting crack-extension resistance, K_R , as a function of effective crack extension results in the R-curve (Figure 4-6).

The extent to which the R-curve can be developed depends on the specimen size and geometry, since incrementally increasing loading will eventually lead to instability and fast fracture of the specimen for M(T) and C(T) specimens or to a toughness plateau for the C(W) specimen. Increasing the width of the specimen will increase the extent of the obtained R-curve (higher possible crack extension prior to failure/plateau). A minimum of three tests each from 2 lots (6 tests) are recommended to determine a valid R-curve.

4.3 Develop Crack Growth Data For Each Location

4.3.1 Background

The fatigue crack growth rate properties are generally expressed as an average crack extension per loading cycle (da/dN). For a given material, heat treat and product form, the da/dN data is presented as a function of the stress intensity range ($\Delta K = K_{max} - K_{min}$) for the applied load cycle. Because the applied stress intensity factor range (ΔK) is a function of both geometry and applied load, da/dN vs. ΔK data is material specific, but independent of geometry and loading.

Fatigue crack growth rate in the form of da/dN dependency on ΔK are available from a number of sources for common aircraft structural materials. The da/dN data is usually presented on a log-log scale (i.e. $\log(da/dN)$ vs. $\log(\Delta K)$). Sample da/dN data is shown in Figure 4-9.

Some sources for da/dN data are listed in Section 4.3.2. Section 4.3.3 presents some examples of da/dN data for 7075-T6 Aluminum alloy. If the crack growth data

is not available for the material, temper and product form of interest, procedures for developing the required data are presented in Section 4.3.4.

Many different equations have been developed to express the relationship between da/dN and ΔK . One of the most commonly used is the Walker equation which has the form,

$$da/dN = C [(1-R)^{m-1} \Delta K]^n$$

Where: $R = \text{stress ratio } (\sigma_{\min} / \sigma_{\max})$

$C, m, n =$ empirical constants determined to provide the best fit to the experimental data.

The NASGRO material database uses a different equation to model da/dN vs. ΔK , and has found widespread application in the industry.

$$\frac{da}{dN} = \frac{C(1-f)^n \Delta K^n (1 - \frac{\Delta K_{th}}{\Delta K})^p}{(1-R)^n (1 - \frac{\Delta K}{(1-R)K_c})^q}$$

Where: $K_c = \text{Plane strain fracture toughness}$

$\Delta K_{th} = \text{Threshold stress intensity (i.e. } da/dN = 0 \text{ for } \Delta K < \Delta K_{th})$

$C, n, p, q, f =$ Empirical coefficients determined from da/dN vs. ΔK data

While most sources for da/dN data give the data in graphs and in tables, some will include the empirical coefficients used in crack growth equations such as the Walker or NASGRO equation. Other equations used for crack growth analysis are the Forman equation, the hyperbolic tangent equation, the Walker-Chang equation and the Collipriest equation.

4.3.2 Sources for Fatigue Crack Growth Data

Fatigue crack growth data can be found in a number of generally available sources. These include, but are not limited to:

- Damage Tolerance Design Handbook (Reference 7)
- Aerospace Structural Metals Handbook (Reference 8)
- NASGRO Material Database (Reference 11)

- AFGROW Material Database (Reference 17)
- ESDU Data Sheets (Reference 18, Volumes 2 and 3)

4.3.3 Sample Fatigue Crack Growth Rate Data

Figure 4-9 shows da/dN data for six middle tension (M(T)) specimens of extruded 7075-T6 aluminum alloy, that were tested at three different R-ratios ($R= 0.1, 0.4$ and 0.7). Figure 4-10 presents the same data after the Walker equation (presented in Section 4.3.1) was applied to account for the R-ratio difference between the tests. The effect of R-ratio is explained in more detail in Section 4.3.5. Figures 4-9 and 4-10 illustrate the benefits of using da/dN vs. ΔK expressions, such as the Walker and NASGRO equations introduced in Section 4.3.1, that approximate the crack growth rate data from tests with different R-ratios. Table 4-2 summarizes the specimen geometry, loading and test conditions for the data shown in Figures 4-9 and 4-10. The coefficients for the tri-slope Walker equation fit to the data are presented in Table 4-3.

FIGURE 4-9

FATIGUE CRACK GROWTH DATA FOR EXTRUDED 7075-T6 FOR DIFFERENT R-RATIOS

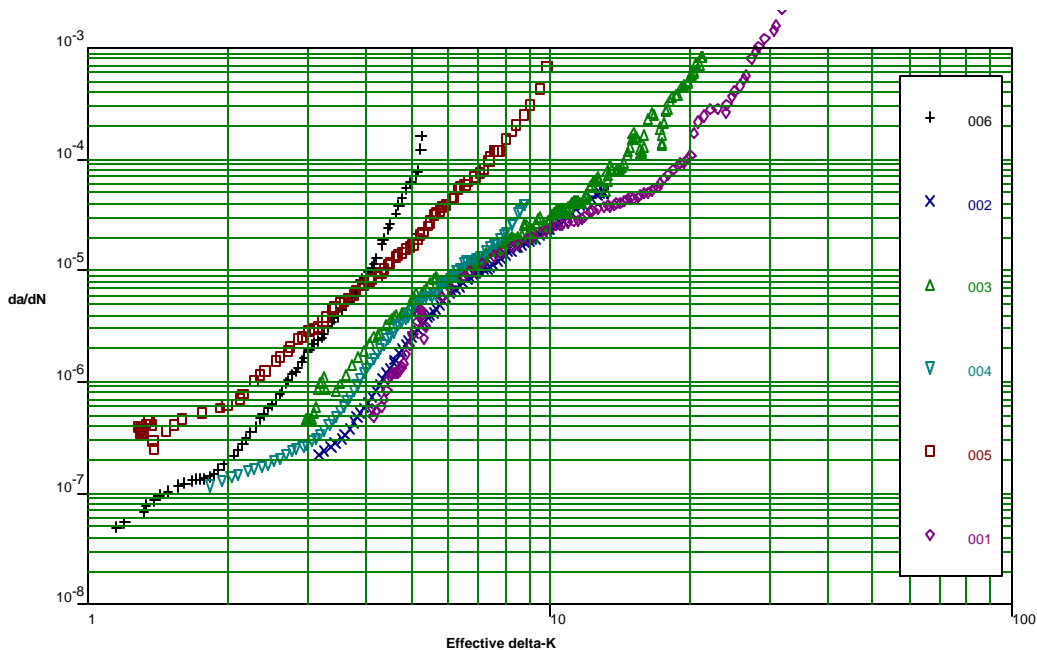


FIGURE 4-10

**FATIGUE CRACK GROWTH DATA FOR EXTRUDED 7075-T6 COLLAPSED
 AND FITTED WITH TRI-SLOPE WALKER EQUATION**

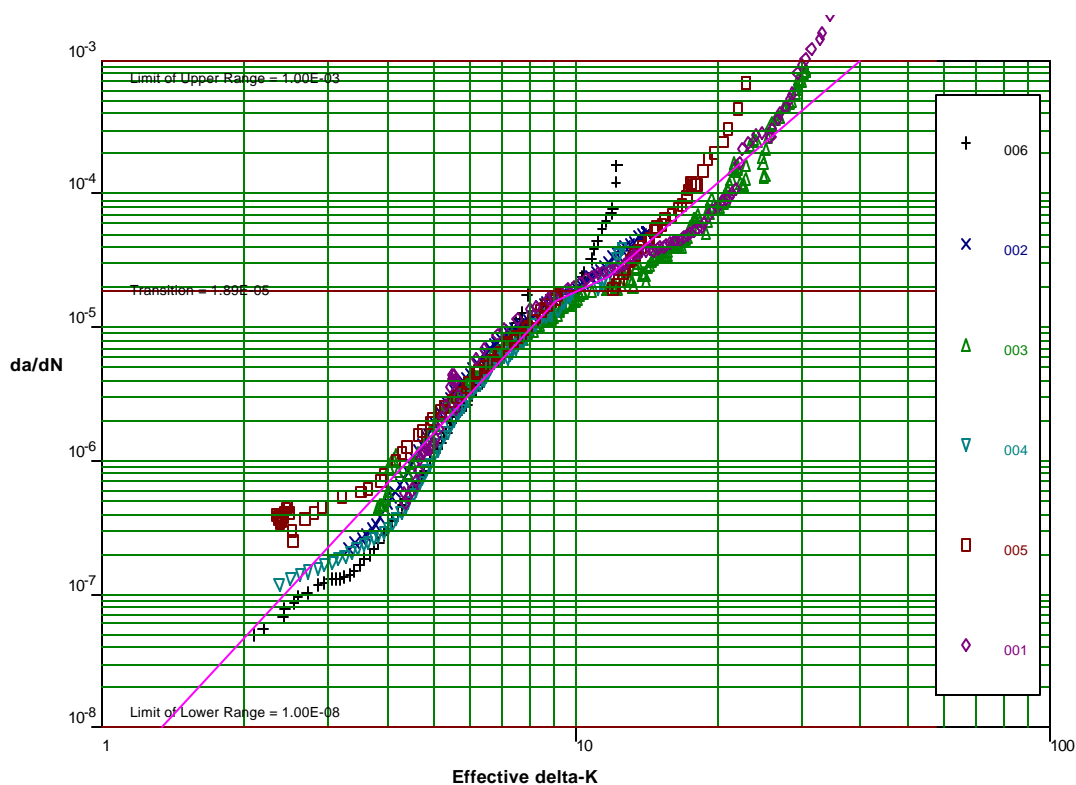


TABLE 4-2

**SUMMARY OF SPECIMEN GEOMETRY, LOADING AND TEST CONDITIONS
 FOR THE EXTRUDED 7075-T6 ALUMINUM ALLOY da/dN VS ΔK DATA**

Specimen	Specimen Type	Grain	Humidity	Frequency	R-Ratio
001	MT	LT	75%	10 Hz	0.1
002	MT	LT	75%	10 Hz	0.1
003	MT	LT	87%	10 Hz	0.4
004	MT	LT	88%	10 Hz	0.4
005	MT	LT	88%	10 Hz	0.7
006	MT	LT	90%	10 Hz	0.7

TABLE 4-3

COEFFICIENTS FOR TRI-SLOPE WALKER EQUATION FOR EXTRUDED 7075-T6 ALUMINUM ALLOY

	C	n	m
Upper Line	2.19025E-08	2.917219	0.40
Transition Line	3.571697E-12	6.845742	0.40
Lower Line	2.19771E-09	3.928524	0.40

4.3.4 Procedures for Developing Fatigue Crack Growth Rate Data

Fatigue crack growth rate testing is carried out per ASTM Standard E647 (Reference 19). The subsequent discussion is intended to introduce some of the concepts used in da/dN testing, but in no way replaces ASTM E647.

4.3.4.1 Specimen Configuration, Size and Preparation

Fatigue crack growth rate tests conforming to ASTM E647 (Reference 19) are usually performed using middle tension (MT) or compact tension (CT) specimens that have been pre-cracked in fatigue. Figures 4-11 and 4-12 show the standard CT and MT specimens. Specimen dimensions for the standard MT and CT specimens are found in Reference 19. Crack growth rate (da/dN) tests can be performed on a wide range of product forms (sheet, plate, extrusions, forgings etc.) in different thicknesses. The specimens are usually in the L-T orientation for extrusions and T-L for all other product forms. Details on the effect of crack orientation on fatigue crack growth rate are given in Section 4.3.5.6. Tensile test specimens are usually also fabricated to evaluate the 0.2% offset yield and the ultimate strength of the material per ASTM E8 (Reference 13), as well as the Elastic (Young's) Modulus per ASTM E111 (Reference 14). Typically, da/dN tests consist of an initial pre-cracking step to induce a crack at the notch tip, followed by steady fatigue cracking of the specimen to failure.

The standard specimen is notched to ensure that the fatigue crack will initiate at the desired location. Acceptable forms of notching include Electric Discharge Machining (EDM), saw cutting, milling, broaching, and grinding. The choice of notch type depends on the material and specimen type and size (see Reference 19).

FIGURE 4-11

ASTM STANDARD COMPACT TENSION (CT) SPECIMEN FOR FATIGUE
 CRACK GROWTH RATE TESTING

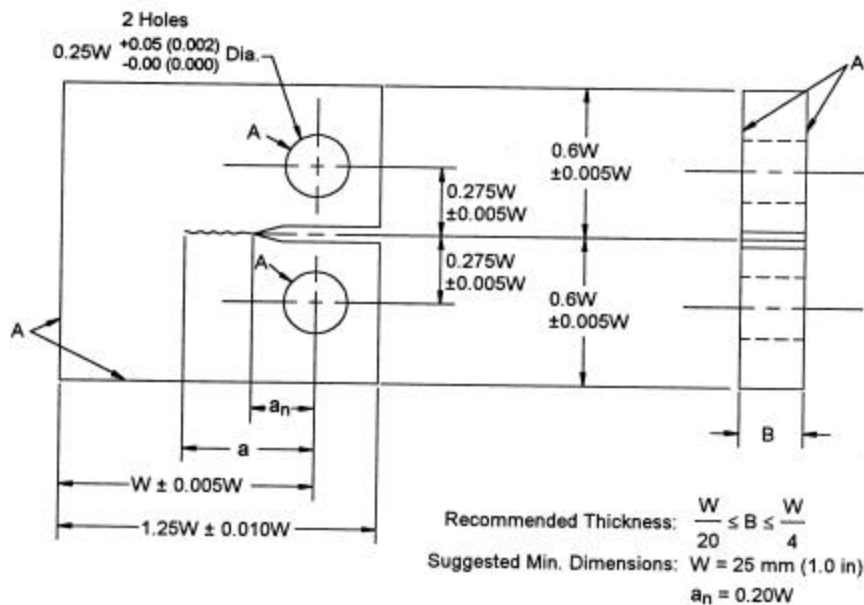
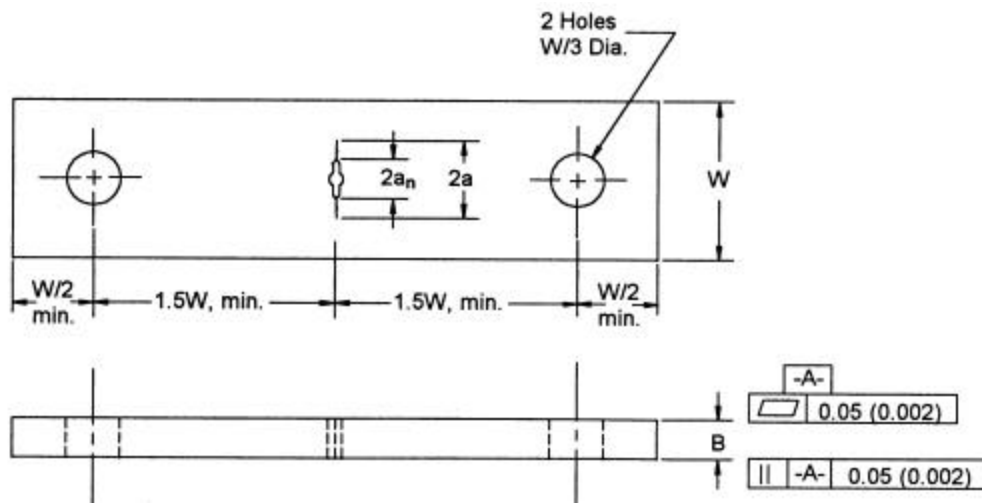


FIGURE 4-12

ASTM STANDARD MIDDLE TENSION (MT) SPECIMEN FOR FATIGUE CRACK
 GROWTH RATE TESTING



4.3.4.2 Pre-Cracking

The purpose of pre-cracking is to provide a sharp fatigue crack of adequate size, straightness and, for MT specimens, symmetry which ensures that 1) the effects of the starter notch are removed from the stress intensity factor calibration, and 2) the effects of changing crack front shape or pre-crack load history on the subsequent crack growth rate data are eliminated.

The loads for pre-cracking are to be chosen, so that K_{Max} at the end of pre-cracking is no larger than K_{Max} at the beginning of the crack growth rate test. It is desirable that the R-ratio for the pre-cracking be the same as in the subsequent fatigue crack growth rate test. In certain cases it may be necessary to start pre-cracking with loads that result in higher than desired K_{Max} values to obtain crack initiation in a reasonable amount of time. In this case, a load shedding procedure is to be used to arrive at an acceptable K_{Max} value at the end of pre-cracking. The reduction in load for each of these steps is to be less than 20% of the maximum load, furthermore, after each load step a minimum increment of crack growth must be achieved before further load shedding or the end of pre-cracking can take place. For details of the procedure refer to ASTM E647 (Reference 19).

The minimum pre-crack length is 0.04 inches or 10% of the specimen thickness, whichever is larger. There are also requirements on crack envelope (straightness), and on symmetry front and back and, for MT specimens, symmetry with respect to specimen centerline.

4.3.4.3 Equipment

The test machine to be used for da/dN testing per ASTM E647 must meet both ASTM E4 (Reference 20) and ASTM E467 (Reference 21) requirements. If the tests are to be performed under high humidity conditions, a specimen mountable high humidity chamber will be required (see Section 4.3.5.4 for a discussion on humidity effects). Environmental chambers can be used to obtain da/dN data at temperatures above or below room temperature, if the analysis location requires such data (see also Section 4.3.5.3 for a discussion on temperature effects).

Various methods are acceptable for measuring crack lengths. The main requirement is that crack extension can be measured to within 0.004 inches or 0.002 of the specimen width, whichever is greater. Possible means of measuring crack length include, travelling microscopes, Crack Opening Displacement (COD) gages, crack gages, still or video photography, electric potential difference (EPD) gages, and strain gages. Note that COD, crack, EPD and strain gages do not directly measure crack extension, but rather measure a change in specimen displacement or resistance, which can then analytically be related to crack extension. Annexes A2 and A3 to ASTM E647 (Reference 19) contain detailed information on the use of COD and EPD methods to determine crack lengths.

4.3.4.4 Crack Rate Growth Testing

Most crack growth rate testing is performed under constant amplitude loading. Reference 19 also contains procedures for decreasing ΔK loading, used to obtain accurate ΔK_{th} values, and alternate ΔK -control tests. The choice for the number of specimens, test loads and R-ratios, test frequency and environment depends greatly on the application of the obtained da/dN vs. ΔK data. Example parameters for a complete material da/dN characterization are presented in Table 4-4.

TABLE 4-4

EXAMPLE PARAMETERS FOR MATERIAL da/dN CHARACTERIZATION

Waveform	Sine
Temperature	Room Temperature
Environment	High Humidity
Stress Ratio (Note 1)	0.05, 0.1, 0.2, 0.4, 0.5, 0.7 and -1.0
Number of specimens at each stress ratio	Varies with each Lot. Minimum of 2 Specimens (Note 2)
Number of Lots	2 Lots

Note 1: Stress ratios are distributed amongst the 2 lots.

Note 2: A minimum of 2 coupons at a given R-ratio are recommended for each lot. If the data is drastically different, a 3rd coupon is needed.

During the test, crack length measurements should be made at intervals so that the da/dN data is evenly distributed over the ΔK interval. The minimum allowable measured crack extension is ten (10) times the crack length measurement precision. Recommended crack length measurement intervals are given in Table 4-5 taken from Reference 19.

TABLE 4-5

RECOMMENDED CRACK LENGTH MEASUREMENT INTERVALS

CT Specimen		MT Specimen	
Crack Length	Interval	Crack Length	Interval
$0.25 \leq a/W \leq 0.40$	$\Delta a \leq 0.04 W$	$2a/W \leq 0.60$	$\Delta a \leq 0.03 W$
$0.40 < a/W \leq 0.60$	$\Delta a \leq 0.02 W$	$2a/W > 0.60$	$\Delta a \leq 0.02 W$
$a/W > 0.60$	$\Delta a \leq 0.01 W$		

4.3.4.5 Data Reduction / Analysis

The raw test data for each test consists of crack length vs. cycle count data, as well as applied load (P_{min} , P_{max}) vs. cycle count data. In thick specimens the phenomenon of crack tunneling may be observed, i.e. the crack is longer in the center of the specimen than it is on the surface. If the fracture surfaces show that crack tunneling has occurred, a crack curvature correction factor needs to be determined, and subsequently used to “correct” all the crack length measurements (for details see Reference 19).

Using the load and crack length data, the ΔK vs. crack length and ΔK vs. cycle count data is generated by using the closed form ΔK solution for the appropriate standard specimen given in Reference 19. For constant amplitude or K-increasing tests either a seven point polynomial or a secant method can be used to obtain da/dN vs. ΔK data, however, the seven point polynomial method is generally preferred. For K-decreasing tests only the secant method is recommended for obtaining da/dN vs. ΔK data. Both of these methods are detailed in Appendix X.1 of Reference 19. The da/dN vs. ΔK data for all of the specimens of the same material, temper, thickness and product form are combined on one da/dN vs. ΔK plot (see Figure 4-9 as an example). With all of the data for a specific material, temper, thickness and product form combined, it is now possible to use curve-fitting techniques to fit the data with any of the generally used da/dN vs. ΔK equations, such as the Walker or NASGRO equations introduced in Section 4.3.1. Because of the generally sigmoidal shape of the da/dN vs. ΔK curve, it may be advantageous to use two or three separate linear segments to model the data (e.g. see the tri-slope Walker fit shown in Figure 4-10 and Table 4-3).

4.3.5 Factors Influencing Fatigue Crack Growth Rate Data

There are a number of factors affecting the crack growth rate. The most common factors and their effects are described in this section. The effects of these factors need to be considered when performing a crack growth analysis and when determining crack growth rate data as outlined in Section 4.3.4.

4.3.5.1 Stress Ratio

The stress ratio (R-ratio) is defined as $\sigma_{\min} / \sigma_{\max}$. Increasing the stress ratio, without changing the applied stress intensity range, ΔK , will lead to faster crack growth rate. This behavior is shown in Figure 4-9, which shows that the da/dN for a given ΔK for specimens with an R-ratio of 0.7 (specimens 005 and 006) can be as much as a factor of 10 higher than the da/dN for the same ΔK which had an R-ratio of 0.1 (specimens 001 and 002). The stress ratio effect is a result of crack closure. As a crack grows it forms a “wake” of plastically deformed material. This wake will tend to hold the crack tip closed, therefore part of the load applied in each load cycle is required to “open” the crack, before further crack extension can occur. Loading conditions with the same ΔK but higher R-ratio, will tend to keep the crack tip open (higher P_{\min}), and therefore, more of the load cycle will be available to extend the crack. Crack growth rate equations, such as the Walker and NASGRO equations account for the stress effect and approximate da/dN for different R-ratios (see Figure 4-10).

4.3.5.2 Material Thickness

Because material thickness has an effect on crack growth rate, it is necessary to use, or develop, da/dN data for material of the same thickness as the material for which data is needed. The crack growth rate increases with material thickness. The increase in da/dN with increasing material thickness is due to the change in stress state as material thickness increases. Thin materials are predominantly in plane stress condition, as the thickness increases the center of the specimen becomes plane strain. As a result of the smaller plastic zone size in plane strain, crack tunneling will occur and the fracture mode changes from plane stress to plane strain. Due to the smaller plastic zone for plane strain, most materials exhibit faster crack growth in plane strain than in plane stress. Therefore, thicker materials, which are mostly plane strain, will have faster growth rates than thin materials, which are mostly plane stress.

4.3.5.3 Temperature

Increasing temperature will generally increase the crack growth rate for metallic materials. The temperature effect is reduced at high ΔK levels, since the fracture toughness of metallic materials generally increases with temperature. The beneficial effect of colder than room temperature operating temperatures is generally neglected in crack growth analysis, and room temperature da/dN data is used. However, components that are exposed to hotter than room temperature operating environments need to be analyzed with material data obtained at elevated temperatures.

4.3.5.4 Humidity

An increase in humidity is usually directly related to an increase in crack growth rate. The increase in da/dN due to humidity is associated with corrosion at the crack tip. The effect of humidity on da/dN is more pronounced for high R-ratios, because the crack is held open for more of the loading cycle, and hence exposed longer to the corrosive effects of high humidity. Even more aggressive environments, such as salt water, further accelerate the crack growth rate. Crack growth rate data (da/dN) is typically determined using a high humidity environment.

4.3.5.5 Frequency

While some of the experimental data seems to indicate that frequency affects crack growth rate (faster growth rate for lower frequencies), it is believed that the observed trend is largely due to the environmental effects. Cycling at lower frequencies exposes the crack tip to potential corrosive environments for longer periods of time, thereby accelerating the crack growth rate. For most applications, frequency effects are neglected in crack growth analysis.

4.3.5.6 Crack Orientation

Crack orientation has an effect on crack growth rate for some materials and product forms. Therefore, data must be obtained for the crack orientation to be analyzed. For rolled products in general (plate, sheet) a crack growing parallel to the rolling direction (T-L, see Figure 4-1) will have faster crack growth rates than cracks perpendicular to the rolling direction (L-T). The same generally holds true for extruded parts, where cracks in the T-L direction will grow faster than cracks in the L-T direction. Because of grain direction, crack growth rates in the S-L, S-T and T-L directions are typically expected to be faster than growth rates in the L-S, T-S and L-T directions. For some product forms, especially forgings, published data does not always support the intuitive grain direction argument. Hence, care must be taken when da/dN data obtained for one crack orientation is used to predict crack growth in a different orientation.

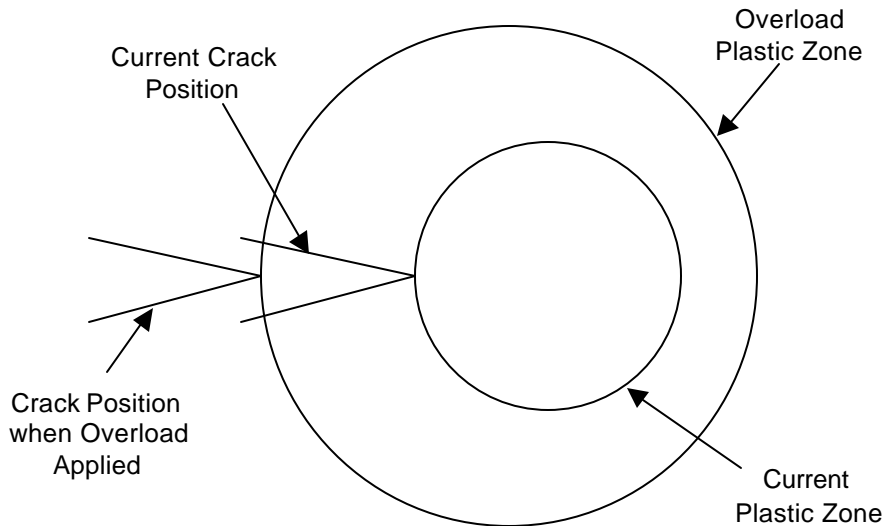
4.3.6 Load Sequence Effects

All the crack growth rate information presented to this point was based on constant amplitude loading. A typical aircraft structure, however, is rarely subjected to constant amplitude loading. A material subjected to variable amplitude loading can experience significant load sequence effects. The most significant load interaction phenomenon is retardation, which is defined as the reduction in crack growth rate observed after an occasional overload. In general, a high load followed by a sequence of low amplitude loads, will cause a decrease in crack growth rate during the low amplitude cycling.

Retardation is the result of plastic deformations that occur at the crack tip during cycling. During loading the material near the crack tip is plastically deformed, resulting in a tensile plastic zone. During the unloading phase of the load cycle the material is elastically unloaded, causing the tensile plastic zone to be subjected to compressive stresses. The size of the plastic zone is related to the crack tip stress intensity factor, which in turn is a direct function of the applied load (i.e., the higher the load, the larger the plastic zone). Since each applied load cycle causes its own plastic zone, a plastic “wake” is developed along the crack and some small distance ahead of the crack tip. The compressive stresses in the plastic wake tend to hold the crack faces shut during load application, reducing the effective stress intensity factor that the crack tip experiences. During constant amplitude loading, the plastic wake stabilizes and a constant effective stress intensity develops. However, if a high load followed by a sequence of lower loads is applied during variable amplitude loading, the overload will cause a large plastic zone, the plastic zones developed by the lower loads immediately following the overload are smaller and do not extend past the plastic zone formed by the overload. Therefore, the large field of compressive stress created by the overload plastic zone will keep the crack tip from opening fully, and hence reduce the crack growth rate. The retardation effect of the overload plastic zone is schematically shown in Figure 4-13.

FIGURE 4-13

RETARDATION DUE TO PLASTIC ZONE FROM OVERLOAD



The retardation effect of an overload diminishes as the crack propagates through the plastic zone formed by the overload. In the same manner that high tensile loads cause retardation, high compressive loads, which result in tensile residual stresses in the vicinity of the crack tip, can either diminish retardation due to tensile overloads, or even cause crack acceleration.

Several load interaction models have been proposed in the literature. The most commonly used load interaction models, most of which are incorporated in commercially available crack growth codes, are various forms of the Willenborg crack retardation model. The three commonly used forms of the Willenborg model are the original Willenborg model (Reference 22), the generalized Willenborg model (Reference 23, 24) and the Willenborg/Chang model (Reference 12). All of these models determine the amount of retardation based on the difference in the size of the overload plastic zone and the plastic zone caused by the current load cycle. All three forms of the Willenborg model utilize an overload shut-off ratio to characterize the retardation behavior, which needs to be determined experimentally for a given material and spectrum. Some generally used overload shut-off ratios for common aerospace materials are presented in References 12 and 25. However, the overload shut-off ratios published in the literature should be used with caution.

For a given material and spectrum, coupon tests subjected to the stress spectrum experienced by the analysis location should be performed to ensure that the chosen overload shut-off ratio is conservative. The coupons need to be of the same material, thickness, geometry, crack type and grain orientation as the analysis location. The overload shut-off ratio for a given analysis location and spectrum is determined by performing spectrum crack growth analyses with varying shut-off ratios. The aim is to determine the shut-off ratio that best predicts the experimental crack length versus cycle data obtained from the spectrum loaded coupon tests. However, in practice one overload shut-off ratio is chosen for a given material and subsequently used for all analysis locations made from the same material. In this case, the spectrum coupon test data is only used to verify that the overload shut-off ratio chosen for a given material will result in conservative crack growth predictions for the spectrum in question. Crack growth rate testing, as described in Section 4.3.4, should also be performed on material from the same lot as the spectrum test specimens. This eliminates material crack growth behavior as a variable from the spectrum coupon test program. Another conservative option is to neglect the beneficial effects of retardation all together, and perform the crack propagation analyses without load interaction effects.

4.4 Stress-Life (S-N) Fatigue Testing

4.4.1 Background

The stress-life (S-N) approach to fatigue has been around for over a century. The S-N approach is still widely used in design application of parts that have long lives. The S-N approach is also used to determine the initiation, or crack formation life, where the crack initiation life is the time to form a crack of given length. The remaining life of the structure is then determined using LEFM crack growth methods, starting with the initiation crack size.

The basis for S-N analysis is the S-N diagram, which plots constant amplitude maximum stress (or in some cases alternating stress (S) as a function of life (N)), usually on a semi-log plot. Figure 4-14 shows a sample S-N diagram for 2024-T4 aluminum alloy, smooth specimens ($K_t=1.0$) and different R-ratios. There are however different interpretations of the life of a specimen. In many cases the life is the number of cycles to specimen separation (complete failure), while other published data only considers the life to be the number of cycles to reach a certain crack length, (e.g., cycles to a 0.05 inch crack). For high stress levels, the difference between cycles to a fixed crack size, and cycles to complete failure is quite small, but at lower stress levels the difference can be significant.

Another frequently used term in conjunction with S-N diagrams is the endurance limit. The endurance limit is defined as the stress level where the S-N diagram becomes asymptotic, i.e., reducing the maximum stress below the endurance limit does not increase the fatigue life any further. Therefore, a part that is subjected to constant amplitude loading at a stress below the endurance limit has an infinite life. Generally, test specimens with lives in excess of 10^8 cycles are considered to be run-outs, hence they are assumed to have infinite lives.

4.4.2 Sources for S-N Data

S-N diagrams for various materials, tempers, stress ratios and stress concentration (K_t) factors can be found in several generally available sources. These include but are not limited to:

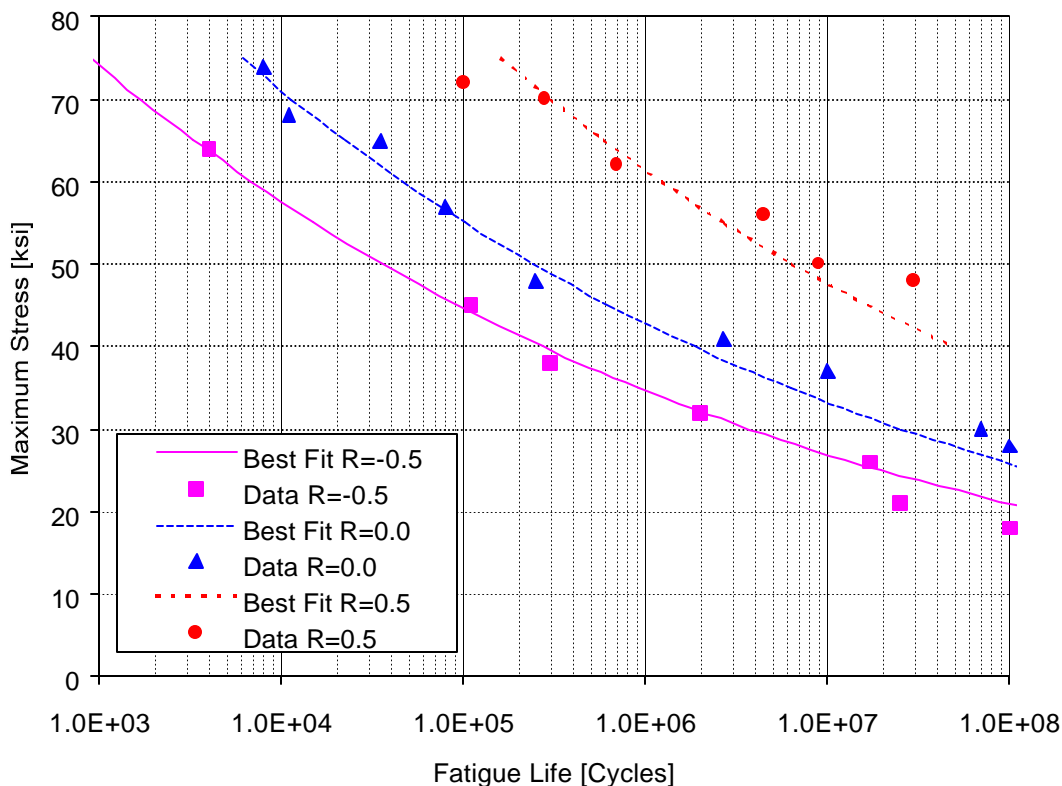
- MIL-HDBK-5G (Reference 6)
- Damage Tolerance Design Handbook (Reference 7)
- Aerospace Structural Metals Handbook (Reference 8)
- ESDU Data Sheets (Reference 18)

4.4.3 Procedures for Developing S-N Data

If S-N diagrams for the material, temper and form to be analyzed are not available from published sources, like the ones discussed in Section 4.4.2, it will be necessary to develop the required S-N diagrams through material testing. S-N diagrams are developed for various stress ratios (R-ratios) and for different notch configurations, characterized by the notch stress concentration factor, K_t . ASTM Standard Practice E466 (Reference 26) defines the specimens and procedures to be used for S-N testing, while ASTM Standard Practice E468 (Reference 27) defines the methods for S-N data presentation. The subsequent discussion is intended to introduce some of the concepts of S-N testing, but in no way replaces ASTM E466 and ASTM E468.

FIGURE 4-14

SAMPLE S-N DIAGRAM: 2024-T4 ALUMINUM ALLOY, SMOOTH SPECIMEN
 (Taken from Reference 6)



4.4.3.1 Specimen Configuration, Size, and Preparation

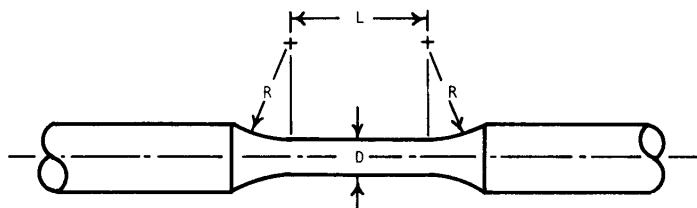
For smooth ($K_t=1.0$) specimen testing, four standard specimens are recommended by ASTM E466. The standard specimens, shown in Figure 4-15 taken from Reference 26 are either round or rectangular, and either have a uniform thickness test section or a continuous radius between the ends. While no standard exists for notched specimens, the notch configuration and radius should be chosen to simulate the desired analysis detail, and the K_t for the chosen notch configuration needs to be known accurately.

The condition of the test specimen and specimen preparation are of utmost importance. Residual surface stresses due to specimen machining are especially detrimental, and care must be taken to minimize them. Appendix X.1 of Reference 26 contains a sample machining and surface preparation procedure that results in minimal residual surface stresses.

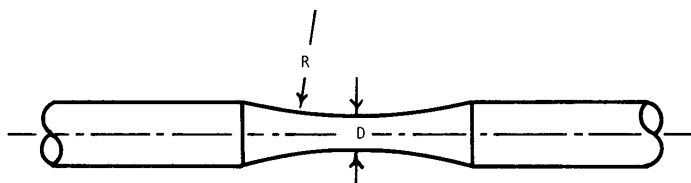
FIGURE 4-15

STANDARD SMOOTH S-N SPECIMENS

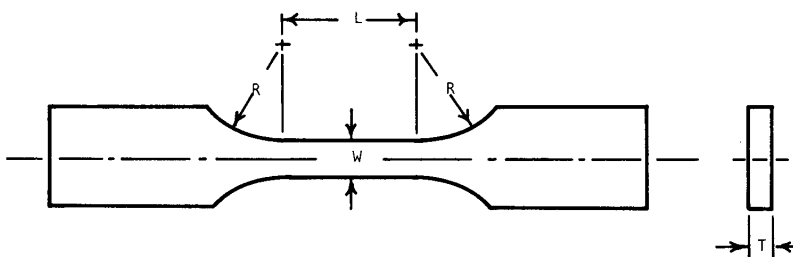
(Taken from Reference 26)



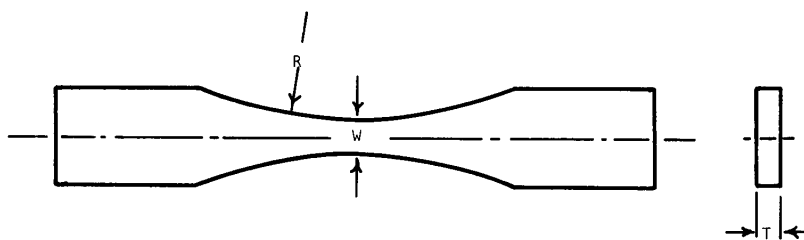
Specimens with Tangentially Blending Fillets Between the Test Section and the Ends



Specimens with a Continuous Radius Between Ends



Specimens with Tangentially Blending Fillets Between the Uniform Test Section and the Ends



Specimens with Continuous Radius Between Ends

4.4.3.2 Test Equipment

Several different test machines meet the requirements of ASTM E466 (Reference 26). The loads generated by the test machine(s) to be used need to be verified in accordance with ASTM E467 (Reference 21) and maintained within 2% of the machine range being used. The required loading for a target stress value is obtained by measuring the specimen dimensions to the nearest 0.001 inch for dimensions equal to or greater than 0.200 inch, and 0.0005 inch for dimensions less than 0.200 inch. Alignment of the specimen is an important consideration and it should be ensured that minimal torsional or bending moments are induced in the specimen while mounting and testing. Alignment can be ensured by using specimen fixtures to align the specimen axis with the load axis.

4.4.3.3 Procedure and Presentation of Results

It is recommended that statistical planning methods, such as the ones described in ASTM STP 588 (Reference 28), be used to determine various test parameters such as the percent replication, the minimum number of specimens and the number of stress levels for a complete S-N test program. The specimens are cycled under constant amplitude loading until failure, which typically is complete separation. However, in some cases it may be desirable to report the life as cycles to a certain crack size, rather than cycles to complete separation. If cycles to a fixed crack size are desired, it is possible to extract the cycles to desired crack size either by back-calculating from the life to separation or through fractographic analysis of the completely failed specimen. Often times a test specimen that sustains 10^8 load cycles without a completely separated failure is considered a run-out specimen, and cyclic testing of the specimen is stopped. Note however, that the run-out limit of 10^8 cycles is not a standard and the appropriate cycle limit for a run-out specimen needs to be evaluated for each S-N test series.

S-N test results are presented following the guidelines presented in ASTM E468 (Reference 27). S-N data can be presented in tabular form, in an S-N diagram or in a constant life diagram. The S-N diagram is the most common way of presenting S-N data and is drawn by plotting the test data with cycles to failure (complete or desired crack length) on a log scale on the X-axis and maximum or alternating stress on the Y-axis (see Figure 4-14).

5.0 Define Aircraft Utilization

The last piece of information required to perform a damage tolerance analysis is usage data. In order for a damage tolerance analysis to be accurate, it is critical that the usage, and therefore the loads, that the aircraft experiences in service are well understood. The detailed procedure to develop aircraft usage estimates is presented in this section. Typical flight lengths are defined through customer surveys and statistical analysis. These flight lengths are used as a basis for determining flight profiles. Aircraft usage estimates are usually presented in the form of defined flight profiles. These flight profiles encompass typical usage of the aircraft and are used to develop gust load spectra (Section 6.0) and stress equations (Section 7.0).

5.1 Flight Length Definition

The first step in determining typical aircraft usage estimates for the aircraft under consideration is defining typical flight lengths. After enough data is gathered, statistical analysis of the data can be performed to determine mean flight lengths and times. These parameters are used as the basis for flight profile definition as described in Section 5.1.2.

5.1.1 Typical Usage Data

For the aircraft under consideration, the derived utilization profile should reflect the average usage of the airplane when in service. It will take into account the number and frequency of typical flights. Since the aircraft under consideration has most likely been in service for a considerable period, such utilization data should be compiled through a survey of aircraft operators. Lists of airplanes and the current operators may be obtained from FAA records if the data is not available from the aircraft manufacturer's customer service records.

Figure 5-1 shows an example of a usage survey. The data that should be collected through the survey includes:

- Altitudes
- Velocities
- Fuel loading (including information on auxiliary fuel tanks)
- Number of passengers
- Baggage and Cargo Loading Configuration
- Flight lengths (distribution of distance or time)

- Type of terrain flown over
- Frequency of flight

This data should be collected for as many operators as possible for good statistical correlation.

FIGURE 5-1

SAMPLE OPERATOR SURVEY - AIRCRAFT USAGE

INFORMATION NEEDED TO DEVELOP FLIGHT PROFILES FOR FATIGUE ANALYSIS

This form should be filled out to accurately describe a **typical** flight¹. Weights, distribution of fuel, altitude above ground or water, speeds, and length of flight all have an effect on the fatigue life expected. The accuracy of the fatigue analysis depends on the accuracy of your information. If the typical flight changes, the individual fatigue analysis no longer would apply.

<u>Aircraft Model</u>				
Number of Times Typical Flight is Flown _____ /week/month/year (circle one)				
Percent Of Total Flight Time This Typical Flight Represents				%
Airport Elevation (ft)	Takeoff -	Landing -		
<u>Auxiliary Tank Locations (outb'd, wing locker, etc.) and Capacity Of Each</u>				
Aux. Tank #	Loc.	gals.		
Aux. Tank #	Loc.	gals.		
Ramp Weight ²	lbs			
Takeoff Fuel Loading ³	Main Tanks	lbs		
	Aux. Tanks	lbs		
		lbs		
Occupants and Baggage ⁴	lbs			
Landing Weight ⁵	lbs			
Landing Fuel Loading ³	Main Tanks	lbs		
	Aux. Tanks	lbs		
		lbs		
<u>Cruise Speed and Altitude</u>				KIAS ft
Terrain flown over and elevation ⁶	land	% water	%	ft
Climb Speeds and Time ⁷	grd --	ft	KIAS	min
		ft	KIAS	min
		ft	KIAS	min
Descent Speeds and Time ⁷		ft	KIAS	min
		ft	KIAS	min
		-- grd ft	KIAS	min
<u>Flight Length (hours or minutes)</u>				

¹ Complete this form for each frequently flown flight profile (significantly different flight pattern).
² This is the total weight of the fueled aircraft, including crew and passengers and any baggage or cargo.
³ This is the total weight of the fuel onboard, with the distribution noted if there are auxiliary tanks used.
⁴ This is the total weight of the crew, passengers, and baggage or cargo.
⁵ This is the weight at which this aircraft lands.
⁶ If the terrain flown over is fairly flat, an average elevation may be used. If flying over varied elevations (i.e. - mountains and valleys) the flight path may be marked on an aeronautical chart that shows terrain elevation and submitted with this form.
⁷ If altitude is over 7,000 ft. break down in 5,000 ft or less increments.

One usage profile or a range of profiles may be applicable to all airplanes of the same airplane type. However, if individual airplanes (or fleets) are used in specialized roles that differ significantly from the average usage profile or environment for the aircraft type, a separate usage profile must be developed. Types of special usage include pipeline survey missions, island hopping or short flights, and flying over mountainous terrain.

5.1.2 Statistical Analysis of Data

After completing the usage survey described in the previous section the data must be reviewed. Data for each special usage aircraft, as defined in the previous section, is separated from the other data. Separate usage profiles must be developed for each specialized aircraft usage. Each set of usage data must be reduced to determine flight profiles and the mean time of each flight. If all the data in a usage category is nearly identical in terms of flight length, flight altitudes, weights, and other flight parameters, then one flight profile can be generated to represent that usage. If there is variation in the data, then a statistical analysis of the data must be conducted.

A Weibull statistical distribution has historically been the best distribution fit for aircraft usage data. Typically a three parameter Weibull distribution fit is used to define the probability of a given flight length (in terms of time) occurring within a population of flight lengths. The Weibull distribution, $p(t)$, is shown in Figure 5-2 and is defined as:

$$p(t) = \frac{\beta}{\eta} \left[\frac{t}{\eta} \right]^{\beta-1} \cdot e^{-\left[\frac{t}{\eta} \right]^\beta}$$

where β = the Shape Parameter, and

η = the Characteristic Life

t = the time of each flight

The total area under $p(t)$ is 1.0. The area under the curve to time t is defined as:

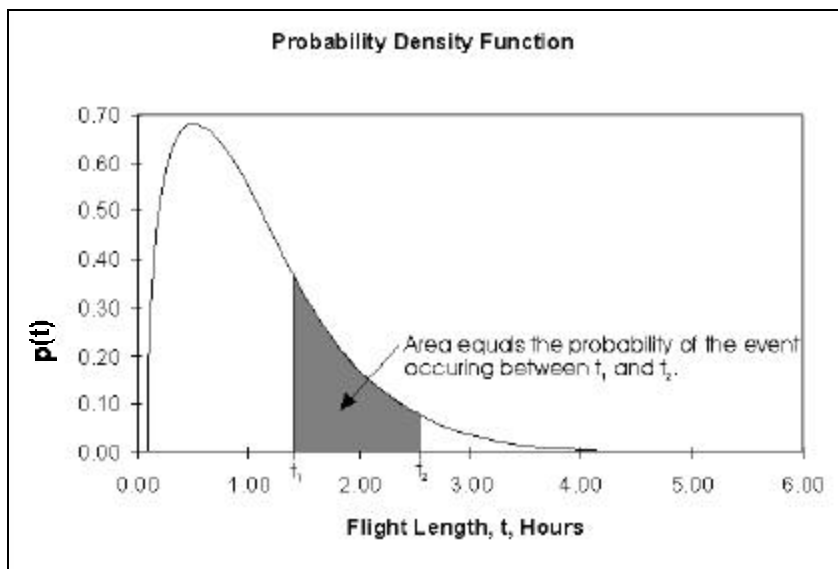
$$F(t) = 1 - e^{-\left[\frac{t}{\eta} \right]^\beta}$$

The area under $p(t)$ between any two flight times, t_1 and t_2 , which represents the percentage of total flights for any given profile is defined as:

$$\text{Area} = F(t_2) - F(t_1)$$

FIGURE 5-2

TYPICAL WEIBULL DISTRIBUTION



Section 1 of Appendix A presents an example of how the Weibull parameters β and η can be calculated from collected usage data using a Microsoft Excel spreadsheet.

After calculating the Weibull parameters, the Weibull Probability Density Function, $p(t)$ curve can be segmented into the desired number of flight profiles. The flight usage surveys should be used to decide on the t_1 and t_2 increments for each flight profile. The mean flight time between t_1 and t_2 represents the flight time for any given profile (see Figure 5-3) and is defined as:

$$\text{Mean} = \frac{\int_{t_1}^{t_2} t \cdot p(t) dt}{\text{Area}} + \Gamma$$

where Γ = the minimum life

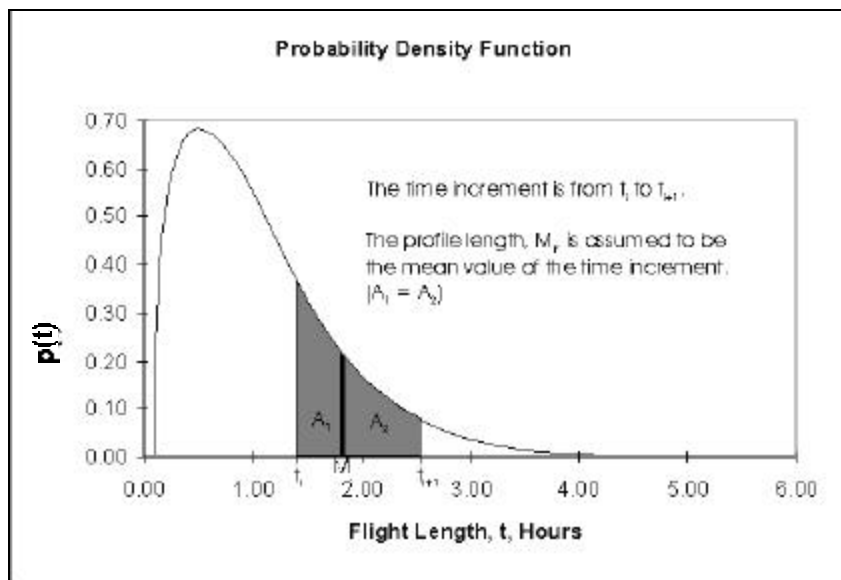
$p(t)$ = Weibull Probability Density Function

Area = $F(t_2) - F(t_1)$

The minimum life is defined as the shortest possible flight time (checkout flight, maintenance flight, or aborted takeoff). For twin engine commuters a minimum life of 0.09 hours is common.

FIGURE 5-3

DEFINITION OF PROFILE FLIGHT LENGTH



Section 2 of Appendix A presents an example of how the usage data can be segmented into the desired number of flight profiles using the usage data contained in Section 1 of Appendix A.

The flight length distribution can be plotted with the Weibull Probability Density Function to verify the data fits a Weibull statistical distribution. Figure 5-4 shows this comparison. If the flight usage data does not fit a Weibull distribution then a different statistical distribution (Normal, Gaussian, etc.) needs to be used to determine the flight profile utilization of the aircraft under consideration.

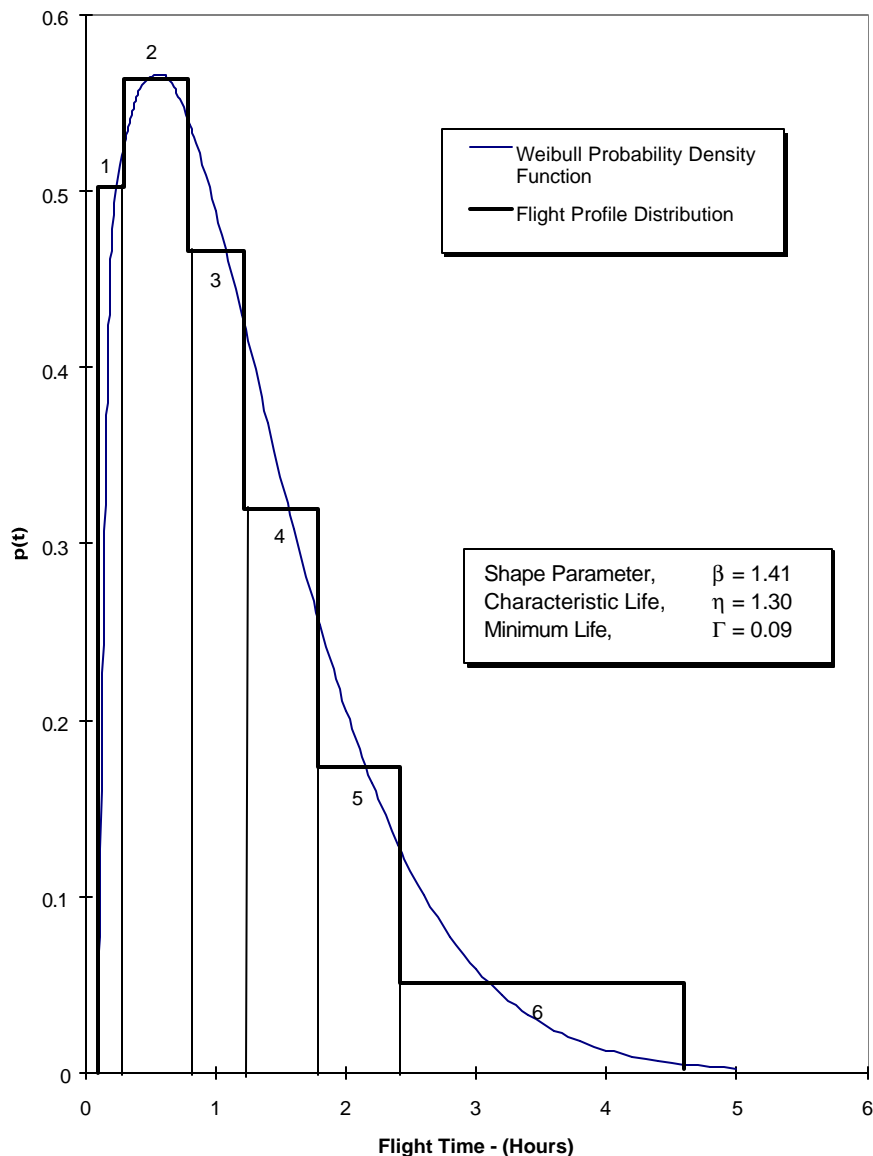
A summary table of the flight times used for each profile should also be presented (Table 5-1). This data is used to calculate flight profile segment data that is used in stress equation development.

TABLE 5-1

PROFILE SUMMARY

Profile Number	t1 (hours)	t2 (hours)	Flight Hours	% Total of Flights	% Total of Flight Hours
1	0.09	0.30	0.250	11.9%	2.4%
2	0.30	0.79	0.636	27.3%	13.8%
3	0.79	1.21	1.080	20.5%	17.6%
4	1.21	1.79	1.562	19.7%	24.5%
5	1.79	2.41	2.150	11.6%	19.8%
6	2.41	4.59	3.101	8.8%	21.8%

FIGURE 5-4
FLIGHT LENGTH DISTRIBUTION

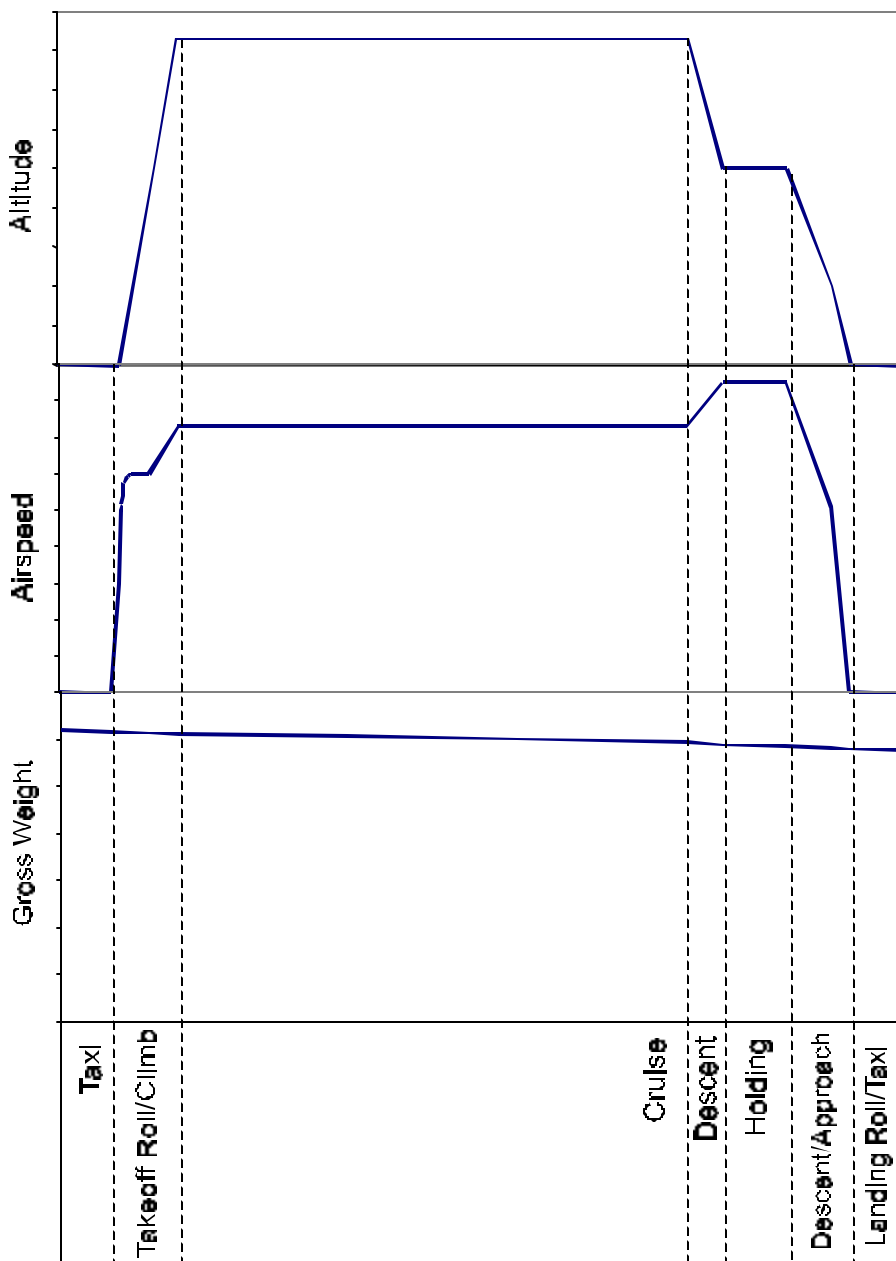


5.2 Flight Profile Definition

A flight profile is defined as a typical flight that represents part or all (if there is only one usage profile) of an aircraft's normal usage. It consists of takeoff, climb, cruise, descent, approach, and landing segments that define the flight. Flight parameters are calculated for each of these segments for use in load spectra and stress calculations. Typically there are up to six flight profiles of varying flight length and altitude that are created to define the typical usage of an aircraft. An example of a mission profile divided into mission segments is shown in Figure 5-5.

FIGURE 5-5

MISSION PROFILE AND MISSION SEGMENTS



5.2.1 Required Data

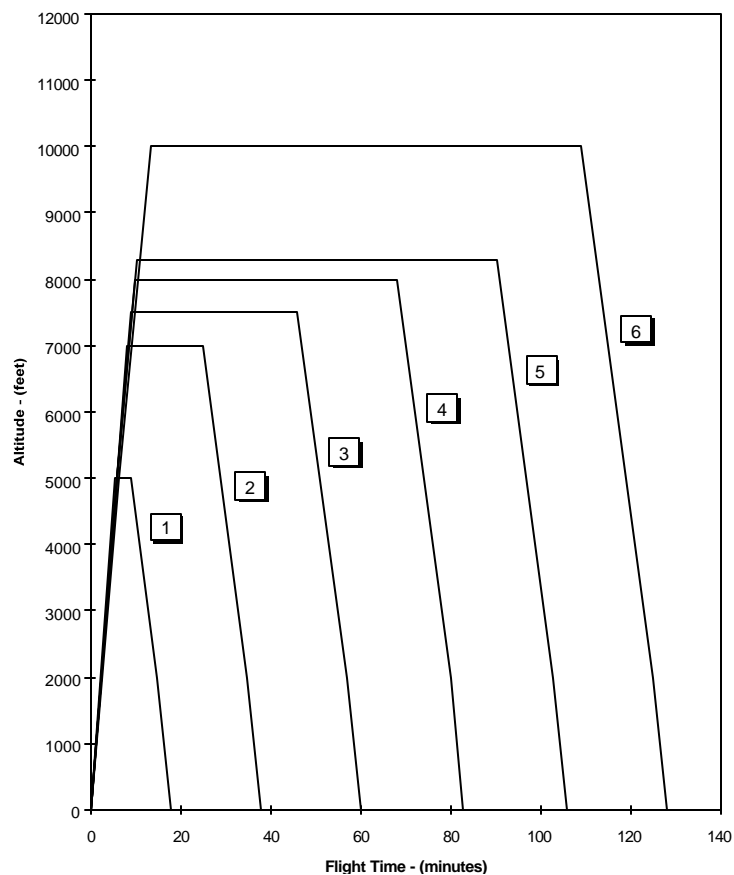
For the aircraft under consideration, the following data must be collected to create the flight profiles:

- Flight lengths (distribution of distance and/or time - Defined in Section 5.1)
- Basic aircraft empty weight (and cg location in airplane)

- Number and weight of passengers (and cg location in airplane)
- Baggage and cargo load configurations (and cg location in airplane)
- Fuel loading (and cg location in airplane)
- Climb, cruise, and descent altitudes for each profile (See Figure 5-6)
- Cruise altitudes and speeds
- Engine fuel consumption rates

FIGURE 5-6

PROFILE ALTITUDES



Some of this data can be found in a Pilot's Operating Handbook (POH). The Pilot's Operating Handbook details climb and descent parameters, center of gravity (cg) locations, mean aerodynamic chord length, and other required flight data. However, typical aircraft passenger, baggage and cargo, and fuel loadings along with the

cruise altitudes and speeds need to be determined through operator surveys or interviews with pilots of the aircraft under consideration.

5.2.2 Weight Configuration Calculations

The first aircraft parameter that needs to be calculated is the gross weight at the beginning of the profile, prior to takeoff. Table 5-2 shows an example of the calculation of the aircraft gross weight for an example profile. For all cases the starting point should be with the aircraft basic empty weight. Occupant loadings should be based on the aircraft usage survey and cg locations taken from the pilot operating handbook. The gross weight calculation is performed for each flight profile, due to the different passenger and fuel configurations.

TABLE 5-2

EXAMPLE AIRCRAFT WEIGHT CONFIGURATION CALCULATION

<u>ITEM</u>	<u>WEIGHT (LBS)</u>	<u>AIRCRAFT CG (F.S.)</u>
Basic Empty Weight	4110	147.12
Crew (1 person)	180	137.00
Passenger 1	180	137.00
Passenger 2	180	175.00
Passenger 3	180	175.00
Passenger 4	180	218.00
Passenger 5	180	218.00
Baggage	120	147.00
Zero Fuel Weight	5310	153.13
Fuel (main tank)	600	152.00
Fuel (auxiliary tank)	275	164.00
TOTAL RAMP (GROSS) WEIGHT	6185	153.50

5.2.3 Flight Profile Segments

The next step in creating a flight profile is to determine how many flight segments make up a profile and to calculate the associated flight parameters for each segment. An example of a flight profile and the required flight parameters is presented in tabular format in Table 5-3. In general, climb and descent segments should not have more than 5,000 ft. altitude changes and the cruise portion should be split into one segment for every 30 minutes of cruise. An approach segment

from 2,000 ft. to 0 ft. should be the last descent segment. The parameters for the approach segment are used for both maneuver segments (approach flaps and landing flaps). All taxi, landing impact, and ground loads should each be represented as flight segments. Each flight profile segment is described below:

- Taxi/Takeoff Roll – This segment represents the portion of the profile from initial taxi through the takeoff roll. This segment is calculated at a weight midway between initial taxi and takeoff.
- Climb - The total number of climb segments depends on the final cruise altitude. Each segment should represent no more than a 5,000 ft. change in altitude. Small altitude changes are defined to assure that the gust environment is accurately represented, since the severity of the gust spectrum is a function of altitude (i.e., the gust spectrum is more severe at lower altitudes). Each climb segment is calculated at the average weight for that segment.
- Cruise - The total number of cruise segments depends on the total time spent in cruise. Each segment will represent no more than 30 minutes of flight. Dividing the cruise segments into smaller segments assures accuracy in the calculated gust loads, since the severity of the gust spectrum is a function of aircraft weight as well as other parameters. Each cruise segment is calculated at the average weight for that segment.
- Descent - The descent segments are defined in the same manner as the climb phase. For descents down to 10,000 ft. the aircraft velocity is restricted only by aircraft limitations. For descents below 10,000 ft. the velocity is limited to 250 KCAS as required by Federal regulations (14 CFR 91.70).
- Holding - When the profile cruise altitude is above 10,000 feet a 5.5 minute holding pattern is included at 10,000 feet.
- Approach - This is the last descent segment prior to landing. The velocity is limited to the approach speed of the aircraft under consideration.
- Maneuvers - Parameters are identical to the approach segment. In general, most maneuvers conducted with an aircraft of this class can be expected to occur just after takeoff and prior to landing (including holding maneuvers). The maneuvers prior to landing can be expected to be the more frequent.
- Approach-to-Landing Flap Deflection - Parameters are identical to the approach segment with the exception of deflected flaps (first in the approach position, then in the landing position).
- Landing Impact – The weight at touchdown is used. This segment is used to calculate the gear loads at touchdown.

- Landing roll/taxi to ramp – Represents the portion of flight from landing to taxi to the ramp. This segment is calculated at a weight midway between landing and taxi to the ramp.

A systematic procedure for calculating flight profile data for each segment is presented in Appendix B for use in hand calculations or the development of a computer program. An example profile is shown in Table 5-3.

TABLE 5-3

EXAMPLE FLIGHT PROFILE TABLE

<u>Flight Load Segment</u>	<u>Start-End Altitude</u>	<u>Total Fuel (lb)</u>	<u>GRWT (lb)</u>	<u>Segment Time-min</u>	<u>KEAS</u>	<u>Mach</u>	<u>ALT (ft)</u>	<u>%CG</u>	<u>Diff. Press (psi)</u>	<u>Thrust (lb)</u>
Taxi/Takeoff Roll		860	6170	N/A	0	0	0	23.21	0	0
Climb	0-5000 ft	834	6144	6.04	120	0.19	2500	23.22	0	874
Climb	5000-8300 ft	816	6126	4.45	120	0.205	6650	23.23	0	801
Cruise	8300-8300 ft	773	6083	26.60	146	0.257	8300	23.24	0	517
Cruise	8300-8300 ft	701	6011	26.60	146	0.257	8300	23.27	0	514
Cruise	8300-8300 ft	629	5939	26.60	146	0.257	8300	23.30	0	514
Descent	8300-2000 ft	574	5884	12.60	170	0.282	5150	23.33	0	451
Approach	2000-0 ft	543	5853	2.97	102	0.158	1000	23.34	0	76
Maneuver - 15° Flap		543	5853	N/A	102	0.158	1000	23.34	0	76
Maneuver - 45° Flap		543	5853	N/A	102	0.158	1000	23.34	0	76
Landing Impact		531	5841	N/A	0	0	0	23.34	0	0
Landing Roll/Taxi to Ramp		516	5826	N/A	0	0	0	23.44	0	0

5.3 Mission Mix Definition

After determining the utilization of each of the flight profiles (see Section 5.1), a mission mix must be determined for crack growth analysis. A mission mix is defined as the distribution or number of each flight of each profile occurring in a predefined loading block. If the loading block is 1,000 flights, then the 24 flights that make up the six profiles used as an example in Section 5.1 would have to occur a total of 1,000 times. This mission mix is used by crack growth programs to define how often and when each flight in the stress spectrum occurs.

Table 5-4 shows the percentage and mean flight time of each of the six flight profiles from the example problem. To determine the mission mix of the aircraft under consideration, multiply the % Total of Flights column by 1000 to get the number of flights of each profile in the 1000 flight block. Next, multiply the number of flights by 0.9 (90%) to determine the number of 1/1 flights, and multiply the number of flights by 0.09 (9%) to determine the number of 1/10 flights. Multiply the number of flights by 0.009 (0.9%) to determine the number of 1/100 flights, and finally multiply the number of flights by 0.0009 (0.09%) to determine the number of 1/1000 flights. Repeat these steps for each flight profile. Table 5-4 shows sample flight numbers for the example in Appendix A for a 1,000 flight block.

TABLE 5-4

FLIGHT DISTRIBUTION EXAMPLE (1000 FLIGHT BLOCK)

Flight Profile	% Total of Flights	Total Flights (1000 flt block)	1/1 Flights (90% Tot. flts)	1/10 Flights (9% Tot. flts)	1/100 Flights (0.9% Tot. flts)	1/1000 Flights (0.09% Tot. flts)
1	11.9%	119	107.1	10.71	1.07	0.107
2	27.3%	274	246.6	24.66	2.47	0.247
3	20.5%	206	185.4	18.54	1.85	0.185
4	19.7%	197	177.3	17.73	1.77	0.177
5	11.6%	116	104.4	10.44	1.04	0.104
6	8.8%	88	79.2	7.92	0.79	0.079
	$\Sigma = 100\%$	$\Sigma = 1000$				

After determining the number of each of the flights that occurs in a 1,000 flight block, each flight needs to be rounded to a whole number. Since none of the 1/1000 flights would round to 1, one of them should be chosen to appear in the mission mix. In this example, the 1/1000 flight from Profile 2 is chosen to occur once because it is larger. The other five profiles' 1/1000 flights will not occur in the mission mix. Table 5-5 shows the final mission mix for the example.

TABLE 5-5

MISSION MIX EXAMPLE (1000 FLIGHT BLOCK)

Flight Profile	1/1 Flights	1/10 Flights	1/100 Flights	1/1000 Flights	
1	107	11	1	0	
2	247	25	2	1	
3	186	18	2	0	
4	177	18	2	0	
5	104	10	1	0	
6	79	8	1	0	
	$\Sigma = 900$	$\Sigma = 90$	$\Sigma = 9$	$\Sigma = 1$	$\Sigma = 1000$

The mission mix should be reviewed to verify that the sums of each flight type are correct and that the total number of flights equals 1,000. By adding a 1/1000 flight, sometimes a 1/100 flight will need to be subtracted for the same profile so that the respective columns in Table 5-5 add to 900, 90, 9, and 1.

After the mission mix is defined, the order of the flights is usually randomized before adding it to the stress spectrum file. This is done because the flight order sequencing has an effect on the crack growth rate when retardation (load interaction) is considered. Retardation effects are influenced by the order in which high loads are encountered. The 1/1000 and 1/100 flights will have higher loads than the 1/1 and 1/10 flights. Therefore the order in which the flights occur will affect the crack growth life of the critical area of the PSE under consideration. The format of the mission mix depends on the crack growth computer program used.

5.4 Alternate Approach

As an alternate approach to defining a mission mix with several flights, the flight representing the most severe usage may be chosen to represent all flights. The advantage of using the most severe flight is that the flight profile definition will be simplified as well as the damage tolerance analysis. The disadvantage is that the inspection intervals and replacement times will be shorter than necessary for airplanes that are not flown as severely as what was analyzed. The trade-off in savings between reduced analysis time versus the increased maintenance costs due to additional inspections/replacements will have to be evaluated.

6.0 Development of Load Spectrum

Before a damage tolerance analysis can be conducted, the load factor spectrum must be developed. The load spectrum is used to generate a stress spectrum for each critical area of a PSE selected as discussed in Section 7.0. In turn, the stress spectrum for each PSE is used for analytical fatigue and crack growth calculations.

In a static structural analysis, only the magnitude of the load is required. In a fatigue analysis, the frequency and the magnitude of the loads must be established. When an aircraft is certified, the airplane must have met specific limit and ultimate load factors. With the exception of fuselage pressurization, fatigue loads are based on the airplane load factor, N_z . N_z is the vertical acceleration of the airplane's center of gravity, expressed in terms of the earth's acceleration of gravity, $g \approx 32 \text{ ft/sec}^2$. For straight and level flight, $N_z = 1$.

The load spectra can be developed in two categories:

- Spectra for major airframe components Section 6.1
- Spectra for landing gear components Section 6.2

If spectrum load data has been recorded for the airplane type under consideration (representing typical service), then this data should be used in preference to the data referenced in this section.

6.1 Airframe Load Spectra

The loading spectrum is a function of the "type" of aircraft (pressurized, non-pressurized, single or twin-engine) and utilization (normal or severe). Usage data from similar type aircraft has been gathered and is used in this section to aid in definition of the load spectra. Maneuver loads are a significant contributor to the fatigue load spectra. Air turbulence (gust) is the largest contributor to the fatigue spectra which can exceed 70% of the load cycles in light twin-engine commuter aircraft. The rest of the loads are due to landing, taxiing, etc. Table 6-1 summarizes the load spectra discussed in this section which are to be considered in the damage tolerance evaluation of all airframe PSEs depending upon their location in the airframe. The table also references the section where each load spectra is described in more detail.

For each load spectra type, a table of load factors and load occurrences must be developed. These tables are used to generate the stress spectrum described in Section 7.0.

TABLE 6-1
TYPICAL AIRFRAME LOAD SPECTRA SUMMARY

<u>Load Spectra</u>	<u>Section</u>	Airframe Component				
		<u>Wing and Carry-Through</u>	<u>Fuselage</u>	<u>Horizontal Tail</u>	<u>Vertical Tail</u>	<u>Engine Support</u>
Maneuver	6.1.1	X	X	X	X	X
Vertical Gust	6.1.2	X	X	X	X	X
Lateral Gust	6.1.2		X	1	X	X
Taxi	6.1.3	X	X	X		X
Landing Impact	6.1.4	X	X			X
Ground-Air-Ground (GAG)	6.1.5	X	X	X	X	X
Balancing Tail Load	6.1.6			X	1	
Thrust	6.1.7	2	3			X
Cabin Pressurization	6.1.8		X			
Propeller Slipstream	6.1.9			X		

- 1 May be significant for T-tail configurations.
- 2 Significant when engine mounted on wing.
- 3 Significant when engine mounted to fuselage.

NOTE: Load spectra for unique features such as canards and winglets are addressed in ACE-100-01 (Reference 29).

6.1.1 Maneuver Loads

The maneuver load spectrum is defined in terms of load factor (N_z) at the aircraft center of gravity. Maneuver loads are encountered when the aircraft is turned. For most aircraft, turning maneuvers are experienced right after takeoff and just before landing. However, depending on the usage of the aircraft under consideration, turning maneuvers could be experienced throughout all segments of the flight. The effects of pitching and rolling are generally considered negligible for most airframe components. Therefore, maneuvers are considered symmetric steady state conditions, with gradual initiation.

Maneuver loads for commuter type aircraft are normally encountered during steady, coordinated turns. These loads usually do not exceed 1.3 g's ($N_z = 1.3$). The bank angle and the aircraft's speed during the turn determine the load factor encountered for that particular turning maneuver. Figure 6-1 shows a sample flight in which load factor vs. time is plotted. This particular example shows an aircraft that experiences maneuver loads throughout each segment of the flight. It also illustrates how the fatigue load spectrum is obtained from a series of maneuver loads. It is obtained by counting only the positive and negative peak excursions and grouping them into cycles as shown in the lower graph.

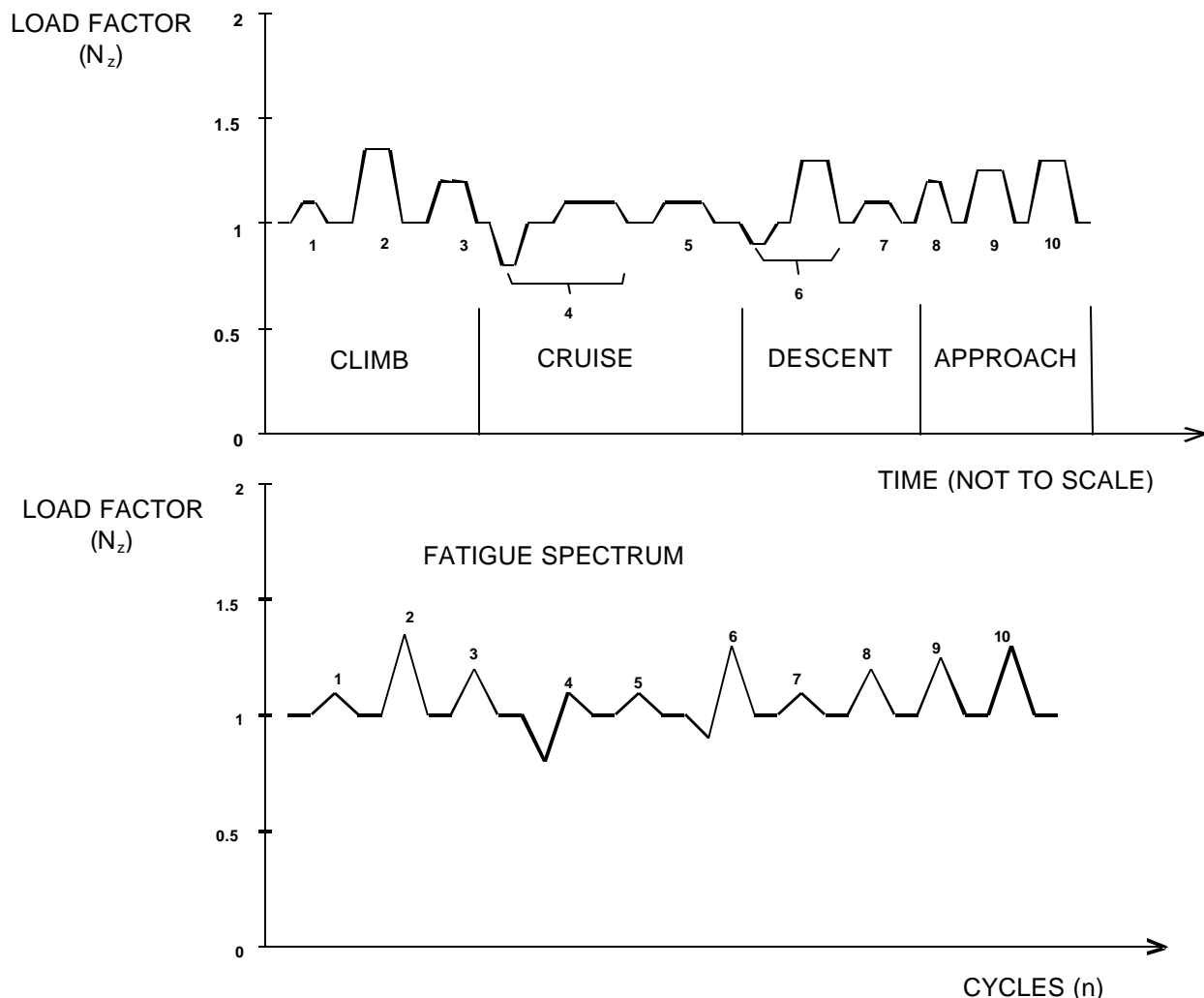
For the aircraft under consideration, similar type and usage data should be used to make a maneuver occurrence table for analysis. Maneuver exceedance curves can be found for several types and usages of aircraft in the following references.

- | | |
|-------------------------------|--------------|
| • FAA Report No. AFS-120-73-2 | Reference 30 |
| • DOT/FAA-CT-91/20 | Reference 31 |
| • TM-84660 | Reference 32 |
| • MIL-A-8866B | Reference 33 |
| • NASA SP-270 | Reference 34 |

Figure 6-2 shows example maneuver exceedance curves from two of the five references for twin engine executive usage. The data in References 30 and 31 are given as the cumulative frequency of exceedance per nautical mile versus load factor fraction. For analysis purposes, this data should be converted to exceedances per 1000 flights. References 32, 33, and 34 are presented in this format. Figure 6-3 shows the converted curve to exceedances per 1000 flights for References 30 and 31, along with data obtained from References 32 and 34 for a fictitious aircraft, the Acme Model 999. References 30 and 31 present a series of equations that can be used to convert the data back and forth between the two chart formats for a specific airplane. The following terms are used in these conversion equations.

FIGURE 6-1

MANUEVER SPECTRUM TIME HISTORY



a_n = incremental load factor, expressed in terms of g's = ΔN_z

a_{nLLF} = design limit load factor for a certain flight condition (i.e. maneuver or gust), expressed in terms of g's

a_n/a_{nLLF} = acceleration fraction, dimensionless

Appendix C presents an example of the conversion process from cumulative frequency of exceedance per nautical mile format to exceedances per 1000 flights format.

FIGURE 6-2

MANEUVER LOAD FACTOR SPECTRUM (CUM. EXCD/NAUT. MILE)

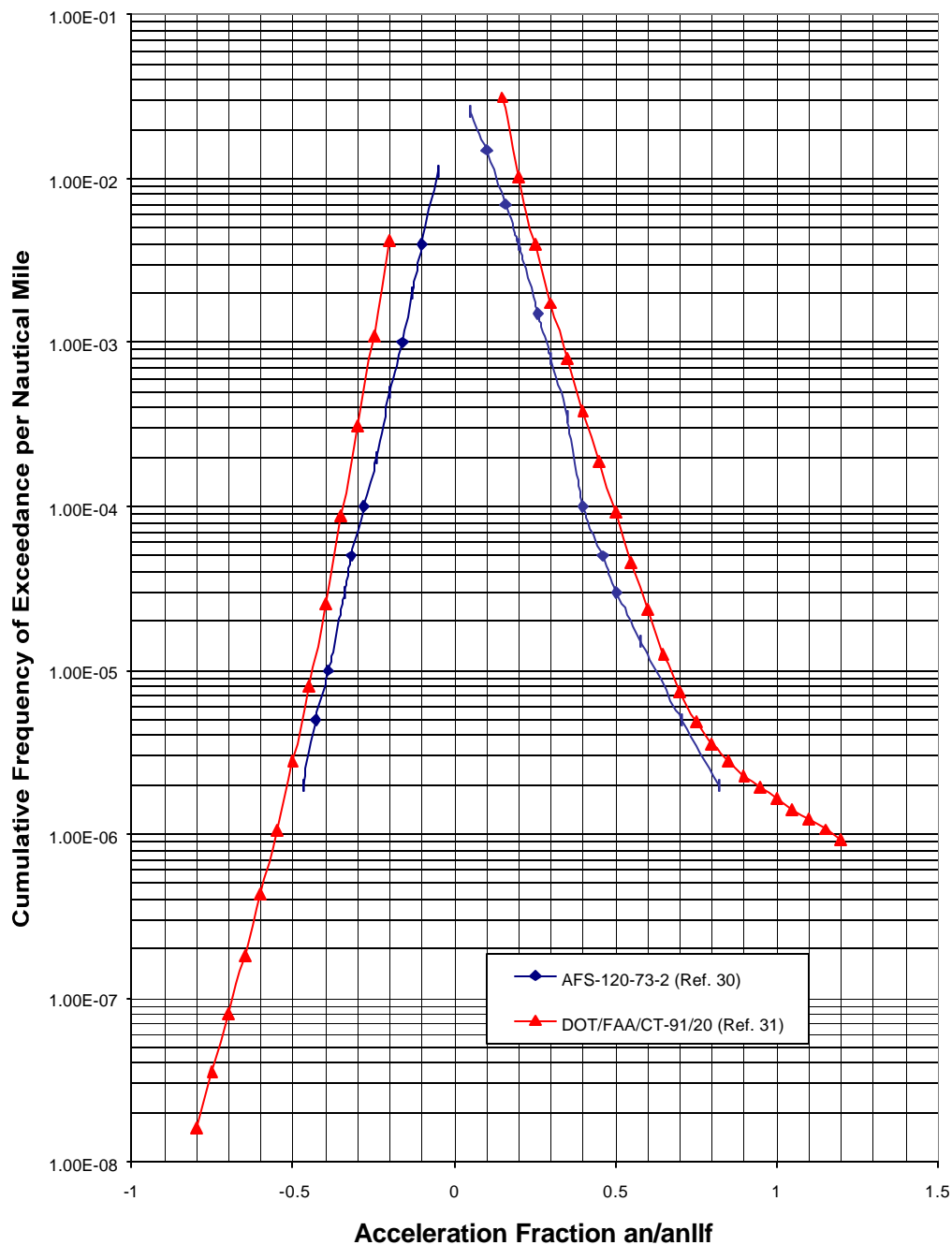
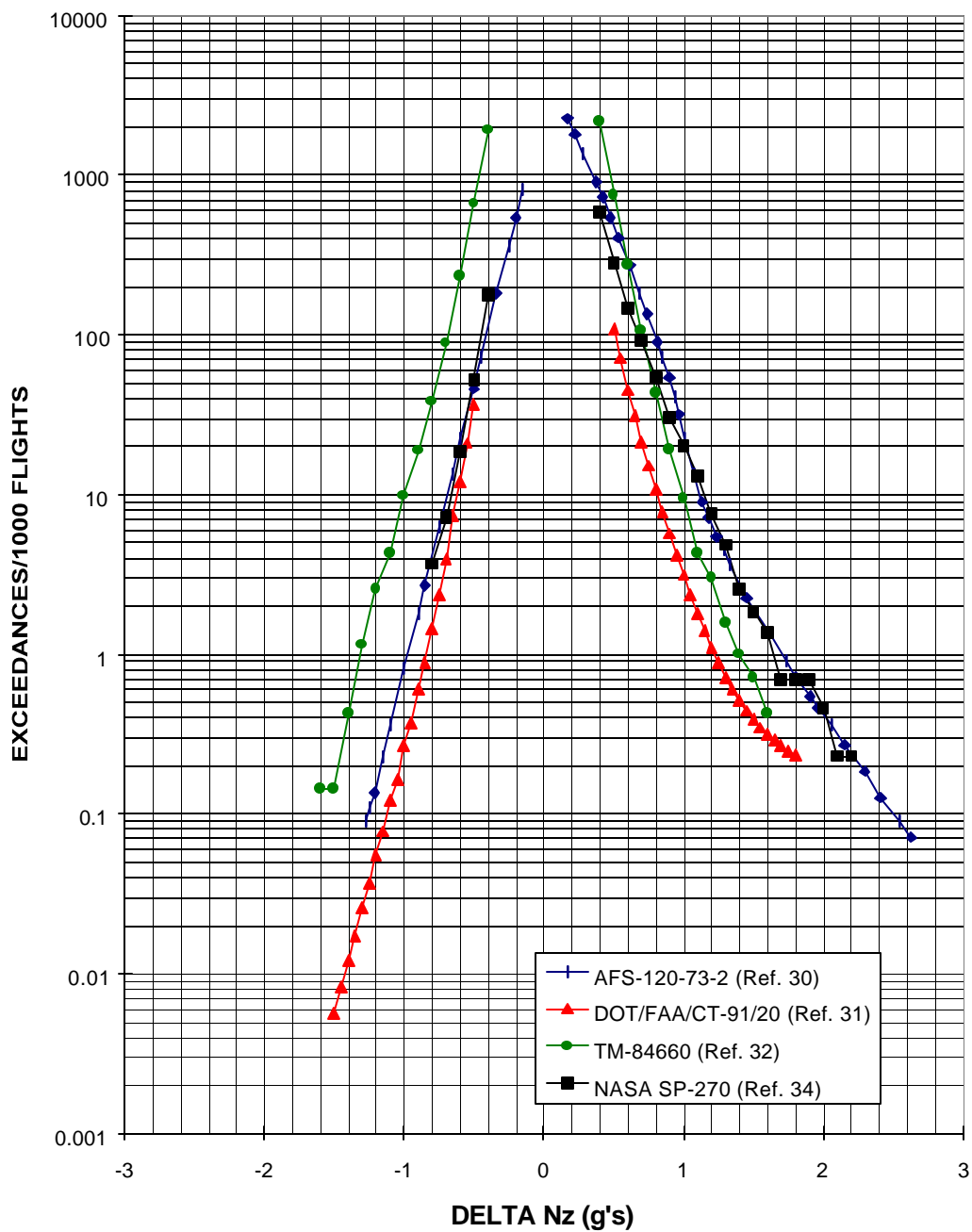


FIGURE 6-3

MANEUVER LOAD FACTOR SPECTRUM (EXCD/1000 FLTS)
FOR THE ACME MODEL 999 AIRCRAFT



The terms exceedance and occurrence will be used frequently in this section to describe the load factor spectrum generation methods. Exceedances are defined as the number of times a certain level or value is exceeded, whereas occurrences are defined as the number of times a certain level or value is attained. An occurrence table provides the best example for these definitions. In Table 6-2, a column of load occurrences is presented to indicate how many times each load factor level is attained. Exceedances will be calculated next to the occurrences to demonstrate how to go from occurrences to exceedances. Starting at the bottom of the table, a 2.60 N_z maximum load factor is reached 0.4 times. Since this is the highest level reached it is only exceeded by this level's number of occurrences, 0.4. Therefore, at a N_z of 2.60, there are 0.4 exceedances. At the next lower level, 2.50 g's, there are 0.3 occurrences. The number of exceedances at this level are 0.3 + 0.4 from the 2.60 g level. Therefore, there are 0.7 exceedances of the 2.50 g load level. To calculate exceedances, the previous level's exceedances are added to the current level's occurrences.

The occurrences for the Reference 32 curve of Figure 6-3 are listed in Table 6-2 in the form of load factor occurrences per 1000 flights. Load cycles and occurrences are defined from the curves of Figure 6-3 by combining positive and negative incremental load factors at the same exceedance level. The difference between the current and previous exceedance levels equals the occurrences for the current exceedance level. A table like Table 6-2 (minus the Exceedances/1000 Flights) should be directly entered into a load file. This load factor occurrence file will be used to calculate stress spectra as described in Section 7.0.

TABLE 6-2

SAMPLE MANEUVER LOAD FACTOR OCCURRENCES (REF. 32)

Maximum N_z	Minimum N_z	Occurrences per <u>1000 Flights</u>	Exceedances per <u>1000 Flights</u>
1.4	0.6	1400.0	2000.0
1.55	0.5	400.0	600.0
1.62	0.39	160.0	200.0
1.81	0.2	30.0	40.0
2.0	0.0	5.0	10.0
2.1	-0.08	3.0	5.0
2.27	-0.22	1.3	2.0
2.5	-0.35	0.3	0.7
2.6	-0.40	0.4	0.4

6.1.2 Gust Loads

An airplane in flight encounters gusts of random magnitude at random times. Up to 70% of the total fatigue load cycles may be due to gust load cycles. The airplane

load factors associated with gusts are generally symmetrically distributed above and below the 1g condition. In order to determine the contribution of gust to the fatigue load spectra, analysis of flight gust data is required.

Gust data, to be used in load spectrum development, can be found for several types and usages of aircraft in the following references.

- FAA Report No. AFS-120-73-2 Reference 30
- DOT/FAA-CT-91/20 Reference 31
- ESDU 69023 Reference 35
- PSD Gust Spectrum Analysis, Part 2-5
Appendix G to 14 CFR Part 25 of the FAR's

The data from the first three references represents a compilation of measured data. This data is discussed in Section 6.1.2.1. An alternate way to generate a vertical or lateral gust load spectrum is to use a Power Spectral Density (PSD) function to predict the load exceedances on the aircraft structure. PSD methods are discussed in Section 6.1.2.2.

Two types of gust loading are used in the analysis of airframe PSEs: vertical gust and lateral gust. Vertical gusts are usually expressed in terms of vertical acceleration (N_z) at the aircraft center of gravity location. Lateral gusts are usually defined in terms of lateral gust velocity (U_{de}) at the aircraft cg or at the vertical tail center of pressure location.

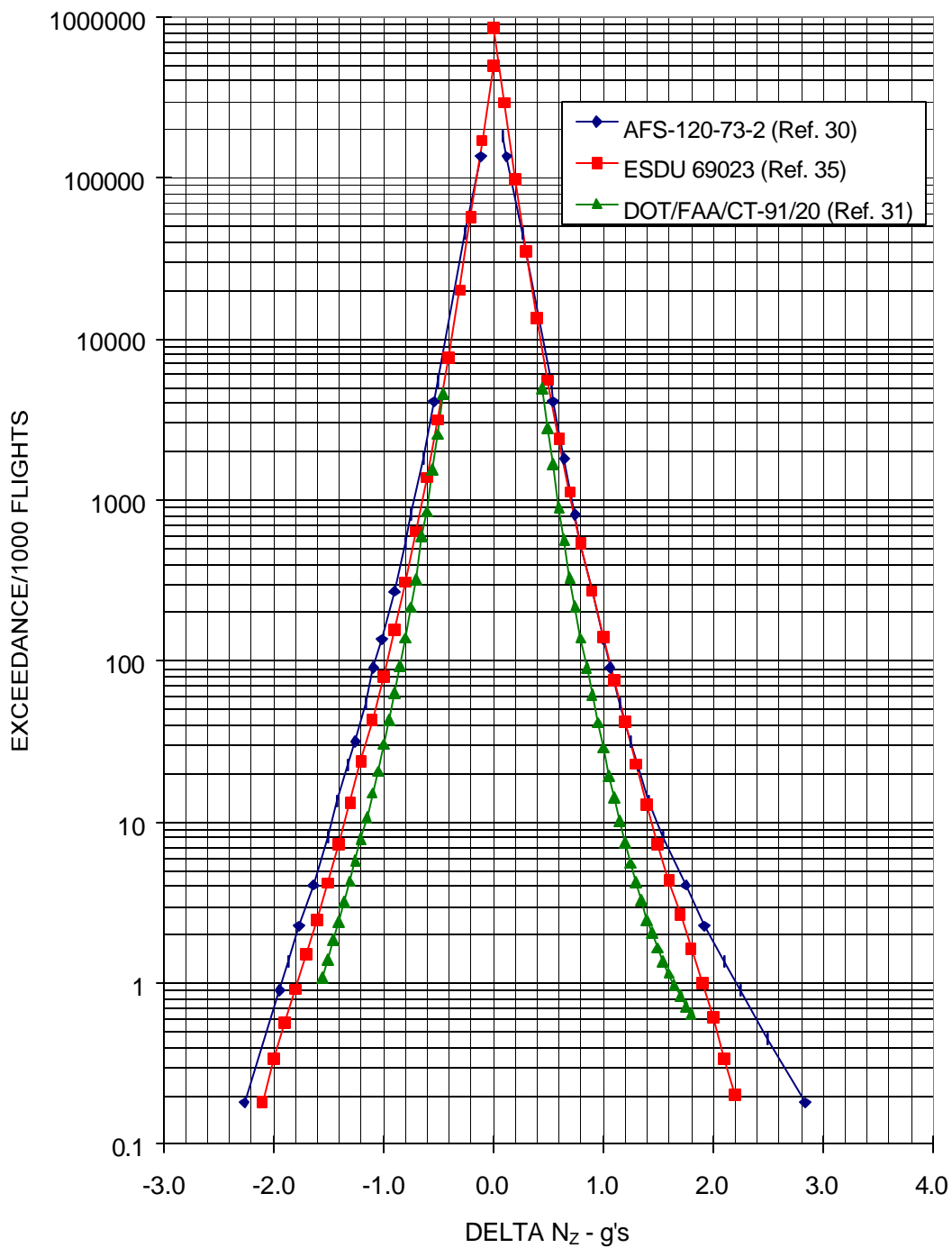
6.1.2.1 VGH Gust Data

Figure 6-4 shows a comparison of overall vertical load factor exceedance data compiled from the three references noted in the previous section for the Acme Model 999 aircraft. The data presented in these three references is derived using the VGH (Velocity, acceleration, and altitude) recording method. This comparison is based on data representing twin-engine executive usage. References 30 and 31 are expressed in terms of a_n/a_{nLLF} and are converted to ΔN_z as described in Appendix C.

The data presented in ESDU 69023 is a compilation of normalized gust exceedances obtained from subsonic transport aircraft in scheduled operation. Dynamic effects (structural flexibility) are not included, although twin-engine propeller aircraft are considered relatively stiff structures, requiring little or no adjustment for dynamic effects. Of References 30, 31 and 35, ESDU is the

FIGURE 6-4

VERTICAL GUST LOADS EXCEEDANCE COMPARISON
FOR THE ACME MODEL 999 AIRCRAFT



preferred method of obtaining gust load data. A computer program can be developed to convert ESDU data to incremental load factor ΔN_z exceedances as a

function of aircraft weight, altitude, aircraft geometry and aerodynamics. Some of the required program input data for each profile flight segment, as determined in Section 5.0 includes:

- Weight
- Altitude
- Mean Chord
- Slope of Lift Curve
- Velocity
- Wing Area
- Mach Number
- % time of total flight profile

Some of the intermediate calculations include:

- Nautical miles flown to encounter a 10 fps gust
- Ratio of up gusts to down gusts occurrences
- Gust alleviation factor
- Delta N_z factor (ΔN_z) (or ΔU_{de} for lateral gusts)

Load cycles and occurrences are defined from the exceedances by combining positive and negative incremental load factors at the same exceedance level. Each flight profile composite is the sum of the individual segment exceedances multiplied by the individual segment mission factor. The composite N_z exceedances multiplied by the corresponding percent of total flight hours for the individual profiles is shown in Figure 6-4 and in table format in Table 6-3 for the Acme Model 999 aircraft.

The lateral gust load spectrum is defined in terms of gust velocity exceedances. This spectrum can also be developed from Reference 30, 31, or 35 data. For the same gust velocity, lateral gust exceedances are assumed equal to vertical gust exceedances. Therefore the exceedance curves from References 30 or 31 can be used for lateral gust after conversion of a_n to U_{de} to L_{tv} as described in Appendix C. Two assumptions must be made: (1) the overall gust environment is isotropic, and (2) a lateral gust in one direction is followed by one of equal magnitude in the opposite direction. For vertical aerodynamic surfaces (fin, rudder, winglets), the occurrence factor of 2 is applied to lateral gust occurrences to account for maneuver loading and the dynamic response of the empennage to lateral gusts. This is done because there is no rational vertical tail maneuver spectrum or dynamic analysis of the empennage response to a gust spectrum. This approach has been recommended by some foreign certification agencies. A computer program can be developed to convert ESDU data to gust velocity exceedances as a function of aircraft weight, altitude, aircraft configuration and aerodynamics. The input parameters and procedures used to calculate the gust velocity exceedances are nearly identical to those used for the vertical gust spectrum. Table 6-4 and Figure 6-5 show an example lateral gust spectrum for the Acme Model 999 aircraft expressed in terms of ΔU_{de} .

TABLE 6-3

VERTICAL GUST LOAD EXCEEDANCES FOR ACME MODEL 999
(FROM REFERENCE 35)

<u>Maximum N_z</u>	<u>Minimum N_z</u>	<u>Occurrences/1000 Flts</u>
1.10	0.95	300,000
1.30	0.78	40,000
1.45	0.65	10,000
1.72	0.35	1,000
1.93	0.15	200
2.10	-0.05	70
2.30	-0.25	20
2.50	-0.40	6
2.75	-0.65	2
2.95	-0.83	0.8
3.10	-0.95	0.4
3.20	-1.10	0.2

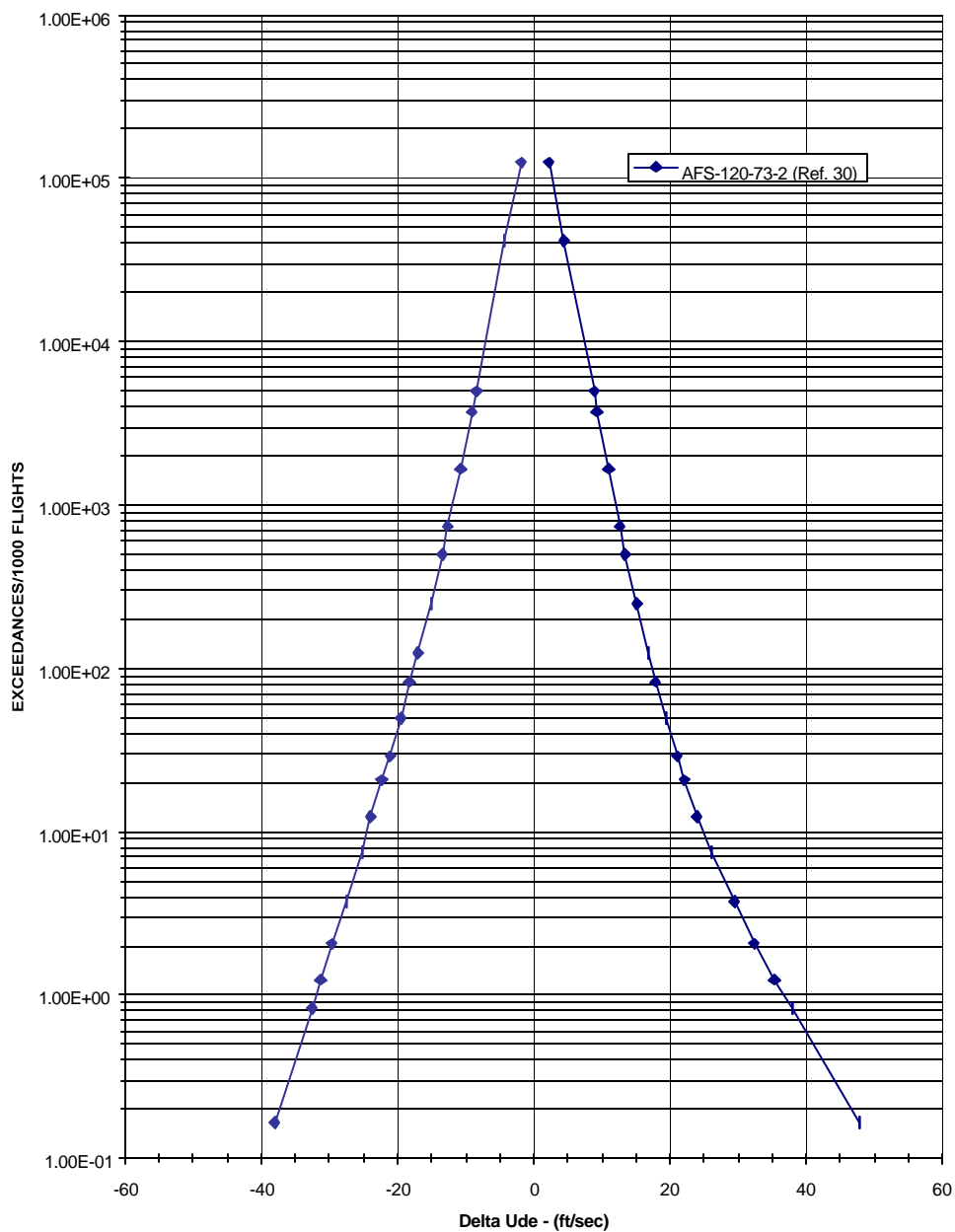
TABLE 6-4

LATERAL GUST LOAD EXCEEDANCES FOR ACME MODEL 999
(FROM REFERENCE 30)

<u>Maximum U_{de} (ft/sec)</u>	<u>Minimum U_{de} (ft/sec)</u>	<u>Occurrences/1000 Flts</u>
2.15	-1.89	82955.00
4.42	-4.42	36500.00
8.84	-8.42	1244.30
9.26	-9.05	2073.90
10.94	-10.73	912.50
12.62	-12.62	248.86
13.47	-13.47	248.86
15.15	-15.15	124.43
16.83	-17.00	41.48
17.89	-18.31	33.18
19.36	-19.57	20.74
21.04	-21.04	8.30
22.09	-22.30	8.30
23.90	-23.99	4.98
26.09	-25.25	3.73
29.46	-27.56	1.66
32.32	-29.67	0.83
35.35	-31.35	0.41
37.87	-32.61	0.66
47.76	-38.09	0.17

FIGURE 6-5

LATERAL GUST LOAD SPECTRUM (EXCD/1000 FLTS)
FOR THE ACME MODEL 999 AIRCRAFT



6.1.2.2 PSD Gust Loads

An alternative way to generate vertical (in terms of normal acceleration, ΔN_z) and lateral (in terms of lateral velocity, ΔU_{de}) gust loads is to use a Power Spectral Density (PSD) function to predict the load exceedances on an aircraft structure. The Continuous Gust Design Criteria (PSD) of Appendix G to 14 CFR Part 25 of the Federal Aviation Regulations (FAR's) spells out the PSD method of gust load calculations. The PSD approach has an advantage over the other approach in that it accounts for structural dynamic effects. PSD parameters \bar{A} , N_0 , and y_{one-g} are analytically determined for primary loading terms (shear, and/or bending moment, and/or torque) over all areas of the aircraft. The \bar{A} , N_0 terms are calculated from dynamic models of the aircraft structure (finite element models that are modeled to approximate the dynamic response of the aircraft to loading). The y_{one-g} terms are taken from static loads analyses and from flight strain survey data. These loads are generally developed from aircraft flight profile data (see Section 5.0). From these values, an exceedance curve of applied load is developed, from which a spectrum of stresses is derived.

The frequency of load-exceedance for each flight profile segment is found by:

$$N(y) = t N_0 \left[P_1 \cdot \exp\left(-\frac{|y - y_{one-g}|}{b_1 \bar{A}}\right) + P_2 \cdot \exp\left(-\frac{|y - y_{one-g}|}{b_2 \bar{A}}\right) \right]$$

where:

t = selected time interval (1000 hours)

y = net value of the load for which an exceedance value is needed (whether moment, shear, torque, or load factor)

y_{one-g} = value of load at 1g level flight

$N(y)$ = number of exceedances for the chosen load value, y

N_0, \bar{A} = PSD parameters

P_1, P_2, b_1, b_2 = parameters defining the probability distributions of rms gust velocity (Figures 6-6, 6-7). Note that $P_1, P_2, b_1,$ and b_2 are taken from Appendix G to 14 CFR Part 25 of the FAR's. These values are subject to change. The latest values should be used.

Figure 6-8 presents an outline of the steps taken to develop the gust load spectra. Steps A thru F are explained in the following paragraphs.

FIGURE 6-6

PSD PROBABILITY DISTRIBUTIONS b1 AND b2

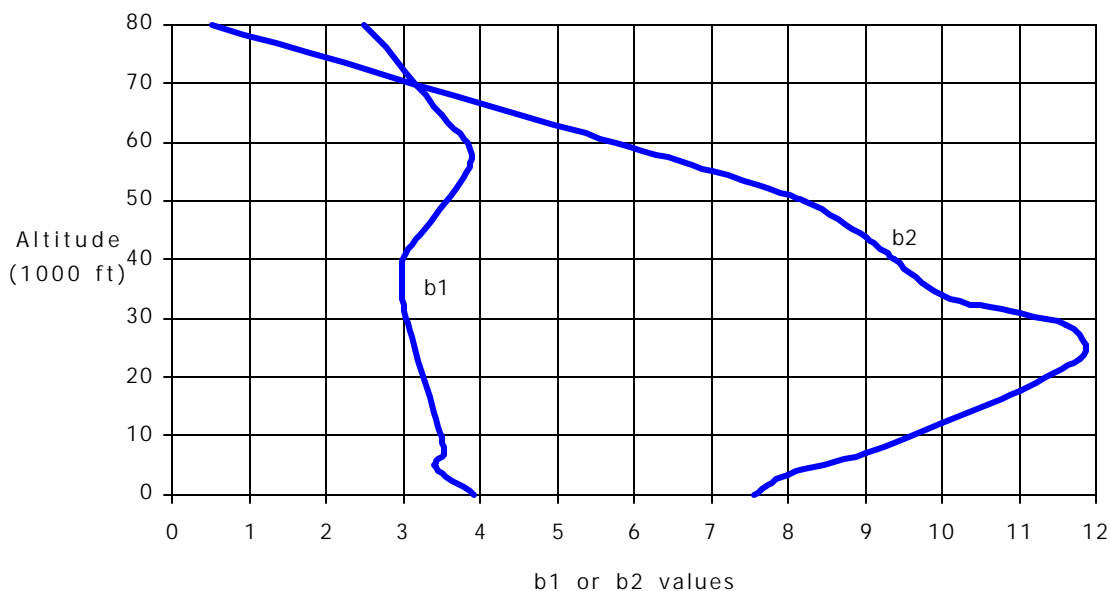


FIGURE 6-7

PSD PROBABILITY DISTRIBUTIONS P1 AND P2

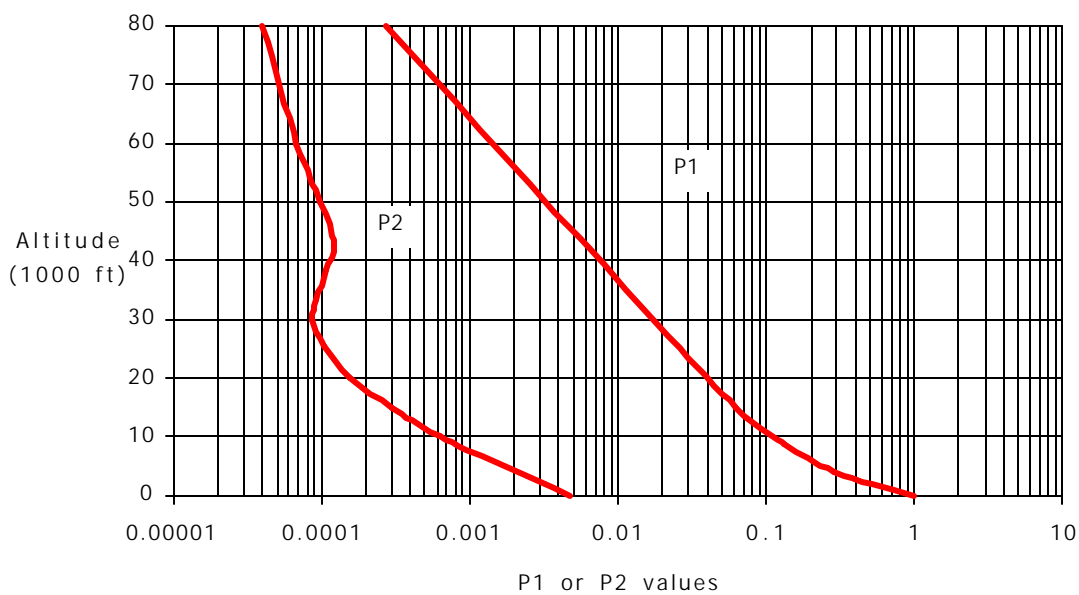
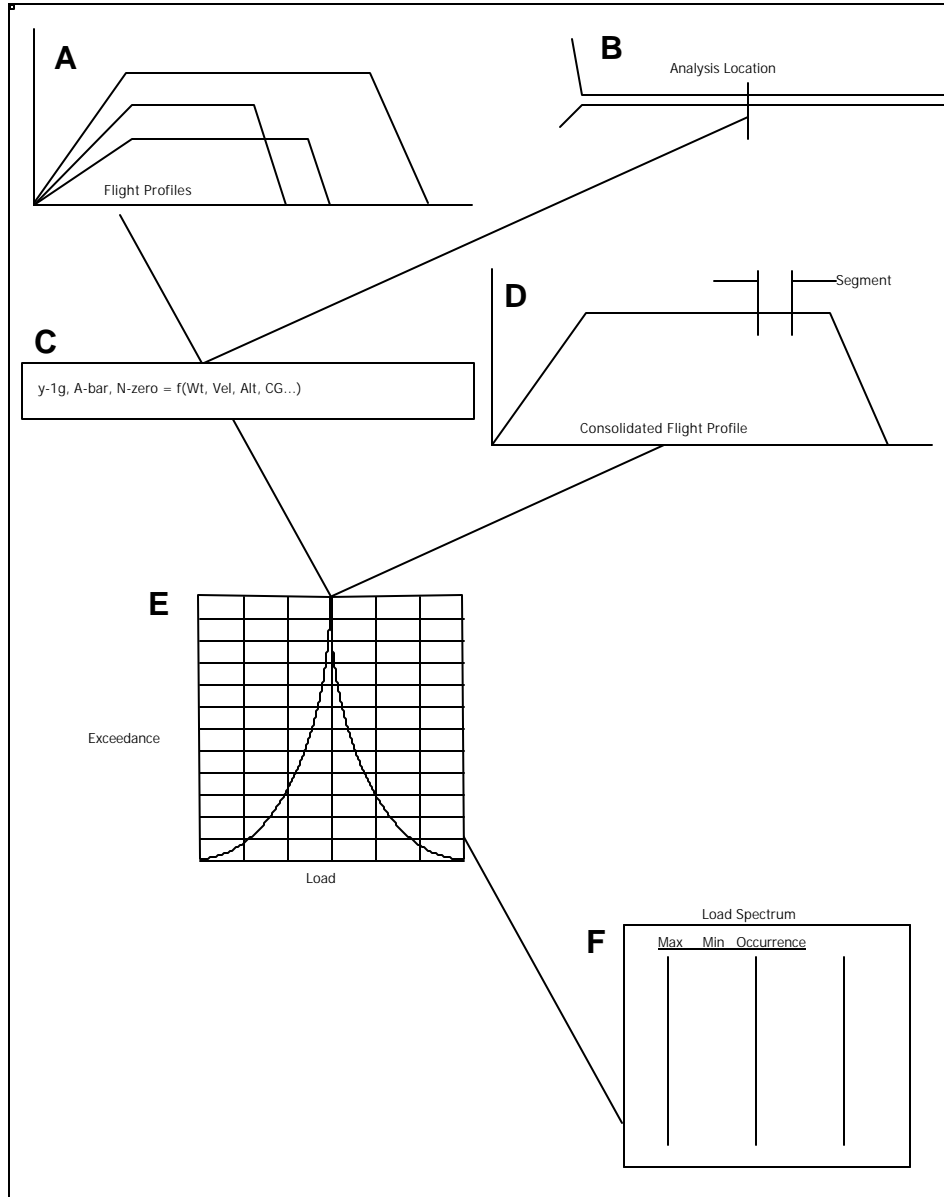


FIGURE 6-8

GUST SPECTRUM DEVELOPMENT – PROCESS FLOW



The PSD terms, $\bar{\Delta}$, N_0 , y_{one-g} , (and therefore the spectrum) are not calculated directly in terms of stress for each analysis location. Instead, the terms are developed first for the loading type (shear, bending moment, or torque), and then the resulting load type spectrum is converted to a stress spectrum through a constant transfer stress factor for each location. The transfer factor is derived from flight

strain data or analysis. This approach simplifies, without loss of accuracy, the number of locations for which PSD terms must be developed.

Additionally, instead of calculating the PSD terms directly for each flight segment, a general equation (for each PSD term) is first developed as a function of flight parameters (velocity, weight, altitude,...) from which the required terms can then be determined. This approach will not require repeated loads development for each flight profile and loading configuration.

$\bar{\Delta}$'s and N_0 's are calculated for a wide range of aircraft parameters (Step A, Figure 6-8) for the critical areas of the PSEs (Step B, Figure 6-8). Steady-state maneuver loads are also calculated for these same locations and conditions using a variety of load factors (avoid any non-linear regions of the flight envelope such as pre-stall buffet).

From these specific results a general equation is developed, using multiple regression techniques for each location. The following equations are given as examples of what the general equations may look like (Step C, Figure 6-8).

$$\bar{\Delta} = g_0 + g_1(\text{fuel})^2 + g_2(\text{wt}) + g_3(\text{keas}) + g_4(\text{keas})^2 + g_5(\text{cg}) + g_6(\text{cg})(\text{wt}) + g_7(\text{altitude}) + g_8(\text{thrust})$$

$$N_0 = r_0 + r_1(\text{fuel}) + r_2(\text{wt}) + r_3(\text{cg}) + r_4(\text{kcas}) + r_5(\text{altitude})$$

$$\text{Load} = m_0 + m_1(N_z)(\text{fuel})^2 + m_2(N_z) + m_3(N_z)(\text{wt}) + m_4(\text{keas})^2 + m_5(\text{cg})(\text{keas})^2 + m_6(\text{flap})(\text{keas})^2 + m_7(\text{pressure}) + m_8(\text{thrust}) + m_9(\text{mach}) + m_{10}(\text{mach})^2$$

where:

- fuel = total fuel weight (lb.)
- wt = aircraft weight (lb.)
- cg = aircraft cg as percent MAC
- kcas = calibrated airspeed (knots)
- altitude = pressure altitude (ft)
- N_z = aircraft vertical load factor at cg (g's)
- keas = equivalent airspeed (knots)
- thrust = total aircraft net thrust (lb.)
- pressure = cabin pressure
- mach = mach number of airspeed

and:

The load equation is used to define the y_{one-g} load by setting the ' N_z ' term to 1. The same equation form is used for all areas, hence the use of a pressure term which is set to zero for use with all non-fuselage (pressurized) locations.

For each flight segment of the overall flight profile (Step D, Figure 6-8) the aircraft terms (fuel, keas, wt,...) are combined with the PSD terms to generate the load exceedance curve (Step E, Figure 6-8).

The resulting exceedance curve is continuous for all values of load type away from the center, y_{1g} value. In order to reduce the spectrum size, the curve is limited to the exceedance level representing a load of once per lifetime. Further, the exceedance curve is divided into a minimum of ten even load increments (per side) to define the Max-Min-Occurrence table required to calculate the stress spectrum. Although the maximum value of gust load used in each flight segment will always represent the load exceeded once per lifetime, the smaller (more frequent) loads in the max-min table will not necessarily correspond to equivalent exceedances across different flight segments.

The final spectrum, as defined here, is in terms of the applicable load type at each location. The conversion from load type to stress is accounted for by a constant stress factor.

6.1.3 Taxi Loads

Taxi load factor spectra are usually derived in terms of vertical load factor occurrences at the aircraft center of gravity per 1000 flights. For the aircraft under consideration, similar type and usage data should be used to make a taxi occurrence table for analysis.

Taxi data can be found in the following references:

- AFS-120-73-2 Reference 30
- MIL-A-8866B Reference 33
- MIL-A-87221 Reference 36
- ESDU 75008 Reference 37

Figure 6-9 shows an exceedance curve for References 30 and 33 as an example. Table 6-5 lists the loads and occurrences for the taxi spectrum from Reference 33. Occurrence tables like Table 6-5 should be directly entered into the load file. This load factor occurrence file will be used to calculate stress spectra as described in Section 7.0.

FIGURE 6-9
TAXI LOAD FACTOR SPECTRUM

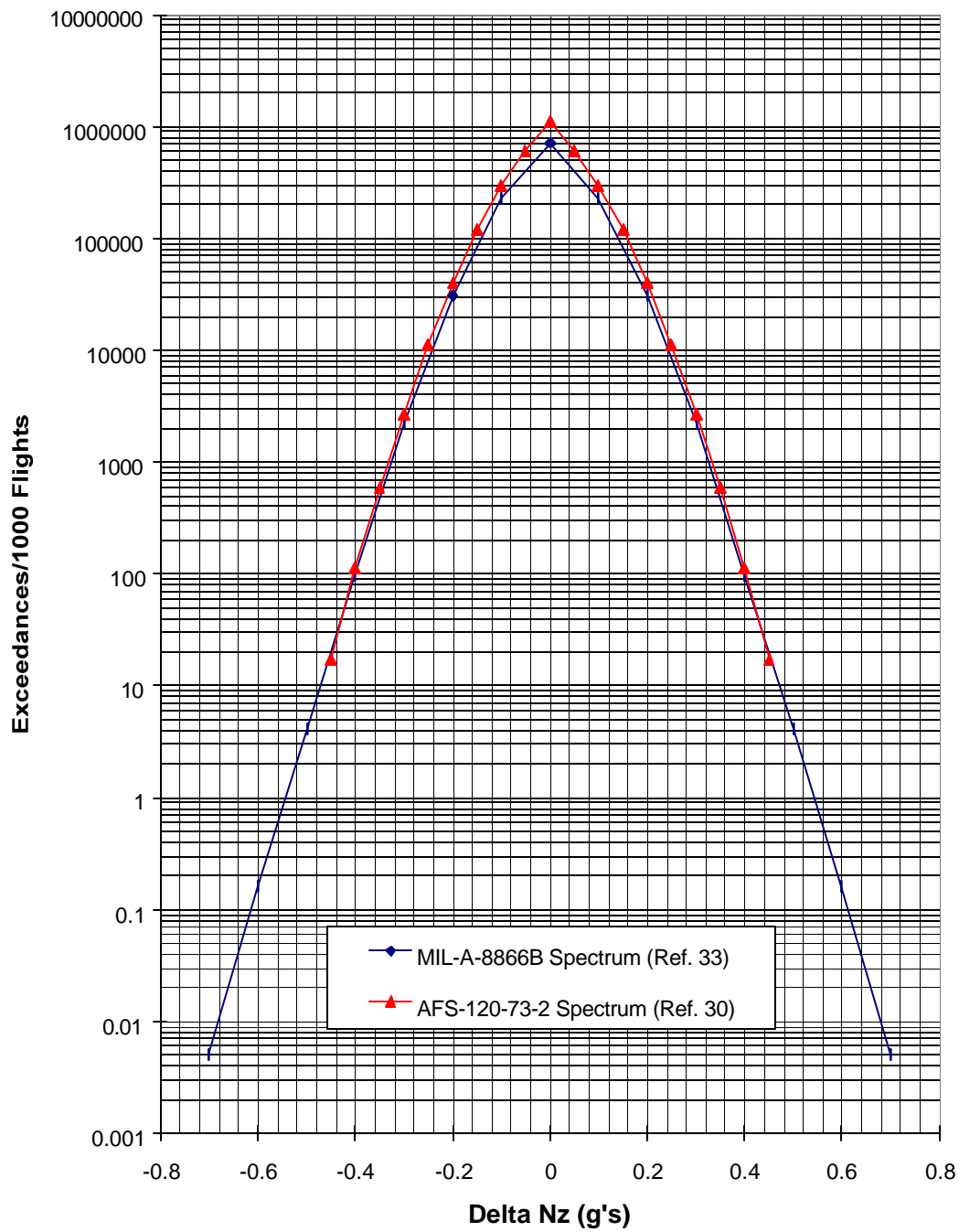


TABLE 6-5

TAXI LOAD FACTOR OCCURRENCES (REF. 33)

<u>Maximum Load Factor (+Nz)</u>	<u>Minimum Load Factor (+Nz)</u>	<u>Occurrences Per 1000 Flights</u>
1.05	0.95	300,000
1.15	0.85	165,000
1.25	0.75	27,000
1.35	0.65	2,000
1.45	0.55	90
1.55	0.45	4
1.65	0.35	0.150
1.75	0.25	0.005

6.1.4 Landing Impact Loads

Landing impact load factor spectra are usually derived in terms of landing sink rate per 1000 flights or landings. Landing impact data can be found in the following references:

- | | |
|----------------|--------------|
| • AFS-120-73-2 | Reference 30 |
| • MIL-A-8866B | Reference 33 |

The sink rates and occurrences for the landing impact spectrum are shown for executive twin usage for Reference 30 in Figure 6-10. Table 6-6 lists the occurrences from Reference 30. A table similar to this can be directly entered into the load file. This occurrence file for sink rates will be used to calculate stress spectra as described in Section 7.0.

6.1.5 Ground-Air-Ground Cycle

The ground-air-ground (GAG) spectrum is defined as the stress cycle per flight encompassing the maximum flight stress excursion and the minimum ground stress excursion. This cycle represents the effect of transition from the landing gear to the wing, and back to the landing gear again, as the support for the aircraft weight. This large stress change occurs once per flight due to the operational cycle. The airplane has negative or low positive loads while on the ground, encounters variable loads while taxiing, is subjected to variable gust and maneuver loads, fuel burn-off occurs, and finally experiences landing and taxi loads (see Figure 6-11, taken from Reference 38). The GAG cycle is not an additional spectrum (as with gust or maneuver), but is instead a method of accounting for the large stress range that otherwise would not be included. Section 7.3.1 addresses the addition of the GAG cycle into the final stress spectrum.

FIGURE 6-10
LANDING IMPACT SPECTRUM

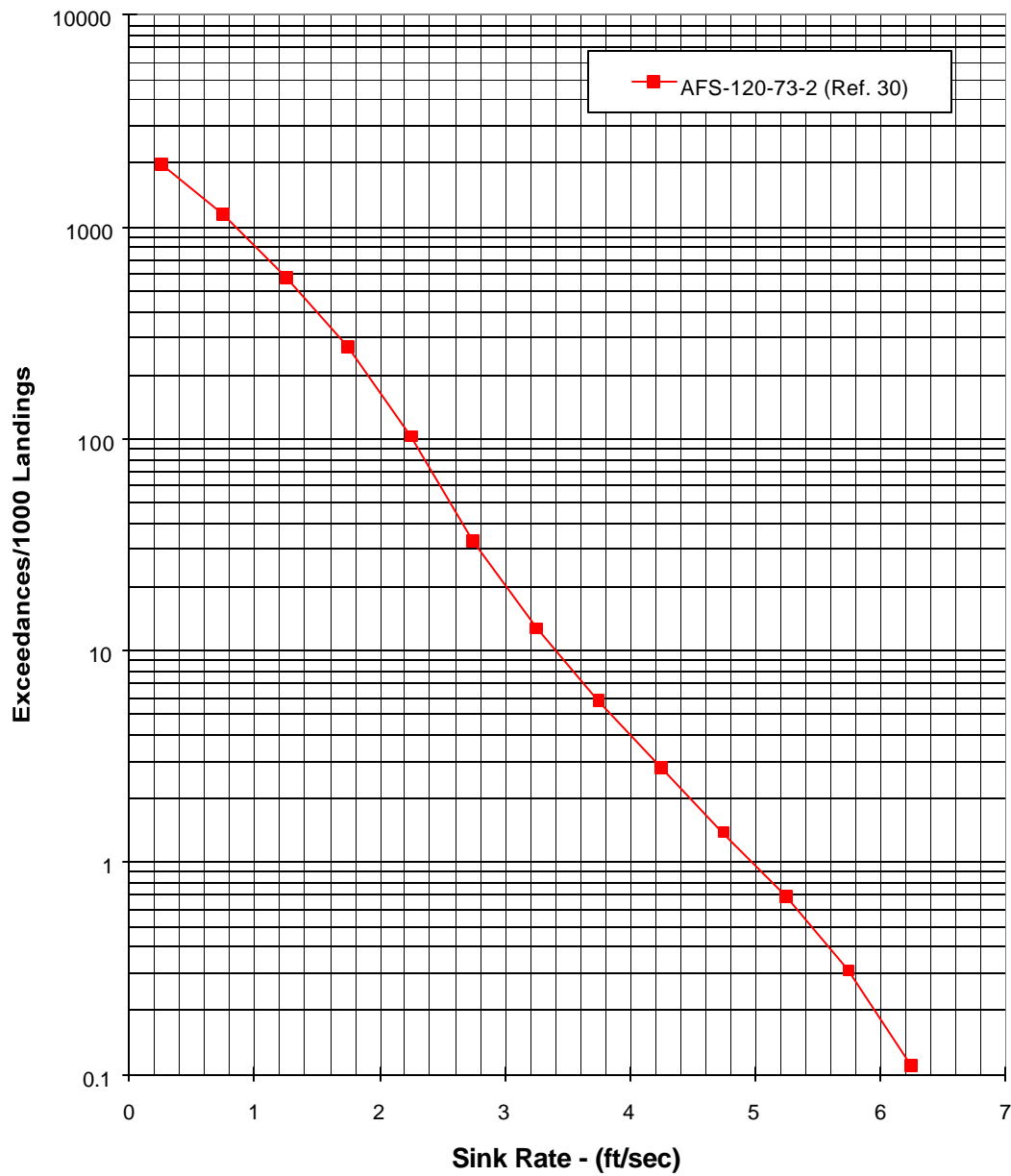


TABLE 6-6

LANDING IMPACT SINK RATE OCCURRENCES (REF. 30)

<u>Sink Rate (Ft./Sec.)</u>	<u>Occurrences per 1000 Landings</u>
0.25	840.0
0.75	570.0
1.25	305.0
1.75	170.0
2.25	70.0
2.75	20.0
3.25	7.0
3.75	3.0
4.25	1.4
4.75	0.7
5.25	0.38
5.75	0.20
6.25	0.11

6.1.6 Balancing Tail Loads

Typically, the most significant contribution to the cyclic fatigue history on the horizontal tail is the change in the level-flight balancing tail load due to flap deflections. Figure 6-12, taken from Reference 29, shows how the stresses vary with flap deflection. Balancing tail load spectra are usually defined in terms of actual maximum and minimum stresses. A balancing tail load stress spectrum should be created for each horizontal tail PSE (and possibly vertical tail PSE depending on aircraft configuration) for each of the flight profiles described in Section 5.0. The spectrum is created using the stress equations calculated in Section 7.0 and the flight parameters listed in Table 6-7. This table lists the conditions and flight parameters that should be used to calculate the balancing tail load stresses for any aircraft under consideration.

Once these stresses are calculated they are assembled into a table as shown in Table 6-8. This table should be directly entered into the load file. Since this spectrum is in terms of stresses instead of load factors, the stress equation coefficients applied to this file as described in Section 7.0 will be 1.0.

FIGURE 6-11

EFFECT OF SPANWISE LOCATION ON GROUND-AIR-GROUND CYCLE

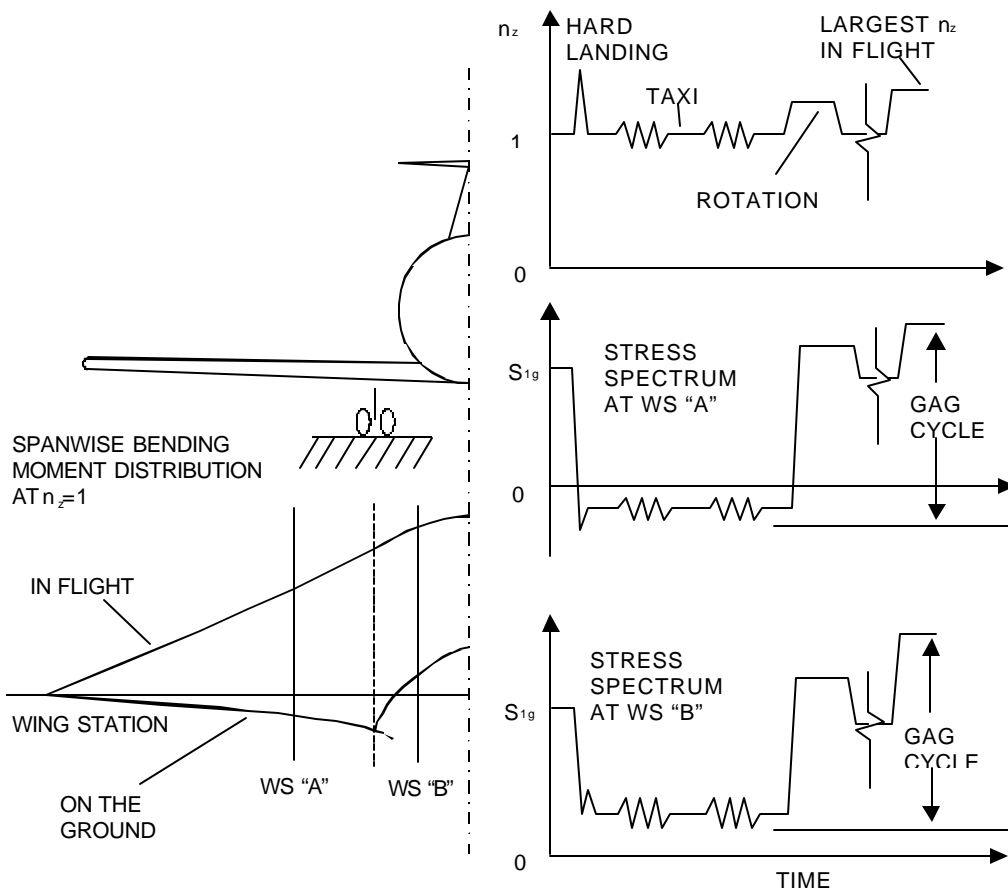


TABLE 6-7

BALANCING TAIL LOAD CYCLES

Condition	Velocity	Flap Position
Takeoff	Takeoff Velocity	Takeoff Flap Position \Rightarrow 0
Cruise	As Required	0
Landing	Approach Velocity	0 \Rightarrow Approach Flap Velocity
Landing	Landing Velocity	Approach Flap Velocity \Rightarrow Landing Flap Velocity

The velocities used reflect the maximum allowable flap deflected speeds for each flap position.

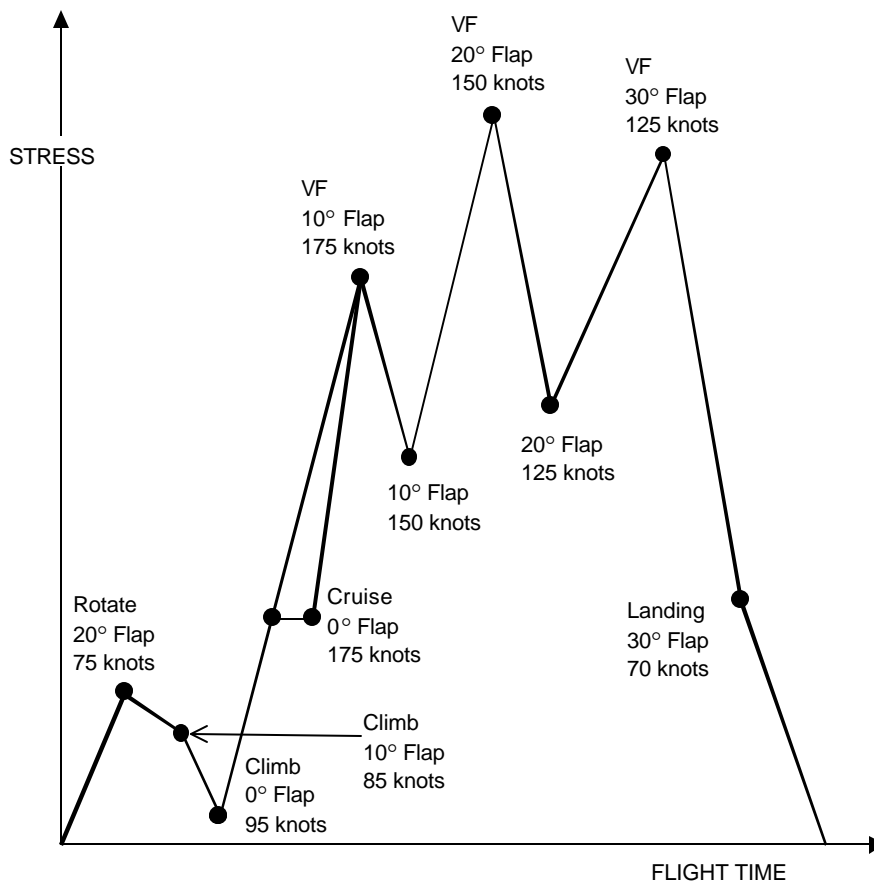
TABLE 6-8

BALANCING TAIL LOAD SPECTRUM TABLE

<u>Maximum Stress (psi)</u>	<u>Minimum Stress (psi)</u>	<u>Occurrences per 1000 Flights</u>
Max Stress Takeoff	Min Stress Takeoff	1000
Max Stress Cruise	Min Stress Cruise	1000
Max Stress Landing	Min Stress Landing	1000

FIGURE 6-12

EFFECT OF FLAP DEFLECTION ON HORIZONTAL TAIL STRESS



6.1.7 Thrust Loads

The effects of engine thrust must be considered in the fatigue evaluation of the engine support structure and other affected airframe components. Examples of other affected components include:

- Wing – when the engines are attached to the wing
- Empennage – when the engines are attached to the aft fuselage

Specific thrust values for the individual flight segments must be calculated. The Pilot Operating Handbook and the engine manufacturer's data can be referenced to calculate specific thrust values based on specific parameters. For piston aircraft these parameters would include engine RPM and manifold pressure.

If thrust reversers are used then the aircraft's strain response may be significant. The strain response should be measured during a flight strain survey on any component that may be influenced by thrust reversers.

6.1.8 Cabin Pressurization Loads

Cabin cyclic pressure and the external loads for typical flight and ground conditions will be considered in the fatigue evaluation of the fuselage. The differential cabin pressure shall be based on 0.5 psi average external aerodynamic pressure and the pressure differential for the maximum operating altitude. For analysis and test purposes, this pressure cycle occurs once per flight. The pressure differential to maintain an 8,000 ft. pressure cabin at 40,000 ft. is calculated in Table 6-9.

6.1.9 Propeller Slipstream Effects

The effects of the propeller slipstream should be considered for inclusion into the stress spectrum. The propeller slipstream affects the horizontal tail and other structure located in the propeller slipstream. To determine the loads on the structure due to the propeller effects, the structure must be gauged and the loads measured. The propeller effects cannot be determined analytically nor is there any publicly available data to determine propeller slipstream effects.

TABLE 6-9

CABIN PRESSURIZATION LOADS

<u>Maximum Operational Altitude:</u>	40,000 ft
<u>Cabin Altitude*:</u>	8,000 ft
Ambient pressure on a standard day at 40,000 ft = (Pressure data is from Standard Atmosphere tables)	2.72 psi
Ambient pressure on a standard day at 8,000 ft = (Pressure data is from Standard Atmosphere tables)	10.92 psi
Pressure difference =	8.20 psi
Required pressure differential =	8.20 psi
Regulator tolerance =	± 0.1 psi
Regular setting (normal operating) =	8.30 psi
External aerodynamic negative pressure = (A suction pressure is pulling out on the fuselage)	0.50 psi
<u>Cabin Pressure =</u>	8.80 psi

* Cabin Altitude is defined as the altitude and its corresponding standard atmospheric pressure that the fuselage is pressurized to for the passengers comfort. A “cabin altitude” of 8,000 ft means that inside the fuselage a person would be subjected to the standard atmospheric pressure corresponding to 8,000 feet.

6.2 Landing Gear Load Spectra

This section describes the spectra that are specific to either the nose gear or the main gear. The taxi and landing impact spectra are covered in Sections 6.1.3 and 6.1.4 respectively. Other ground handling loads including turning, braking, towing and pivot loads are discussed in the following paragraphs.

6.2.1 Turning Loads

Turning load spectra are usually defined in terms of lateral acceleration (LACG) occurrences at the aircraft center of gravity. Figure 6-13 shows a turning load spectrum from MIL-A-8866A (Reference 39). Table 6-10 lists the occurrences for the turning spectrum shown in Figure 6-13.

TABLE 6-10

TURNING LOAD FACTOR OCCURRENCES

<u>Δ LACG</u>	<u>Occurrences per 1000 Landings</u>
0.15	4000
0.20	3000
0.30	2000
0.40	1000

6.2.2 Braking Loads

Per MIL-A-8866B (Reference 33), full braking with maximum braking effects occur twice per landing and medium braking with half braking effects occur five times per landing. Figure 6-14 shows the braking load spectrum graphically. Table 6-11 lists the occurrences for the spectrum shown in Figure 6-14.

TABLE 6-11

BRAKING LOAD FACTOR OCCURRENCES

<u>Brake Load</u>	<u>Occurrences per 1000 Landings</u>
1/2 Maximum Braking Load	5000
Maximum Braking Load	2000

6.2.3 Towing Loads

Towing loads should be evaluated to determine if these loads produce a significant load on the aircraft landing gear. There are no publicly available references available for towing loads, so towing loads need to be measured for the airplane being evaluated. The towing spectrum should be based on conservative assumptions about ground operations. The towing spectrum should include one towing segment per flight.

FIGURE 6-13
TURNING LOAD FACTOR SPECTRUM

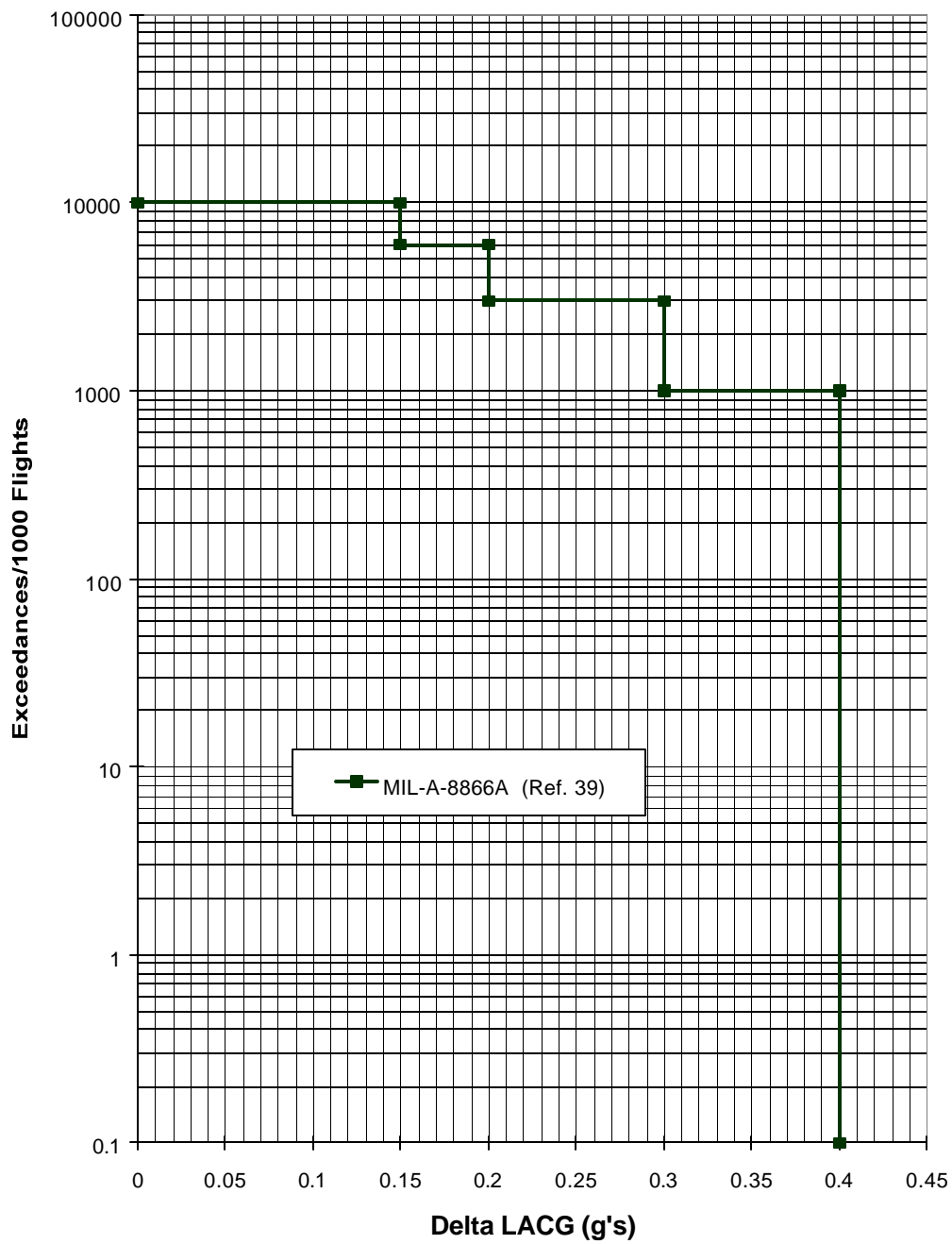


FIGURE 6-14

BRAKING LOAD FACTOR SPECTRUM

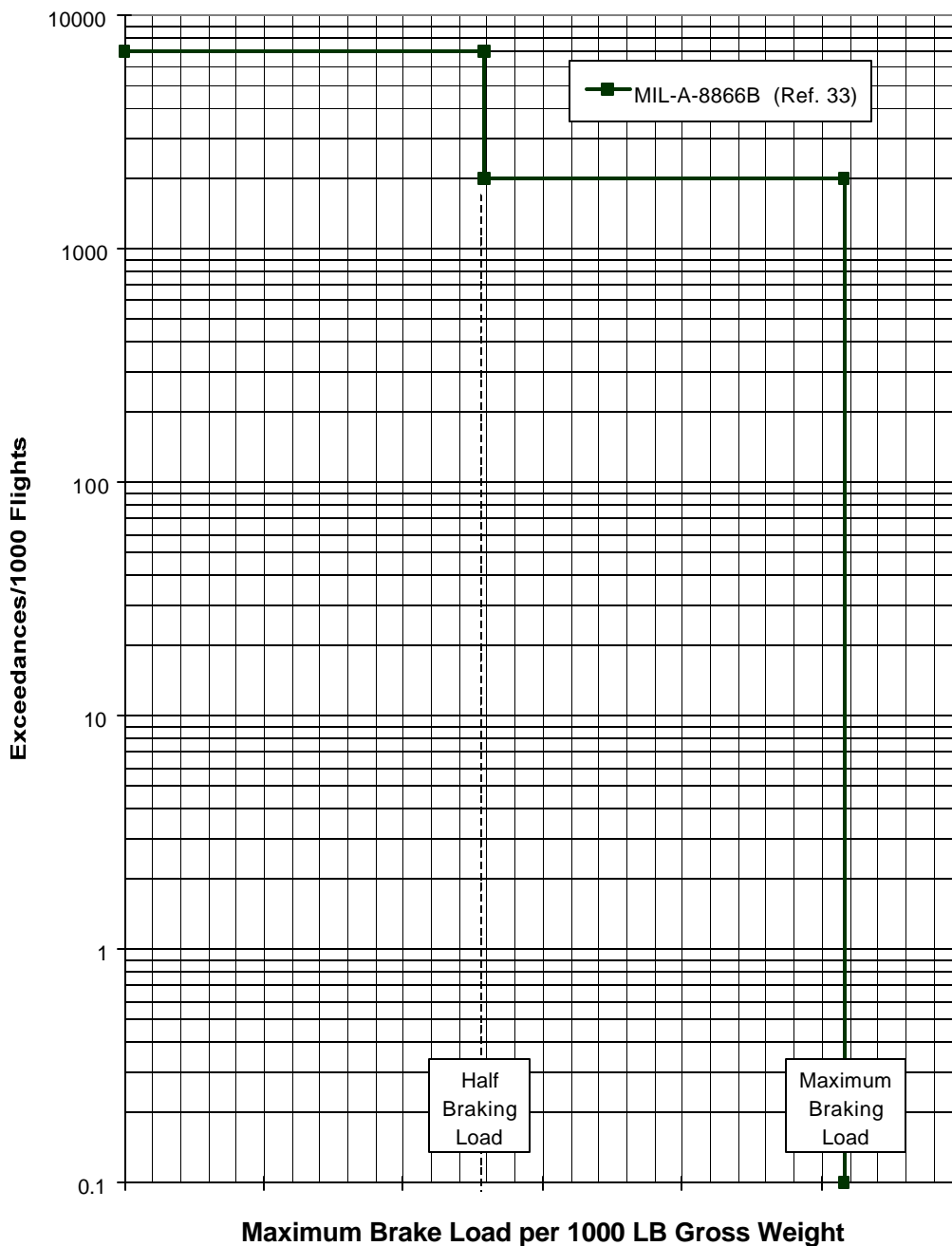


TABLE 6-12

TOWING LOAD SPECTRUM

<u>Towing Load</u>	<u>Occurrences per 1000 Landings</u>
Maximum Towing Load	1000

6.2.4 Pivot Loads

While not commonly used for aircraft that operate out of large commercial airports, locked wheel pivots are used by some operators who routinely fly into and out of small or private airstrips. Due to narrow airstrip widths, single entrance/exit ramps and no bubble turn-arounds, pilots may lock one wheel and use the opposing engine's thrust to turn the aircraft. Pivoting can be one of the most damaging of the landing gear loads to the nose gear. The pivoting spectrum should include two pivots per flight – one during the taxi out segment, and one during the taxi in segment. The pivot occurrences should be split equally between right and left pivots. Since there is no publicly available data as to the magnitude of the expected pivot load, the load must be measured on the aircraft.

TABLE 6-13

PIVOT LOAD SPECTRUM

<u>Pivot Load</u>	<u>Occurrences per 1000 Landings</u>
Right Pivot Load	1000
Left Pivot Load	1000

7.0 Stress Spectrum Generation

Stress spectra are required for fatigue and crack growth analyses for each critical location on a PSE. The process of developing the spectra is shown in Figure 7-1. As shown in the figure, once the flight profiles (Section 5.0) and load spectra (Section 6.0) are determined, the stresses are developed in one of two ways. The first method is to use finite element models to generate stress relationships to loads for a number of unit load cases. This method is presented in Section 7.1. The second method is to measure strains from a flying test aircraft along with relevant flight parameters and create strain equations, as described in Section 7.2. The measured strains can then be converted to stresses. Once stresses have been developed, the general guidelines for creating a stress spectrum are presented in Section 7.3. Since the stress spectra developed are required for crack growth analysis, gross area stress spectra are calculated. If fatigue analysis is desired, net area stress spectra are required.

7.1 Analytically Derived Stresses

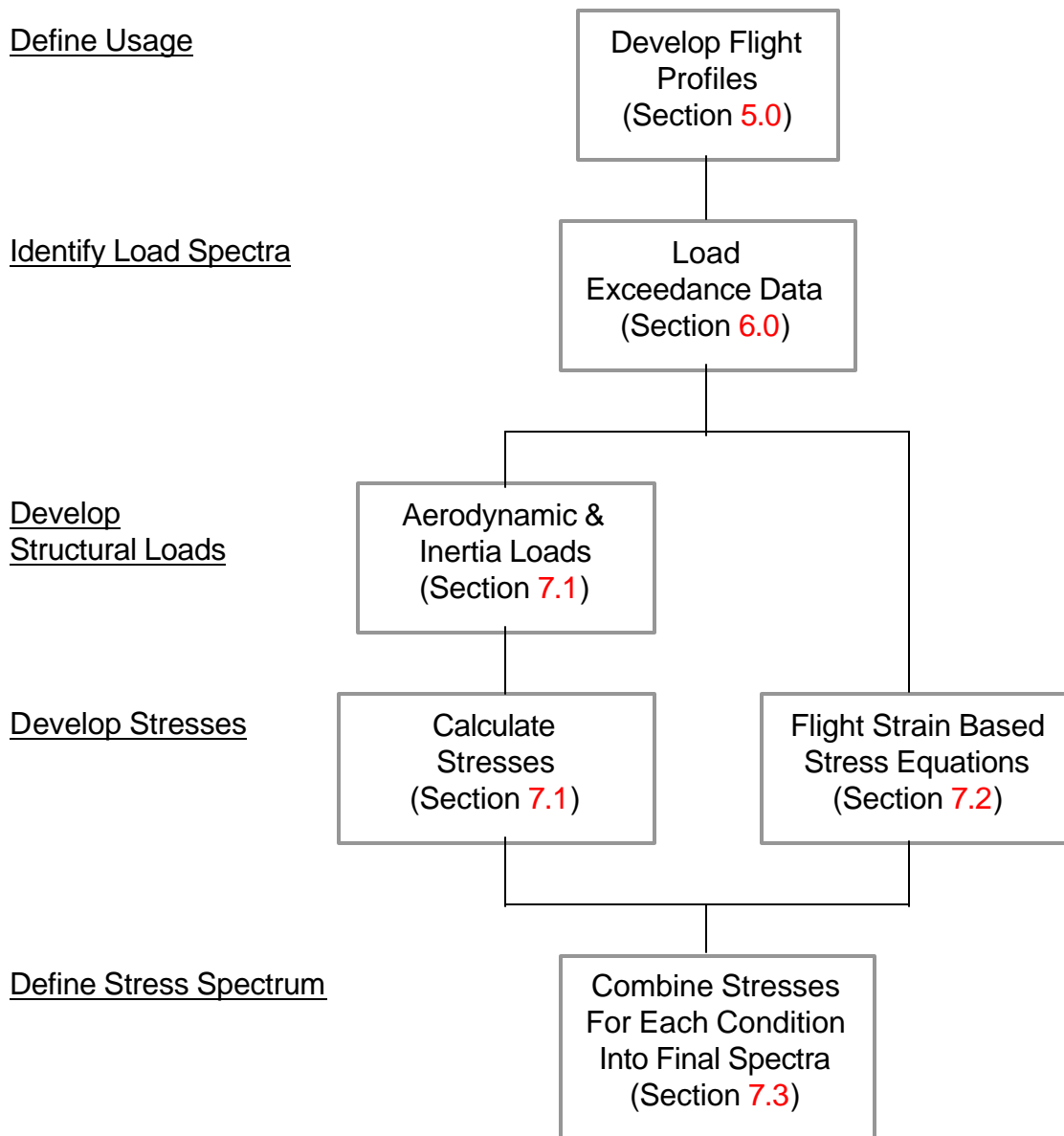
Based on a finite element model (FEM) and classical stress analysis methods, stresses can be determined at the critical location of the PSE based on known shear, moment and torque values. At or near the critical location of a PSE the internal stress can be determined from the FEM output for a specific load condition.

After a finite element model is developed as described in Section 3.2.1, shear, moment and torsion distributions must be determined. For each significant flight phase in a flight profile configuration (i.e., gross weight, fuel weight, cg, etc., as described in Section 5.0), the following unit load cases are developed:

- A 1g level flight case. Also, a case for each significant flap setting may be required.
- A unit vertical gust ($N_z = 2.0$ g's) case.
- A unit lateral gust case for a nominal lateral gust velocity ($U_{de}=10$ ft/sec).
- A 1g on the ground case. This case will be used for taxi conditions.
- A unit cabin pressure case, if the airplane is pressurized.

FIGURE 7-1

STRESS SPECTRUM DEVELOPMENT PROCESS



Other loads, such as thrust for wing-mounted engines may be included in the above load cases. For a specific critical location not all of the above load cases would be developed. For example on a wing, lateral gust and cabin pressurization cases would not be developed.

Actual load calculations are beyond the scope of this document. FAR Part 23 Subpart C, Sections 23.321 through 23.511, presents some of the equations for calculating loads. Some structural design handbooks such as Reference 36 also provide guidance in calculating airframe loads. Using reliable aerodynamic data validated by flight test, surface spanwise airload shears, moments, and torques are developed. Inertia loads must also be calculated. The aerodynamic and inertia loads are then distributed at the nodes of the finite element model. Stresses at the critical area of the PSE are extracted from the finite element model. It is desirable to have experimentally derived stresses from previous static and fatigue tests to verify the stresses derived from the finite element model.

Once the stress due to a unit load is developed, the load spectra can be converted to stress spectra. If References 30 and 31 are used to obtain load data, exceedance data plotted as the cumulative frequency of exceedance per nautical mile vs. the acceleration fraction experienced by the aircraft must be converted to a curve of exceedances per 1000 flights versus the incremental load factor from 1g experienced by the airplane (Section 6.0). References 32, 33 and 34 present the data in an exceedance per 1000 flights format. Next, the stresses in the finite element model developed from the 1g load cases can then be ratioed to determine the stresses for other g levels and paired with the corresponding exceedances. Appendix C presents an example of how to develop the load spectra from exceedance data that can then be converted to an “uncounted” stress spectra. The spectra are then cycle counted as described in Section 7.3.3 before inputting into a crack growth program. Figure 7-2 flowcharts this process.

7.2 Flight Strain Survey Derived Stresses

Flight strain survey programs are used to determine stress equations as a function of flight parameters (N_z , weight, speed, altitude, etc.) for use in stress spectra development. By flying an instrumented aircraft through a variety of representative conditions, enough data points can be recorded to perform statistical regressions to obtain strains that are converted to stresses.

Several steps are required to get to the end goal of experimentally determined stresses. First, the aircraft must be instrumented. The required instrumentation and technical considerations are described in Section 7.2.1. Next, the flight conditions to be flown are planned. Considerations in planning the flight conditions are discussed in Section 7.2.2. After the flight data has been collected, the data must be analyzed. Data regression techniques used for the data analysis are presented

in Section 7.2.3. A flowchart of the Flight Strain Survey Process is shown in Figure 7-3.

FIGURE 7-2
ANALYTICAL STRESS SPECTRUM DEVELOPMENT

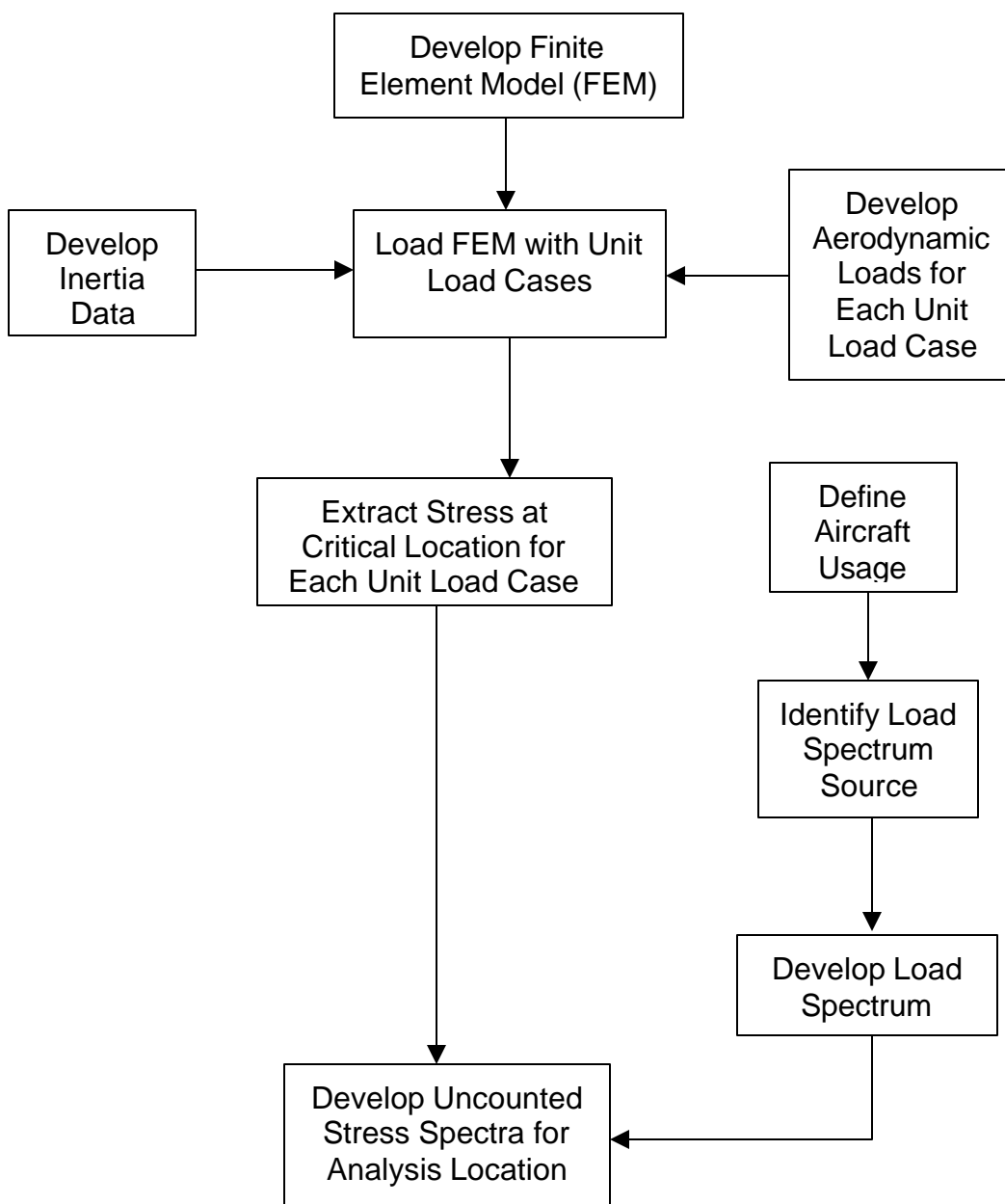
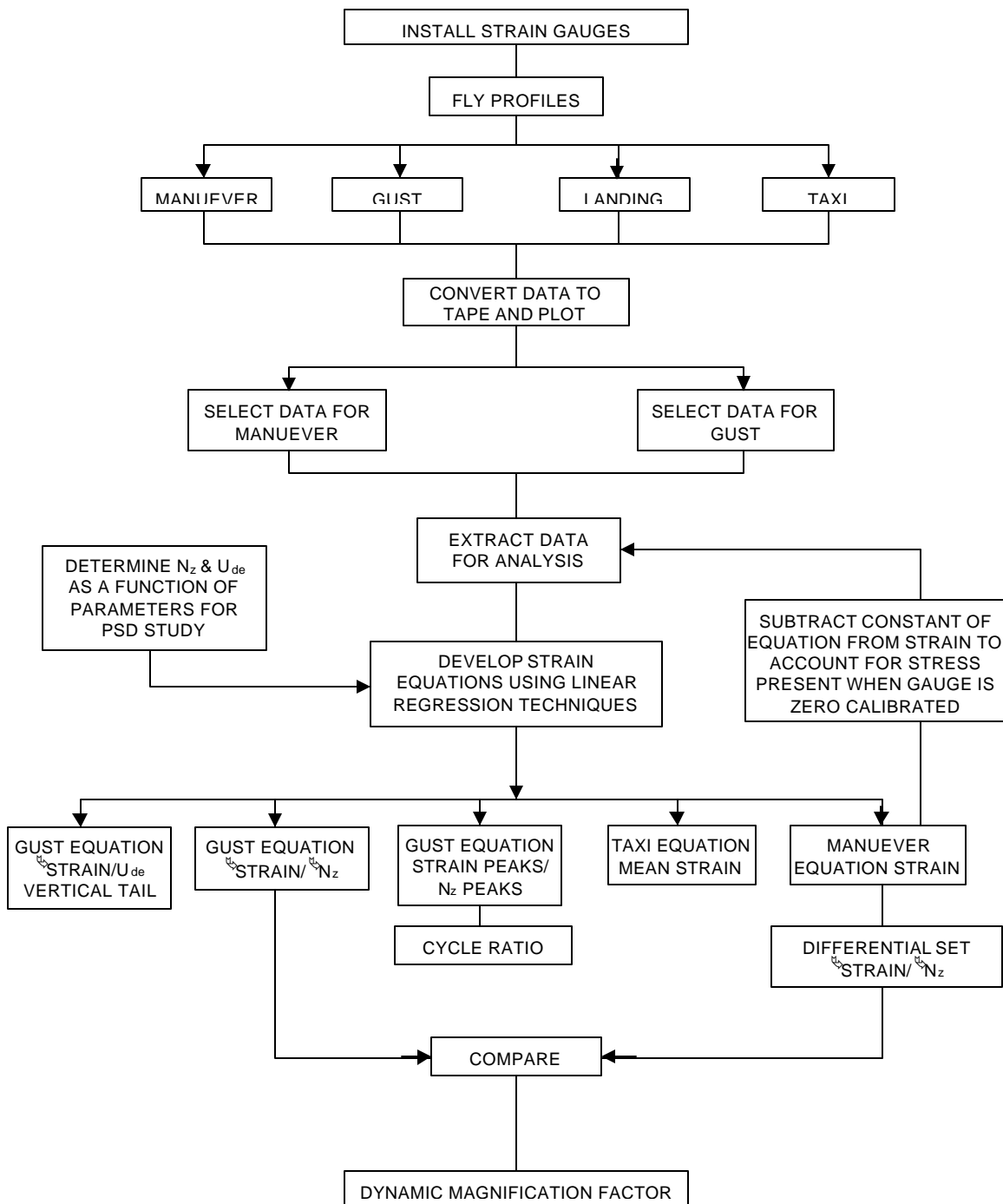


FIGURE 7-3
FLIGHT STRAIN SURVEY PROCESS



7.2.1 Instrumentation

During a flight strain survey, numerous flight parameters and structural strains need to be measured. In order to record all of this data, the aircraft undergoing the flight strain survey needs to be instrumented. A vertical accelerometer should be installed near the aircraft center of gravity. Lateral accelerometers should be installed at the center of gravity of the aircraft and near the vertical fin center of pressure. Flight parameters such as airspeed, gross weight, fuel weight, altitude, left/right engine speed (RPM), left/right engine manifold pressure, and flap position all should be recorded. Strain gages should be installed on the aircraft at the critical area(s) of each PSE. Technical considerations for the installation of strain gages are discussed in Section 7.2.1.1. Specific items to measure are presented in Section 7.2.1.2.

When installing strain gages at the PSE locations, it is a good idea to install a few extra gages at an opposite location to use for comparison. For instance, if a PSE is located on the right wing or horizontal stabilizer, a strain gage should also be installed at the same location on the left side wing or horizontal stabilizer. This comparison can be used to make sure measurements are believable for symmetric loading conditions.

Since PSE locations usually are in spar caps rather than skin, efforts should be made to mount strain gages directly on spar caps if possible. If access is not available to the underside of a spar cap, spot facing is an option to allow direct spar cap mounting of a strain gage. Spot facing is the drilling out of a quarter sized hole through the skin and stopping before penetrating the spar cap below. This method gives direct access to spars or other components underneath the skin.

After the instrumentation of the aircraft is complete, an onboard flight data recording system is required to record the desired data. Data is normally recorded in Pulse Code Modulation (PCM) format with a Programmable Conditioning Unit (PCU) system similar to the Aydin Telemetry PCU-816. Data is usually recorded and stored on Digital Linear Tape (DLT) with various storage capabilities.

7.2.1.1 Technical Considerations

This section will discuss flight strain measurement and will reference Micro-Measurements Division, Measurements Group, Inc. technical notes and tips for detailed information (References 40-47). Installation considerations, temperature compensation, frequency response, filtering considerations, and engineering unit calculations are covered.

7.2.1.1.1 Installation

- 1) Bridge Type - Installations are typically configured as a $\frac{1}{4}$ Wheatstone bridge type. The $\frac{1}{4}$ bridge configuration provides a simple setup that will yield a micro-strain output without the requirement to calibrate the structure for loads.
- 2) Connection - A 3 wire connection may be used if the I*R excitation drop is determined to be insignificant. If excitation drop becomes a significant factor, signal conditioning with excitation sense may be used to eliminate this error. Measurement of the actual excitation voltage at the gage location may also be used to account for excitation drop.
- 3) Gage Selection – (See Reference 40) A type CEA 13 gage from Micro-Measurements is a universal general purpose strain gage for use on aluminum. This type of gage is encapsulated in polyimide to improve its durability. The required gage size is determined by the unique installation requirements of the critical area. Generally a large gage to dissipate excitation heating is desirable and will provide greater flexibility when choosing excitation levels, assuming a uniform strain across the gage.
- 4) Excitation Selection – (See Reference 41) Consider all measurements to be of a static nature when selecting excitation values. A 5 to 10 watt/in² excitation value will yield a highly accurate static measurement on aluminum aircraft structure.
- 5) Bonding Considerations - Selection of an adhesive requires consideration of each unique application. Installation duration, moisture, exposure to fuels, operating temperature, ability to clamp the installation, and the ability to cure the adhesive should be considered when selecting an adhesive. Measurements Group Inc. manufactures a variety of adhesives for virtually all applications. If the strain program will be of short duration and the aircraft can be kept out of moisture then Mbond 200 may be used for bonding considerations. Mbond 200 allows for a simple installation of strain gages on aircraft structure. The gage still must be coated to protect it from moisture and high humidity. Even with a protective coating, care should be taken to avoid exposure to moisture. The life span of the gage will be short due to moisture creep under the lead wires.
- 6) Terminal Application – See References 42 (TT-603 The Proper Use of Bondable Terminals in Strain Gage Applications) and 43 (TT-604 Lead Wire Attachment Techniques for Obtaining Maximum Fatigue Life of Strain Gages) for terminal application techniques.
- 7) Instrumentation Calibration

- a) With Shunt Calibration – See Reference 44
- b) Without Shunt Calibration - Some bridge amplifier instrumentation have programmable gains which enables an accurate gain to be selected. The calibration of the system is to determine if the instrument is operating within its specified accuracy. A system error analysis to include gain, excitation, offset, and lead wire excitation voltage drop error can be performed to determine if the overall system will yield satisfactory results. Overall this method is quicker to implement for large scale programs.

7.2.1.1.2 Temperature Compensation

Strain measurements on aircraft must consider temperature drift. Although a gage can be purchased with a general temperature characteristic to match the material under test, additional measures must be used to obtain accurate data. See Reference 45 for detailed techniques and procedures.

7.2.1.1.3 Frequency Response Considerations

An aircraft strain program must respond to all gust input induced on the airframe. An upper frequency of 20Hz is generally accepted to be the upper frequency extent of the gust spectrum. Unfortunately for this application the strain gage frequency response is much greater than the desired 20Hz upper limit. An anti-aliasing filter is used to remove unwanted noise prior to digital sampling of the measurement. The slope of the anti-aliasing filter is used to set the sample rate of the data acquisition system. See Reference 46 for detailed filtering techniques.

7.2.1.1.4 Micro-Strain Calculation

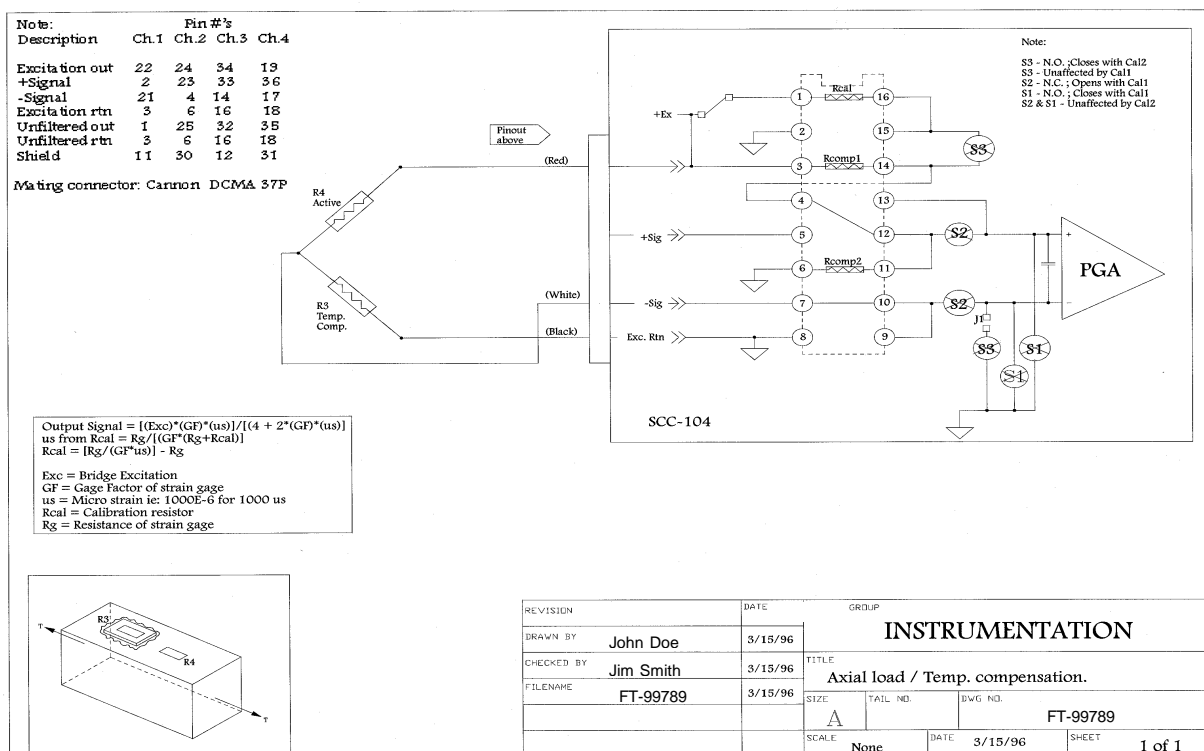
See Reference 47 (TN-507 Errors Due to Whetstone Bridge Nonlinearly) and Reference 44 (TN-514 Shunt Calibration of Strain Gage Instrumentation) for details in micro-strain calculation.

7.2.1.1.5 Typical Application

Figure 7-4 shows a schematic diagram of a typical flight data recording system. This example uses a $\frac{1}{4}$ bridge with dummy temperature compensation with the Aydin Telemetry SCC-104 signal conditioner.

FIGURE 7-4

TYPICAL FLIGHT DATA RECORDER SCHEMATIC DIAGRAM



7.2.1.2 Items to Measure

In the previous section, instrumentation was installed on the aircraft to measure flight parameters and strain. Most of these parameters need to be recorded simultaneously with the strain values. Some, such as flap position, engine rpm, and manifold pressure do not need to be recorded continuously – it is sufficient to mark the time in the flight log. This section will detail each item to be measured and why.

- Vertical Acceleration (N_z) - Required for use in deriving vertical gust, maneuver, and taxi strain equations.
- Lateral Acceleration (N_y ⇒ U_{de}) - Required for use in deriving lateral gust strain equations.
- Airspeed (KEAS) - Required as a flight parameter in strain equation regressions.
- Gross Weight (GW) - Required as a flight parameter in strain equation regressions.

- Fuel Weight (FW) - Required as a flight parameter in strain equation regressions.
- Altitude (h) - Required as a flight parameter in strain equation regressions.
- Left/Right Engine Speed (RPM) or Engine Fan Speed - Required as a flight parameter in engine thrust calculations.
- Left/Right Engine Manifold Pressure or Engine Thrust directly - Required as a flight parameter in engine thrust calculations.
- Flap Position (FLAP) - Required as a flight parameter in strain equation regressions.
- Cabin Pressure - Required for the strain equation for cabin pressurization.
- Strain ($\mu\epsilon$) - Strain at each PSE recorded in micro in/in. Strain should be recorded at each PSE with an axial type strain gage installed with the long axis of the gage parallel to the line of stress. In other words, install the strain gage along the direction of expected stress.
- Center of Gravity (cg) - Required as a flight parameter in strain equation regressions.
- Sink Rate - Required for landing impact strain equation.
- Thrust Reverser Position (if applicable) - Required for thrust cycle strain equation.

7.2.2 Flight Conditions

The most accurate and useful stress equations are those developed using a wide range of flight and configuration parameters, ideally with the same distribution of values as the final flight spectrum. At a minimum, data should be collected for ground taxi, maneuver, gust and landing. When collecting data, the extreme points (of the cg envelope) are generally not part of a typical flight profile, and may not yield valid data for stress equations. Enough data points are needed to establish credible equations. In general, at least three separate data groupings are required for each parameter that will be used. Three flights at different zero fuel weight configurations are usually enough to satisfy this requirement. Data for three fuel configurations (near full, near half full, and near empty) should be recorded. In addition, during each flight the normal fuel burn should provide enough data points for the gross weight and fuel weight terms.

The following guidelines are presented to aid in the flight planning for a strain survey:

- The following loading events should be considered when developing a flight plan: taxi, takeoff, 1-g flight, gust loading, maneuvering, landing, and thrust reverse operation (if applicable). One-g flight and maneuver events should be recorded with and without flaps extended. Additional events such as braking, pivoting, and turning may also be required.
- High-altitude (35,000 ft. and above) flights are relatively uncommon; data should be recorded at lower altitudes where gust and maneuver loads are more likely to occur.
- A full range of velocities should be recorded. Note, though, that extreme points (near stall or near maximum speed) are generally not representative of final spectrum speeds, and can induce dynamic loading (stall buffet, for example) that cannot be characterized by stress equations.
- For pressurized aircraft, the aircraft should be pressurized to 1.0 psi on the ramp while fuselage strain gages are read. This data will be used to calculate cabin pressurization stress equations.
- Taxi data should be recorded at each of the zero fuel weights and with as many fuel weights as is practical. The surface should be consistently rough and the taxi speed should be at normal levels. A minute of recorded data at each configuration should provide enough data to develop stress equations.
- Maneuvers should be smooth, coordinated maneuvers that cover the full range of the flight envelope. High g levels are unnecessary because these points would be omitted from the final spectrum anyway. Dynamic effects and yaw effects should also be avoided. Avoid maneuvers with both positive and negative g loading; the structure will be cyclically loaded, and hysteresis will be present for part of the maneuver. Specify either push-over or pull-up maneuvers, but not both in a single maneuver sequence.
- In order to obtain acceptable gust response equations the aircraft N_z excursions should regularly exceed at least 0.7 g's during the flight; higher levels (above 1.0 g's) are preferable. The gust response equation (σ/N_z) is usually a strong function of fuel weight so data should be collected over a wide range of fuel weights. Gust flights should be at 1 g level flight. Parameter recording accuracy and frequency (accelerations and strains) are more critical for dynamic loading events than for steady state events. It is suggested a sampling rate of at least 124 samples per second be used for measuring gust data. A sample rate of 31 samples per second is sufficient for steady state events. As a rule, data should be recorded at a sample rate of 5 times the expected load frequency.
- Landings should be recorded over a wide range of fuel weights along with all zero fuel weight configurations. At least twelve landings should be recorded. The pilots should be instructed to record both hard and normal landings. Usually

both types of landings have been performed for each configuration. Measured stress histories may be used in the spectrum to determine the effects of landing impact on the structure (see Figure 7-5).

- Signal filtering should be used to keep high vibration and resonance of the signal out of the recorded data. A 20 Hz filter, for example, attenuates the part of the signal above 20 Hz. Some of the peaks that are recorded at or above 20 Hz would be lowered. A higher frequency filter could be used, but this exposes the recorded data to more signal noise. A 20 Hz filter is generally used for flight strain surveys.
- Attention should be given to how strain gages are zeroed. Strain due to one-g inertia loads (set at zero strain when the gages are installed) can yield significant errors when developing stress equations. Zeroing engine beam gages with the engines removed works well. For other gages, using a static test article with identical gages can be used with some success. It is also noted that zeroing of gages needs to be completed only once during the flight strain survey. If signal drift becomes a problem with the instrumentation then the gages should be zeroed before each data collection flight.

7.2.3 Data Regression

After the flight data is recorded, the data is transferred from the recording medium (for example, 8mm magnetic tape) to a computer. Flight data software (for example, Probe) is used to view, and in some cases reduce the flight data. In addition, strip charts of the measured data are useful for reviewing the data (see Figure 7-6).

Before regressing the flight data it must be reviewed for erroneous or non steady-state maneuvers. Valid data streams need to be selected and extracted from the data tapes for regression. After determining valid data streams, the data is separated into discrete time slices where the strain and all flight parameters are known for a specific time. Over a valid data stream there should be enough time slices (at least 100) to use in a regression analysis. Any obvious data spikes or errors should be removed from the time slices used for regression.

FIGURE 7-5

TYPICAL FLIGHT STRAIN SURVEY STRESS HISTORY PLOTS

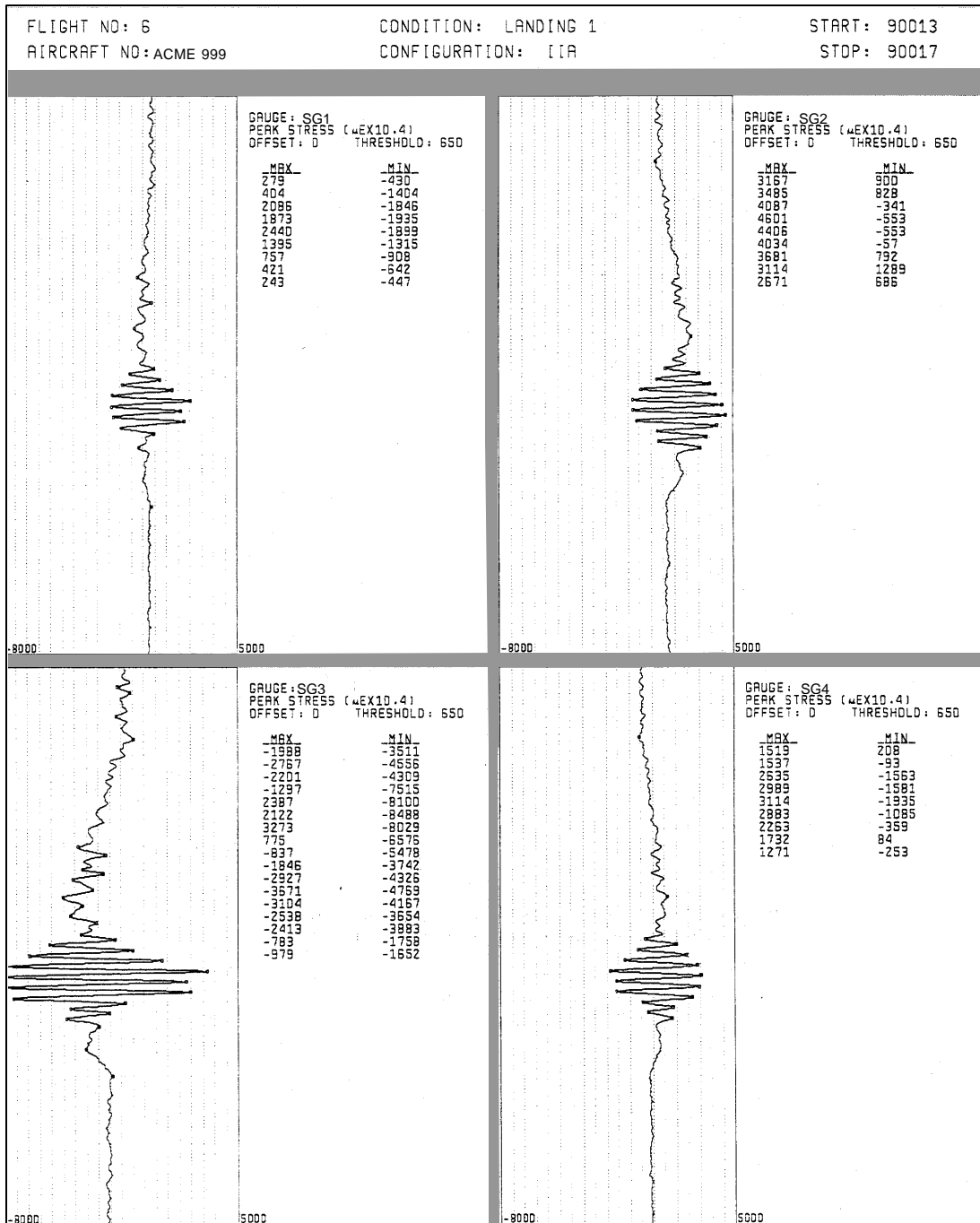
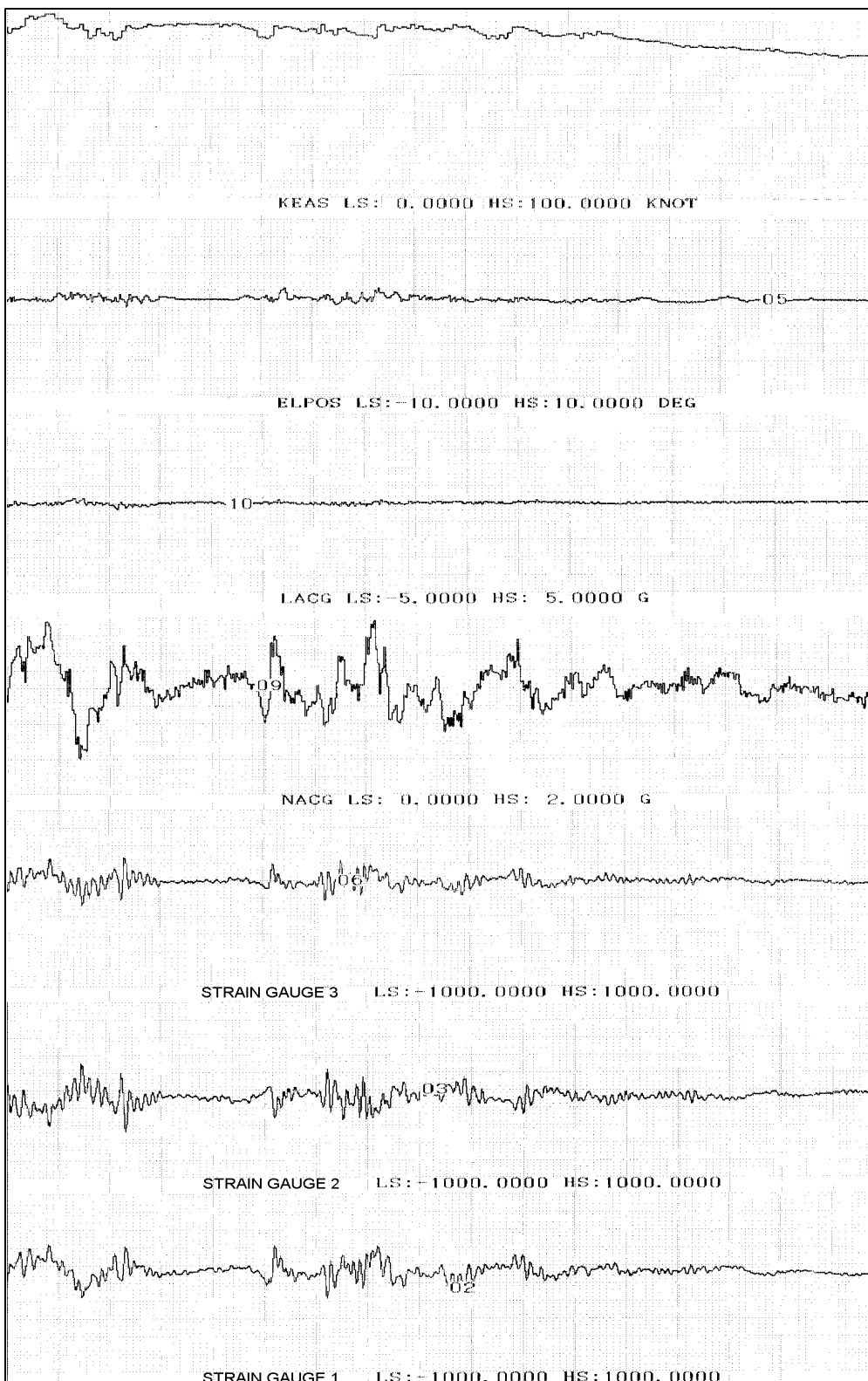


FIGURE 7-6

TYPICAL MEASURED DATA STRIP CHARTS



A linear least squares regression technique should be used to regress the flight data and strains into a strain equation. Microsoft Excel has a regression tool that is useful for this operation. Whichever way the regression is completed, a number of statistical values are computed. A review of these values will tell whether a valid correlation between the strain and flight parameters has been calculated. Figure 7-7 shows an example regression for determining the maneuver stress equation. The following statistical values should be reviewed for data validity:

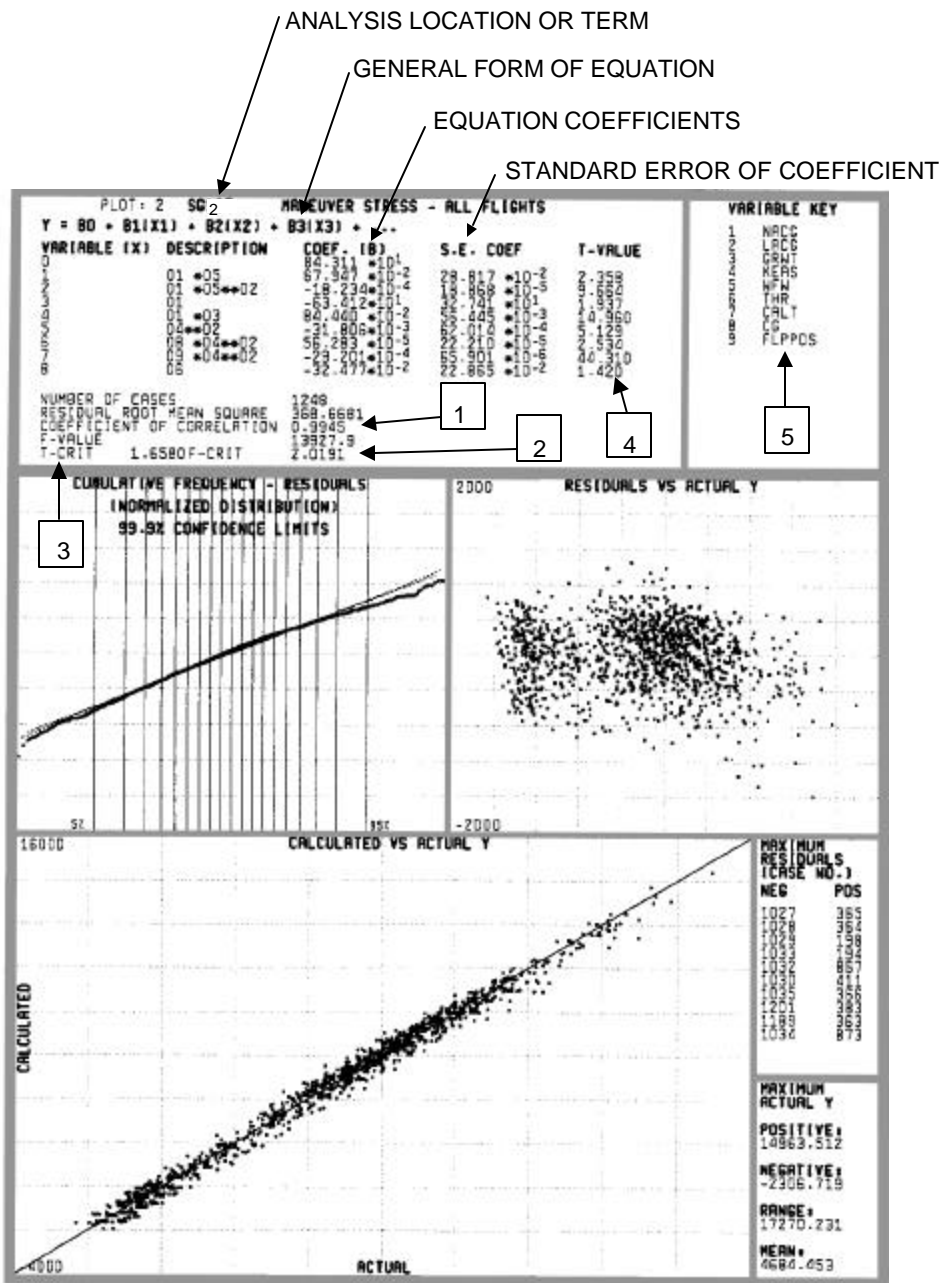
- r^2 - Coefficient of Correlation [Item 1, Figure 7-7] - Compares estimated and actual y-values (the value that is trying to be correlated) and ranges in value from 0 to 1. If it is 1 there is a perfect correlation in the sample (there is no difference between the estimated and actual y-value). If the value is 0, then the regression equation is not helpful in predicting a y-value (Reference 48).
- F - The F Statistic [Item 2, Figure 7-7] - The F statistic is used to determine whether the observed relationship between the dependent and independent variables occurs by chance. There is a relationship among the variables if the F-observed value is greater than the F-critical value. A F_{crit} value can be found in a statistical handbook and depends on the number of variables in the regression and the confidence level of the regression (Reference 48).
- t - The t Statistic [Item 3, Figure 7-7] - The t statistic is used to determine whether a certain variable in the regression equation is useful in predicting the y-value. The variable under consideration has a significant impact on the prediction of the y-value if its t statistic is greater than a t_{crit} value. The t-critical value can be found in a statistical handbook and depends on the number of variables in the regression and the confidence level of the regression (Reference 48).

When trying to predict a valid regression analysis, some variables may be taken out of the regression if their t statistic is lower than t_{crit} [Items 4 & 5, Figure 7-7]. After removing a variable, the regression should be redone and the F and t statistics should be rechecked because the critical values of F and t will change when the number of variables changes. In some instances, more variables will be needed to predict a useable regression equation. The variables that should be tried first are squared terms (i.e., GW^2) of variables and cross products (i.e., $GW*CG$) of two or more variables.

Gust stress equations should be regressed in an alternating stress format. Root mean square (RMS) stresses and corresponding RMS load factors are computed over several seconds to determine the deviation stress resultant.

FIGURE 7-7

EXAMPLE REGRESSION ANALYSIS OUTPUT



Because the cycles of stress and load factors are not necessarily equivalent, the ratio of stress cycles to load factor (cycle ratio) needs to be measured. This means that if the aircraft cg is hit with a 1.5 g up gust, the outer tip of the wing may oscillate 2.25 times for every one oscillation at the aircraft cg. The cycle ratio is determined by comparing the number of N_z exceedances to strain exceedances at the analysis location. This cycle ratio term is used in computing the number of occurrences for

each stress level in the stress spectrum. The load factor used for vertical gust (horizontal tail, wing, fuselage and engine beams) is N_z while the load factor used for lateral gusts (vertical tail and fuselage) is N_y . Strain gage measurements can be used to determine this value by counting the number of strain peaks at the strain gage for each gust peak at the accelerometer.

The Dynamic Magnification Factor (DMF) is a factor that can be applied to the maneuver strain to give gust strains. It is defined as the amplifier required on the maneuver strain to match the gust strain at a certain strain gage location. An efficient way to calculate the DMF is to differentiate the maneuver equation. This equation is then compared to the $\Delta\text{strain}/\Delta N_z$ equation developed with actual gust data.

7.2.3.1 Strain Equations

Before stress equations can be derived, strain equations from the flight strain survey data need to be regressed. This section gives suggested formats for strain equations. Some of the parameters which should be considered as variables in the strain equations are presented in Table 7-1. The following list shows the abbreviations used for each flight parameter in the strain equations.

NACG	Vertical Acceleration, N_z , at the aircraft cg - g's
GRWT	Total Aircraft Gross Weight - lbs
WFW	Total Aircraft Wing Fuel Weight - lbs
KEAS	Aircraft Velocity in Knots Equivalent
FLPPOS	Flap Position - degrees
THR	Engine Thrust (one engine) - lbs
CG	Aircraft cg position in Percent Mean Aerodynamic Chord (MAC)
PRES	Cabin Pressure

Some example wing strain equations are:

Maneuver Strain (in/in) = $C_1(\text{NACG} \cdot \text{WFW}) + C_2(\text{NACG} \cdot \text{WFW}^2) + C_3(\text{NACG}) + C_4(\text{NACG} \cdot \text{GRWT}) + C_5(\text{KEAS}^2) + C_6(\text{CG} \cdot \text{KEAS}^2) + C_7(\text{FLPPOS} \cdot \text{KEAS}^2) + C_8(\text{THR})$

Taxi Mean Strain (in/in) = $C_1(\text{WFW}) + C_2(\text{WFW}^2) + C_3(\text{CG} \cdot \text{NACG}) + C_4(\text{THR})$

Taxi Alternating Strain (in/in) = $C_1(WFW) + C_2(WFW^2) + C_3(CG*GRWT)$

Vertical Gust Strain (in/in) = $C_1(WFW) + C_2(WFW^2) + C_3(GRWT) +$
 $C_4(KEAS^2) + C_5(CG*KEAS^2) + C_6(THR)$

TABLE 7-1

STRAIN EQUATION PARAMETERS

	GRWT	NACG	WFW	KEAS	FLPPOS	THR	CG	PRES
Maneuver								
Wing	X	X	X	X	X	X	X	
Engine Beam	X	X		X	X	X		
Fuselage	X	X	X	X	X	X	X	X
Horiz. Stab.	X	X		X	X	X	X	
Vertical Gust								
Wing	X	X	X	X		X	X	
Engine Beam	X	X		X		X		
Fuselage	X	X	X	X		X		X
Horiz. Stab.	X	X		X		X	X	
Taxi Mean								
Wing	X	X	X			X	X	
Engine Beam	X	X				X		
Fuselage	X	X	X				X	
Horiz. Stab.	X	X						
Taxi Alternating								
Wing	X	X	X			X	X	
Engine Beam	X	X				X		
Fuselage	X	X	X				X	
Horiz. Stab.	X	X						
Lateral Gust								
Vertical Fin	X	X	X	X			X	

7.2.3.2 Stress Equations

After deriving strain equations from regression techniques, the strain equations need to be converted to gross area stress equations. This is accomplished by multiplying the strain equation by the Modulus of Elasticity (E) for the PSE's material. These stress equations are the same format as the strain equations presented in Section 7.2.3.1.

Next, segment-by-segment stress equation coefficients need to be determined for all the profiles and strain gage locations, so that the stress is represented by an equation of the form:

$$\sigma = C_1 * N_z + C_3$$

This format allows the load spectrum, which is in terms of N_z to be easily converted to stress (see Section 7.3). The following symbols and definitions are used in stress equation development:

σ = Stress, psi

$\frac{\Delta S}{\Delta N_z}$ = Incremental Gust Stress, psi/g

N_z = Normal Acceleration at Aircraft Center of Gravity, g

C_1 = Coefficient of N_z in Stress Equation, psi/g

C_3 = Constant Term in Stress Equation, psi

Subscripts:

t = Taxi

m = Maneuver

g = Gust

alt = Alternating component

mean = Mean component

ss = Steady state component

For each profile segment, as described in Section 5.0, the parameters (i.e., fuel weight, gross weight, velocity, etc.) are entered into each of the strain equations (multiplied by E to convert to stress) to determine C_1 and C_3 . The method to determine the C_1 and C_3 coefficients for taxi, maneuver and gust are described in the following paragraphs.

7.2.3.2.1 Taxi Stress Equation

The taxi stress equation is defined as a mean stress, $s_{t_{mean}}$, plus an alternating component, $s_{t_{alt}}$. These terms were expressed as a function of several variables such as wing fuel weight, gross weight, and cg location. The taxi stress can be represented as:

$$\begin{aligned} \sigma_t &= \sigma_{t_{alt}} + \sigma_{t_{mean}} \\ &= \frac{\sigma_t}{\Delta N_Z} \cdot \Delta N_Z + \sigma_{t_{mean}} \\ &= \frac{\sigma_t}{\Delta N_Z} \cdot (N_Z - 1) + \sigma_{t_{mean}} \\ &= \frac{\sigma_t}{\Delta N_Z} \cdot N_Z - \frac{\sigma_t}{\Delta N_Z} + \sigma_{t_{mean}} \end{aligned}$$

The stress equation was re-written as:

$$\sigma_t = C_{1t} N_Z + C_{3t}$$

where:

$$C_{1t} = \frac{\sigma_t}{\Delta N_Z}$$

$$C_{3t} = - \frac{\sigma_t}{\Delta N_Z} + \sigma_{t_{mean}}$$

7.2.3.2.2 Maneuver Stress Equation

The maneuver stress equation should be developed as a steady state condition based on several variables such as wing fuel weight, gross weight and equivalent airspeed. It can be represented as:

$$\sigma_m = \frac{\sigma_m}{N_z} * N_z + \sigma_{m_{ss}}$$

The equation can be re-written as:

$$\sigma_m = C_{1m} * N_z + C_{3m}$$

where:

$$C_{1m} = \frac{\sigma_m}{N_z}$$

$$C_{3m} = \sigma_{mss}$$

7.2.3.2.3 Gust Stress Equation

The gust stress equation is developed as a change in stress per change in normal acceleration, $\frac{\Delta \sigma_g}{\Delta N_z}$, plus a 1 'g' steady state stress, σ_{ss} . The 1 'g' maneuver stress is used to develop σ_{ss} . The gust equation is represented as:

$$\sigma_g = \frac{\Delta \sigma_g}{\Delta N_z} \cdot \Delta N_z + \sigma_m @ 1g,$$

Since:

$$\Delta N_z = N_z - 1 \text{ and } \sigma_m @ 1g = C_{1m} + C_{3m},$$

$$\sigma_g = \frac{\Delta \sigma_g}{\Delta N_z} \cdot N_z - \frac{\Delta \sigma_g}{\Delta N_z} + C_{1m} + C_{3m}$$

This equation was re-written as:

$$\sigma_g = C_{1g} \cdot N_z + C_{3g}$$

where:

$$C_{1g} = \frac{\Delta \sigma_g}{\Delta N_z}$$

$$C_{3g} = C_{1m} + C_{3m} - \frac{\Delta \sigma_g}{\Delta N_z}$$

Vertical gust stress equations must be calculated for each flight segment of the profiles created in Section 5.0 (i.e., climb, cruise, and descent).

7.3 Stress Spectrum Development

A separate stress spectrum for each critical area of a PSE is required for crack growth analyses. If a flight strain survey was conducted, the stress spectrum is the result of combining the typical usage load spectra (Section 6.0) and the stress equations (Section 7.2.3.2). A computer program is usually used to combine the load spectra and stress equations and create a low-hi block stress spectrum for each flight profile segment. This method of stress spectra development is explained in Section 7.3.1. If the stress spectrum was generated analytically as described in Section 7.1, the method for developing the spectra is discussed in Section 7.3.2. After the spectrum is defined in a low-hi block stress order, another computer program then takes the single-flight stress spectrum and converts it into four flights then cycle counts each flight (reorders the spectrum to pair up high and low stresses within the flight). These computer programs will probably have to be developed due to the lack of commercially available spectrum generation programs.

When creating each spectrum, some options available to the user are cycle counting, clipping, and spectrum stress transfer factors. These options exist to correctly represent the stress spectrum for a damage tolerance analysis, and are not uniformly applied to all stress spectra. Cycle counting, spectrum clipping and transfer factors are explained in Sections 7.3.3 thru 7.3.5.

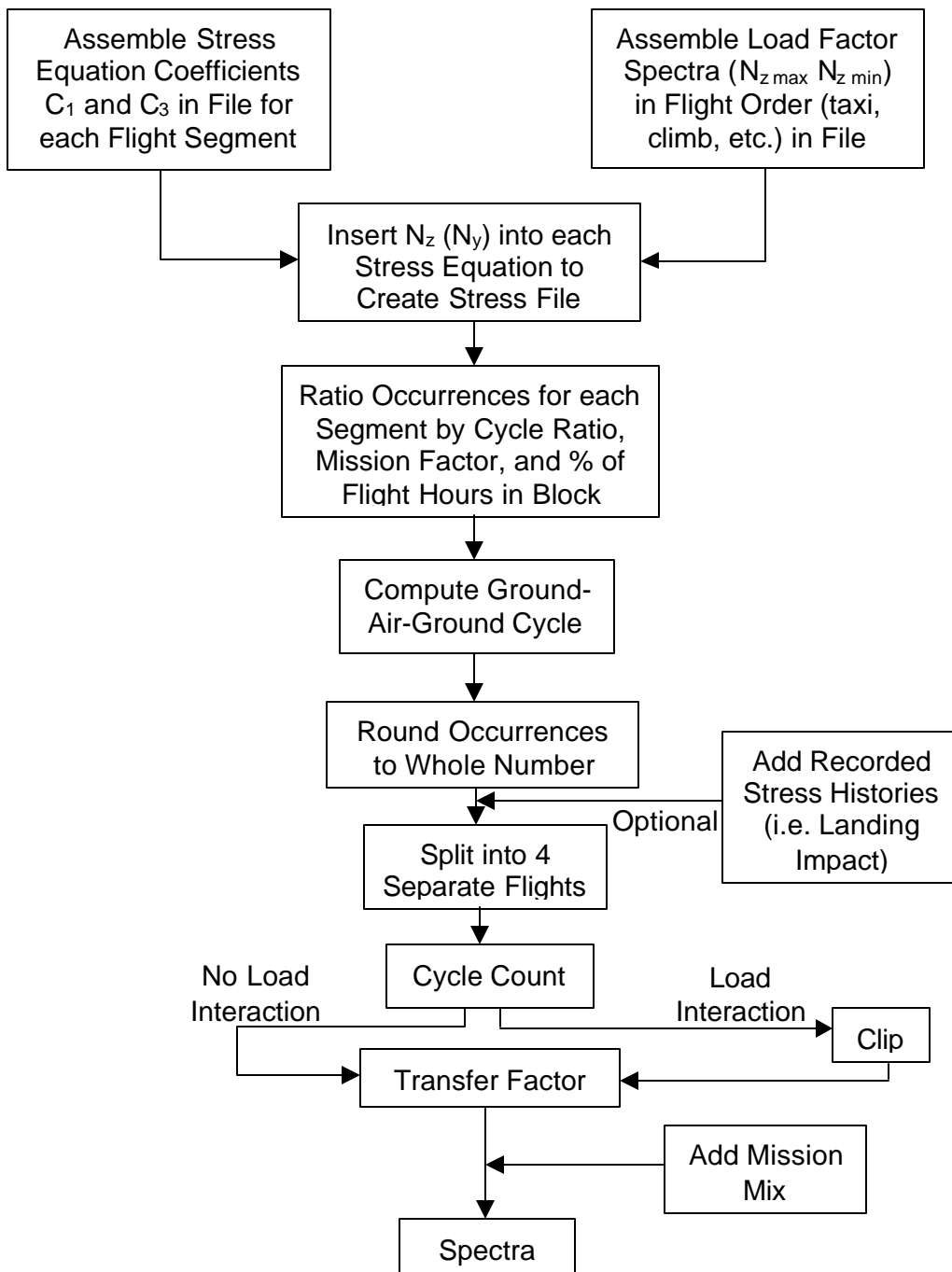
7.3.1 Stress Spectrum Construction For Flight Strain Equations

Usually two computer programs are used to create stress spectra due to the large volume of numerical calculations involved. The first such program creates a block stress spectrum for each flight profile (defined in Section 5.0). The second program splits that block spectrum into four flights and cycle counts each one.

The first step in creating a stress spectrum is to assemble the load factor spectrum into an input file. Each load spectrum (i.e., maneuver, gust, taxi, etc.) which is applicable to the critical area of a specific PSE is entered into an input file in the proper flight order (for example: taxi, climb gust, cruise gust, descent gust, maneuver and taxi). This file consists of maximum and minimum N_2 s and occurrences. The stress equation coefficients C_1 and C_3 for each flight segment of each flight profile are put into another input file. The spectrum program reads in the load spectra and stress equation coefficients and combines them to create a stress spectrum. Each segment of each profile is computed separately. Maximum and minimum stresses are calculated from the maximum and minimum load factors (N_2) for that particular load segment. Occurrences for that load set are read from the load factor spectrum and factored by the cycle ratio (see Section 7.2.3), the mission factor (see Section 5.3), and the percentage of flight hours in a 1,000 hour block that the profile makes. Figure 7-8 illustrates this procedure.

FIGURE 7-8

FLIGHT STRAIN SURVEYBASED STRESS SPECTRUM FLOWCHART



At this point no truncation is performed for flight segments. A once-per-flight taxi loading is retained for the ground-air-ground transition. The ground-air-ground is the stress cycle occurring once per flight containing the maximum positive flight stress paired with the maximum negative ground stress. The maximum and

minimum stresses are paired together and the stresses used to make the GAG cycle are removed from the stress spectrum so the total number of cycles remains unchanged. Next, the number of occurrences of each stress cycle in the spectrum is rounded to a whole number. Fractional occurrences less than 0.5 are summed and rounded to the nearest whole number.

The next step in creating a stress spectrum is to split the block stress spectrum for each profile into 4 separate flights representing a once per one (1/1), once per ten (1/10), once per one hundred (1/100), and once per one thousand (1/1000) flight. Progressively, each of these flights is more severe than the flights included in the mission mix (see Section 5.3). This method of splitting the block spectrum into separate flights accounts for the stress pairs with very low occurrence levels. These stress pairs are included in the 1/100 and 1/1000 flights. Some stress pairs with occurrence levels below 0.0005 are not included in any flights because they happen so infrequently, it would bias the spectrum in a severe manner. Any additional cycles such as a stress history of landing impact, need to be added to the spectrum.

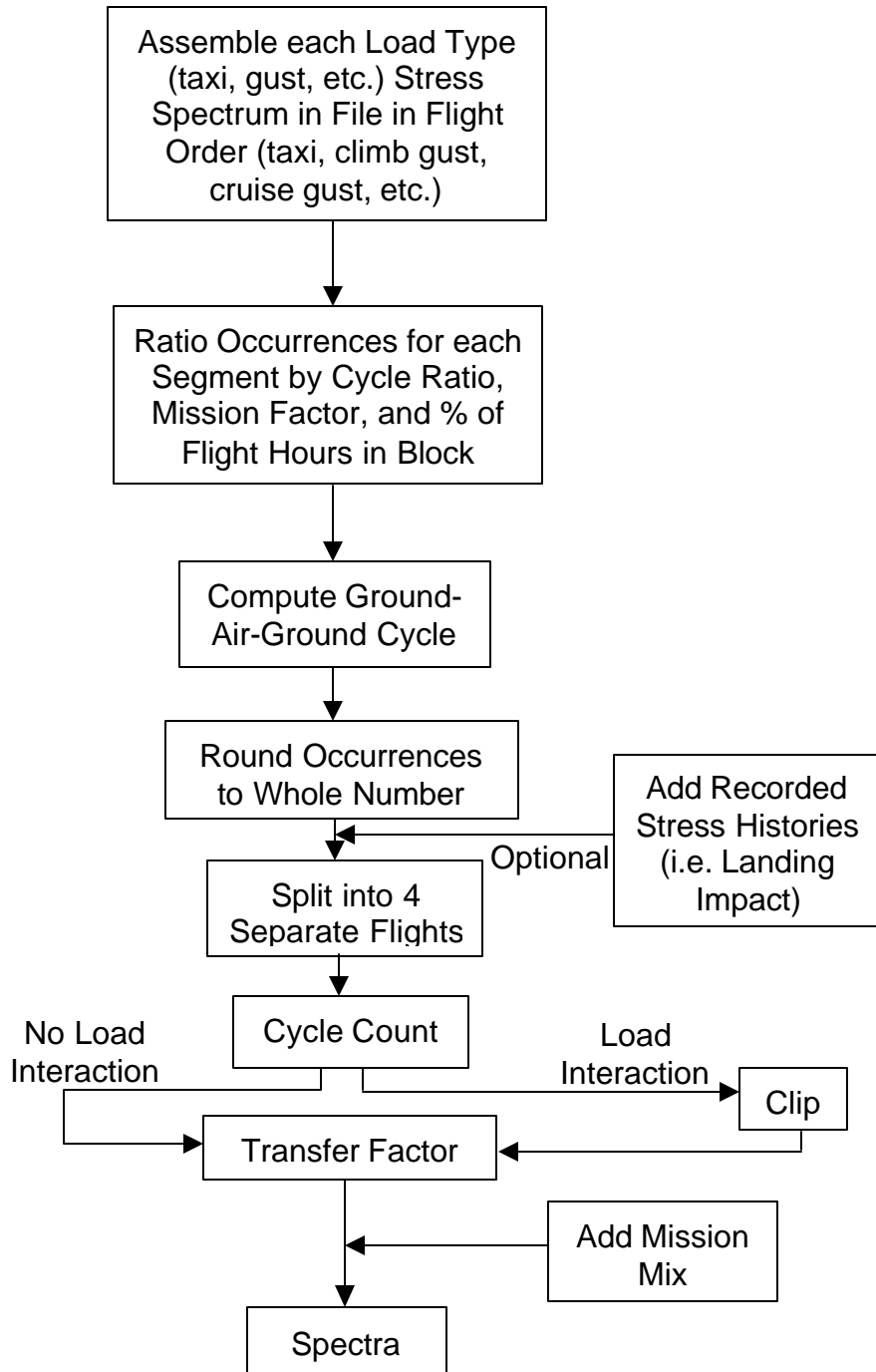
After each profile's block spectrum is split into four flights, these flights are all individually cycle counted. Cycle counting is explained in Section 7.3.3. After cycle counting, each flight is clipped if load interaction effects are considered in the damage tolerance analysis as explained in Section 7.3.4. The final gross area stress spectrum is output to a file that contains four flights for each profile in the spectrum. A mission mix that defines the distribution of these flights in a predefined block (i.e. 1000 flights or 1000 flight hours) is added to the stress spectrum file. The mission mix determines the order of the separate flights in the crack growth analysis. At this point, the stress spectrum is ready for use by damage tolerance programs.

7.3.2 Stress Spectrum Construction For Analytical Stresses

The first step in creating a stress spectrum is to assemble the stress spectrum created in Section 7.1 into an input file. Each stress spectrum (i.e., maneuver, gust, taxi, etc.) which is applicable to the critical area of a specific PSE is entered into an input file in the proper flight order (for example: taxi, climb gust, cruise gust, descent gust, maneuver and taxi). Occurrences for that load set are read from the load factor spectrum and factored by the cycle ratio, the mission factor (see Section 5.3), and the percentage of flight hours in a 1,000 hour block that the profile makes. Figure 7-9 illustrates this procedure.

FIGURE 7-9

ANALYTICALLY DERIVED STRESS SPECTRUM FLOWCHART



At this point no truncation is performed for flight segments. A once-per-flight taxi loading must be present for the ground-air-ground transition. The ground-air-ground is the stress cycle occurring once per flight containing the maximum positive flight

stress paired with the maximum negative ground stress. The maximum and minimum stresses are paired together and the stresses used to make the GAG cycle are removed from the stress spectrum so the total number of cycles remains unchanged. The number of occurrences of each stress cycle in the spectrum is rounded to a whole number. Fractional occurrences less than 0.5 are summed and rounded to the nearest whole number.

The next step in creating a stress spectrum is to split the block stress spectrum for each profile into 4 separate flights representing a once per one (1/1), once per ten (1/10), once per one hundred (1/100), and once per one thousand (1/1000) flight. Progressively, each of these flights is more severe than the flights included in the mission mix (see Section 5.3). This method of splitting the block spectrum into separate flights accounts for the stress pairs with very low occurrence levels. These stress pairs are included in the 1/100 and 1/1000 flights. Some stress pairs with occurrence levels below 0.0005 are not included in any flights because they happen so infrequently, it would bias the spectrum in a severe manner. Any additional cycles such as a stress history of landing impact need to be added to the spectrum.

After each profile's block spectrum is split into four flights, these flights are all individually cycle counted. Cycle counting is explained in Section 7.3.3. After cycle counting, each flight is clipped if load interaction effects are considered in the damage tolerance analysis as explained in Section 7.3.4. The final gross area stress spectrum is output to a file that contains four flights for each profile in the spectrum. A mission mix that defines the distribution of these flights in a predefined block (i.e. 1000 flights or 1000 flight hours) is added to the stress spectrum file. The mission mix determines the order of the separate flights in the crack growth analysis. At this point, the stress spectrum is ready for use by damage tolerance programs.

7.3.3 Spectrum Cycle Counting

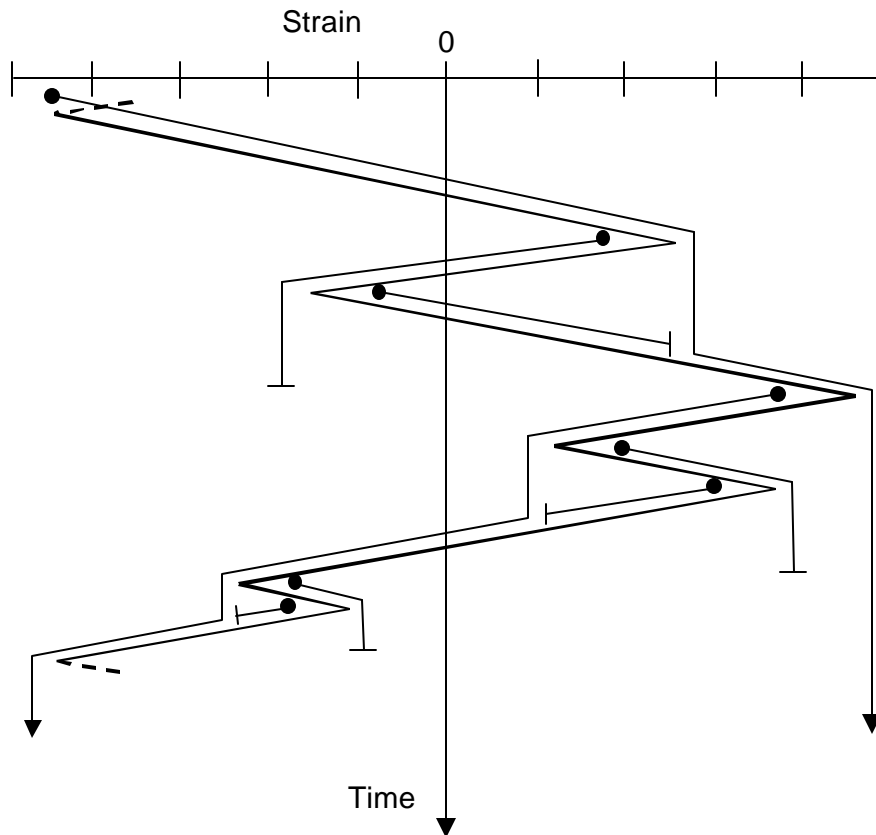
Spectrum cycle counting is used to summarize irregular load histories by counting the number of times cycles of various sizes occur (Reference 49). The cycle counting method sequences the stress spectrum in a low-high-low order for fatigue or damage tolerance analysis. A low-high-low order means that lower stresses are at the beginning of the spectrum but are gradually increasing. The highest loads of the spectrum usually occur in the middle of the flight and then the loads lower again as the flight nears completion. Methods that cycle count in this low-high-low fashion are called "rain-flow" methods.

Reference 49 gives a step-by-step guide to understanding and creating an algorithm for several cycle counting algorithms including three rain-flow cycle counting methods. The three rain-flow methods produce essentially the same spectrum but from a different approach. The rain-flow method turns the graphical display of the stress history vertical and treats the stress excursions as a series of

stacked roofs (see Figure 7-10). Rain is imagined to flow down the rooftops onto one another. After applying several rules, the range of the rain flow is considered the range of the stress. For segments of a load history that are repeatedly applied, the “simplified rain-flow” counting method can be used. Reference 49 details the methods of applying each of these three counting methods.

Reference 49 also addresses other cycle counting methods which are commonly used such as the range-pair method. The range-pair method counts a range as a cycle if it can be paired with a subsequent loading in the opposite direction.

FIGURE 7-10
RAINFLOW CYCLE COUNTING



7.3.4 Stress Spectrum Clipping

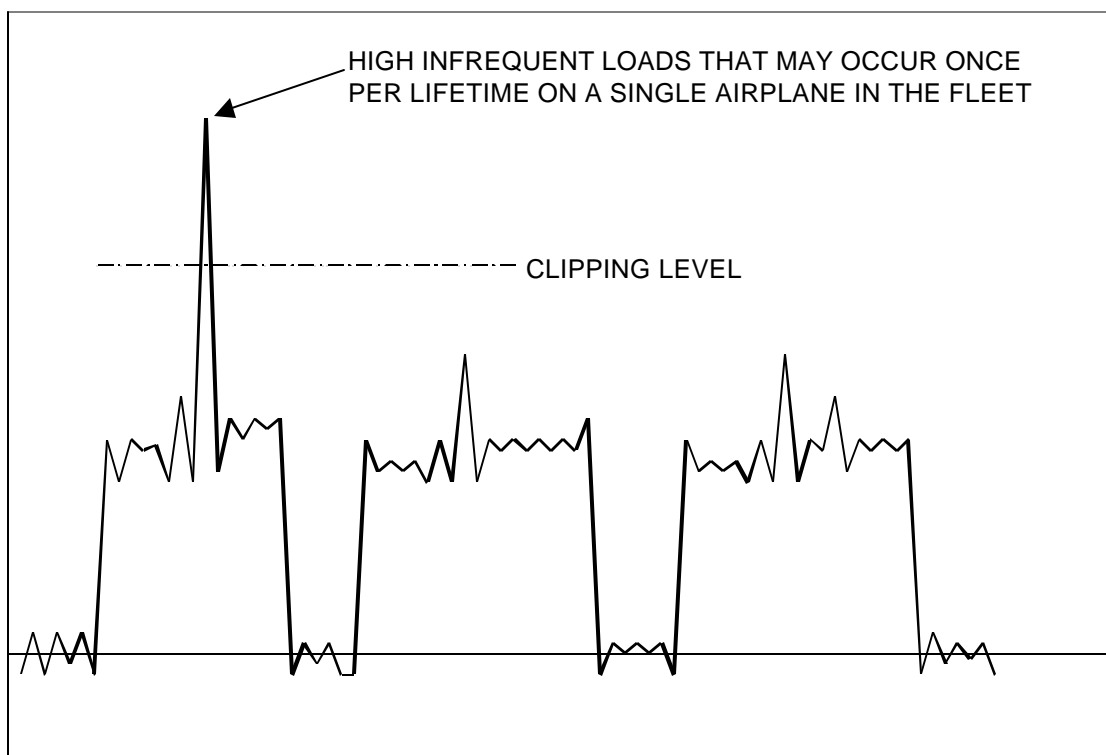
During construction of the stress spectrum, certain high load peaks could be included in the spectrum. These high stresses have very low occurrence levels and are usually only seen by one or two aircraft in the fleet during their service life. If load interaction is used, it is unconservative to include these high loads in a stress

spectrum that is supposed to represent typical fleet usage. Since these high peak loads usually cause considerable crack growth retardation, a longer crack growth life would be predicted than the fleet would actually see.

To account for this phenomenon, the stress spectrum is “clipped” at a level that represents the highest commonly seen loads. The act of clipping a spectrum does not cut out a peak stress, it just reduces its magnitude down to the defined clipping level. Figure 7-11 shows this stress level reduction.

FIGURE 7-11

PEAK STRESS CLIPPING EXAMPLE

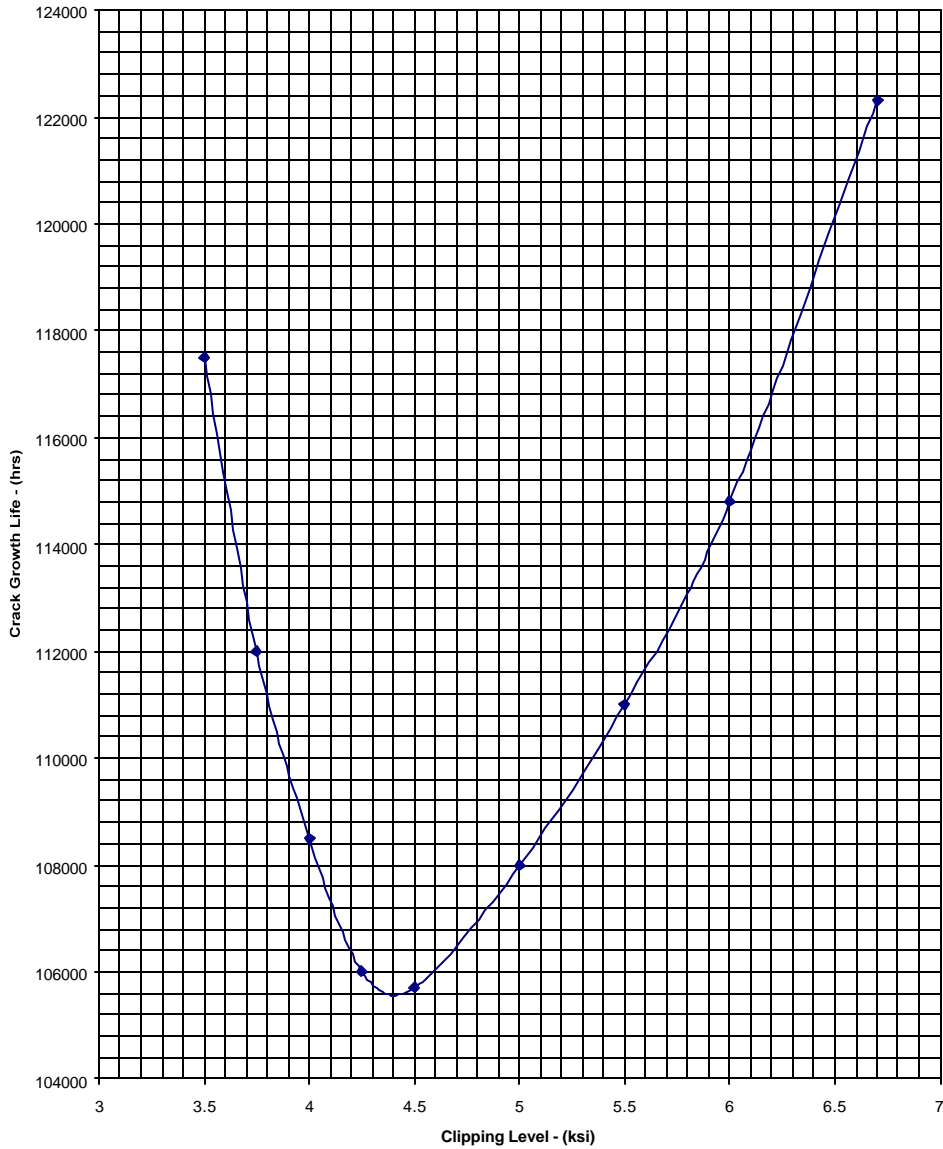


The effects of clipping a stress spectrum can be graphically seen in a crack growth vs. clipping level chart (Figure 7-12). The upper-right hand part of the figure is the normal location of the unclipped spectrum life. As the peak stresses are clipped to a lower and lower level, the crack growth life reduces because the effects of retardation are lessening due to lower peak stresses. There will be a point where the curve bottoms out and then starts going back up again to the left. The lowest most point on this curve is the correct clipping level for this particular stress spectrum. As the curve begins going back up, meaning the crack growth life is

increasing, the effects of retardation are being outweighed by the fact that too many high peak stresses have been removed so slower crack growth is occurring.

FIGURE 7-12

CLIPPING EFFECTS ON CRACK GROWTH EXAMPLE



The Air Force damage tolerance procedures recommend that the spectra be clipped at the 1/10 exceedance level. Maximum stresses above the maximum clipping level are changed to the maximum clipping level; likewise, minimum stresses below the minimum clipping levels are changed to the minimum clipping levels.

7.3.5 Transfer Factors

Before using the spectra in crack growth and fatigue calculations, certain adjustment factors may be required to obtain the stress at the critical area of the PSE location. The adjustment factors are the transfer factor and the net area factor. These factors are described as follows:

- 1) Transfer Factor, TF: A transfer factor is defined to transfer the stress from the strain gage to the PSE location. This is accomplished by dividing the stress at the analysis location (PSE) by the stress at the strain gage location as determined from a finite element model.
- 2) Net Area Factor, NAF: The net area factor (NAF) is applied to the basic stress spectrum to account for the reduction in cross-sectional area due to the absence of material at fastener locations. The NAF is calculated by dividing the gross cross-sectional area by the net-sectional area. Net area stresses are used for classical fatigue damage analyses only. The crack growth analyses use gross area stresses.

8.0 Damage Tolerance Analysis

The damage tolerance (crack growth) analysis phase consists of six (or in some cases seven) steps, which form the analytical background used to determine the inspection requirements outlined in Section 9.0. The steps in the damage tolerance analysis phase are:

- 1) **Determine Initial Flaw Size:** Initial flaws of given size, shape and orientation are assumed to be present in each analysis location and serve as starting points for the crack growth analysis (Step 2). Initial flaw sizes are discussed in Section 8.1.
- 2) **Perform Crack Growth Analysis:** The initial flaws specified in Step 1 are analytically grown using the material property data gathered per Section 4.0, and the stress spectra obtained from following the procedures outlined in Section 7.0. The crack growth analysis procedure is presented in Section 8.2.
- 3) **Determine Critical Crack Length:** For each analysis location the critical crack length, i.e., the crack length at which the part can no longer meet residual strength requirements, is determined. The critical crack length is used to establish the life of the structural detail by specifying an upper limit for the crack growth curve determined in Step 2. Section 8.3 presents the method for determining the critical crack length.
- 4) **Establish Inspection Threshold:** The inspection threshold (i.e., initial inspection) of the critical area of the PSE is established based on crack growth analysis and/or fatigue analysis depending on the fail-safe capability of the aircraft structure. Methods to determine the inspection threshold are presented in Section 8.4.
- 5) **Establish Repeat Inspection Intervals:** The repeat inspection interval for each analysis location is determined as a function of (a) the largest flaw size that has a low probability of escaping detection during an in-service inspection and (b) the time required for such a flaw to grow to a critical size. The repeat inspection interval is discussed in Section 8.5.
- 6) **Fatigue Analysis:** A fatigue analysis is generally not a part of a damage tolerance analysis. However, fatigue (safe-life) analysis is allowed on parts for which damage tolerance is impractical. Landing gear and its attachments are examples. Fatigue analysis is also allowed to establish the initial inspection threshold in multiple load path crack arrest "fail-safe" structure. Fatigue analysis procedures are presented in Section 8.6.
- 7) **Determine Onset of Widespread Fatigue Damage:** Widespread fatigue damage (WFD) is a major threat to the continued airworthiness of aging aircraft. Methods to identify areas susceptible to WFD based on analysis, test evidence and in-service experience are discussed in Section 8.7.

8.1 Initial Flaw Size

The initial (pre-existing) flaw shapes, sizes, and local orientation assumed for the damage tolerance analysis are presented in this section. The flaws are intended to provide the basis for analytical crack growth predictions to determine the initial and recurring inspection requirements for the aircraft.

The initial flaws defined in this section are identified as either primary or secondary flaws. Primary flaws are intended to provide the primary crack initiation site in a part, and they are representative of gross manufacturing defects. Secondary flaws are intended to provide the crack initiation site(s) for continuing growth after primary growth is arrested by growth to the edge of the part or into an adjacent hole. Secondary flaws are representative of typical manufacturing quality.

8.1.1 Primary Flaws

Initial (primary) flaws are assumed to exist in the aircraft from the time of manufacture. These flaws, along with their subsequent growth under flight conditions, will establish the initial inspection times for the aircraft. The initial flaws are assumed to exist at holes, edges of cut-outs or edges of parts and exist at the most unfavorable location and orientation with respect to the applied stresses and material properties. These flaws will be quarter-circular corner cracks, except when the part thickness is less than or equal to the initial flaw size, in which case the flaw will be a through-the-thickness crack. The initial cracks will be assumed to start from the side of the hole nearest the edge of the part (when an edge of a part is present). For locations away from holes, cut-outs or edges of parts, initial flaws are semi-circular surface flaws except where the part thickness is less than or equal to the initial flaw size, in which case they will be considered through-the-thickness.

Only a single primary flaw is assumed to exist at each location analyzed. However, in those cases where manufacturing operations exist such that a common flaw could exist in more than one element (common drilled holes) then a primary flaw is assumed to exist in each element.

The size of the initial flaw must be based on the largest initial flaw that can be expected. To determine this size, manufacturing inspection data should be reviewed. Data from initial crack sizes found in fatigue tests or service should be considered. Commercial and military service experience has provided the background to make a reasonable estimate of what the size of this initial flaw should be. The initial flaw sizes for cracks originating from fastener holes and the edge of a part, based on military specification AFGS-87221A (Reference 50), are presented in Table 8-1 and shown in Figures 8-1 and 8-2. The initial flaw sizes for surface flaws are shown in Table 8-1 and Figure 8-3. The primary flaw size for fuselage skins is set equal to the assumed minimum visible detectable crack length. For fuselage panels, this crack length is typically 2.00". The proposed initial flaw

sizes must be submitted to the FAA Aircraft Certification Office for approval prior to completing the final analysis.

The fastener type also has an influence on the size of the initial flaw. There are several techniques, such as interference fit pins, cold-working the holes, etc., that can reduce the effect of the stress concentration around a fastener hole. Therefore, it may be reasonable to reduce the initial flaw size but not account for the stress changes from the fastener installation. This is based on the rationale that the combined possibility of a poor installation and a severely flawed hole is low enough to be ignored. In the case of cold-worked holes, USAF damage tolerance specifications allow cold-worked (Cx) holes to be based on an analysis for a non-cold worked hole with a reduced initial assumed flaw size, considering the hole as being filled. Traditionally, a cold-worked hole is analyzed using a 0.005" initial flaw size.

TABLE 8-1

PRIMARY FLAW SIZE ASSUMPTIONS

Flaw Location	Flaw Shape	Thickness		
		t - in.	c _i - in.	a _i - in.
Hole/Edge	Part-Through	> .05	.05	.05
Hole/Edge	Through	≤ .05	.05	t
Surface	Part-Through	> .125	.125	.125
Surface	Through	≤ .125	.125	t

8.1.2 Secondary Flaws

The secondary flaw size is the “typical” flaw size representative of the initial quality of the structure. This is the minimum flaw size assumed to exist in any fastener hole. Data obtained from fatigue tests or service should be considered in determining this minimum flaw size. Secondary flaws are assumed to grow independently of the primary flaw up to the point that the primary flaw induces a failure. During the time that it takes a primary flaw to grow from a fastener hole to the edge of the part (ligament failure), a secondary flaw will be assumed to be growing opposite the primary flaw. At failure of the ligament, the continuing damage will include the growth of the secondary crack. For dual load path members, after the failure of the member which contains the assumed primary flaw, the second member must have enough residual strength to support the load.

FIGURE 8-1

PRIMARY FLAW SIZE ASSUMPTIONS FOR HOLE FLAW LOCATION

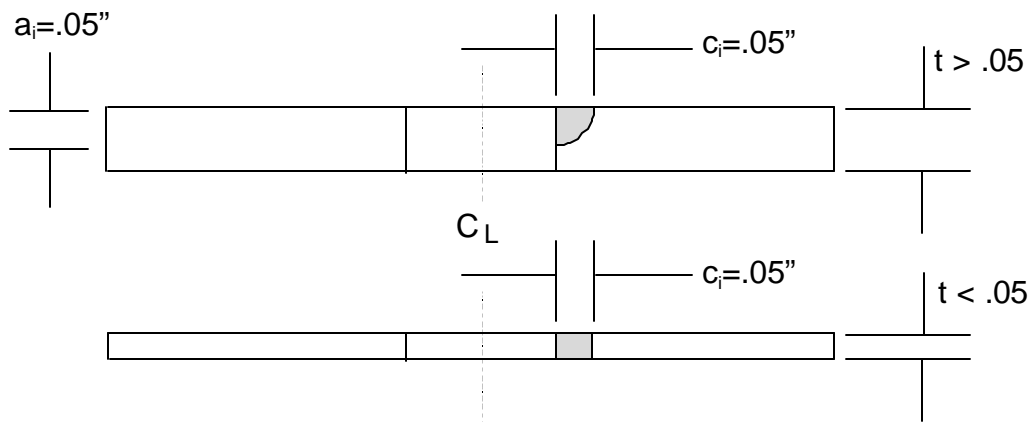


FIGURE 8-2

PRIMARY FLAW SIZE ASSUMPTIONS FOR EDGE FLAW LOCATION

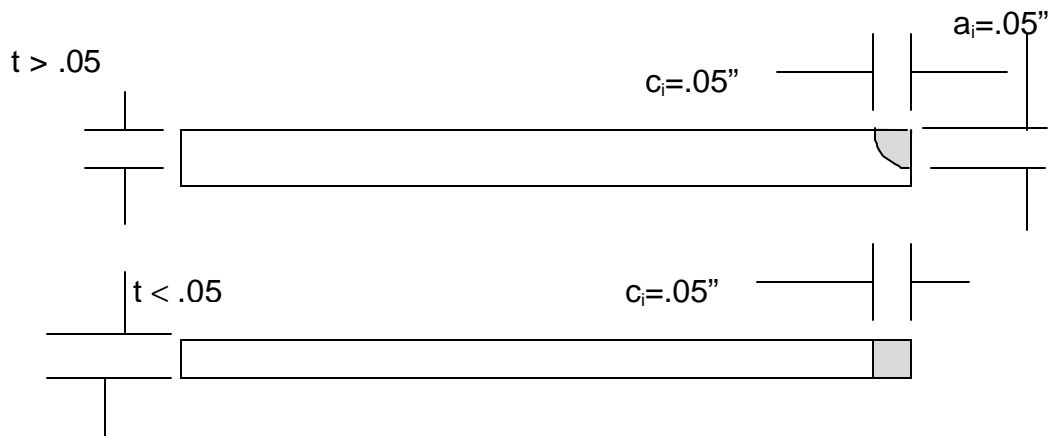
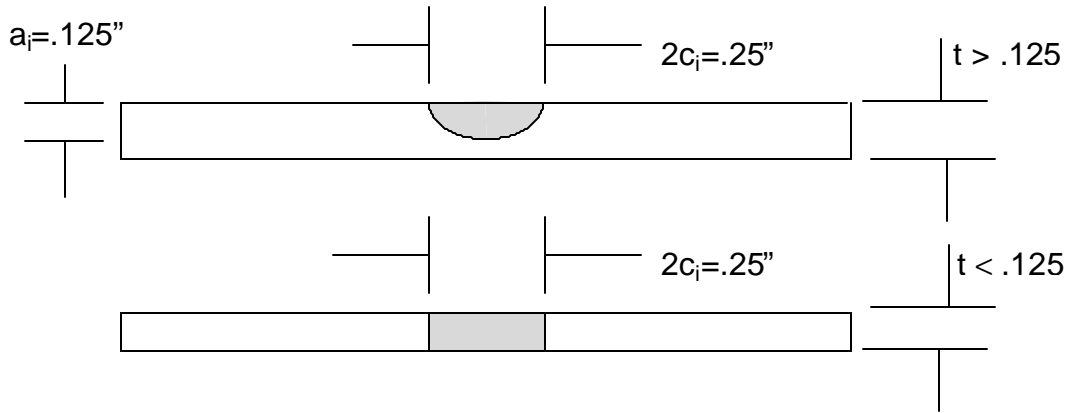


FIGURE 8-3

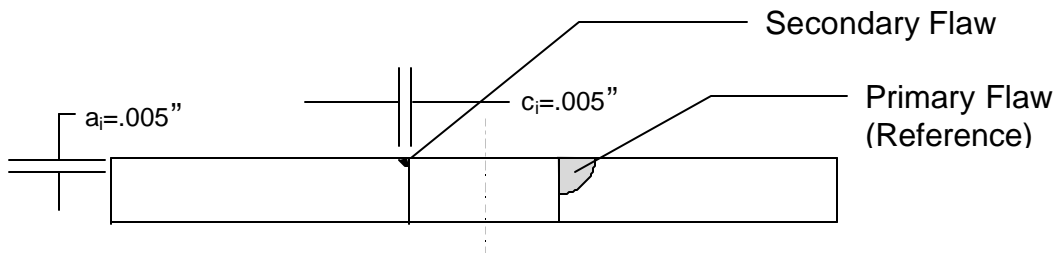
PRIMARY FLAW SIZE ASSUMPTIONS FOR SURFACE FLAW LOCATION



A suggested secondary flaw size for all structure is shown in Figure 8-4. As with the proposed primary flaw sizes, the proposed secondary flaw sizes must be submitted to the FAA Aircraft Certification Office for approval prior to completing the final analysis.

FIGURE 8-4

SECONDARY FLAW SIZE ASSUMPTIONS



8.1.3 Maximum Undetectable Flaws

Maximum undetectable flaws are defects that remain undetected in the structure after an inspection. The maximum size of these flaws will form the basis for the determination of required repeat inspection intervals, discussed in Section 8.5.

For visual inspections, a maximum undetectable flaw size may be on the order of 2.0 inches. This flaw size would include fuselage skin cracks (where detection due to pressure leaks would occur) and wing skin cracks (where detection due to fuel leaks would be obvious). For all other NDI inspections (cracks in caps, fittings, etc.) the flaw size is dependent on the location and the method of inspection used as described in Section 9.0.

8.2 Crack Growth Analysis

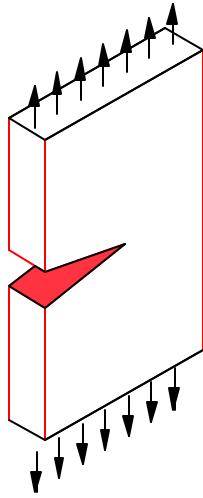
A crack growth analysis is required to determine the initial and repeat inspection intervals (Sections 8.4 and 8.5) for the critical area of each PSE. The methods of crack propagation analysis used by various manufacturers are generally different, and vary from extremely simplistic to extremely complicated. The simplistic methods are usually easy to implement for the manufacturer but tend to produce conservative results, which may be burdensome to the operator. The more sophisticated methods are more difficult to implement by the manufacturer but are usually more accurate, resulting in inspection frequencies that may not be as burdensome to the operator. Regardless of which method is utilized, the analysis is based on growth under spectrum loading (Section 7.0) from the maximum crack size that can remain undetected following an inspection to the critical size at limit load. This section presents some of the commonly used methods.

8.2.1 Basic Background

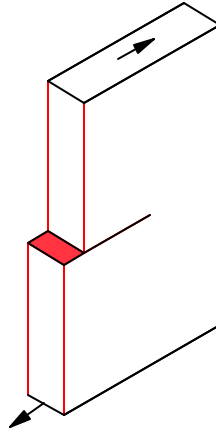
The application of fracture mechanics to solve crack problems is based on the assumption that the elastic stress field in the neighborhood of the crack tip controls the crack behavior. The significance of this stress field can be measured in terms of the stress intensity factor, K . One factor influencing K is the mode of crack extension, of which there are three independent types as shown in Figure 8-5. The tensile mode, Mode I, is the principal mode observed in practice and is thus the mode that is addressed through crack growth analysis and testing. While fractures induced by shear stresses can occur, they are infrequent.

FIGURE 8-5

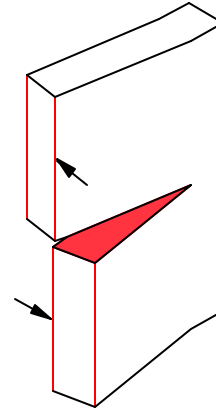
FRACTURE MODES



Mode I
Opening



Mode II
Shear



Mode III
Tearing

Linear elastic fracture mechanics (LEFM) analysis provides a good approximation to the localized stress state near the crack tip. It is widely accepted as an approach for evaluating crack growth in aircraft materials. Since LEFM is based on elastic stress analysis, it is implicitly assumed that any localized plastic deformation is small and contained within the surrounding elastic stress field. Application of linear elastic stress analysis to Mode I cracks such as that illustrated in Figure 8-6 shows that the stress field close to the crack tip ($r \ll a$) is given by:

$$\sigma_x = \frac{K_I}{\sqrt{2\pi} r} \cos \frac{\theta}{2} \left[1 - \sin \frac{\theta}{2} \sin \frac{3\theta}{2} \right]$$

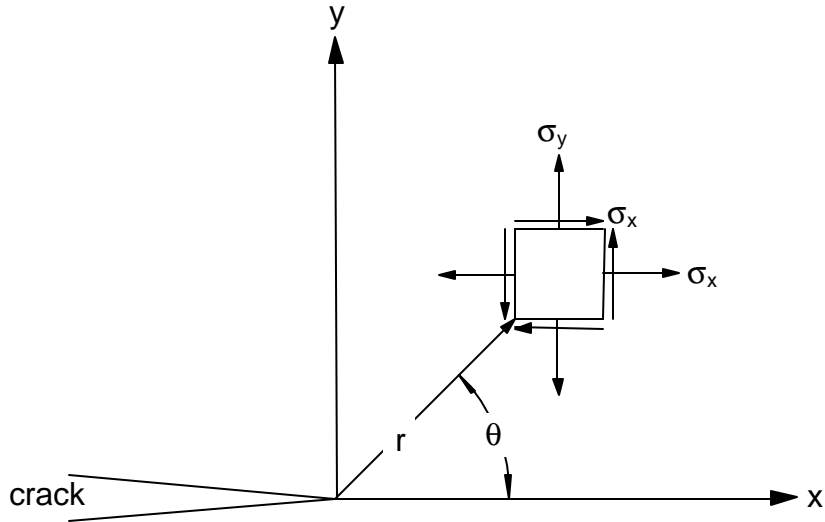
$$\sigma_y = \frac{K_I}{\sqrt{2\pi} r} \cos \frac{\theta}{2} \left[1 + \sin \frac{\theta}{2} \sin \frac{3\theta}{2} \right]$$

$$\sigma_{xy} = \frac{K_I}{\sqrt{2\pi} r} \sin \frac{\theta}{2} \left[\cos \frac{\theta}{2} \cos \frac{3\theta}{2} \right]$$

where r and θ are polar coordinates and K_I is known as the Mode I stress intensity factor. The remaining stresses are given by $\sigma_z = \sigma_{xz} = \sigma_{yz} = 0$ for plane stress problems, and by $\sigma_{xz} = \sigma_{yz} = 0$ and $\sigma = \nu(\sigma_{xz} + \sigma_{yz})$ for plane strain problems. These equations are valid for all Mode I cracks, regardless of geometry or loading.

FIGURE 8-6

DEFINITION OF X-Y PLANE STRESSES NEAR CRACK TIP



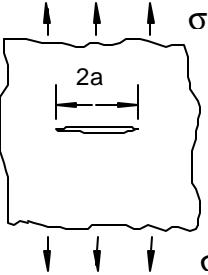
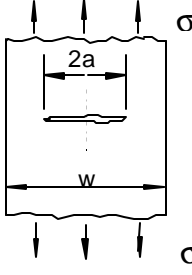
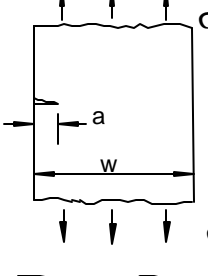
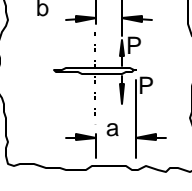
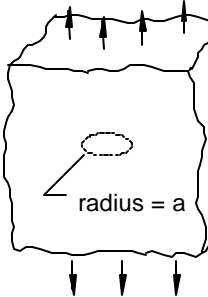
The parameter K_I that occurs in the equation for each of the three stresses determines the intensity or magnitude of the stress in a small region around the crack tip. The applied loads and geometry of the cracked part influence the crack tip stresses through K_I . The stress intensity factor is thus a single parameter characterization of the crack tip stress field. As the applied loads on the cracked part change, the crack tip stresses change accordingly through K_I , and the potential for crack propagation changes.

Figure 8-7 shows stress intensity factors for several simplified configurations. As indicated from the K_I expressions, the stress intensity factors can all be put in the general form:

$$K_I = \sigma \sqrt{\pi a}$$

FIGURE 8-7

SIMPLIFIED STRESS INTENSITY FACTOR SOLUTIONS

<u>Geometry</u>	<u>Description</u>	<u>K_I</u>
	Center cracked infinite plate with remote tension load	$\sigma\sqrt{\pi a}$
	Center cracked finite width plate with remote tension load	$\sigma\sqrt{\pi a \sec\left(\frac{\pi a}{w}\right)}$
	Edge cracked finite width plate with remote tension load	$1.12\sigma\sqrt{\pi a}$, $a \ll w$
	Center cracked infinite plate with symmetric wedge load	$\frac{P}{t\sqrt{\pi a}} \sqrt{\frac{a+b}{a-b}}$, $t = \text{thickness}$
	Imbedded penny crack in infinite plate with remote tension	$\sigma\left(\frac{2}{\pi}\right)\sqrt{\pi a}$

where the crack length is “a”, the factor β is a function of the part geometry and crack length, and σ is the reference stress. The reference stress is usually the far-field uniform or bending stress. In problems where the applied load is a pin load, the reference stress is usually bearing stress.

Most commonly used stress intensity factor solutions are available in handbooks such as References 51-54 and in libraries contained in most crack growth programs, as noted in Section 8.2.3. The derivation of stress intensity solutions is not generally straightforward. Several methods of approximation are discussed in Section 8.2.4.

8.2.2 Crack Growth Models

The following information must be available to model crack growth behavior analytically:

- 1) The far-field reference stress (or load) spectrum (Section 7.0) for the analysis location.
- 2) Constant amplitude crack growth rate (Section 4.3) and fracture toughness (Section 4.2) data for the material and relevant environment.
- 3) The stress intensity factor, K_I , and,
- 4) An algorithm that uses the stress spectrum and stress intensity factor to integrate the crack growth rate, producing a crack growth curve.

Cracks at each analysis location are propagated in a variable amplitude cyclic stress environment defined by the stress spectrum. The spectrum contains a history of flight-by-flight reference stresses specified on a random cycle-by-cycle basis. The stress spectrum is used to derive a stress intensity factor history, as discussed below.

The increment of crack growth per loading cycle, or crack growth rate, is primarily a function of the stress intensity factor history and material properties. Constant amplitude crack growth test data is used to express the rate of change of crack length with respect to the number of applied loading cycles (N) as an empirical function of ΔK and material properties:

$$\frac{da}{dN} = f(\Delta K, \text{Material})$$

where ΔK is the stress intensity factor range for the stress cycle. Using the expression for K_I in Section 8.2.1, ΔK can be expressed as:

$$\Delta K = \Delta \sigma \hat{a} \sqrt{\delta a}$$

where $\Delta \sigma$ is the stress range of the cycle, i.e., $\Delta \sigma = \sigma_{\max} - \sigma_{\min}$.

The time for a crack to grow from an initial length (a_i) to a final length (a_f) is found by substituting the above equation for da/dN into the expression for K_I and integrating:

$$N = \int_{a_i}^{a_f} \frac{1}{f(\Delta K, \text{Material})} da$$

In practice, the above integration is carried out numerically using a crack growth program. A damage integration algorithm within the program is employed to evaluate variable amplitude crack growth on a cycle-by-cycle basis. It accounts for the influence of material, structural geometry, and the maximum and minimum peak stresses in the stress spectrum. Crack growth is accumulated monotonically from the initial size according to:

$$a = a_i + \sum^N \Delta a$$

where a_i is the initial crack length, Δa is the crack growth increment, and a is the current crack length associated with N increments of growth.

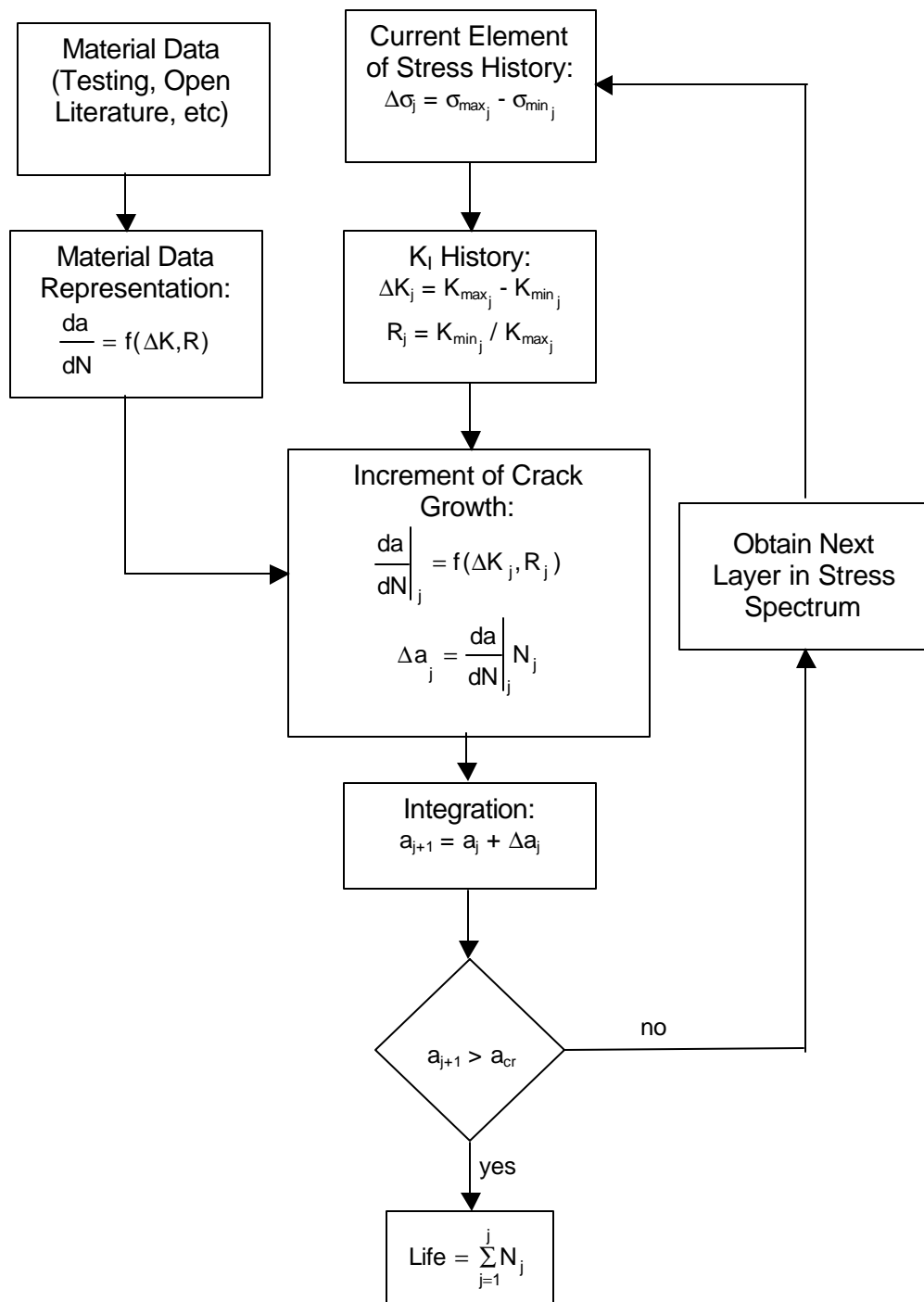
Baseline crack growth rate testing is performed under constant amplitude loading conditions, but aircraft structures are subjected to variable amplitude loading. The ordering of cycles in the stress spectrum can influence crack growth life. This phenomenon results from crack tip plastic effects, and is referred to as load interaction. It describes the observation that the rate of crack growth during a particular cycle depends not only on the stresses in that cycle, but also on the stresses in the previous cycles. Some crack growth models ignore load interaction effects, and are referred to as linear models. The more sophisticated models that include such effects are referred to as load interaction models. Examples of each are given in the following sections.

8.2.2.1 Linear Crack Growth Models

Linear crack growth models neglect the effects of load interaction. They require a stress spectrum, a way of representing constant amplitude material behavior, a stress intensity factor solution, and a damage integration algorithm. The crack growth computations are typically carried out numerically using a procedure similar to that represented in Figure 8-8. Two commonly used methods of modeling constant amplitude material behavior are discussed in this section.

FIGURE 8-8

CRACK GROWTH COMPUTATION PROCEDURE FOR PROBLEMS WITHOUT
 LOAD INTERACTION (REFERENCE 51)



8.2.2.1.1 Walker/Chang Material Representation

This section presents the use of the Walker/Chang crack growth rate equation (Reference 9) to model constant amplitude material behavior. Similar versions of the model are included in several programs.

Constant amplitude material data represented with the Walker/Chang equation use the K_{max} Walker equation to represent positive stress ratios and the Chang equation for negative stress ratios:

$$\frac{da}{dN} = C[(1-R)^m K_{max}]^n \quad R_{cut} > R > 0 \text{ and } \Delta K > \Delta K_{th}$$

$$\frac{da}{dN} = C[(1+R^2)^q K_{max}]^n \quad R_{cutn} < R < 0 \text{ and } \Delta K > \Delta K_{th}$$

$$\frac{da}{dN} = 0 \quad \Delta K < \Delta K_{th}$$

where:

- $\frac{da}{dN}$ = crack growth rate
- R_{eff} = effective stress ratio
- K_{max} = maximum stress intensity factor
- C, m, n = empirical constants
- q = acceleration index
- R_{cut} = positive stress ratio cutoff limit, above which the material does not exhibit additional stress ratio effects.
- R_{cutn} = negative stress ratio cutoff limit, below which the material does not exhibit additional stress ratio effects.

The values of C , m , n and q are obtained from a best fit to the material data. For values of R that exceed R_{cut} , R_{cut} is used in place of R in the K_{max} Walker equation. Similarly, for values of R less than R_{cutn} , R_{cutn} is used in place of R in the Chang equation. Also, there is no crack growth below the threshold value of ΔK . The threshold is a function of R and material:

$$\Delta K_{th}(R) = \Delta K_{th}(0) \cdot (1 - A_{th} R) \quad R > 0$$

$$\Delta K_{th}(R < 0) = \Delta K_{th}(0) \quad R < 0$$

8.2.2.1.2 NASGRO Material Representation

The NASGRO equation (Reference 11) of crack growth appears in the NASGRO program and several other programs that use the NASGRO database. It is given by:

$$\frac{da}{dN} = C \left[\left(\frac{1-f}{1-R} \right) \Delta K \right]^n \frac{\left(1 - \frac{\Delta K_{th}}{\Delta K} \right)^p}{\left(1 - \frac{K_{max}}{K_c} \right)^q}$$

where: $\frac{da}{dN}$ = crack growth rate
 R = stress ratio
 C, n, p, q = empirical constants
 f = crack opening function
 ΔK_{th} = threshold stress intensity factor
 K_c = critical stress intensity factor

The values of C, n, p and q are obtained from the material data.

8.2.2.2 Crack Growth Models with Load Interaction

Typical aircraft loading results in a mixture of high and low stresses associated with varying stress ranges. The crack growth increment produced by any given load cycle depends upon the prior load history. The term “load interaction” is used to describe these effects. Load interaction results from the plastic deformations that occur as the crack propagates. An overload tends to result in less crack growth on a given subsequent load cycle than would be produced by the same load cycle under constant amplitude conditions, a phenomenon known as retardation. Conversely, an underload following an overload results in a reduction of the retardation effect of the overload.

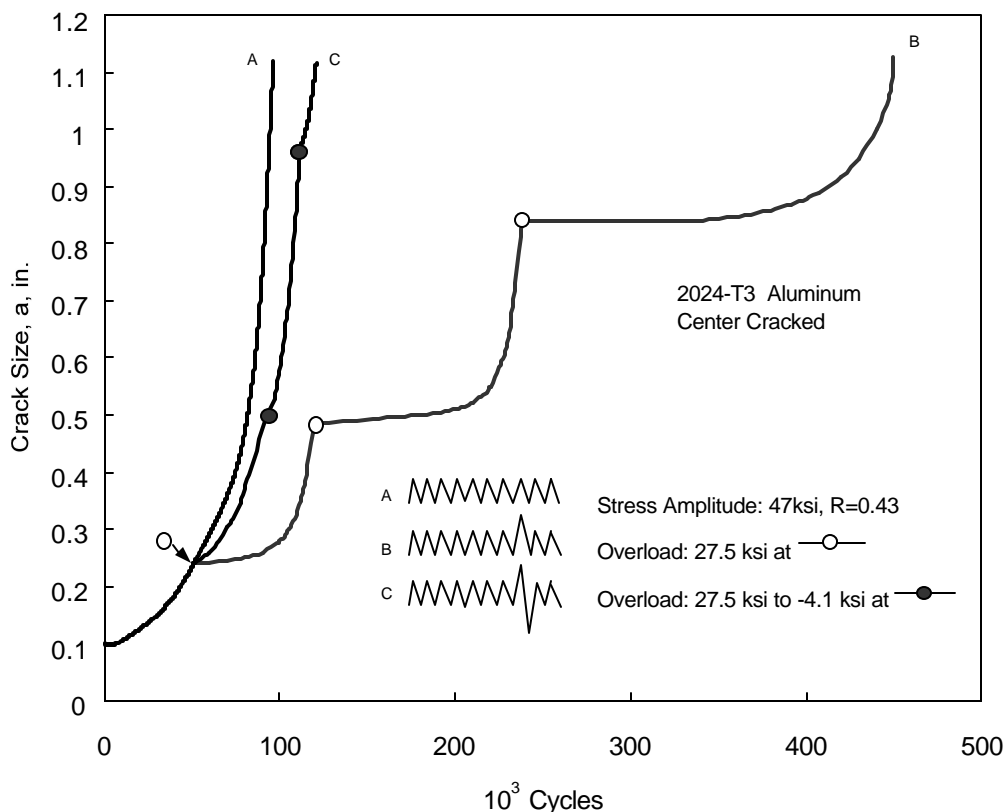
The effects of load interaction are illustrated in Figure 8-9. The baseline crack growth curve (A) was obtained from a constant amplitude test. In a second experiment (B), the same constant amplitude loading was interspersed with overload cycles. During the loading portion of the overload cycle, the material at the crack tip is plastically deformed in tension. Upon unloading, the surrounding material is unloaded elastically, leaving the material at the crack tip in compression. Following each application of the overload, the residual compressive stresses resulted in a crack growth rate that was reduced to near zero over several subsequent cycles, after which the original growth rate was gradually approached. In the third experiment (C), the tensile overload was followed by a compressive overload which caused reverse plastic deformations at the tip of the crack. The effect of reverse plastic deformations was to reduce the beneficial effect of the tensile overload.

Crack growth computations that account for load interaction effects, are typically carried out numerically using an extension of the procedure employed for problems

without load interaction, as illustrated in Figure 8-10. Two load interaction models are discussed in the following sections.

FIGURE 8-9

**RETARDATION DUE TO OVERLOAD AND OVERLOAD/UNDERLOAD CYCLES
 (REFERENCE 55)**



8.2.2.2.1 Generalized Willenborg-Chang

The Generalized Willenborg-Chang load interaction model is illustrated in this section. The model presented in this section is used in the CRACKS98 crack growth program, Reference 56. Similar versions of the model are included in other programs. The model predicts that immediately following an isolated overload cycle, such as that represented in spectrum B of Figure 8-9, an enlarged compressive plastic zone is created ahead of the crack tip. The plastically deformed material is assumed responsible for a retardation in the subsequent crack growth rate through the zone. As long as the plastic zone of the current cycle measured from the current crack tip ($a + r_y$) is less than the extent of the plastic zone produced by the overload ($a_{OL} + r_y^{OL}$), as illustrated in Figure 8-11, load interaction effects are taken into account. If the overload is followed by a compressive spike as shown in spectrum C in Figure 8-9, the overload retardation effect is reduced.

FIGURE 8-10

CRACK GROWTH COMPUTATION PROCEDURE FOR PROBLEMS WITH LOAD INTERACTION (REFERENCE 51)

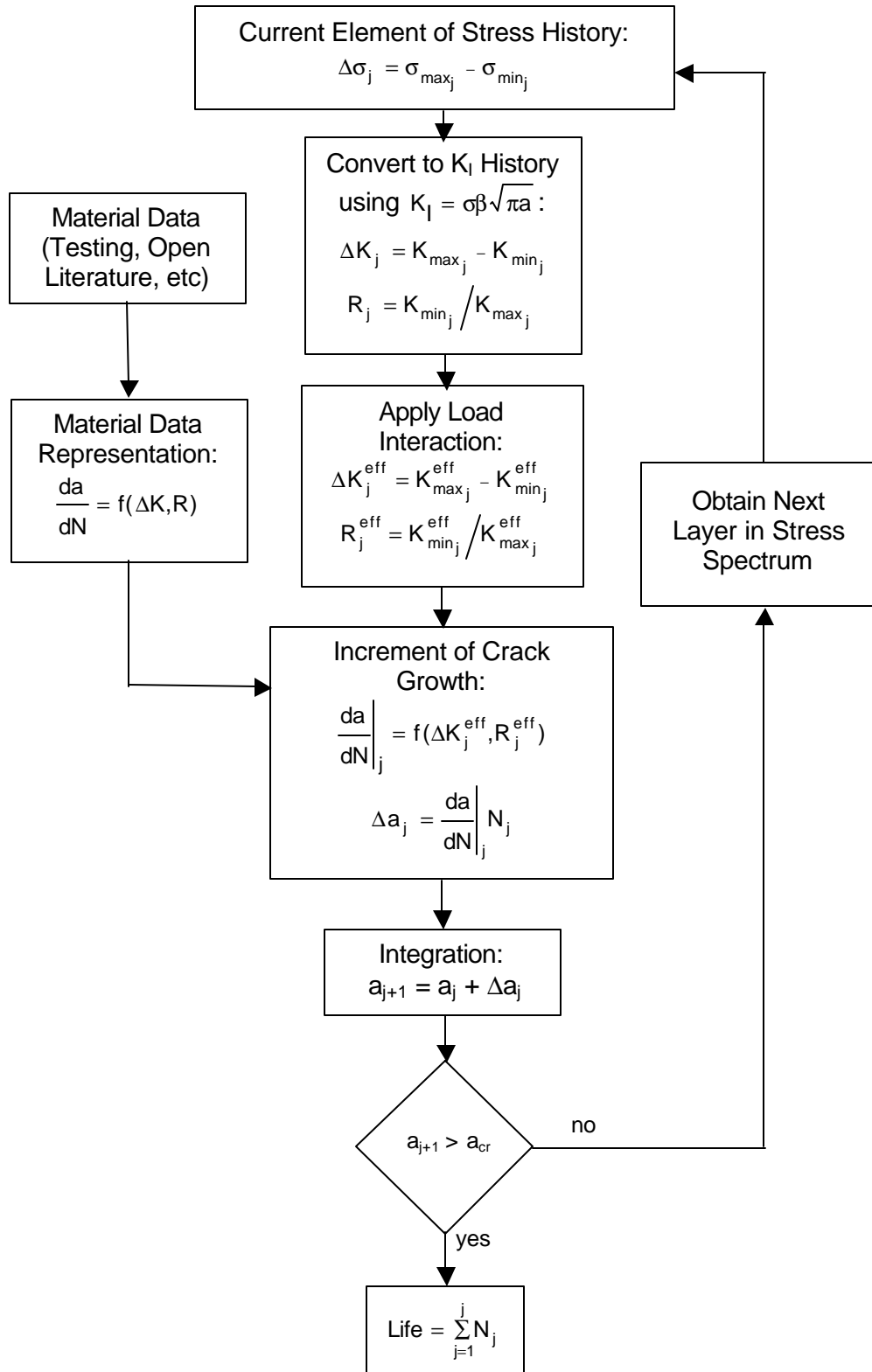
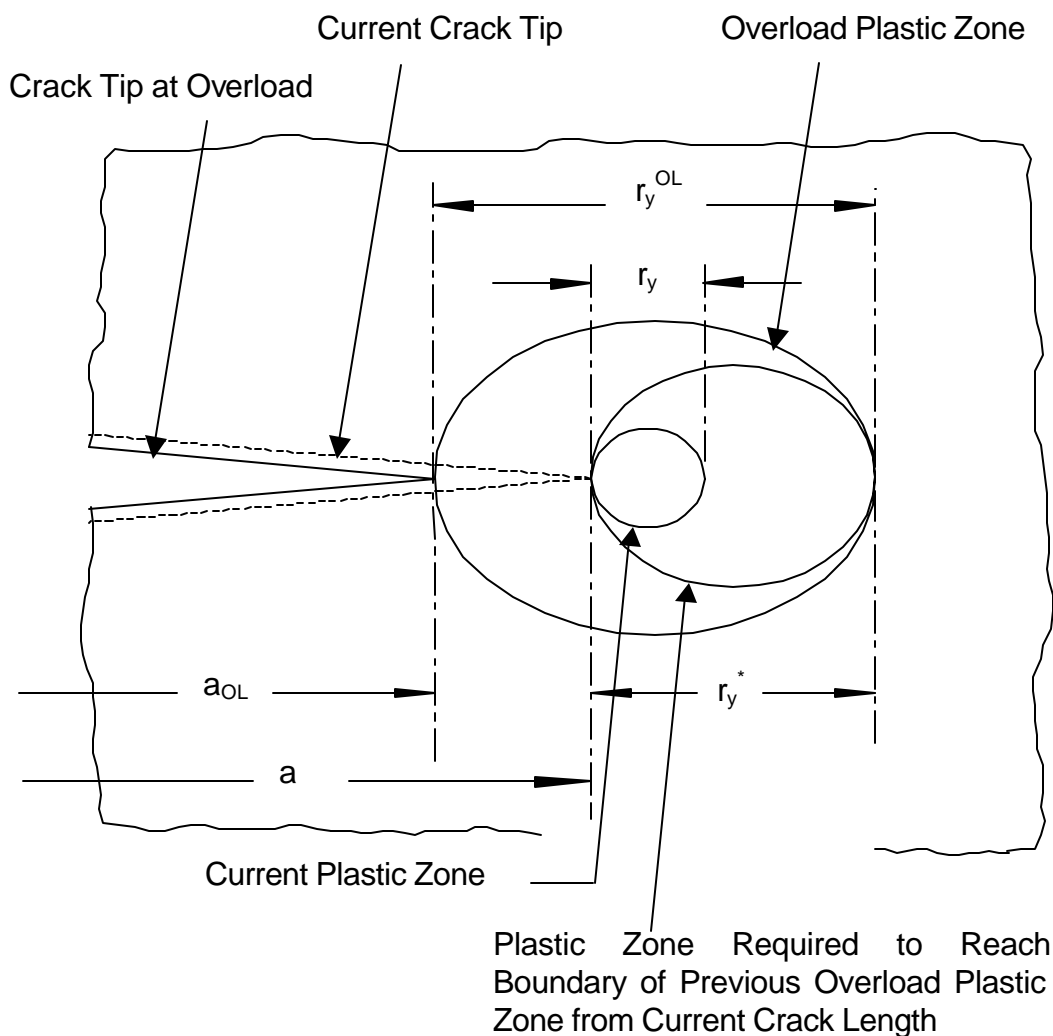


FIGURE 8-11

GENERALIZED WILLENBORG-CHANG LOAD INTERACTION MODEL



Computationally, the load interaction behavior is implemented by replacing the values of K_{min} , K_{max} , and R for the current cycle with effective values K_{min}^{eff} , K_{max}^{eff} , and R_{eff} :

$$K_{min}^{eff} = K_{min} - K_{red}$$

$$K_{max}^{eff} = K_{max} - K_{red}$$

$$R_{eff} = K_{min}^{eff} / K_{max}^{eff}$$

where K_{red} is the residual stress intensity factor. Letting K_{max}^* represent the stress intensity factor required to generate a load interaction zone coincident with the load

interaction zone due to the overload, K_{red} is assumed to be proportional to the difference between K_{max}^* and the current K_{max} :

$$K_{red} = \Phi (K_{max}^* - K_{max})$$

If $K_{red} < 0$, then $K_{red} = 0$

where:

$$K_{max}^* = K_{max}^{OL} \sqrt{1 - \frac{a - a_{OL}}{r_y^{OL}}}$$

$$K_{max}^{OL} = \text{maximum stress intensity factor of prior overload}$$

$$= \sigma_{max}^{OL} \hat{a} \sqrt{\alpha a_{OL}}$$

$$r_y^{OL} = \text{plastic zone size created by previous overload}$$

$$= \frac{1}{\alpha \hat{\sigma}} \left(\frac{K_{max}^{OL}}{F_{t_y}} \right)^2$$

F_{t_y} = material yield strength

$\alpha = 2$ typically for plane stress, and

$\alpha = 4\sqrt{2}$ typically for plane strain

and the proportionality factor Φ is given by:

$$\Phi = \frac{1 - (\Delta K_{th_0} / K_{max})}{R_{so} - 1}$$

where:

ΔK_{th_0} = threshold stress intensity factor range at $R = 0$

R_{so} = overload shutoff ratio.

The overload interaction zone is reduced whenever the stress intensity factor ratio is negative and the current loading cycle is an overload condition. If K_{min}^{OL} is less than zero, then the extent of the plastic zone associated with the overload is decreased to:

$$r_y^{OL} = \left(1 + \frac{K_{min}^{OL}}{K_{max}^{OL}} \right) r_y^{OL}$$

where:

K_{\max}^{OL} = maximum stress intensity factor due to overload
 K_{\min}^{OL} = minimum stress intensity factor due to overload

and the stress intensity factor of the overload is decreased to

$$K_{\max}^{OL} = F_{t_y} \sqrt{\dot{a} \ddot{r}_y^{OL}}$$

The Generalized Willenborg-Chang model requires a single value for the overload shutoff ratio R_{so} . The overload shutoff ratio is defined as the ratio of the maximum stress intensity factor of the overload cycle to the maximum stress intensity factor of the current cycle of interest at which no fatigue crack growth occurs. For variable amplitude fatigue crack growth, R_{so} varies with both material and spectrum parameters such as stress ratio and magnitude of the compressive loads. Typical values for aluminum range from 2.3 to 2.7.

8.2.2.2 Crack Closure

The most realistic load interaction model developed to date is the crack closure model proposed by Elber (References 55 and 57) and further developed by Newman (Reference 58). The model is based on the phenomenon that during crack propagation a zone of residual plastic deformation is left in the wake of an advancing crack tip. On unloading, these deformations interfere with the closing crack and tend to result in crack closure above zero load. The crack remains closed until the applied loads are sufficiently increased to re-open the crack. Determination of the crack closure stress, S_{OP} , is thus an important step in the application of the model. The effective stress intensity range, ΔK^{eff} , for a stress cycle is then based on the effective stress range $\Delta S^{eff} = S_{\max} - S_{OP}$ rather than $\Delta S = S_{\max} - S_{\min}$ if S_{\min} is less than S_{OP} .

The crack closure model can be used to make accurate predictions of the effect of retardation on crack growth under spectrum loading. However, in its most general form, the model requires a numerical analysis of the elastic-plastic stress near the crack tip, making the calculations much more involved than those required for the Willenborg model. For this reason, simplified closure models are included in some crack growth programs.

8.2.3 Crack Growth Programs

Several crack growth programs are available commercially. This section gives a brief description of three programs that have found widespread use. It is not meant to be a comprehensive list of programs or capabilities. It is, rather, intended to

summarize some of the useful features available in general purpose crack growth codes.

8.2.3.1 CRACKS98

The University of Dayton Research Institute's (UDRI) CRACKS98, Reference 56, is a crack growth life calculation algorithm which is based on the linear elastic fracture mechanics approach for estimating the life of a component with a crack. It contains several methods of representing material data, loading spectra, and K_I solutions. The code currently includes:

- Five crack growth rate behavior descriptions – Power Law, Forman Equation, Walker Equations, Sinh Equation, and tabular interpolation.
- Six load interaction models – no load interaction, basic Willenborg, generalized Willenborg, Willenborg/Chang, Wheeler, and the Hsu models.
- A spectrum input routine which can process a variety of variable amplitude histories.
- Stress intensity factor calculations from a library of solutions that includes the solutions available in NASGRO, from tabular interpolation of beta factor input data, and from weight functions.
- An option for evaluating the effect of a residual stress state on crack growth, and,
- Options for evaluating continuing damage.

8.2.3.2 NASGRO

NASGRO version 3.0 (Reference 11) is a suite of computer programs comprised of three modules: NASFLA, NASBEM, and NASMAT. The NASFLA program is based on fracture mechanics principles that can be used to calculate stress intensity factors, compute critical crack sizes, or to conduct fatigue crack growth analyses. Crack growth analyses may be performed either interactively or in a batch mode. Material properties can be chosen from a large database supplied with the program by selecting from a menu of options. Crack growth properties may also be entered as either a 1-D table or a 2-D table. The fatigue loading spectra can be input easily from a standard file or individual files. User-defined material properties and fatigue spectra may also be supplied manually and saved for future use. The second module, NASBEM, incorporates the boundary element method of analysis for solving problems with complex crack configurations. The third module, NASMAT, is designed for processing fatigue crack growth data in a laboratory and obtaining curve fits to the NASGRO equation.

Crack growth can be modeled with the effects of load interaction. Five models, the Generalized Willenborg, the Modified Generalized Willenborg, the Willenborg-Chang, the Strip Yield and the Constant Closure models have been implemented. Some of these models account for the crack growth retardation only and the others account for both acceleration and retardation resulting from overloads and underloads in fatigue loading spectra.

Several options are available for defining fatigue loading spectra of arbitrary size. The format for fatigue loads can be of the standard NASGRO type or of the sequential type common in the aircraft industry.

8.2.3.3 AFGROW

The AFGROW (Air Force Grow, Reference 17) program is a general purpose crack growth program developed over several years with funding from the U.S. Air Force and U.S. Navy. The program has a state-of-the-art user interface and runs on UNIX and Windows platforms. AFGROW is maintained by the Air Force Wright Aeronautical Laboratories (AFWAL/FIBEC).

Material data can be represented using one of five methods provided in AFGROW. These include the Walker Equation, Forman Equation, NASGRO Equation, Harter T-Method, and tabular lookup.

Variable amplitude spectra may be evaluated with or without load interaction. If load interaction is desired, the available models include Generalized Willenborg, Wheeler, and a plasticity based closure model.

Typical industry loading spectra can be represented. They include constant amplitude, blocked, or cycle-by-cycle spectra.

Stress intensity factors can be determined from the AFGROW internal library, or input manually. The AFGROW stress intensity solution library includes two types of solutions:

- Solutions using standard stress intensity factors
- Solutions based on weight functions.

In addition, an option is available for user input beta solutions.

AFGROW also includes an option to account for the effect of a bonded composite repair patch on crack growth life. The method is based on the Green's function method.

A server version of AFGROW for Windows 95/98/NT4 is available, and may be used interactively or by other windows programs. Microsoft's Component Object Module (COM) Server technology has been incorporated into the server version of

AFGROW, allowing users to efficiently perform multiple crack growth analyses and have the results sent directly to the calling program.

New capabilities are under development including methods to analyze multiple cracks and time dependence. The developers continuously seek to improve the capabilities of AFGROW by encouraging comments and suggestions from users in government and industry through an online users consortium.

8.2.4 Stress Intensity Factor Solution Development

The most commonly used stress intensity factor solutions involve pin loaded holes in tension fields and are available in handbooks such as References 51-54 and in libraries contained in most crack growth programs. The solutions found in many program libraries include a sufficiently broad class of geometry and loading types to represent most practical problems. When handbooks or solution libraries cannot adequately depict important aspects of the local geometry or applied loading, a variety of alternate solution methods are available. The methods used in deriving solutions vary greatly in complexity. An example of a simple method is superposition as shown in Figure 8-12. In this case, a component with a crack is subjected to more than one load type. The stress intensity factor for the combined loading can be obtained by adding the K_I values from each separate load case.

A less trivial procedure is illustrated in Figure 8-13. This example illustrates how the stress intensity solution for a complex geometry can be determined by breaking the geometry down into separate, simpler configurations with known K_I values and then multiplying the effect of each configuration. This is known as the compounding method.

Occasionally, local geometric or loading effects may require finite element modeling using codes such as Stress Check (Reference 59) or FRANC2D/L (Reference 60). Boundary element codes such as BEASY (Reference 61) or the BEM code in NASGRO are also available for modeling such problems.

In certain situations, the applied load or stress distribution is too irregular to employ the above methods. Frequently the solution of such problems can be approximated using weight functions (References 62-67). Weight functions are available in some crack growth programs, including CRACKS98 and AFGROW.

FIGURE 8-12

EXAMPLE OF SUPERPOSITION

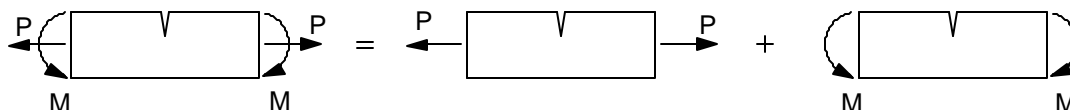
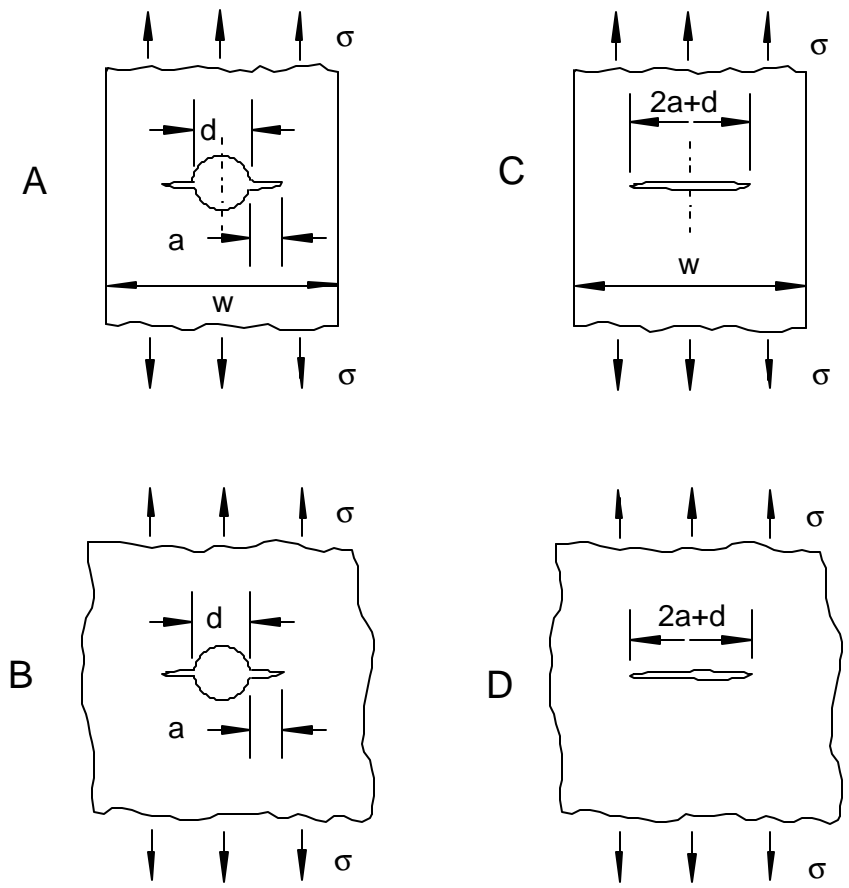


FIGURE 8-13

EXAMPLE OF COMPOUNDING



$$\frac{K_A}{K_B} = \frac{K_C}{K_D}$$

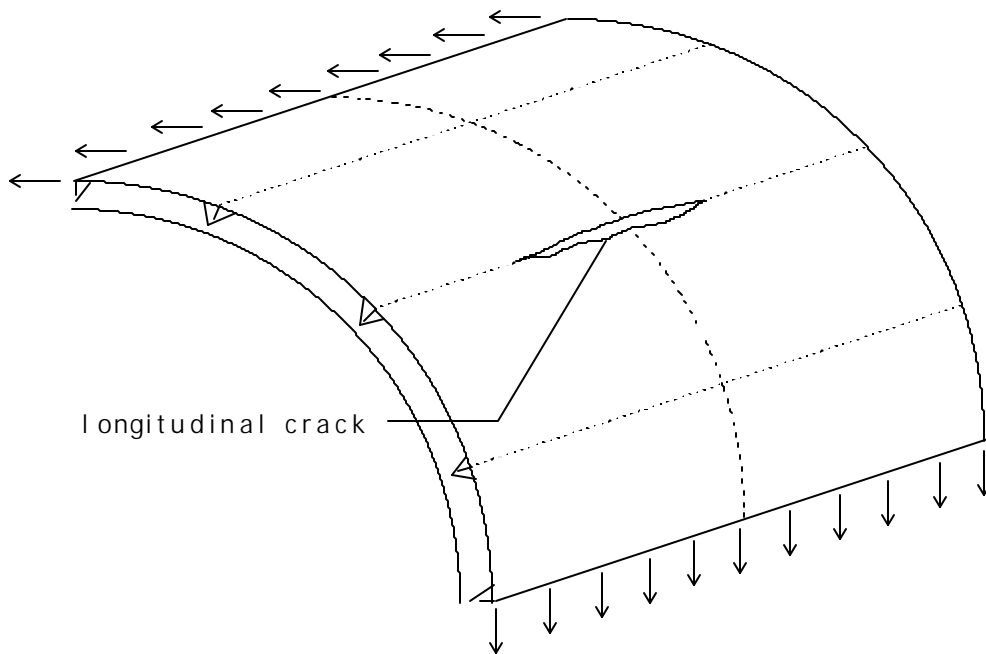
$$K_A = K_B \frac{K_C}{K_D}$$

8.2.5 Special Case: Pressurized Fuselage Structure

For most crack configurations and load cases stress intensity factor solutions are either contained in the databases of the crack growth software, are available from the various handbook references or can be obtained using compounding or weight function techniques as described in Section 8.2.4. However, the stress intensity factor solution for a crack in a stiffened, pressurized fuselage, one of the critical stress intensity factor solutions for aircraft damage tolerance analysis, is not readily available from handbooks, or obtainable through compounding or weight function approaches. Therefore one accepted process for obtaining stress intensity factors for cracks in pressurized fuselage structures is presented in this section. An example of a longitudinal fuselage crack is shown in Figure 8-14.

FIGURE 8-14

LONGITUDINAL CRACK IN PRESSURIZED FUSELAGE STRUCTURE



In general, the stress intensity factor solution for this case is broken down into two separate solutions, and the total stress intensity factor is obtained through compounding. The two cases are:

- A crack in a flat, stiffened panel subjected to uniaxial tension. The crack can either lie between two stiffeners, centered under an intact center stiffener with intact stiffeners on either side, or centered under a broken center stiffener with intact stiffeners on either side.
- A correction factor, called the bulge factor, to account for the effects of panel curvature, biaxial stress field, pressure loading, and out-of-contour deformation of the crack faces for longitudinal cracks in pressurized aircraft fuselages. For circumferential cracks, no such correction is necessary, and hence the bulge factor is equal to one.

It is beyond the scope of this handbook to provide all the details of the stiffened panel and bulge factor analyses. An overview of the procedures and assumptions of the analyses is presented below. For details of the calculations refer to the references listed in the respective sections.

8.2.5.1 Displacement Compatibility Method for Stiffened Panels

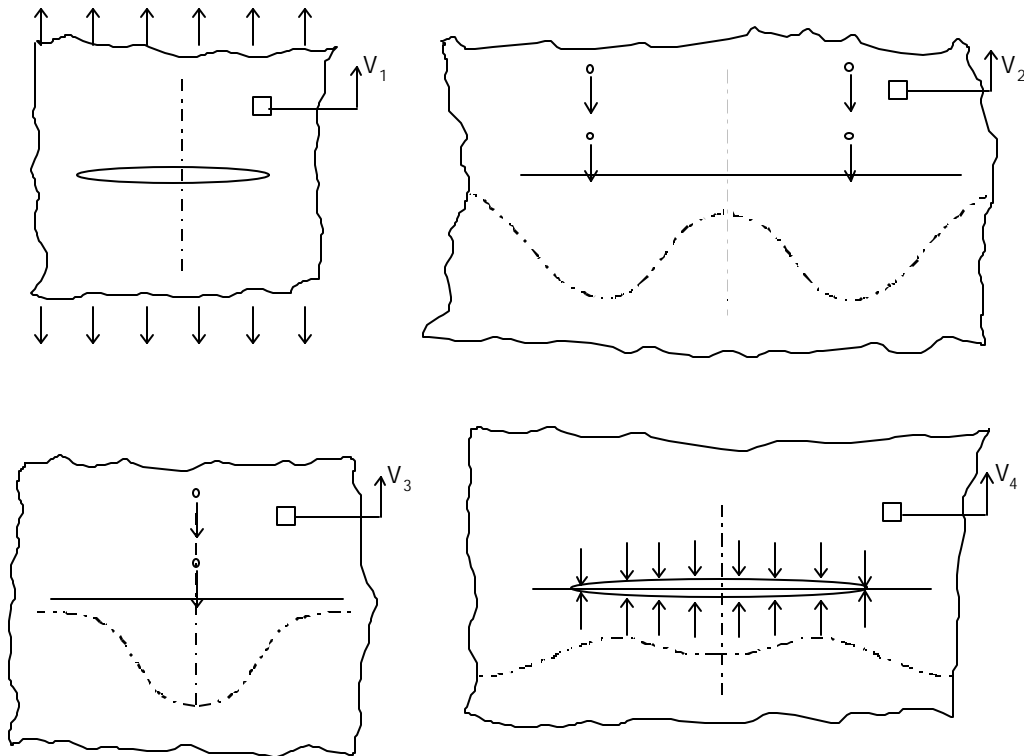
The displacement compatibility method is a closed form, purely analytical approach that does not rely on finite element solutions. The displacements in the cracked skin are defined as equal to the displacements in the stiffeners at each rivet location. The method accounts for fastener deflections, as well as stiffener extension and bending. The structure (including fasteners) is assumed to behave linearly at all times. In the following sections the basic procedure for the displacement compatibility method is presented for the sample case of a crack centered under a broken center stiffener with intact stiffeners on either side. The methodology for the two other cases of interest is analogous, the only difference is the choice of the appropriate displacement functions for each case. The set of equations that need to be solved simultaneously for the various cases are contained in a series of papers by Tom Swift (see References 68-71).

8.2.5.1.1 Skin Displacement

For the case of a crack centered under a broken stiffener, with intact stiffeners on either side, the total skin displacement is determined by the superposition of the four load cases shown in Figure 8-15.

FIGURE 8-15

SKIN DISPLACEMENT SUPERPOSITION LOADING CASES



where:

- V_1 = Displacement in skin due to the overall gross stress applied to the cracked sheet.
- V_2 = Displacement in uncracked skin due to intact, outer stiffener fastener loads.
- V_3 = Displacement in uncracked skin due to broken, center stiffener fastener loads (fundamentally the same technique as V_2).
- V_4 = Displacement due to uncracked skin stress distribution (equal and opposite to the stress caused by the fastener forces) applied to crack face.

8.2.5.1.2 Stiffener Displacement

The total stiffener displacement (measured at the fastener shear face) is defined as the sum of displacements from:

- Shear fastener loads

- Overall axial stresses
- Bending loads from fasteners

The displacements due to shear fastener loads, and axial stresses are calculated using elasticity solutions (see References 69-71). The displacement due to induced bending from the fasteners is calculated using the local moments shown in Figure 8-16 and the stresses determined using the 3-moment method (from Figure 8-17). A separate derivation to calculate bending stresses is used depending on whether the frame (stiffener) is broken or intact.

FIGURE 8-16

IDEALIZED FRAME LOADING

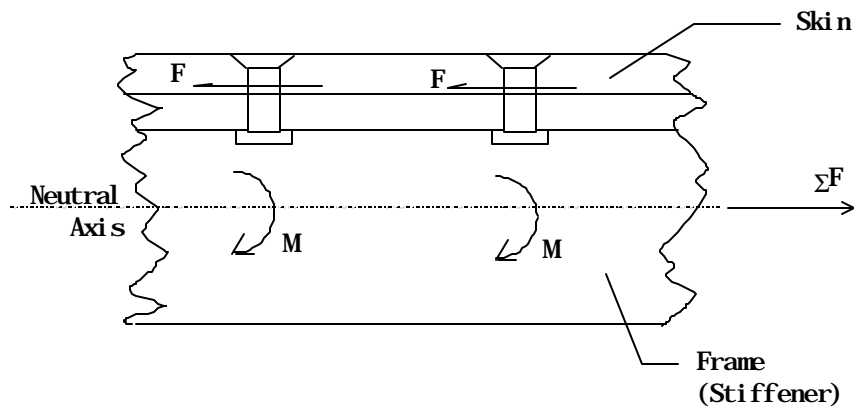
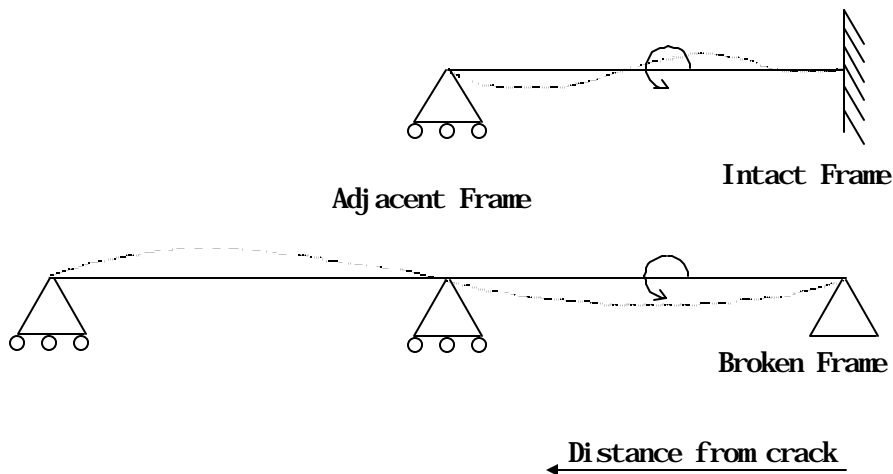


FIGURE 8-17

FRAME BENDING IDEALIZATION



8.2.5.1.3 Fastener Displacement

The fastener deflections are assumed to be linear with applied load (plasticity ignored). Additionally, all fasteners are assumed to remain connected regardless of the actual capability of each fastener (failure ignored). Each of these assumptions can have an effect on the final answer to varying degrees as documented by Swift. Nevertheless, a purely elastic solution will provide valid, accurate results for most cases if the user is aware of these limitations and regards solutions with highly loaded (beyond yield) fasteners with some suspicion.

In the absence of any actual test information, the fastener stiffness should be calculated using the methods presented in Reference 68 or NACA TN-1051 (Reference 72). For bonded elements, the bond surface is divided into a series of bonded rectangles, each of which is then treated the same as for actual fasteners as shown in Reference 69.

8.2.5.1.4 Displacement Compatibility

The displacement of the skin is set equal to the displacement of the frame while accounting for the fastener deflection. A system of simultaneous equations is then set up for each of the above displacement terms. Solving these equations gives the total load for each fastener. Swift presents the results of parametric studies that indicate that accounting for the loads in 15 fasteners (above the crack) is sufficient (Reference 71). Therefore, the final matrix size to be solved is 30 x 30 for a two-bay crack and 15 x 15 for a one-bay crack.

8.2.5.1.5 Crack Tip Stress Intensity and Beta Solution

The crack tip stress intensity in the skin is determined through superposition of the stress intensity factor of the overall stress in the skin and the stress intensity factor due to each loaded fastener. The stress intensity due to the overall stress is based on the solution for a finite width center cracked plate. The stress intensity solution for each fastener (or point load) is calculated using the complex variable method shown below.

$$K = \frac{P}{2t\sqrt{\pi c}} \left\{ \sqrt{\frac{c+z}{c-z}} + \sqrt{\frac{c+\bar{z}}{c-\bar{z}}} - \left[\gamma \left(\sqrt{\frac{c-z}{c+z}} \frac{c}{(c-z)^2} - \sqrt{\frac{c-\bar{z}}{c+\bar{z}}} \frac{c}{(c-\bar{z})^2} \right) \right] i \right\}$$

where:

$$z = x + yi$$

$$\bar{z} = x - yi \text{ (complex conjugate of } z\text{)}$$

$$\gamma = \frac{1+\nu}{2} \text{ (for plane stress)}$$

and:

c = half-crack length

x = fastener location (along axis of crack growth)

y = fastener location (perpendicular to axis of crack growth)

P = fastener load (perpendicular to crack face)

t = skin thickness

v = Poisson's ratio

The geometry factor for the stiffened panel, $\beta_{\text{stiffened}}$, can then be obtained directly

from the compounded stress intensity factor solution as: $\beta_{\text{stiffened}} = \frac{K}{\sigma\sqrt{\pi c}}$.

8.2.5.2 Bulge Factors

The bulge factor is an adjustment to the stiffened panel stress intensity factor solution for longitudinal cracks in pressure vessels, that accounts for the effects of panel curvature, pressure loading, biaxial stress field and out of contour displacement of the crack faces. Bulge factor solutions reported in the literature were either obtained from experimental data (References 73, 74) or from sophisticated nonlinear finite element analyses (References 75, 76). The bulge factors reported in References 73-76 were obtained for unstiffened pressure vessels, so a further correction for the reduction in bulge at the stiffeners is required. One such correction was developed by Swift and is reported in Reference 70.

It is important to note that all of the bulge factor solutions referenced here were developed for transport category aircraft. When applying any of these solutions to commuter size aircraft, significant extrapolation beyond the data for which the bulge factors were determined is required. At the writing of this report bulge factor development work is continuing. A review of bulge factor data available in the open literature should be conducted at the time a SID is developed, to ensure that the most current available data is used.

8.2.6 Example Problem

This section illustrates, by example, some of the general considerations that must be addressed in performing a typical crack growth analysis. The example used for discussion is a typical lower wing spar cap shown in Figure 8-18. It will be assumed that a hole in the cap, common to both the cap and skin, has been selected as a critical location in the PSE.

Setting up the crack growth analysis involves several steps. The basic steps can be summarized as follows.

- 1) Establish the initial crack geometry; that is, the initial crack size and orientation (Section 8.1). For this example, assume that a 0.05" initial primary crack is

located at the edge of the fastener hole such that it will grow toward the near edge of the cap as shown in Figure 8-19. This orientation places the crack face in the maximum principal stress plane. Independent of the primary crack, a secondary crack is assumed to exist on the opposite side of the hole with an initial crack length of 0.005". Following failure of the near side ligament, the secondary crack continues to grow until failure.

- 2) Determine the material properties (Section 4.0) including crack propagation (da/dN vs. ΔK) data and fracture toughness. Assume, for the example, that the crack growth material data can be represented by the Walker/Chang equation (Section 8.2.2.1.1) and neglect the effects of load interaction. The material data used for the crack growth analysis is given in Table 8-2.

TABLE 8-2

EXAMPLE MATERIAL DATA

Material Parameter	Value
K_{IC}	38 ksi $\sqrt{\text{in}}$
$\Delta K_{th} @ R = 0$	2.38 ksi $\sqrt{\text{in}}$
A	0.833
Walker C	2.20×10^{-9}
Walker n	3.0
Walker m	0.60
Chang q	0.15
R_{cut}	0.90
R_{cutn}	-0.50

- 3) Determine the stress spectrum for the location (Section 7.0). The process of defining the stress spectrum involves determining the stresses at the critical location. The stress distribution in the wing structure is usually defined using a finite element model similar to that shown in Figure 8-20, in which the skins and webs are represented with plate elements and the caps and stringers with beam elements. Local stresses in the spar cap are obtained from beam element stresses, and fastener loads are based on skin shear as illustrated in Figure 8-21.
- 4) Obtain a K_I solution. A number of simplifications and assumptions are made in choosing a K_I solution for the spar cap. The cap cross section is idealized as a finite width rectangular plate with an eccentric hole as shown in Figure 8-19. Additional restraint from adjacent structure (as from web or skin) is not considered, and any influence from other fasteners on the crack tip is ignored.

The applied stresses include the bypass stress, out-of-plane bending, and fastener bearing stress. A representative K_I solution consisting of a superposition of the three cases shown in Figure 8-22 was chosen for the example.

- 5) Run the crack growth analysis and determine the inspection intervals. The crack growth curve for the spar cap is shown in Figure 8-23, along with the determination of the threshold and recurring inspection intervals.

FIGURE 8-18

EXAMPLE CRITICAL LOCATION

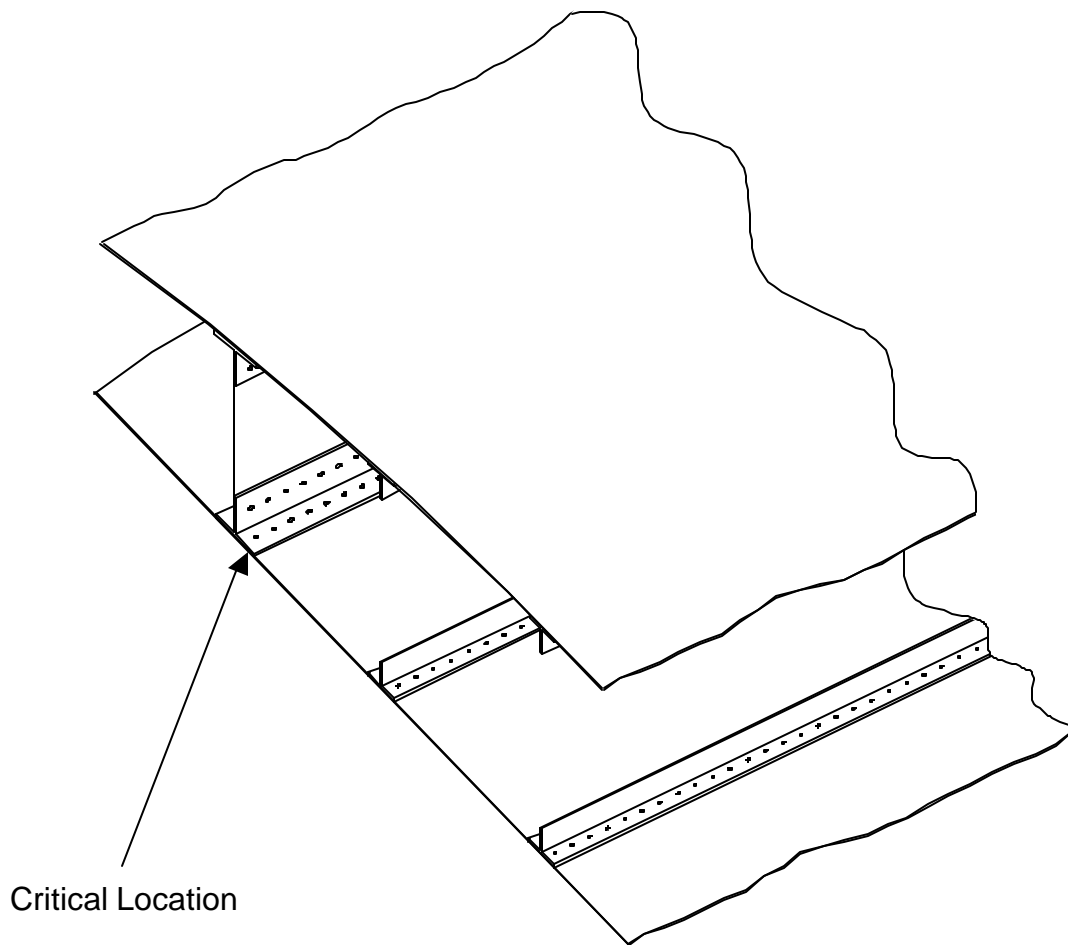


FIGURE 8-19

GEOMETRY IDEALIZATION

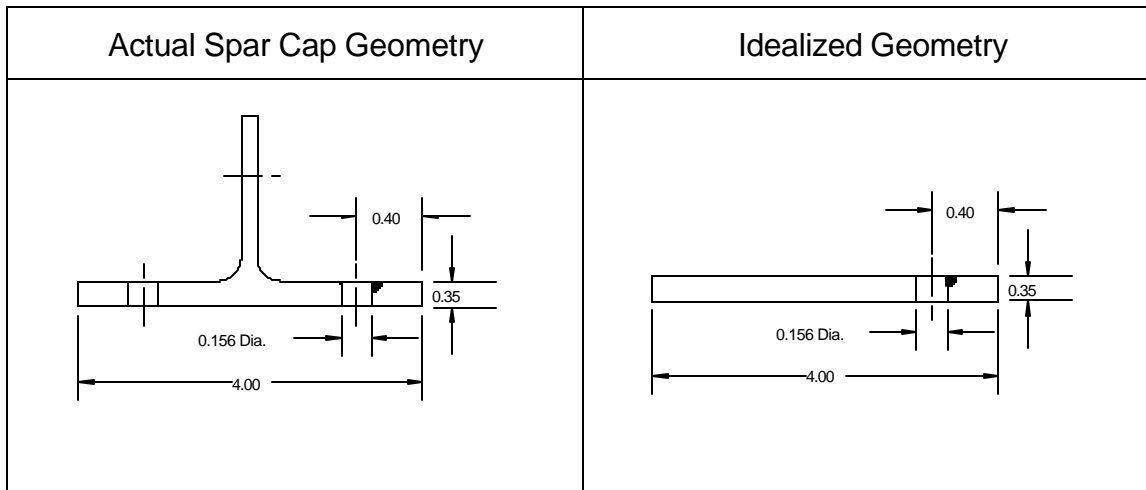


FIGURE 8-20

EXAMPLE OF WING AND CARRY-THRU FINITE ELEMENT MESH

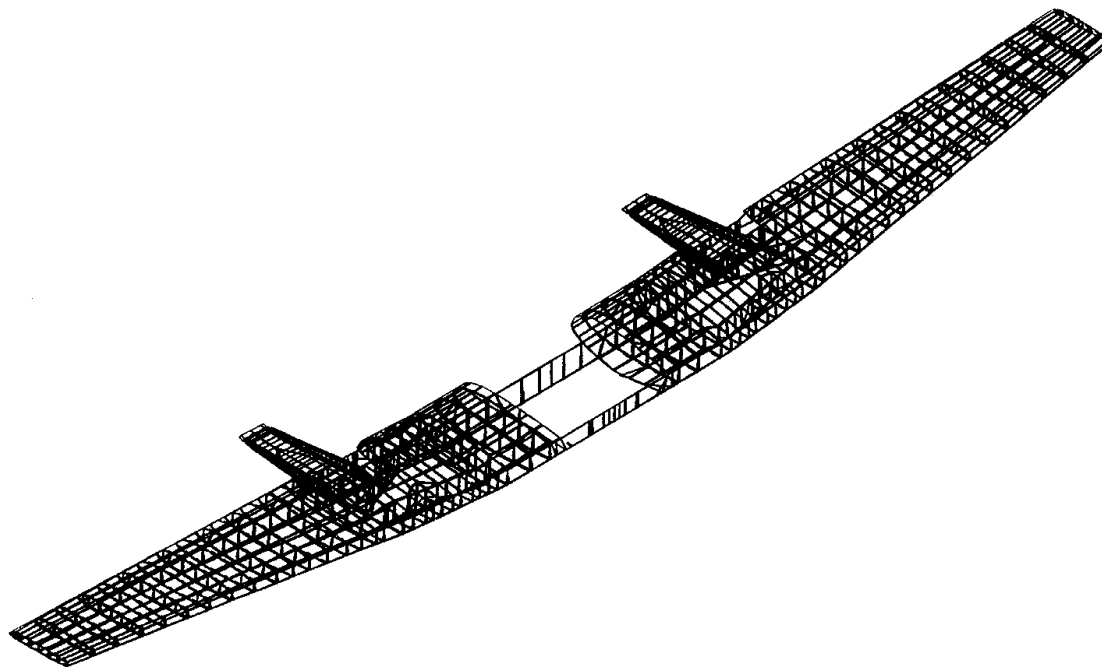


FIGURE 8-21

LOCAL STRESSES AND FASTENER LOADS IN SPAR CAP (REFERENCE 44)

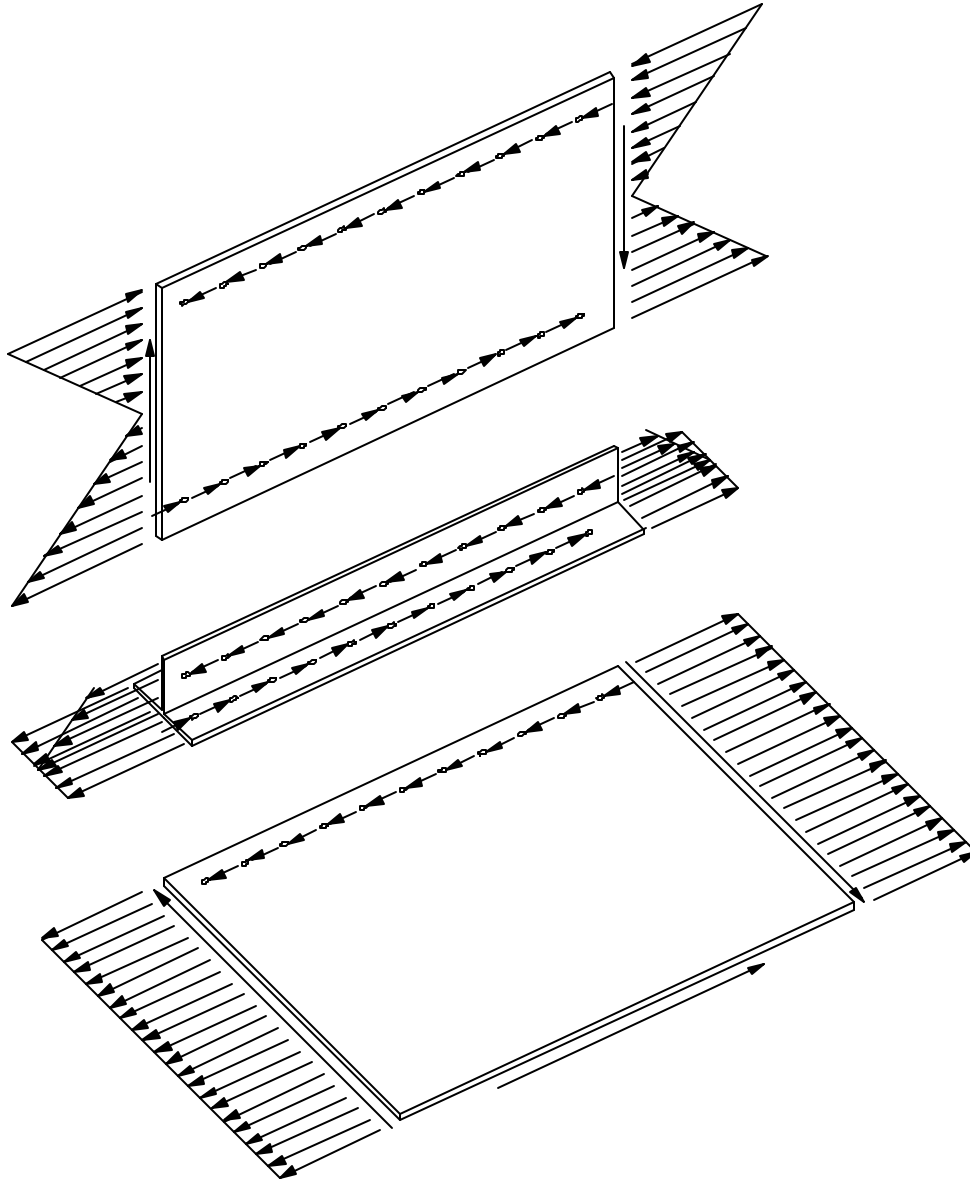


FIGURE 8-22

STRESS INTENSITY FACTOR SOLUTION CC02 (REFERENCE 11)

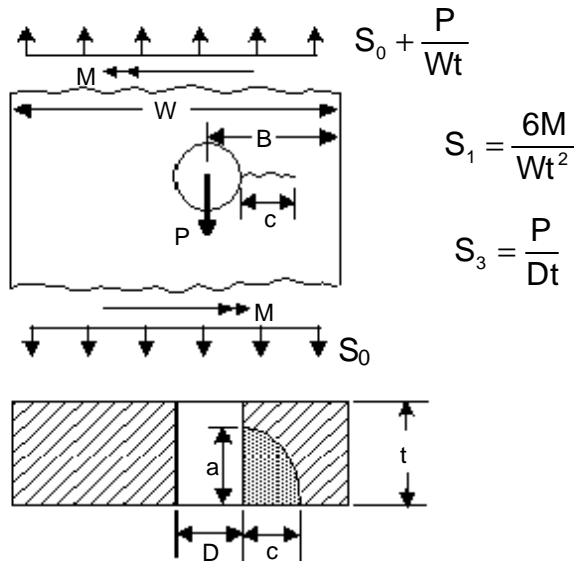
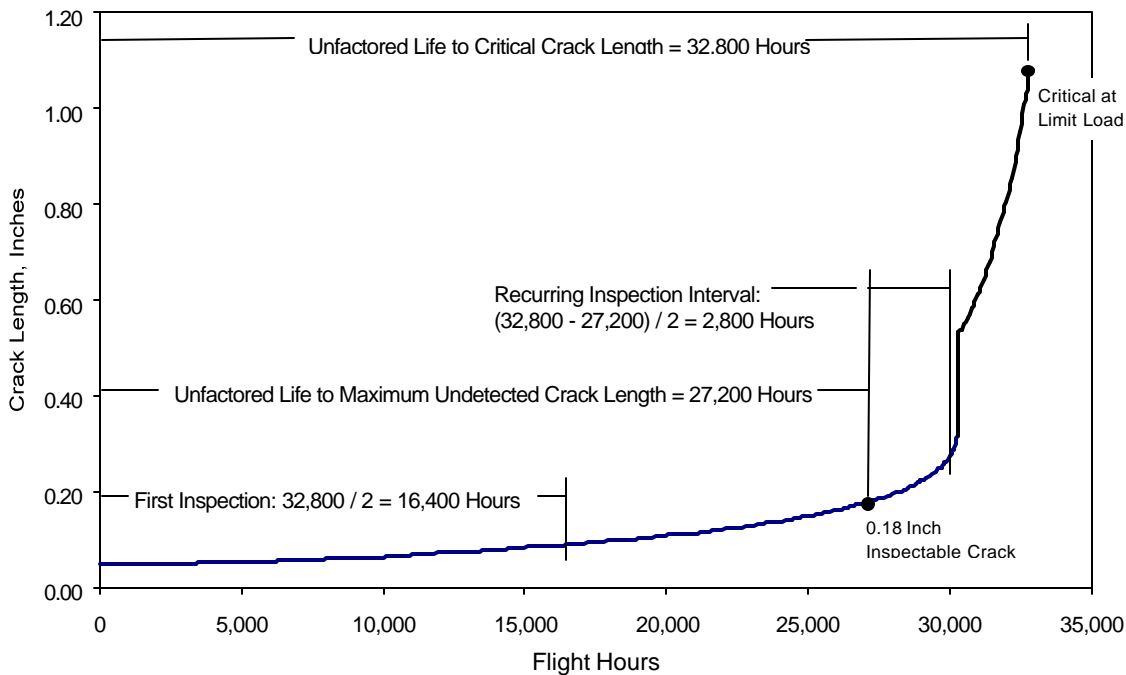


FIGURE 8-23

SPAR CAP SKIN FLANGE HOLE CRACK GROWTH CURVE



8.3 Critical Crack Length

The crack growth life of a structural component is defined as the time it takes for a crack to grow from an initial length to a critical length. The initial crack sizes to be used in a damage tolerance analysis are presented in Section 8.1, and the crack growth history is obtained from the crack growth analysis discussed in Section 8.2. The final piece required to determine the crack growth life of a structure is the critical crack length, discussed in this section.

Fracture failure of a part or system of parts occurs when, due to the presence of a crack, the part no longer has sufficient residual strength to withstand application of additional load. In an unflawed structure, the residual strength is based on the allowable tensile strength (F_{t_u}) of the material. In a cracked structure, the residual strength is less than F_{t_u} , and decreases non-linearly as the crack increases in size. Complete or partial failure of a part does not necessarily lead to failure of the aircraft, nor even to total failure of the part itself (e.g., crack arrest in stiffened structure).

In general, the residual strength analysis can be used to solve either of the following problems:

- 1) Determine the load carrying capability of a structural member containing a crack of known length, or
- 2) Determine the critical crack length corresponding to a particular load level (limit load or max spectrum load).

The general stress intensity formula can be used to determine the solution to either of these problems:

$$K = \sigma \sqrt{\pi c} \beta$$

By rearranging the equation to the form:

$$\sigma_{crit} = \frac{K_{crit}}{\sqrt{\pi c} \beta}$$

The critical stress (σ_{crit}) can be calculated for a known crack length, where:

- K_{crit} = Fracture Toughness (K_c or K_{1c})
- c = Crack length for a single crack tip, and
- β = Total geometric correction factor, which may be compounded from the various geometric correction factors applicable to the structural detail.

The critical crack length is of more interest here, since the critical crack length is one of the determining factors when setting inspection periods and intervals. If the limit stress (σ_{crit}) for a given structural component is known the critical crack length is obtained by rearranging the general stress intensity equation to the form:

$$c_{crit} = \frac{1}{\pi} \left(\frac{K_{crit}}{\sigma_{crit} \beta} \right)^2$$

This allows for the calculation of the limit load critical crack length (c_{crit}). However since β is a function of crack length, the solution becomes iterative. A more convenient solution is to graph the function σ_{crit} vs c_{crit} to determine the critical crack length. This method also permits incorporating upper boundary conditions for small cracks. For crack lengths approaching zero a boundary condition corresponding to 95% F_{t_u} is chosen.

In some cases, net section yielding can occur at stresses lower than fracture. The stress required to cause yielding over the net section containing the crack is given by:

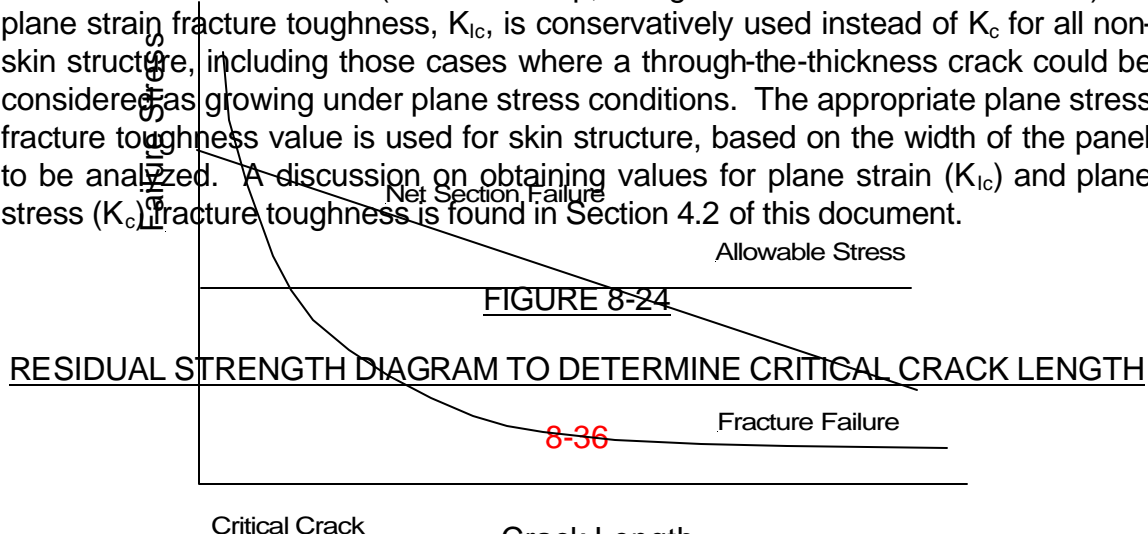
$$s_{crit} = F_{T_y} \left(\frac{A_{n'}}{A_g} \right)$$

where:

- $A_{n'}$ = Gross Area - Fastener Area - Crack Area
- A_g = Gross Section Area, and
- F_{T_y} = Yield Strength.

Since this may influence the ultimate strength if it causes load redistribution in a redundant structure, it is a useful reference.

Failure occurs at the minimum stress that exceeds either the net-section yielding or fracture toughness (K_{Ic} or K_c) allowable, as illustrated in Figure 8-24. The fracture toughness parameter to be used depends on the structural detail to be analyzed. For most structural details (such as a cap, stringer or other non-skin structure) the plane strain fracture toughness, K_{Ic} , is conservatively used instead of K_c for all non-skin structures, including those cases where a through-the-thickness crack could be considered as growing under plane stress conditions. The appropriate plane stress fracture toughness value is used for skin structure, based on the width of the panel to be analyzed. A discussion on obtaining values for plane strain (K_{Ic}) and plane stress (K_c) fracture toughness is found in Section 4.2 of this document.



8.4 Inspection Threshold

This section presents the procedure for setting the inspection threshold for each critical area. For the critical locations determined in Section 3.2, the inspection threshold is established based on crack growth analyses and/or fatigue analyses depending on the structural category of each location as defined in Section 3.3. Table 8-3 shows under what conditions it is acceptable to use fatigue instead of crack growth analysis for determination of the inspection threshold.

When crack growth analyses are conducted, it is assumed that the structure contains an initial flaw of the maximum probable size (usually 0.05") that could exist as a result of manufacturing or service induced damage (see Section 8.1). The procedures to determine the inspection threshold for each critical location based on crack growth analyses are presented in Section 8.4.1.

As can be seen in Table 8-3, for some structural categories, the decision as to whether to use crack growth or fatigue analyses to determine the inspection threshold is based on whether or not the structure is fail-safe. Therefore an evaluation should be made by analysis and/or by tests to determine the fail-safe features, if any, of the structure. If it can be shown that a load path failure in crack arrest "fail-safe" structure will be detected and repaired prior to failure at limit load of the remaining structure, the inspection threshold can be established using either (1) fatigue analyses and tests with an appropriate scatter factor or (2) by crack growth analyses. The requirements and guidelines for conducting fail-safe analyses and tests are presented in Section 8.4.2.

Care should be exercised in assessing the fail-safe capability of the structure. In the past, structures have been designated as fail-safe if they have been capable of sustaining fail-safe loads with a single principal structural element failed. This assumption has not always been true. When a single principal element fails due to fatigue, some secondary fatigue damage is usually present which may tear in a slow manner to critical size during application of fail-safe load. This phenomenon, which can degrade the fail-safe qualities of the structure, is described in more detail by T. Swift in References 77 and 78.

The rationale for allowing a fatigue evaluation, which does not account for initial manufacturing or induced service damage, to establish the initial threshold for a fail-safe structure is that fail-safety provides a second line of defense. Thus, in the event that cracking occurs prior to the threshold determined by the fatigue analysis, fail-safety will prevent catastrophic failure of the structure at limit load. Similarly, in single load path structure or in multiple load path structure which is not fail-safe, fatigue analysis is not allowed because no second-line of defense exists for this type of structure.

TABLE 8-3
METHOD OF INITIAL THRESHOLD DETERMINATION

Structural Category	Crack Arrest "Fail-Safe" Structure	Initial Threshold Determination Method	
		Fatigue	Crack Growth
Safe-Life		X	
Damage Tolerant – Obvious Damage Evident	YES	X	X
	NO		X
Damage Tolerant – Single Load Path Structure			X
Damage Tolerant – Multiple Load Path Structure – not inspectable for less than load path failure	YES	X	X
	NO		X
Damage Tolerant – Multiple Load Path Structure – inspectable for less than load path failure	YES	X	X
	NO		X

For components with inspection thresholds that can be determined using classical fatigue (crack initiation) analyses, the analysis procedures are discussed in Section 8.4.3.

8.4.1 Initial Threshold Based on Crack Growth

This section provides the guidelines for determining the initial inspection requirements based on crack growth to ensure continued safety in the event of an undetected failure.

The initial inspection times are a function of:

- Initial flaw size - The initial flaw sizes (c_{init}) are discussed in Section 8.1 and are generally assumed to be 0.05" quarter-circular for most structure.
- Spectrum loaded crack growth - The crack growth is defined as a function of flight hours and is naturally unique for each location. The development of the spectra used for the analysis is presented in Section 7.0 and the crack growth methodology is presented in Section 8.2 of this document.
- Critical flaw size – The critical flaw size (c_{crit}) for a critical location is determined using the information presented in Section 8.3.

The maximum allowable flaw size (c_{crit}) is the crack size beyond which the part can no longer take the maximum required load. There is no direct relationship between the maximum spectrum stress used to define the crack growth and the maximum (limit) load that the part is required to withstand. Figure 8-25 graphically presents the inspection requirements. This approach defines the inspections for all airframe locations.

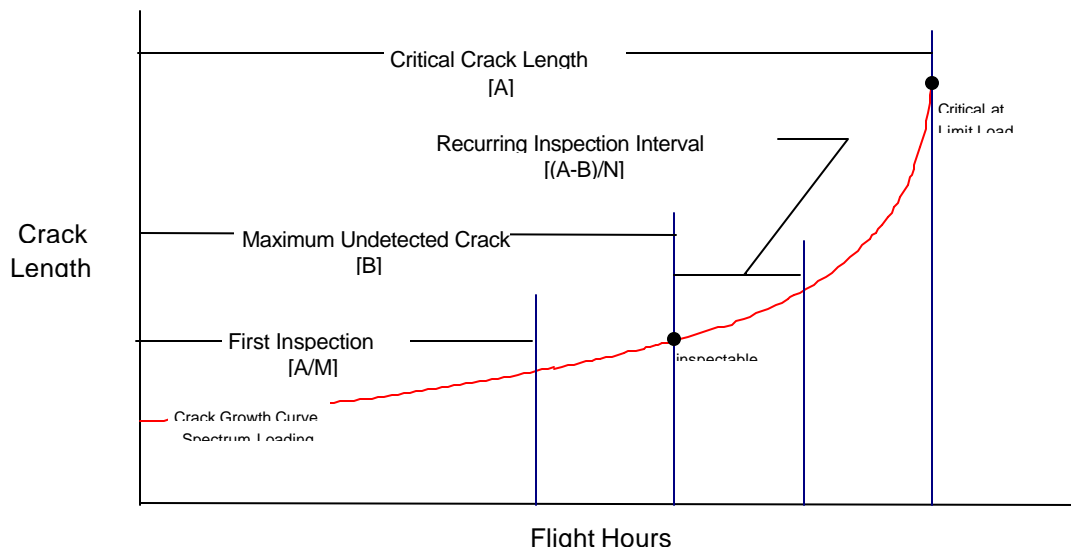
$$\text{Initial Inspection} = \frac{[\text{Flight Hours}@c_{critical} - \text{Flight Hours}@c_{initial}]}{M}$$

where $M=2$ for multiple load path structure which is crack arrest "fail-safe."
 and $M=3$ for single load path structure or multiple load path structure
 which is not crack arrest "fail-safe."

Recurring inspections, discussed in Section 8.5, are performed after the initial inspection at intervals equal to a defined fraction of the time it takes for a crack to grow from the detectable length to the maximum allowable flaw size. This provides at least two chances to detect a crack before it grows to the maximum allowable flaw size.

FIGURE 8-25

INITIAL INSPECTION INTERVAL



8.4.2 Fail-Safe Tests

While technically not part of the damage tolerance evaluation, fail-safe testing and analyses should be performed to document the fail-safe capability of multiple load path structures. The fail-safe tests and analyses need to demonstrate that

catastrophic failure or excessive deformation which could adversely affect the aircraft flight characteristics will not occur after fatigue failure or obvious partial failure of a single principal structural element (FAR 23.571, FAR 23.572). For both FAR 23.571 and FAR 23.572, the requirements are for the structure to withstand an ultimate static load factor of 86.25% of critical limit load (75% of critical limit load and dynamic factor of 1.15). However, the structure should be evaluated to limit load as suggested in AC 91-MA "Continued Airworthiness of Older Small Transport and Commuter Airplanes; Establishment of Damage-Tolerance-Based Inspections and Procedures".

8.4.2.1 Selection of Fail-Safe Test Conditions

The selection of the fail-safe conditions to be tested or analyzed is typically based on field experience as well as an extensive analytical evaluation of the structure.

Detailed finite element models (FEM) of the structure are studied to determine the critical structural components for the various load cases as outlined in Section 3.2.1. The models are then modified with the critical components failed for the critical load case. The results are reviewed to determine which component failures are most critical (significant loss of margin of safety in the remaining intact structure). These critical locations are the ones to be tested in the fail-safe test article(s).

8.4.2.2 Fail-Safe Testing

A component in good condition, perhaps from a salvage yard, can be used to conduct the fail-safe tests, as well as the static tests discussed in Section 3.2.2. Two types of fail-safe damage typically used for fail-safe testing are: 1) bolt removal and 2) saw cuts. When possible, it is desirable to remove bolts to simulate damaged or failed members to preserve the test article as much as possible. After completing the test for a critical location, the test article is returned to the original or equivalent strength by replacing the bolts or by structural repair of the saw cuts, in order to allow other critical locations to be tested.

The test article is to be loaded to 100% of the critical limit load. Recording strain gage data during each fail-safe test provides valuable data for comparison with the predicted stresses from the numerical models. This data can be used to verify the finite element model for fail-safe analysis at locations not tested.

8.4.2.3 Fail-Safe Analyses

Fail-safe analyses using finite element models can be used in lieu of testing to show that a structure with a principal structural element failed can still withstand limit load. However, verification of the models through comparison with measured strains on test articles, particularly fail-safe test articles, is strongly encouraged.

8.4.3 Initial Threshold Based on Fatigue

Fatigue (crack initiation) analysis can be used to establish the inspection threshold for components which are classified as safe-life or for multiple load path crack arrest “fail-safe” structure where the damage will be detected and repaired prior to failure of the remaining structure. The procedure for determining fatigue lives based on linear cumulative damage theory is discussed in Section 8.6. The analytical life predicted by the fatigue analysis is defined as the time when 50% of the fleet aircraft are expected to have developed small cracks (typically assumed 0.05 inches in length). The calculated fatigue life is reduced by dividing by a scatter factor to account for variabilities. The scatter factor to be used should be based on the guidelines presented in Reference 30 and AC 25.571-1C. Typically, for locations where fatigue test data is available a scatter factor of 4 is chosen, while for locations without test data, a scatter factor of 8 is to be used. The FAA Aircraft Certification Office must approve the scatter factors chosen.

8.5 Repeat Inspection Intervals

This section provides the procedure for determining the repeat inspection requirements to ensure continued safety by detecting a crack prior to it reaching a critical length. The repeat inspection intervals are based on crack growth analyses. The initial inspections are set based on Section 8.4 (Inspection Threshold). Repeat inspections are performed after the initial inspection at intervals equal to a defined fraction of the time it takes for a crack to grow from the detectable length to its critical size. The repeat inspection times are a function of:

- Maximum undetectable flaw size - The maximum undetectable flaw size (c_{insp}) is unique for each location and is dependent on the method of inspection used (see Section 9.0). The FAA Aircraft Certification Office must approve the maximum undetectable flaw size chosen.
- Spectrum loaded crack growth - The crack growth is defined as a function of flight hours and is naturally unique for each location. The development of the spectra used for the analysis is presented in Section 7.0 and the crack growth methodology is presented in Section 8.2 of this document.
- Critical flaw size – The critical flaw size (c_{crit}) for a critical location is determined using the analysis procedure given in Section 8.3.

The time required for the flaw to grow from the maximum undetectable flaw size to the critical flaw size is divided by a suitable factor:

- A factor of 2 is used for multiple load path structure which is crack arrest “fail-safe”.

- A factor of 3 is used for single load path structure or multiple load path structure which is not crack arrest “fail-safe”.

Thus, depending on the availability of fatigue test and loads data, a minimum of two opportunities will be available to detect the crack before it grows to the maximum allowable flaw size.

The critical flaw size (c_{crit}) is the crack size beyond which the part can no longer take the maximum required load. There is no direct relationship between the maximum spectrum stress used to define the crack growth and the maximum (limit) load that the part is required to withstand. Figure 8-26 graphically presents the inspection requirements. This approach defines the inspections for the majority of locations.

$$\text{Repeat Inspection Interval} = \frac{[\text{Flight Hours}@c_{critical} - \text{Flight Hours}@c_{inspectable}]}{N}$$

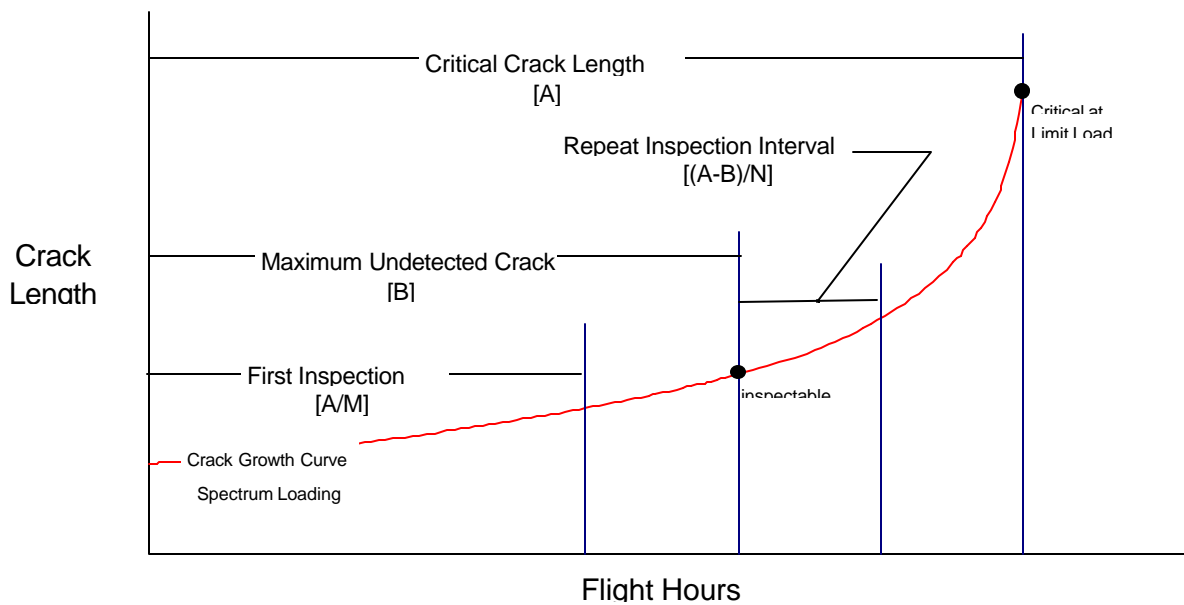
Where N = 2 or 3 based on the above criteria.

8.6 Fatigue Analysis

Fatigue analysis, also referred to as crack initiation analysis, is typically not part of a damage tolerance evaluation. However, older aircraft designed and certified before the advent of damage tolerance, were designed and certified as either fail-safe or safe-life. While the development of a SID is largely based on damage tolerance principles, there are circumstances when fatigue analyses are conducted. Fatigue analysis is required on parts for which damage tolerance is impractical. Landing gear and its attachments are examples. Fatigue analysis is also allowed to establish the initial inspection threshold in multiple load path crack arrest “fail-safe” structure. The FAA has developed a computer program, ACE100-1, which uses Miner’s Linear Cumulative Damage Theory and the data available in AFS-120-73 (Reference 30), to calculate fatigue lives. Another approach to calculating the fatigue lives is presented in the paragraphs below.

FIGURE 8-26

REPEAT INSPECTION CRITERIA



8.6.1 Methodology

The most commonly used fatigue analysis technique utilizes Stress vs. Crack Initiation Life (S-N) curves generated from smooth specimen ($K_t = 1.0$) or notched ($K_t > 1.0$) data (see Section 4.4). The stress input required to determine damage from the curve is the notch stress, obtained using the linear notch stress rule, if the S-N curve is for smooth specimen data, or the net or gross section stress as required for the S-N curve with the specific K_t used. If the S-N curves are to be used directly, the K_t of the analysis location must match the K_t of the curve.

The notch stress will be determined using the Linear Notch Stress rule, which states that the notch stress is equal to the product of the notch stress concentration factor and the applied stress. This is expressed mathematically as follows:

$$\sigma_n = K_t \sigma = K_t \varepsilon E$$

In using the Linear Notch Stress rule the predicted lives are conservative for stress based life techniques. (Note: The Linear Notch Strain rule, when used with a strain life technique, is unconservative).

If the K_t is much different from 1.0, using the S-N for a smooth specimen ($K_t = 1.0$) will produce an overly conservative life estimate resulting from the notch sensitivity of the material. Therefore, using test data for notched specimens is recommended. However, it is rare that notched specimen life data is available for the exact K_t of a particular analysis. In lieu of running a test for the K_t of each analysis location, lives for a particular spectrum may be computed for various S-N curves with different K_t 's and graphed as K_t vs. Life (see Figure 8-27). The life for a particular analysis K_t is then graphically determined as presented in Figure 8-27.

The life, N , is generally taken to be cycles to initiate a 0.050 inch crack, but some S-N curves available from the literature report lives as being cycles to complete failure (see Section 4.4 for a discussion). The spectrum stress cycle will consist of a maximum notch stress and minimum notch stress of "n" reversals. The alternating and mean stresses are computed according to the relations:

$$\sigma_{alt} = \frac{\sigma_{max} - \sigma_{min}}{2} \qquad \sigma_{mean} = \frac{\sigma_{max} + \sigma_{min}}{2}$$

Other useful relations utilize the "R-Ratio" or $R = \sigma_{min}/\sigma_{max}$:

$$\sigma_{alt} = \sigma_{max} \left(\frac{1-R}{2} \right) \qquad \sigma_{mean} = \sigma_{max} \left(\frac{1+R}{2} \right)$$

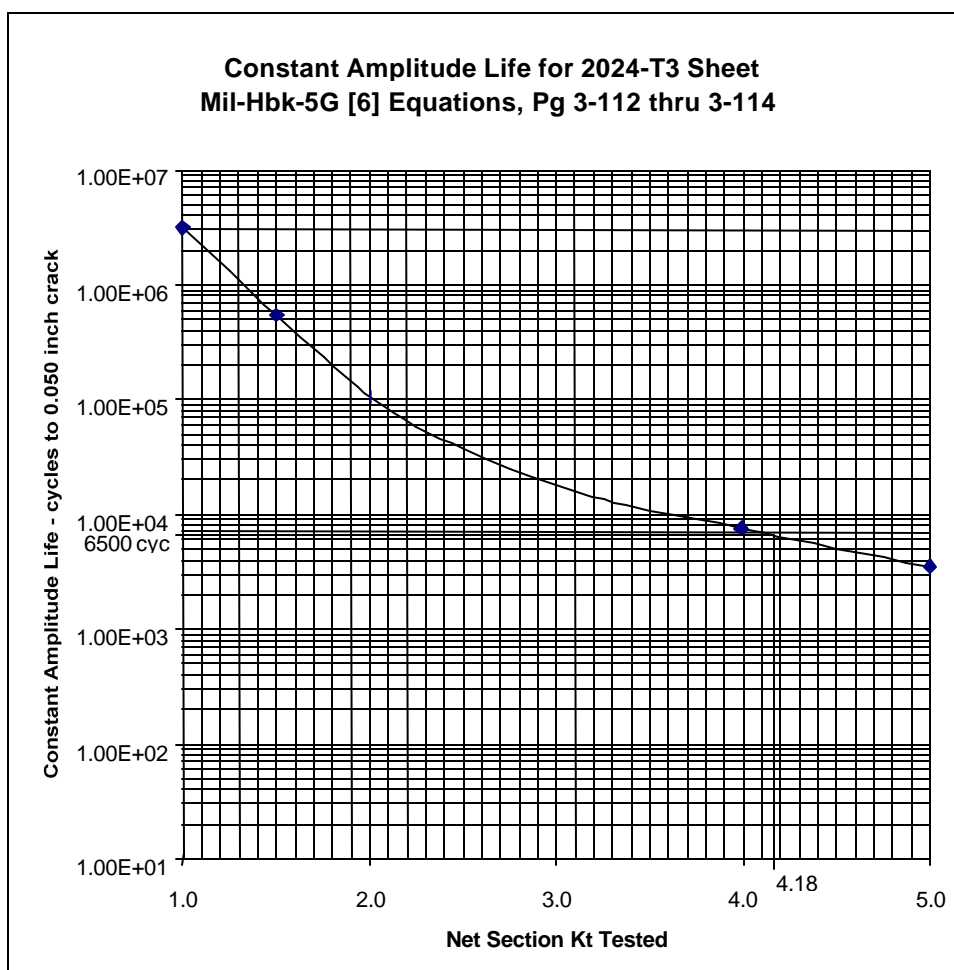
For variable amplitude loading, cycle counted spectra are used and the damage is computed using Miner's linear damage accumulation rule to determine the life for a particular stress spectrum of "n" reversals. Miner's linear damage sums the

damage ratios of n_i/N_i for each stress level in the spectrum until a value of one is reached, indicating failure. The damage ratio of n_i/N_i is the number of cycles at a given stress level in the spectrum, n_i , divided by the number of cycles that would cause failure at that stress level, N_i . The damage ratios are summed for all stress cycles in a given repeated stress spectrum block of S hours (e.g., 1000 flight hours). The predicted time to failure using Miner's linear damage accumulation rule then is:

$$\text{Life} = \left(\frac{S}{\sum n_i/N_i} \right) \text{ which is the time where: } \sum n_i/N_i = 1.0, \text{ by definition.}$$

FIGURE 8-27

SAMPLE K_t VS. LIFE CURVE



8.6.2 K_t Determination

Stress concentration factors (K_t), need to be computed for each load component, such as bypass, bearing, bending, etc. The total or equivalent K_t , which is used to

scale the fatigue analysis is computed based on the principle of linear superposition of all load components. The baseline K_t 's are based on gross section areas but are not limited to that reference. For example, for a hole, the K_t analysis is based on the following equation for tension loading:

$$K_{t_t} = K_{t_{eq_t \text{ gross}}} = \frac{\sigma_{bp \text{ max}} + \sigma_{bnd \text{ max}} + \sigma_{brg \text{ max}}}{\sigma_{ref \text{ gross}}}$$

where $\sigma_{ref \text{ gross}}$ is a reference stress (based on the "gross" area) for some total load (bypass + bearing + bending) representative of the spectrum. The subscripts "bp", "bnd", and "brg" stand for bypass, bending, and bearing, respectively. Shear stresses may need to be added as required. Substituting the relation: $\sigma_{max} = K_{t \text{ gross}} \sigma_{gross}$ gives the result:

$$K_{t_t} = K_{t_{eq_t \text{ gross}}} = \frac{K_{t_{bp \text{ gross}}} \sigma_{bp \text{ gross}} + K_{t_{bnd \text{ gross}}} \sigma_{bnd \text{ gross}} + K_{t_{brg \text{ gross}}} \sigma_{brg \text{ gross}}}{\sigma_{ref \text{ gross}}}$$

The bearing stress based on bearing area may be used so long as the $K_{t_{brg}}$ is compatible with that stress. Net area K_t 's may also be used in a similar fashion. The proper equation for compression loading is of the form:

$$K_{t_c} = K_{t_{eq_t \text{ gross}}} = \frac{K_{t_{bp \text{ gross}}} \sigma_{bp \text{ gross}} + K_{t_{bnd \text{ gross}}} \sigma_{bnd \text{ gross}}}{\sigma_{ref \text{ gross}}}$$

to accommodate the elimination of the bearing stresses and variations of the basic K_t 's for compression loading.

The same approach can accommodate other geometry using "unit load" cases (i.e. drag load, vertical load, or wing bending moment).

Other factors may affect the basic tension and compression K_t 's. The basic bypass and bending stress concentrations are usually for straight shank open holes and may be affected by filled hole effects. Bearing stress concentrations are affected by filled hole effects, thru thickness bearing variations, and hole condition. The basic K_t 's for tension, bearing and bending loading can be found in the literature. Some of the most useful resources for K_t data are:

- Pilkey, W. D., "Peterson's Stress Concentration Factors" (Ref. 79)
- Heywood, R. B., "Designing Against Fatigue of Metals" (Ref. 80)
- Niu, M. C. Y., "Airframe Structural Design" (Ref. 81)

As an example, the basic K_t 's for holes are defined by the following:

$K_{t\text{ bp}} = K_{t\text{ oh}} K_{\alpha} K_{\beta}$	Tension/Compression
$K_{t\text{ bnd}} = K_{t\text{ oh}} K_{\alpha} K_{\beta}$	Tension/Compression
$K_{t\text{ brg}} = K_{t\text{ oh}} K_{\alpha} K_{\beta} K_{\theta}$	Tension
$K_{t\text{ brg}} = 0$	Compression

where:

- $K_{t\text{ oh}}$ = basic K_t for an open hole for axial, bending or bearing stress (see References 79 or 80). (Note: $K_{t\text{ fh}}$ signifies a filled hole K_t used in some cases or $K_{t\text{ fh}} = K_{t\text{ oh}} * K_{\beta}$.)
- K_{α} = factor relating the effective change in K_t due to hole condition (see Reference 81).
- K_{β} = factor relating the change in K_t due to hole filling (see Reference 81).
- K_{θ} = factor relating the change in K_t due to thru-thickness bearing (see Reference 81) gradient effects.

For all other problems, the basic K_t 's are defined by the following:

$K_{t\text{ bp}} = K_{t\text{ ax}}$	Tension/Compression
$K_{t\text{ bnd}} = K_{t\text{ b}}$	Tension/Compression
$K_{t\text{ shear}} = K_{t\text{ s}}$	Tension/Compression

where:

- $K_{t\text{ ax}}$ = basic K_t for axial stress
- $K_{t\text{ b}}$ = basic K_t for bending stress
- $K_{t\text{ s}}$ = basic K_t for shear stress.

Additionally, bypass, bending, and bearing K_t 's are adjusted to reflect the effective change in stress needed to predict variations in crack initiation life observed due to differences in hole type (e.g., countersunk), fretting or surface finishes. These effects can be accounted for by using appropriate correction factors to adjust the K_t values.

The resources given in Reference 79 through 81 can be used to develop K_t estimates for the majority of cases encountered. In complex cases or cases where the geometry does not lend itself to simplification, a Finite Element Model or Boundary Element Model will need to be developed to accurately determine the K_t and load transfer. When numerical models are used to determine notch stresses, P-element FEM (i.e., ProMechanica or Poly-FEM) are highly recommended over H-element (i.e., NASTRAN, Abacus, Adina, CATIA-FEM) models due to the required accuracy of the notch stress.

Once the equivalent K_t 's are determined, a $K_t\sigma$ (notch stress) vs. Spectrum Life is computed by performing a crack initiation analysis using Miner's linear damage accumulation rule using smooth specimen S-N data.

8.7 Widespread Fatigue Damage (WFD) Evaluation

Widespread Fatigue Damage (WFD) is a damage condition that is a concern in aging aircraft, and refers to the degradation in structural integrity as a result of prolonged service. This section addresses the issues associated with, and the procedures required for a WFD evaluation. First, however, widespread fatigue damage is defined along with the two common types of widespread fatigue damage: multiple site damage (MSD) and multiple element damage (MED).

- 1) Widespread Fatigue Damage (WFD): Widespread fatigue damage in a structure is characterized by the simultaneous presence of cracks at multiple structural details that are of sufficient size and density whereby the structure will no longer meet its damage tolerance requirement (i.e., to maintain its required residual strength after partial structural failure).
- 2) Multiple Site Damage (MSD): Multiple site damage is a source of widespread fatigue damage characterized by the simultaneous presence of fatigue cracks in the same structural element (i.e., fatigue cracks that may coalesce with or without other damage leading to a loss of required residual strength). An example of MSD is shown in Figure 8-28. MSD cracks typically develop at a number of initiation points which have similar design and stress levels.
- 3) Multiple Element Damage (MED): Multiple element damage is a source of widespread fatigue damage characterized by the simultaneous presence of fatigue cracks in adjacent structural elements. An example of MED is shown in Figure 8-29. MED fatigue cracks typically develop simultaneously in similar adjacent structural details operating at similar stress levels.

Unfortunately there is no precise way to determine what extent of MSD or MED cracking represents the onset of WFD. Depending on the structural detail, local loading, consequences of failure, ease of inspection etc., different levels of MSD or MED may be tolerated before a structural detail is deemed to have WFD. The general process for evaluating WFD is presented in the following paragraphs. References 82-86 should be consulted for additional information on WFD.

FIGURE 8-28

EXAMPLE OF MSD

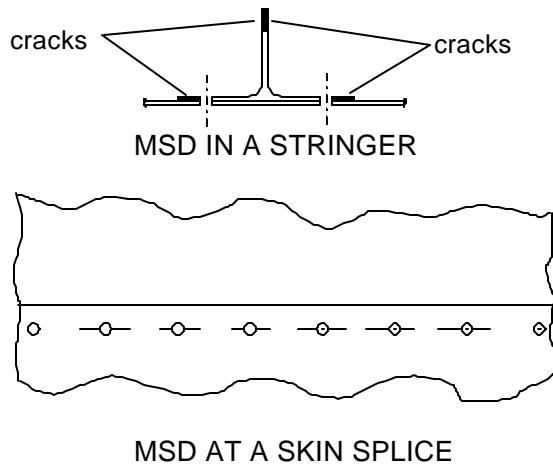


FIGURE 8-29

EXAMPLE OF MED

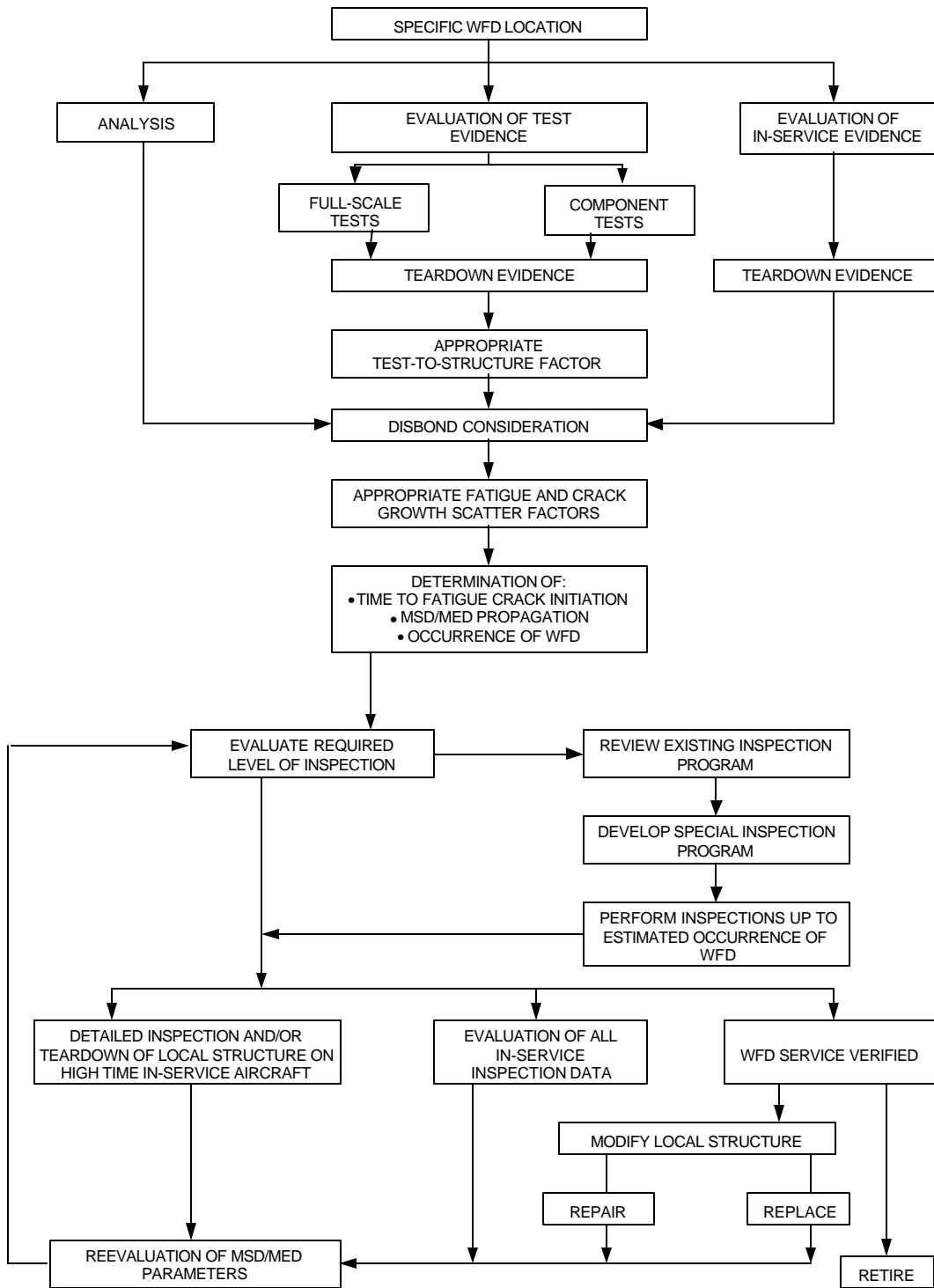


8.7.1 WFD Evaluation Flow Chart

The general process to be followed for a WFD evaluation is based on evaluation guidelines presented in the final report of the AAWG committee on Widespread Fatigue Damage reported in Reference 86, and is presented as a flow chart in Figure 8-30.

FIGURE 8-30

FLOW CHART OF WFD EVALUATION PROCESS



It is important to note, that as of the writing of this report no generally accepted tools and methods are available to perform MSD/MED crack propagation and residual strength analyses. References 82 through 86 present some of the WFD analysis methods that have been proposed in the literature. Therefore, the portion of the flow chart shown in Figure 8-30 that deals with reviewing or developing inspection requirements for WFD is currently not applicable. Section 8.7.2 presents the various steps involved in a WFD evaluation, assuming MSD/MED crack growth and residual strength analysis tools are available. With all the aging aircraft research initiatives currently underway, it is likely that the required MSD/MED analysis tools will become available in the future.

8.7.2 WFD Evaluation For A Specific Location

Each location on an aircraft that is considered susceptible to WFD will require a detailed WFD evaluation. Some of the locations that are typically susceptible to MSD or MED cracking are listed below. Note, however, that this is by no means an exhaustive list, and a careful survey of a particular aircraft model is required to determine all the possible locations that are susceptible to WFD.

Fuselage:

- Longitudinal skin joints, frames and tear straps
- Circumferential joints and stringers
- Fuselage frames
- Pressure bulkhead outer ring and web splices
- Stringer to frame attachments
- Window surround structure
- Wing fuselage attachments
- Non-plug door hinges and latches
- Skin at large doubler run-out

Wing & Empenage:

- Chord wise splices
- Rib to skin attachments
- Skin at large doubler run-out
- Stringer run-out

The process is described in the following section.

8.7.2.1 Identifying WFD Critical Locations

One of the major tasks in performing a WFD evaluation is determining the critical locations that require a detailed WFD analysis. Generally a combination of analysis, test evidence and in-service experience is used to identify WFD critical

locations. The following sections outline the procedures for identifying WFD critical locations based on analysis, test evidence and in-service experience.

8.7.2.1.1 Analysis

Analysis tools, such as finite element methods or durability or damage tolerance analyses, can be used to help with the selection of locations for detailed WFD evaluation. Locations that need to be considered for WFD evaluation are areas that have high stresses, stress concentrations, high load transfer, load eccentricities, severe loading spectra, or material fatigue properties, which would indicate a lower crack initiation or growth life. Special attention needs to be given to structural elements where either a significant part of the element is considered critical, such as skin splices (i.e., potential for MSD), or where several adjoining details are critical, such as stringer splices (i.e., potential for MED). Many secondary factors also need to be considered including: inspectability, susceptibility to corrosion, susceptibility to accidental damage or impact, and production and field support issues.

8.7.2.1.2 Test Evidence

Full-scale and component cyclic tests, especially when they are followed by a detailed teardown, are valuable in determining areas that require a detailed WFD evaluation. Whenever possible, a fractographic analysis of the naturally occurring cracks should be performed to determine the crack growth history.

Structural details previously designated as PSEs are of special interest. If the teardown shows multiple crack origins in PSEs the detail in question will need to be considered for a detailed WFD evaluation. If multiple crack origins are found in a structural detail not previously identified as a PSE, an evaluation will need to be made to determine, if the detail in question requires a WFD evaluation.

When data obtained from full-scale, component or even coupon tests is to be used for a WFD evaluation, appropriate test-to-structure factors may need to be used to account for the potential differences between the test and the actual structure and usage. The test-to-structure factor needs to consider an adjustment for the following sources of potential differences:

Full-Scale Fatigue Test:

- Load spectrum
- Local stress
- Local design and manufacturing details

Component Test: same as full-scale test plus

- Size effects

Coupon Test: same as component test plus

- Boundary conditions
- Shape effects
- Bi-axial or uni-axial stress field
- Effect of local bending
- Load redistribution effects

8.7.2.1.3 In-Service Experience

High-time aircraft are an excellent source of information when it comes to determining areas, which might require a WFD evaluation.

A detailed review of FAA Service Difficulties Reports (SDR) will give an indication of some of the structural details that are prone to cracking or other forms of damage (e.g., corrosion) that can occur in service. Similarly, a review of Service Bulletins/Letters for the specific aircraft provides information on structural details that are prone to in-service damage.

Performing a teardown on a high-time aircraft, preferably one that has seen severe usage, may provide valuable information. Not only will it produce some indication of MSD and MED cracking locations, but it will also give data on the extent and location of corrosion damage, and if applicable, areas of disbond. Whenever possible, a fractographic analysis of crack surfaces should be performed to obtain crack growth rate information.

If a teardown of a high-time aircraft is not feasible, a detailed NDI program for areas identified through analysis, test or in-service experience to be susceptible to WFD will give further details on the extent of MSD/MED cracking. In order for the detailed NDI to be of significant value, the inspection methods to be used must have small enough detectable crack lengths and high enough reliabilities to ensure that the small cracks that are characteristic of MSD/MED cracking can be found with good confidence.

8.7.2.2 Consider Additional Damage

As an aircraft ages, fatigue cracking is not the only source of damage that causes degradation of structural integrity. Some of the other damage types that are typically encountered in aging aircraft, and their effects on structural integrity and interaction with WFD are discussed below.

8.7.2.2.1 Disbonds

The presence of disbonds can present a structural integrity concern in itself. In this section, however, the concern is the detrimental effect that disbonds can have when combined with MSD/MED. The load transfer capacity that was lost due to the disbonds needs to be carried by other means, which typically are mechanical fasteners in the area. The additional load transfer through the mechanical fasteners will increase the local notch stress at the fasteners, leading to reduced crack initiation lives and faster crack growth rates.

The effect of disbonds on crack initiation and growth needs to be included in detailed WFD evaluations of structural details that contain bonds. Of special concern are structural details that combine bonding with mechanical fasteners (e.g., lap/butt splice with rivets and bond). For these details, a conservative crack initiation or propagation analysis would assume the bond ineffective, and all the load transfer occurs through the mechanical fasteners.

8.7.2.2.2 Corrosion

Corrosion plays a role in WFD evaluations in several ways. 1) Corrosion pits are potential crack initiation sites, 2) corrosion increases the stress levels in the structure because of material loss, and 3) corrosion can weaken bond lines or cause disbonds which in turn decrease crack initiation and growth lives. Therefore, corrosion control is an important part of any aging aircraft program.

The detrimental effect of corrosion on crack initiation and growth lives must be considered when performing a WFD evaluation of a specific structural detail, especially when in-service experience has shown the area to be susceptible to corrosion. At the writing of this report there are, unfortunately, no generally accepted procedures for predicting the formation of corrosion or the growth of corrosion pits.

8.7.2.2.3 Fretting

Fretting is one of the primary origins of fatigue cracking in mechanically fastened joints. Since mechanically fastened joints and splices are generally prone to MSD, fretting is an important issue. However, at this point there is no readily accepted analysis to account for the effect fretting has on both crack initiation and growth.

8.7.3 Recommended Action

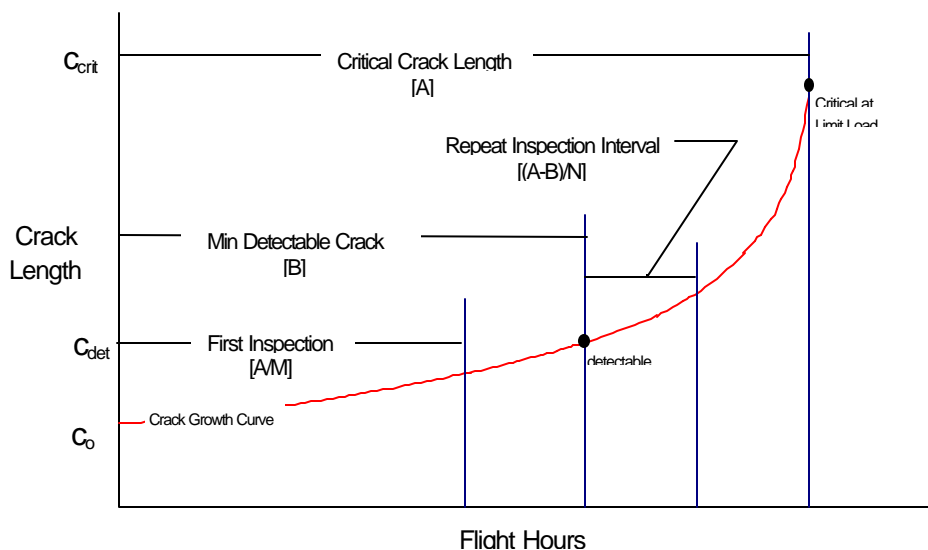
References 83 through 86 discuss some of the deterministic and probabilistic approaches to the determination of the number of flight hours when the structure first experiences WFD. The analysis to determine the onset of WFD needs to consider the minimum acceptable level of damage from corrosion, fretting, discrete source damage, etc. The time when fatigue cracking in the structure degrades the fail-safety from these sources of damage, represents the onset of WFD. The deterministic analysis uses the degradation in residual strength below limit load capability, due to the presence of fatigue cracking in the structure, as the measure. For the probabilistic analysis, the measure is the conditional probability of failure, given that the structure has sustained damage. Once a validated analysis shows that the structure has WFD, the course of action is to repair or replace the structural detail or to retire the aircraft.

9.0 Inspection Requirements

The final step before writing the SID document is to determine the airframe inspection requirements. This involves selecting and evaluating state-of-the-art non-destructive inspection (NDI) methods applicable to each PSE, and determining a minimum detectable crack length, c_{det} , for each NDI method. The minimum detectable crack length is used in conjunction with the critical crack length, c_{crit} , to define the flight-hour interval for the crack to grow from c_{det} to c_{crit} as: $(\text{flight-hours at } c_{crit} - \text{flight hours at } c_{det})/N$, where N is 2 or 3 (see Section 8.5). This interval is used to define the repeat inspection frequency for the SID program's required inspections. The initial inspection occurs at the number of flight-hours to c_{crit} divided by M , where M is 2 or 3 (see Section 8.4.1). For a given NDI method and PSE, c_{det} corresponds to a crack size with a 90% probability of detection. An example of initial and repeat inspection interval determination is shown in Figure 9-1.

FIGURE 9-1

DAMAGE TOLERANT STRUCTURE INSPECTION CRITERIA



The detectable crack length, c_{det} , and the probability of detection for an inspection program are affected by a number of factors. These factors include human factors (such as qualifications of the inspector), size of the inspection task, inspection method, equipment reliability, instrument calibration procedure, structural geometry and the degree of physical access. The objective is to define inspection methods that ensure a small detectable crack length with a 90 percent probability of detection and a 95 percent confidence level.

The objective of this section is to (1) explain the nondestructive inspection methodology, (2) provide guidance in determining the inspectable fatigue crack

lengths for each critical location and (3) define the inspection technique. To meet these objectives, the inspection methods and frequencies are briefly discussed in Section 9.1 and the NDI personnel qualifications in Section 9.2. Next, the basic principles of each NDI inspection method as well as the basic advantages and disadvantages of each method are presented as follows:

- Visual Section 9.3
- Penetrant Section 9.4
- Magnetic Particle Section 9.5
- Eddy Current Section 9.6
- Ultrasonic Section 9.7
- Bond Inspection Section 9.8
- Radiographic Section 9.9

Once the basic principles of the available NDI methods are understood, other factors must also be considered. These factors are discussed in the following sections:

- Minimum Detectable Discontinuity Section 9.10
- Selection of an Inspection Method Section 9.11
- Detection Limits Section 9.12
- Accessibility Section 9.13

Finally, Section 9.14 addresses other considerations in creating a field inspection program, including cost and method availability. For more information refer to References 87 through 99.

9.1 Inspection Methods and Frequencies

The use of Nondestructive Evaluation (NDE) to determine the size of a discontinuity can't be divided into a checklist type of operation. Many factors can make a routine appearing inspection situation into an extremely difficult proposition. It is necessary that properly qualified NDE personnel be included in the selection of an inspection procedure. The purpose here is to present some general information about each of the methods and address some specific topics that can be of use to the SID developer.

9.2 Personnel Qualifications

Each Nondestructive Inspection (NDI) program must have FAA approval to perform aircraft inspection. A vital requirement of a successful NDI program is properly qualified personnel. Despite the science that underlies the various detection methods, NDI is still to some extent an art. There are some inspection situations where detection is based only on the interpretation skills of the inspector. Physical confirmation of the discontinuity may not be possible without extensive disassembly

or destructive methods. Science may provide the information, but it is often up to the inspector to determine the source of what is presented. First, the levels of certification will be discussed and then the requirements for certification.

9.2.1 Levels of Certification

The basic NDI personnel rating system consists of three “Levels” of certification with Level I at the lower end and Level III at the upper end. A separate certification is required for each method of inspection used.

9.2.1.1 Level I

Level I is the entry level certification. A minimum amount of training and experience is required for certification. A Level I is expected to be able to perform inspections under the guidance of a Level II or Level III. This certification is usually viewed as a stepping stone toward qualification as a Level II.

9.2.1.2 Level II

Level II is the technician level certification. Additional training and experience are required to attain this level. The Level II is expected to be capable of performing inspections where experience is the major factor in interpreting discontinuity signals. They are able to interpret established specifications in determining inspection requirements and results. Level II is also responsible for training and supervision of Level I. Most inspection requirements will specify at least a Level II inspector.

9.2.1.3 Level III

Level III is the supervision or super technician level certification. Additional training or experience is required to attain this level. The Level III is expected to be capable of establishing inspection specifications where none exist. They also determine the methods and procedures for inspection. A Level III may or may not be required to perform inspections. They are responsible for the certification and qualification of the Level I and II.

9.2.2 Requirements for Certification

NDI certification is earned. In addition to the training and experience requirements, each level of certification requires the candidate to pass a written examination of the general concepts of that method. Another examination is required over the specific requirements of that industry or company. Finally, a practical examination of inspection skills is needed. A composite score is determined for the three exams and a minimum score established to successfully complete certification by the

program administrator. At specific intervals, these examinations are repeated to maintain certification. Last, an annual eye examination is usually required to ensure that the inspector is capable of seeing the indications presented.

9.3 Visual Inspection

This section presents some of the basic physical principles of visual inspection, followed by a brief description of the method and an overview of the basic advantages and disadvantages. While many of these will be reviewed in more detail in later sections, they are included here to give a general understanding of the methods employed.

9.3.1 Visual Inspection Principles

Visual inspection is the original NDI method. The inspector discovers the discontinuity when it has become large enough to be seen. In the most basic application, it consists of just an inspector and the surface inspected. Lighting and magnifiers may be used to increase the visibility of the indication.

The main factor in the visibility of a discontinuity for visual inspection is the contrast between it and the visible surroundings. A discontinuity that creates no change in its visible surroundings has no chance of detection. An example might be a corroded skin under paint. The corrosion must progress to the point where it changes its visible surroundings by pillowing the surface or similar action. This will create the contrast necessary in order to make detection possible. Lighting is commonly used to either cast shadows or cause reflections. This increases the contrast, thus making the discontinuity more apparent.

Magnifiers can range from simple hand held loop magnifiers to microscopes. The primary purpose is to increase the apparent size of the discontinuity in relation to the surrounding area. The primary limitation is that as the magnification increases, the field of view decreases, affecting the ability to inspect large areas.

9.3.2 Boroscopes

The primary purpose of a boroscope is to allow visual inspection of areas that would not be accessible with other means. They are available in a variety of sizes and lengths to fit most inspection needs.

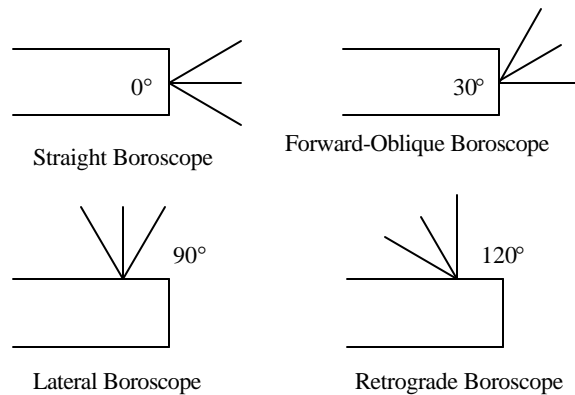
9.3.2.1 Types

Boroscopes can generally be classified as rigid or flexible. A rigid boroscope consists of a rigid tube with a series of lenses and a prism to bring light from the objective lens at one end of the tube to the eyepiece at the other end. The number and specific characteristics of the lenses will depend on the length of the tube and

any magnifiers used. A number of angles of view are available to the inspector. Figure 9-2 presents the standard types. A variable light source is included to illuminate the viewed area.

FIGURE 9-2

BASIC BOROSCOPE TYPES



A flexible boroscope generally uses a glass fiber bundle to transmit the light to the eyepiece of the boroscope. The end with the objective lens is capable of being manipulated through at least 90° . This allows the boroscope to be maneuvered into areas not accessible to the rigid type. A manipulating wheel is usually placed at the eyepiece end to allow the operator to move the objective lens while watching through the boroscope.

9.3.2.2 Additional Options

Various options are available to increase the efficiency of the boroscope inspection. These usually involve magnification and manipulation of the view output. Various magnifying eyepieces are available which are similar to those used in laboratory microscopes. These allow the inspector to zoom into an inspection area once located with a wider view.

Operator fatigue can limit boroscope inspections when the eyepiece is located in an area that is rather small or one where the inspector must be placed in an uncomfortable position while viewing. Video output allows remote viewing. This makes equipment size the primary limitation on the location of the boroscope rather than the ability of the inspector's head to reach the location and view the output. Adding a computer to the boroscope allows the inspector to manipulate the output through various contrast or color enhancement schemes.

One of the difficult things to do with a boroscope is to accurately determine the size of a discontinuity. Without some aid, the size becomes a matter of how large the inspector believes it to be. A number of devices are available to aid the inspector. These usually involve comparing the discontinuity to an object of a known size or distance from the objective lens. Computer software is available to accomplish the same result.

9.3.3 Visual Inspection Process

There are two common types of visual inspection. The first is simply a mechanic checking some interior location of the aircraft with a flashlight. The major factor controlling the minimum detectable discontinuity is the distance between the inspector and the surface. An inspector peering through an access hole two feet from the surface is much more likely to miss relatively smaller discontinuities than an inspector who is six inches from the surface. Many times the inspector will also have a magnifier to check suspect areas. The surfaces are normally not stripped or prepared beyond basic cleaning as necessary.

The other common visual inspection uses the boroscope. No cleaning can usually take place due to the remote nature of the inspection location. Access is usually through the hole created by removing a bolt or rivet. Using a rigid boroscope, the inspection location is in a straight line from the access hole. With a flexible boroscope, the probe is maneuvered through the structure to the inspection location. Depending on the nature of the location, many pictures, instructions, and maybe a model of the path may be needed to ensure that the right location is reached.

In any case, the inspector is seeking visual clues that the surface under the paint contains a discontinuity. Cracked paint and sealer, blistered or discolored paint, and parts that appear misaligned, are among the major indicators.

9.3.4 Visual Inspection Advantages and Disadvantages

Visual inspection is the most widely used method to inspect aircraft. The primary advantage is that it costs very little in the way of equipment and consumables in its most basic form. It provides a relatively quick and inexpensive inspection. Boroscope inspections can provide access to areas of the aircraft that may prove to be too isolated for other NDI methods. An example would be an installed jet engine turbine or compressor. Finally, for most purposes, no NDI specific qualification or certification is required of the inspector.

The major problems arise from two factors. The inspection results are the interpretation of what the inspector sees. The inspector must decide if the crack is just in the paint or is it in the underlying structure. Often, other NDI methods are needed to check suspect areas. The other factor involves the surface. Without

stripping paint or other surface coatings, the discontinuity must be able to cause a change in the paint layer. Some paints and coatings are designed to allow for stretching and shrinking. These factors result in only being able to detect relatively large discontinuities. It should always be remembered that excess paint, sealant, and other coatings could mask underlying discontinuities.

9.4 Penetrant Inspection

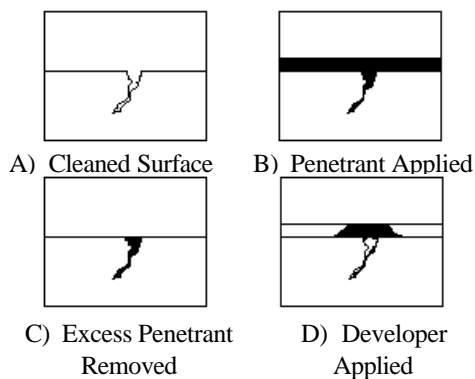
This section presents some of the basic physical principles of penetrant inspection, followed by a brief description of the method and an overview of the basic advantages and disadvantages. While many of these will be reviewed in more detail in later sections, they are included here to give a general understanding of the methods employed.

9.4.1 Penetrant Inspection Principles

The basic penetrant inspection is capable of detecting a discontinuity which is open to the surface. The process consists of variations of three steps (Figure 9-3). First, a penetrating liquid is placed on the surface to be inspected. This liquid penetrates into the cavity formed by the discontinuity. Second, the surface liquid is removed while that in the cavity remains. Last, the liquid left in the cavity must be brought back to the surface for viewing.

FIGURE 9-3

PENETRANT INSPECTION PROCESS



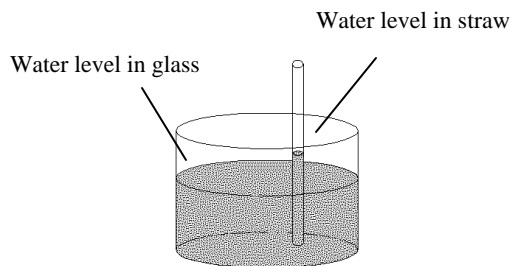
The basic physical property that governs the ability of the penetrant to enter a cavity is that of capillary action. This can be defined as the tendency of certain liquids to travel or climb when exposed to small openings. This principle can be demonstrated through a simple experiment. If a thin glass tube is placed in a container of water, the level of the water in the tube will be higher than the level of the surrounding water, see Figure 9-4. Other experiments show that varying the size of the opening increases the pressure within the crevice.

FIGURE 9-4

CAPILLARY ACTION

The simple nature of this method often overlooks the complex interaction that takes place between the different steps. In the next few sections some of the basic details of each of these steps are discussed. First is a brief description of the chemicals needed, then some of the details of its use and effect on the total inspection process.

9.4.2 Penetrant Inspection Process



The penetrant inspection process requires several steps to complete. Each step of the process is described in the following paragraphs.

9.4.2.1 Penetrant Classification and Application

Penetrant is the chemical without which none of the rest of the process is possible. It is formulated to promote the capillary action previously discussed. Penetrant is generally classified two ways. The first is by the method of viewing the indication and the other by the method needed to remove the excess from the part surface.

Penetrant is classified as “types”, based on the method of viewing the indication, either visible, fluorescent, or dual penetrant. Visible penetrant is designed for viewing in natural (white) light. A high contrast between the indication and the background is necessary to view the inspection. In fluorescent penetrant, the chemical contains dyes that react to ultraviolet (black) light. The main advantage of this method is that indications are significantly enhanced by the greater contrast provided with ultraviolet lights in a darkened viewing area. A third classification is that of dual penetrant. This is designed for use as either a visible or a fluorescent penetrant depending on the inspector’s needs. Due to the contrast and sensitivity issues, fluorescent penetrant is usually the only one authorized for use with aircraft structures.

Penetrant is also classified into four methods based on the method used to remove them from the inspection surface. Method A (water washable) uses water as the removal method. Its main advantage is ease of use. Its main disadvantage is corrosion problems presented by water. It is generally not used for critical aircraft inspections since small and tight discontinuities require detection.

Method B (post emulsifiable, lipophilic) is an oil based penetrant. This method is usually used in stationary penetrant inspections. The use of large tanks allows processing of a range of parts from small to extremely large. The main disadvantage of this method is that it requires many quality controls and is generally not field portable.

Method C (solvent removable) uses a solvent as a remover. This method is usually used for fieldwork as portable kits. All the necessary chemicals are available in aerosol cans. The main disadvantage is that the use of the cans makes inspection of large areas or parts impractical.

Method D (post emulsifiable, hydrophilic) uses a water based penetrant. Like the method B, this method is usually used in stationary penetrant inspection lines for processing a range of parts from small to extremely large. The main disadvantage of this method is that it requires many quality controls and is generally not field portable. However, method D has several significant advantages over method B and is replacing it in most industrial applications.

Penetrant is also produced at different levels of sensitivity. Level 1 is the low sensitivity penetrant. It is suitable for the detection of large, gross discontinuities. Level 2 is medium sensitivity. Level 3 is high sensitivity. This is usually the lowest sensitivity allowed for aircraft inspection. Level 4 is the ultra-high sensitivity penetrant.

Since the penetrant must be able to have direct contact with the discontinuity, the surface of the part must be clean and the suspected discontinuity open to the surface. Once the part has been prepared, the penetrant is applied. This is usually done by flowing, spraying, brushing or dipping. After application, time is allowed for capillary action to occur. This is referred to as the dwell time. A dwell time of between ten minutes and two hours may be necessary depending on the type of discontinuity. The longer times are needed for extremely small or tight discontinuities.

9.4.2.2 Penetrant Removal

The penetrant must be removed from the part surface after the required dwell period. How it is removed depends on the method applied. The goal is to remove the surface layer of penetrant while leaving it inside the discontinuity which is open to the surface.

Method A is the water washable penetrant. As the name implies, water is used to remove it.

Method B is the post emulsifiable, lipophilic method. This penetrant is emulsified by an oil based chemical know as an emulsifier. It is usually applied by dipping or flowing in order to assure an even layer. The emulsifier is left on the surface for a specific amount of time and removed by a water spray.

Method C is the solvent removable method. The penetrant is removed by application of a solvent. Application is done by spraying the solvent on a cloth and wiping the area of interest.

Method D is the post emulsifiable, hydrophilic method. This penetrant is emulsified by a water-based chemical. It is usually applied by spraying or flowing in order to assure an even application.

9.4.2.3 Developer

In order to view the resulting indication, the penetrant must be brought back out of the discontinuity and to the surface of the part. This is the function of the developer. It serves two purposes depending on whether visible or fluorescent penetrant is used. In visual applications, the developer draws out the penetrant from the discontinuity and provides a contrasting background to enhance viewing. In fluorescent applications, the developer is used to draw out the penetrant from the discontinuity. The combination of penetrant fluorescence and the ultraviolet light used provide the contrasting background for viewing. The developer dwells for about half the penetrant dwell time to allow the penetrant to be absorbed from the discontinuity. Developer is available in dry, aerosol, and water based forms.

9.4.2.4 Interpretation

Now that the penetrant has been brought back to the surface with the developer, inspection can occur. The basic rules depend on whether visible or fluorescent penetrant was used. Regardless of which penetrant was used, the indications will take on the same form. The inspector will look at the indications formed by the remaining penetrant and determine their cause by their shape and location.

If using visible penetrant methods, plenty of light is needed to enhance the contrast between the penetrant and the developer. When using fluorescent methods, eliminating as much of the white light as possible is necessary. The white light will interfere with viewing the fluorescent indications. Therefore the inspection should be conducted in darkness with the ultraviolet light.

9.4.3 Advantages and Disadvantages

Penetrant inspection is a very popular and efficient method for detecting surface discontinuities. It is easy to use and relatively inexpensive. In simpler forms, it may consist of just two or three aerosol cans. Penetrant inspection is also very versatile. It can be used on most surfaces which are not too porous. Part size need not generally be a major concern.

The penetrant method will not detect discontinuities that are not open to the surface. For example, smeared metal or other debris trapped in a crack opening will block penetration. Similarly, paint or other coatings will block penetration. Proper cleaning of the surface is vital to the success of the inspection. Since interpretation is based on visual methods, the inspector must have adequate access to reach, clean and view the inspection area.

There are other drawbacks to using the penetrant method. It contains many steps where operator error in applying and using the chemicals can alter the results of the inspection. A variety of chemicals are available with varying sensitivity, making it important to ensure that the right ones are used. Of course, safety is also a consideration. Vapors and hot ultraviolet lights preclude the use of this method in confined or explosive environments.

Only special types of penetrant may be used in environments where they may contact liquid or gaseous oxygen. The wrong penetrant could lead to a reaction resulting in fire or explosion. Another important consideration is chemical reaction with the material under test. The sulfur and chlorides in some chemicals can induce corrosion and hydrogen embrittlement in certain high temperature alloys.

9.5 Magnetic Particle Inspection

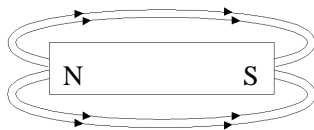
This section presents some of the basic physical principles of magnetic particle inspection, followed by a brief description of the method and an overview of the basic advantages and disadvantages. While many of these will be reviewed in more detail in later sections, they are included here to give a general understanding of the methods employed.

9.5.1 Magnetic Particle Inspection Principles

The inspection consists of the following steps: 1) a magnetic field is introduced into a part, 2) magnetic particles are deposited in the area of inspection, and 3) this particle build up is then evaluated by the inspector. Magnetic particle inspection depends on the interaction of a magnetic field in the part and the magnetic particles introduced onto the part.

FIGURE 9-5

BAR MAGNET MAGNETIC FIELD



The magnetic field in the part can be demonstrated using a bar magnet (Figure 9-5). Here, the magnetic field is illustrated radiating between the north and south poles of the magnet. If the bar magnetic is bent so that its ends move close together, the magnetic field becomes concentrated between the poles such as a horseshoe magnet (Figure 9-6). Taking this one step further, if the ends of the magnet are brought together, a circular magnet results (Figure 9-7). The significant fact about this magnet is that no external magnetic field is present. The entire field is contained within the magnet. This represents the normal inspection situation.

FIGURE 9-6

HORSESHOE MAGNET MAGNETIC FIELD

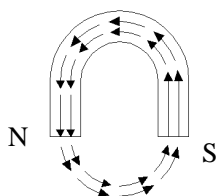
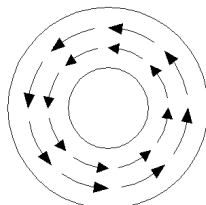


FIGURE 9-7

CIRCULAR MAGNET MAGNETIC FIELD

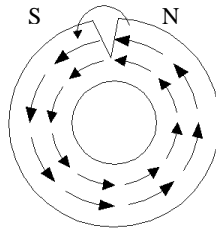


So far, all that has been accomplished is to create a magnetic field that can't be detected since no portion of it is external to the surface. Now, a useful property of magnets comes into play. If a magnet is cut into smaller pieces, each smaller

magnet will have a north and south pole just like the original magnet. Therefore, if a notch is cut into the circular magnet, a north and south pole will be present on the sides of the notch (Figure 9-8).

FIGURE 9-8

CIRCULAR MAGNET WITH A SURFACE BREAK



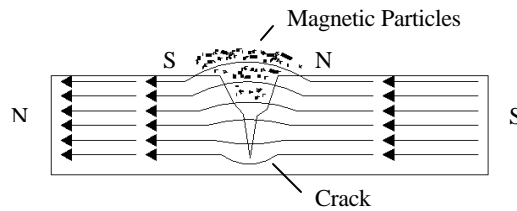
Notch cut into surface.

Two magnet properties become important at this point. The first is the creation of a leakage field. The second is the path of least reluctance. The magnetic field is forced to cross the air gap made by the introduction of the notch. This is called the leakage field. If given the opportunity, the magnetic field will follow the path of least reluctance. Reluctance is a measure of how hard it is for a magnetic field to flow through a material. Air is a high reluctance material. If a material of low reluctance were placed into the leakage field, the magnetic field would tend to flow through that material rather than the air.

This is where the magnetic particles are introduced. They are essentially iron-based filings produced in various shapes and sizes to enhance their visibility, mobility, and magnetic characteristics. If magnetic particles are placed into the area of a discontinuity (Figure 9-9), the magnetic field of the part will tend to flow through the magnetic particles rather than continue through the air. This interaction will hold the magnetic particles at the discontinuity. Since the magnetic particles are made of a magnetic material, they become magnetized by the magnetic field of the part. The magnetized particles will tend to attract additional particles to the discontinuity. This increases the build up of particles at the discontinuity location. A discontinuity located below the surface may or may not produce a leakage field. It depends on many process factors, the material magnetic characteristics, and the depth of the discontinuity.

FIGURE 9-9

EXAMPLE OF A SURFACE CRACK INDICATION



9.5.2 Magnetic Particle Inspection Process

The magnetic particle inspection process consists of variations of three basic steps. First, the part must be magnetized. Second, the magnetic particles must be introduced into the area of the discontinuity. Finally, the resulting indications must be interpreted. Cleaning and demagnetization are accomplished to the extent necessary. All parts inspected using this method must be able to be magnetized and then have enough field strength to allow for magnetic particle accumulation. Following is a brief description of different aspects of a magnetic particle inspection.

9.5.2.1 Magnetic Particles

Magnetic particles are the medium through which the discontinuity becomes visible for inspection. They are essentially iron based filings which have many shapes and sizes to enhance their use. Particles are classified as either wet or dry and fluorescent or visible.

Magnetic particles are generally introduced onto the part in one of two methods: wet or dry. Wet magnetic particles are suspended in a carrier fluid and flowed or sprayed onto the part. Dry particles are usually introduced onto the part by blowing or dusting. The wet particles are more mobile than the dry particles. This makes it easier for them to move to a site on the surface. This added mobility does not work as well as the dry particles concerning subsurface discontinuities. The weaker magnetic field present here may not have enough strength to hold the wet particles in place. Once attracted to the discontinuity site, the dry particles need only a small leakage field to hold them in place.

Visible magnetic particles are designed for viewing in natural light. They are manufactured in several colors. The main criterion for selection is that which gives the best contrast with the background color of the part. Fluorescent magnetic particles are designed with coatings that react to ultraviolet light. This fluorescence

greatly enhances the visibility of discontinuities. Due to these factors, fluorescent magnetic particles are usually the only ones permitted for use on aircraft parts.

9.5.2.2 Equipment

There are three types of magnetic particle equipment. Each is based on the amount of current produced. The largest is the stationary units. They come in a variety of sizes and are capable of magnetizing very large parts. Next are the portable units. These are mounted on small carts or trailers and are capable of inspecting medium size parts or areas in a field environment. The last are the yoke type units. These are hand held units with moveable legs for use with small parts or areas in field inspections.

Other types of equipment include magnetic coils, prods, permanent magnets and clamps. Prods are not generally used on aircraft parts due to electrical arcing and localized heating concerns. Clamps may be used if the problems associated with the prods can be avoided. Permanent magnets are also not generally used as their magnetic characteristics can't be altered to suit the inspection requirements.

9.5.2.3 Interpretation

Once the magnetic field has been established and the particles applied, the interpretation of the particle build up occurs. This requires an experienced inspector. Anything that changes the magnetic field of the part may result in an indication. If the part has large differences in thickness, a complex geometry, or discontinuities expected in multiple directions, several inspections may be required to assure adequate coverage.

If a visible method was selected, the inspector merely looks for the indications of particle build up and interprets their cause. It is important to select a visible magnetic particle that has a highly contrasting color to the background material.

The fluorescent method requires a dark area for inspection. The fluorescence of the indication is relied upon to show the location of a discontinuity. Thus, the inspection occurs in a darkened location with an ultraviolet light to enhance interpretation. Again, the inspector looks for indications of particle build up and interprets their cause.

9.5.2.4 Demagnetization

Once the inspection is completed, the part may need to be demagnetized. This requirement depends on the later use of the part. If it is going to be in an environment where the residual magnetic field may cause interference, the residual field must be removed. It is generally recognized that total demagnetization is not possible. Depending on the magnetic properties of the material, some amount of

residual field may always remain. It may take several attempts to effectively remove the residual field.

The basic method to remove the residual magnetic field is to place the part in another magnetic field. This field will have its polarity continually reversed and its intensity gradually lowered to zero. This will effectively replace the existing magnetic field with another of reversed polarity and a slightly lower intensity. Alternating current (AC) can be used for the field reversal and a gradual decrease in the current will lower the intensity.

9.5.3 Advantages and Disadvantages

The advantages of magnetic particle inspection make it one of the most popular NDI methods. It is relatively easy to use and requires minimum training. It provides results very quickly. Magnetic particle inspections are also inexpensive and cover a wide range of situations.

The major disadvantages relate to the magnetic fields needed for inspection. First, magnetic particle inspection is limited to magnetic materials. Some parts may be difficult to demagnetize. The final two difficulties concern subsurface discontinuities. It is not possible using magnetic particle inspection alone to determine discontinuity depth. In addition, depending on the part and inspection characteristics, the depth of penetration into the part may be limited.

9.6 Eddy Current Inspection

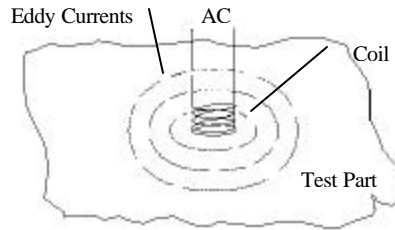
Each section presents some of the basic physical principles of eddy current inspection, followed by a brief description of the method and an overview of the basic advantages and disadvantages. While many of these will be reviewed in more detail in later sections, they are included here to give a general understanding of the methods employed.

9.6.1 Eddy Current Inspection Principles

The basic premise of eddy current inspection is that a magnetic field is altered when it interacts with materials placed in close proximity. The basic arrangement of an eddy current probe is presented in Figure 9-10. An alternating current (AC) is generated in the coil of the probe. The current flow through the coil will cause a magnetic field (the primary magnetic field) to form around the coil. If an object is placed near the coil, this magnetic field will impinge upon the object. The same basic principles used for eddy current inspection are also found in other devices such as electrical motors, transformers, and metal detectors.

FIGURE 9-10

EDDY CURRENT COIL ARRANGEMENT

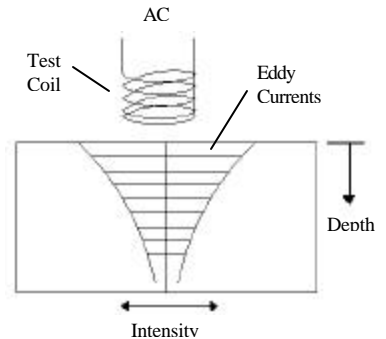


In the object being tested, the primary magnetic field will cause current to flow in a circular direction as illustrated in Figure 9-10. These are called eddy currents. The requirement for current flow means that eddy current inspection can only be done on a conductive material. The current flow in the object will in turn cause a second magnetic field (the secondary magnetic field) to form. This field opposes changes in the primary magnetic field. Changes in the material properties of the object alter the flow of the eddy currents. This results in changes to the characteristics of the secondary magnetic field. Then, the changes in the secondary field will alter the electrical characteristics of the primary magnetic field. The changes to the primary field are then detected by the circuits of the instrument.

The use of alternating current is important as these magnetic fields are caused by the changing current. The quicker the rate of current reversal, the more intense the magnetic fields. The detectable portion of the secondary magnetic field has a limited depth of penetration into the surface (the standard depth of penetration) which is dependent on several factors. At increasing depth from the surface, the field becomes narrower and less sensitive. The basic shape of the eddy current field inside a part is presented in Figure 9-11.

FIGURE 9-11

CROSS SECTION OF AN EDDY CURRENT FIELD



An eddy current probe responds to changes in the material properties such as geometry, homogeneity, electrical conductivity, and magnetic permeability. This results in a versatile instrument that can be used for thickness testing (geometry), discontinuity detection (homogeneity), and conductivity testing.

9.6.2 The Eddy Current Instrument

The eddy current instrument in its basic form is not extremely complicated. It measures the change across the coil of either the impedance, the phase or both. These are measured by splitting the electrical current into a reference signal and the signal going into the probe. The signal returned from the probe will have different characteristics due to the interacting magnetic fields in the part under test. These are the impedance and the phase. Impedance is the total opposition to the flow of the electrical current. The instrument outputs the changes between the reference signal and the signal from the probe using a bridge circuit. The ability to detect changes in both phase and impedance allows the operator to determine the specific location of many signals.

There are predominately two display types used in eddy current inspection. They are a meter display and a cathode ray tube (CRT). The meter display shows the change in the impedance of the signal as the deflection of a needle on a meter. The phase change is not independently presented. The CRT display shows the change in impedance and the phase independently on an X - Y grid coordinate system. This type display is known as the impedance plane. The phase change can present important clues as to the origin of an indication. However, it is not vital for most applications. A CRT display instrument is usually much more expensive than a meter display one. Therefore the meter display unit is generally more readily available in field situations than a CRT display unit.

9.6.3 Eddy Current Inspection Process

The actual operation of an eddy current instrument has become rather simple. The days of setting knobs, buttons, and switches have been largely replaced by automation. Now the entire set up can be accomplished in a matter of seconds. Despite the apparent ease of use, many factors can affect the inspection process that must be considered before beginning operation. In the next sections, some of these influences will be discussed.

9.6.3.1 Part Influences

The major part influences that cause an instrument reaction are the conductivity, the permeability, the homogeneity, and the mass. The conductivity of the part affects the density of the eddy currents at the surface. The magnetic permeability of the part also affects the strength of the magnetic fields within the object. The homogeneity can be compared to how constant the part is in its content. A crack, for example, would represent an interruption in the homogeneity of the part. The mass can be thought of as the shape and thickness of the part. Edges and thickness changes might intercept the eddy current field and result in an indication. An indirect part influence is the temperature. As the temperature decreases, the conductivity of the part increases.

9.6.3.2 Probe Influences

Some factors of the eddy current probe can influence the inspection process. These include the frequency and the distance from the probe to the part. Each of these is operator selected and can be very important to the success of the inspection.

Frequency selection affects the inspection in two ways. The faster the polarity of the electrical current changes (the frequency) the more intense the magnetic fields. The more intense the field, the less the depth of penetration. Therefore, the higher the frequency used, the more sensitive the probe and the less the depth of penetration.

The distance from the probe to the part is referred to as magnetic coupling or lift off. It was shown in Figure 9-11 that the eddy current field is narrower and less sensitive farther from the probe. This is the reason that lift off is important. The further the probe from the discontinuity sought, the less sensitive the inspection becomes. Nonconductive coatings on the part such as paint contribute to lift off. Of course, a point is eventually reached where there is too much lift off present for an effective inspection.

9.6.3.3 Calibration

Calibration is the process of selecting the inspection parameters and checking for an appropriate response from the instrument. This consists of placing the probe on the reference spot and then nulling or balancing the instrument. This tells the unit that this is the condition where the instrument should read no change. The goal is to maximize the difference between an acceptable condition and the expected discontinuity.

An example might be calibrating a unit for crack detection. Here the instrument would be nulled on an area of the standard away from a crack. Scanning over an area without a crack would cause no response from the unit. Scanning over a crack would create a response from the unit.

9.6.3.4 Interpretation

Interpretation of the eddy current instrument response is largely a matter of operator experience. This is not generally as difficult as it seems in simple applications. Rather localized responses such as one from a crack occur rapidly while scanning. First, nothing, then it is there and then it is gone. Area responses such as a conductivity change generally occur more gradually. Situations can occur, such as near geometry changes, where experience is the key to a successful inspection.

The phase information presented on the impedance plane can provide clues as to response origin. For instance, a metered instrument may detect the crack in a tube wall, but the impedance plane instrument can determine whether it is located on the inner or outer wall.

9.6.4 Conductivity and Thickness Testing

There are a number of dedicated conductivity and thickness testers that use eddy current principles. They work on the same principles as described, but use a digital readout rather than a meter or CRT. It is important to remember that the limitations discussed for eddy current fields also apply to these instruments.

When conductivity testing, a larger diameter probe is used. This keeps the instrument from responding to localized changes in material properties. The frequency is usually a fixed value. This makes depth of penetration particularly important. If the surface is not thicker than the depth of penetration, the conductivity measured will be affected by the eddy current field emerging through the far side of the part. Similarly, other coatings or materials will affect the reading. Thus it is important to have the same material, approximate thickness and coating situation for reference standards as on the actual part.

Thickness testing has similar limitations. Again, a larger diameter probe is used and the frequency is usually fixed. This also leads to penetration limits. Here the

eddy current field must extend beyond the far side of the surface to be tested. If the part is too thick, the field will be unable to penetrate far enough to sense the opposite side. Thus these instruments are more accurate with thinner materials. The measurement of lift off can also be used to determine the thickness of nonconductive coatings such as paint. Just as in conductivity testing, conductive materials in contact will affect the output. Standards that duplicate the inspection situation as closely as possible are necessary to ensure a high degree of accuracy.

9.6.5 Advantages and Disadvantages

The eddy current method has a number of advantages that make it a popular inspection method. It can be used in the presence of coatings such as paint. The area to be inspected can usually be rapidly scanned and a determination of condition made. Some metered instruments, conductivity and thickness testers are relatively inexpensive. It also does not take large amounts of training and experience to begin on simpler applications.

The eddy current method also has some important limitations. The first is that it can only be performed on a conductive material. Another is the sensitivity and depth of penetration interdependence. If deeper penetration is required, the sensitivity to smaller discontinuities suffers. Similarly, there is a limit on the depth of penetration into the part. Another is the inability to accurately determine the depth of a subsurface discontinuity with the meter instruments. Estimates can be made based on experience, but too many factors can influence the instrument response to accurately determine depth as a matter of routine. The eddy current method is also relatively ineffective at detecting discontinuities parallel to the surface.

9.7 Ultrasonic Inspection

This section presents some of the basic physical principles of ultrasonic inspection, followed by a brief description of the method and an overview of the basic advantages and disadvantages. While many of these will be reviewed in more detail in later sections, they are included here to give a general understanding of the methods employed.

9.7.1 Ultrasonic Inspection Principles

Ultrasonic inspection generally occurs based on the principle of time of flight. A sound pulse is generated by the instrument and transferred into the surface of a test part. The velocity of sound is constant for a particular material. So, if the velocity and time elapsed are known, the distance traveled by the sound pulse can be determined.

The characteristics of the sound pulse in the material have important properties that affect the inspection. The sound pulse has the same basic properties as a beam of

light. It reflects, refracts, and spreads out as light does. The sound pulse can follow some geometry changes, it can be reflected off an interface to detect discontinuities away from the contact point, and it can be refracted from one material into another.

Useful information is returned by the instrument usually in the form of a reflection at an unexpected location or a loss of signal. Loss of signal (attenuation) can occur when the sound pulse is scattered by a number of small discontinuities or by a larger one oriented such that sound is reflected away from the instrument.

9.7.2 The Ultrasonic Instrument

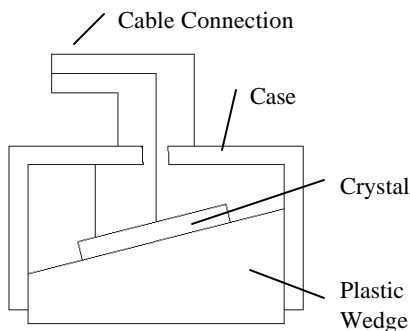
An ultrasonic instrument is a complex piece of equipment. Many internal devices must be properly coordinated. The following sections will not cover all these parts, but will touch upon the two that are the most visible to the user. These are the transducer and the video display.

9.7.2.1 The Transducer

The transducer is the device which transmits the sound pulse into the part and receives the sound returning from the part (Figure 9-12). It is connected to the ultrasonic instrument with a cable which transmits the electrical impulse to and from the transducer.

FIGURE 9-12

ULTRASONIC TRANSDUCER CONSTRUCTION (SHEAR BEAM)



The key is the crystal. It is constructed of a piezoelectric material. This is a material that has the ability to convert electrical energy into mechanical energy (vibration) and vice versa. The material of the crystal determines mechanical efficiency and the crystal thickness determines the frequency of the vibration.

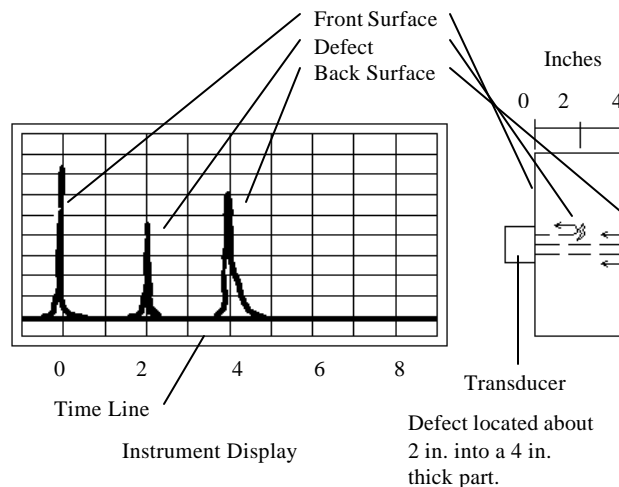
9.7.2.2 Video Display Basics

The video display converts the returned electrical signals into a visual display for interpretation. There are two types of displays in common use. They are the A scan and the C scan.

An A scan presents a display such as that in Figure 9-13. The line at the bottom of the screen is a time line which represents the time it took for the sound to return to the transducer. Since velocity is constant in the material, this can also be thought of as the distance the sound traveled. The vertical signals (amplitude) represent the amount of energy reflected at each interface the sound pulse encountered. This display is the most common among field portable instruments.

FIGURE 9-13

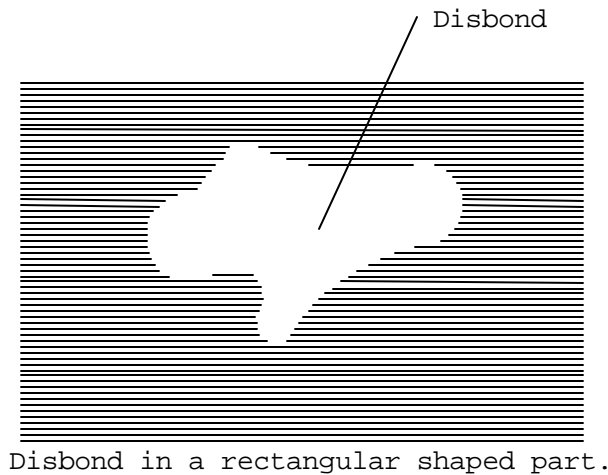
ULTRASONIC A SCAN EXAMPLE



The C scan presents a plan view of the part. Here the ultrasonic instrument is coupled to another device which can follow the movements of the transducer across the part. The amplitude of the return signal is converted into a visual cue. It may be as simple as an on/off command to a plotter (Figure 9-14) or assignment to a color palette on a computer display. The final product is a scaled plan view of the part under test with the amplitude of the return signals presented. This will show the location of the discontinuity, but not its depth. This type display is common among automated units.

FIGURE 9-14

ULTRASONIC C SCAN EXAMPLE



9.7.3 The Ultrasonic Inspection Process

The ultrasonic inspection process has many factors that can affect the quality of the inspection. In this section, the types of inspections, the operator choices, instrument set up, inspection, and interpretation will be covered.

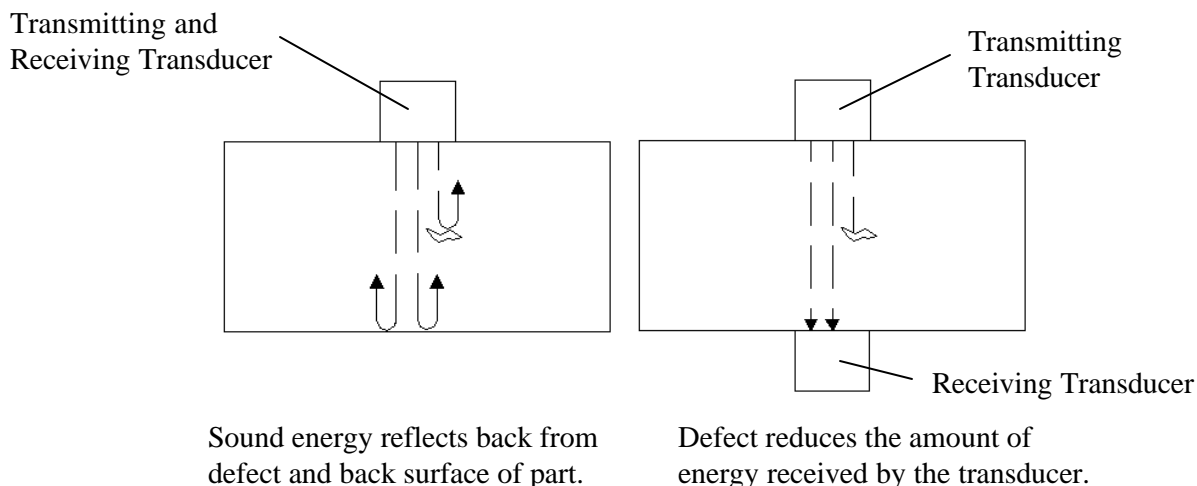
9.7.3.1 Inspection Types

There are several combinations of ultrasonic inspection that can occur. The first is the choice between a contact method and an immersion method. The contact method has the transducer in contact with the part surface. Since the frequency of ultrasonic inspection is generally in the megahertz range, a couplant is required to eliminate the air from between the transducer and the part. The immersion method is done with water used as a couplant. This has the advantage of allowing more movement of the transducer. However, it can involve large amounts of water flowing across the part or placing the entire part under water.

Another choice is between pulse echo inspection and through transmission inspection (Figure 9-15). In pulse echo, the transducer is used to send out and to receive back the signals. The primary advantage is that this allows depth information to be collected. It also requires access to only one side of the part. Through transmission uses separate transducers to send and receive signals. This requires that the transducers be properly aligned on opposite sides of the part. The primary advantage is that about half the energy is needed since the sound does not travel back to the sending transducer. It is also much easier to automate this method. The primary disadvantage is that no depth information is collected.

FIGURE 9-15

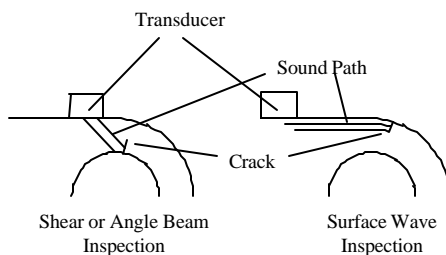
ULTRASONIC PULSE ECHO AND THROUGH TRANSMISSION METHODS



The final major choice is which direction to send the pulse into the part. There are three ways. The first is longitudinal wave: the sound goes straight into the part as illustrated in Figure 9-15. Another is shear wave: the sound is transmitted at an angle into the part. The last is surface wave: the sound is transmitted along the surface of the part. These are shown in Figure 9-16.

FIGURE 9-16

EXAMPLE OF SHEAR AND SURFACE INSPECTIONS



9.7.3.2 Operator Choices

The operator has several choices that will affect the characteristics of the sound beam and the inspection. Among these are the frequency, the transducer diameter, and the use of wedges.

The frequency is probably the most important operator parameter. Like most choices, it represents a compromise of conflicting needs. Higher frequencies allow smaller discontinuities to be located. However, penetration into the part suffers.

The transducer diameter also affects the inspection. A general rule is that the discontinuity sought should be at least half the size of the transducer. Therefore, a smaller transducer will provide a greater relative response to smaller discontinuities.

The final major decision is whether to use some sort of plastic wedge or not. It is generally used for three situations. The first is to angle the transducer so that a specific refracted angle will be present in the part. An example might be taking a longitudinal transducer and angling the wedge to produce a 45° sound beam in a material. Another is to adapt the shape of the transducer to that of the part. An example might be using a wedge to adapt a longitudinal transducer to a curved surface. The last is to remove sound distortion near the transducer face from the part. Removing this from the part allows detection of discontinuities immediately under the part surface.

9.7.3.3 Instrument Calibration

The main purpose of calibration is to ensure a repeatable display that returns the required information. The instrument will initially be set up on an area considered normal. The transducer will be moved to the discontinuity and the signal checked. As an example, the operator may be required to detect a crack. The initial set up would be away from the crack to establish how a normal part should look. The transducer moves to the crack. The display is checked to see if a signal is obtained that is easily interpreted.

It is very important to have a reference standard that accurately simulates the conditions of the inspection. It may seem logical to assume that anything other than a “good” signal is a reject signal. However, since the signal can be caused by a variety of conditions, criteria are set for where and how the signal will appear on the screen. Without the proper standard, it would sometimes be impossible to determine whether the returned signal represented a relevant or non-relevant condition.

9.7.3.4 Inspection

The part is scanned from the surface that provides the best orientation in regard to the discontinuity. The best reflector is one oriented perpendicular to the sound beam. For through transmission, a way must be found to ensure that the two transducers remain aligned.

Care must be taken to ensure adequate coupling to the part. The sound will not transmit through air. Loss of a signal might not be a discontinuity, it might be a loss

of coupling. The surface of the part must also be smooth enough to allow coupling. A rough surface will reflect more sound and may allow air to become trapped in the couplant.

9.7.3.5 Interpretation

Most inspection situations are straightforward. The specification and reference standard provide the information necessary for interpretation. However, there are times when interpretation can be the most challenging part of an ultrasonic inspection. The most common location of discontinuities is in corners, radii, holes and abrupt changes in cross section. Each of these also presents its own signal. The operator must be able to differentiate between the non-relevant and relevant signals.

9.7.4 Thickness Testing

The majority of thickness testers operate on ultrasonic principles. Given the proper conditions, ultrasonic thickness testers can accurately measure thickness in excess of fifteen feet. Most dedicated instruments use a digital readout. They use a variety of frequencies and standoff wedges to increase accuracy or to measure thinner materials.

These instruments operate on the time of flight principle. When calibrating, reference standards of known thickness are used. The operator inputs the thickness into the unit and calibrates to that standard, by having the unit measure the time of flight. Knowing these two, the velocity is calculated. When used for thickness testing, the velocity is now known and the instrument measures the time of flight. The calculated distance traveled is then output on the display. The accuracy of thickness testing is greatly influenced by the accuracy of the reference standards.

9.7.5 Ultrasonic Advantages and Disadvantages

The two primary advantages of ultrasonic NDI are the ability to determine the depth of the discontinuity in a material and its ability to detect laminar discontinuities. These discontinuities, which are parallel to the part surface, can be difficult to detect using other methods. Using the principles of reflection and time of flight, inspection can be accomplished for discontinuities that are not where the transducer is located, such as a shear wave inspection of a weld.

There are disadvantages to ultrasonic NDI. With the sound energy reflecting and refracting off the various surfaces involved in a test, an experienced operator is necessary to set up the test and to interpret the results. Another disadvantage of this method is expense. The equipment and transducers are rather expensive compared to the other NDI methods. All inspections will require some type of standard to compare to the test results. These can sometimes be very expensive.

A final problem is the need for a favorably oriented discontinuity. It may be missed if the sound is reflected away from the expected direction. Since field inspection usually requires some type of contact with a surface, the inspector needs direct access to a surface and it must be smooth enough for scanning. This method might have problems with geometry. It may not be possible to separate a non-relevant signal from a relevant one or to get the sound pulse to the required location.

9.8 Bond Inspection

This section presents some of the basic physical principles of bond inspection, followed by a brief description of the method and an overview of the basic advantages and disadvantages. While many of these will be reviewed in detail in later sections, they are included here to give a general understanding of the methods employed.

9.8.1 Bond Testing Principles

Bond testing instruments generally work on one of four principles. These are high frequency ultrasonic, low frequency ultrasonic, eddy sonic and resonance. The selection of a particular method will depend on the type of information required and the material combination present on the part.

High frequency ultrasonic is the ultrasonic method discussed as applied to bonds. Any of the combinations presented, pulse echo/through transmission; contact/immersion; and longitudinal/shear waves; can be used to determine bond integrity.

The second bond testing method is low frequency ultrasonic. This consists of a transmitter and a separate receiving unit. The transmitter sends out a complex wave pattern which is sensed by the receiver. The instrument detects phase and amplitude changes as the probe passes over a disbanded area.

The third method is the eddy sonic method. A low frequency eddy current coil is used to load and unload the surface of the bonded area. A sensitive ultrasonic detector detects changes in the amplitude of the sound energy transmitted by this process.

The final method is the resonance method. The transducer mechanically sets up a vibration pattern at the resonant frequency of the bonded area. The transducer then detects changes to the amplitude and frequency of the pattern to find discontinuities.

The simplest form of bond inspection involves no dedicated instrument. This is the tap test. The inspector sharply raps with a small tap hammer on the bonded structure. A change in sound quality indicates a disbond.

9.8.2 Bond Testing Process

The actual bond test is usually a relatively simple process. Automation has removed most of the human error side of set up. These units also do not provide much information about the exact nature of the discontinuity. Usually the information returned is that a reject bond condition was found at the probe location. Some testers are able to determine which bond line has the discontinuity in multiple layered structures.

The reference standard is vitally important to this inspection. It must represent the part to be inspected as closely as possible with the same discontinuities as those expected. The probe is placed on the acceptable area of the standard. The instrument will use this as the normal condition. As with most other NDI equipment, the tester is actually measuring the difference between the area being scanned and the signal considered as normal. The written inspection technique will set the limits as to what constitutes a reject signal.

9.8.3 Advantages and Disadvantages

The basic advantage of dedicated bond testers is ease of use and low cost compared to dedicated ultrasonic instruments. A bond tester provides a quick way of determining if something is wrong with a bonded structure. Generally, tap testing does not require special NDI certification.

Unfortunately, the exact nature of the discontinuity is usually not found. For complex or detailed inspection, other methods may need to be employed. Many bond test methods are also limited to simple configurations.

9.9 Radiographic Inspection

This section presents some of the basic physical principles of radiographic inspection, followed by a brief description of the method and an overview of the basic advantages and disadvantages. While many of these will be reviewed in detail in later sections, they are included here to give a general understanding of the methods employed.

9.9.1 Radiographic Inspection Principles

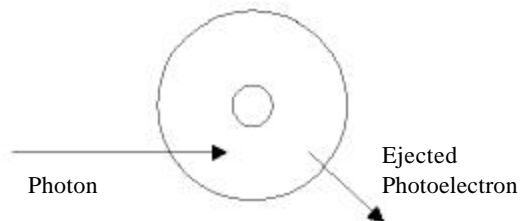
Radiography works on two basic principles. First, radiation is absorbed by different materials at different rates (density). Also, the amount of radiation absorbed depends on the amount of material (thickness). It requires four steps to inspect a structure: the radiation must be somehow generated and directed toward the part, the radiation must then interact with the structure, then the radiation not absorbed interacts with a detector to capture an image, and the image is interpreted.

The key to all this is the interaction between the radiation stream and matter. This is the x-ray photons of the stream interacting with the material being tested, be it aluminum, human bone, or the detection film. At the energy ranges normally used for aircraft inspection, this takes place in two ways, either the photoelectric effect or the Compton effect.

The photoelectric effect is a low energy interaction. An incoming photon encounters an atom of material. The energy of the photon is transferred to the outer electrons of the atom. If enough energy is absorbed, the atom will emit the excess as a low energy photoelectron as the affected electron returns to its normal state. This principle is illustrated in Figure 9-17.

FIGURE 9-17

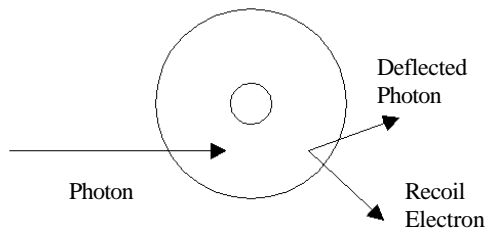
PHOTOELECTRIC EFFECT



The Compton effect is a high-energy interaction. The incoming photon has too much energy for the atom to absorb. Again, the incoming photon interacts with the electrons of the atom. This photon can't transfer all its energy to the atom. It is deflected by the atom and continues with whatever energy was left over. The electrons of the atom have absorbed so much energy that one is ejected from the atom to restore the energy balance. The ejected electron will eventually be captured by another atom and release its energy as either a Compton interaction or a photoelectric one. The Compton effect is illustrated in Figure 9-18.

FIGURE 9-18

COMPTON EFFECT



Through these interactions, each photon of the x-ray beam interacts with the atoms of the material. The photons and those emitted by the material then form the image on the film. The degree of darkening of the film shows how many photons reached the film. Light or clear areas show where few photons reached that area of the film and darker areas indicate that many were present.

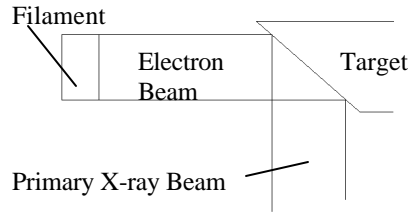
9.9.2 The X-ray Unit

Depending on their power capabilities and physical size, x-ray equipment comes in a variety of configurations. There is usually at least a tube where the radiation beam is created, and a control box. All tubes need some sort of cooling. This is either an internal fan, an internal oil cooler, or an external radiator. Some units are trailer mounted with their own electrical power.

Though the arrangement of a tube may change, the basic steps toward producing a radiation beam remain essentially the same (Figure 9-19). At one end of a tube, the filament is located. This is a source of electrons for the process. The other end of the tube has the target with an electrical charge opposite that of the filament. This electrical difference moves the electrons from the filament to the target. A vacuum is around these components in order to prevent interference with the electron beam.

FIGURE 9-19

GENERAL LAYOUT OF AN X-RAY TUBE



The high velocity electron beam strikes the target. The energy transfer causes the emission of high energy photons from the target. These are the x-rays. Tilting the target aims the majority of the radiation toward the material. A tremendous amount of heat is generated by this process. A large heat sink and cooling system are needed.

The control box is used to set the radiation parameters and to initiate the process. The parameters include the time of exposure, the voltage and the amperage. The voltage adjusts the efficiency of the production process. The amperage adjusts the amount of radiation produced.

A second method of radiography not usually associated with aircraft inspection is the use of a naturally radioactive source. A variety of materials display radioactive decay characteristics producing radiation in the x-ray band. These sources are not usually used for aircraft inspection because the radiation emitted can't be altered. Thus, the only control is how long to expose the film.

9.9.3 Radiation Safety

Radiation safety is a major concern for radiographic inspection. Accumulated or uncontrolled radiation exposure can lead to serious health problems including sterility, tumors and cancers. Exposure to the primary radiation beam can cause death in a matter of weeks from radiation poisoning. Due to these factors, all radiographic operations fall under some type of government regulation.

The primary protections from exposure are provided by distance or shielding. To protect bystanders, a shielded room, or an isolated area is required. To protect the operator, radiation detection devices are required to monitor exposure and to warn of excessive exposure. A medical monitoring system is set up to track this exposure. The body has the ability to repair some damage over time. Therefore, limited amounts of exposure are permitted within certain time limits.

9.9.4 Radiographic Inspection Process

The basic process of industrial radiography is the same for an aircraft as it is for medical radiography of a person. This process is often referred to as making a shot or an exposure.

9.9.4.1 The Parameters

The three ways that the inspector can vary the quality of the radiograph are the position of the tube, the settings on the control box, and film selection. The area to be shot is controlled by aiming the beam. Different angles may be used by off setting the tube to one side of the perpendicular aim point. Just like a flashlight, the distance from the tube to the object determines the area of the radiation beam at the test surface.

At the control box, the operator adjusts the kilovoltage, the amperage, and the time. The kilovoltage controls the quality of the radiation. The amperage controls the rate of radiation production. Time controls the duration of the exposure.

Just like in regular photography, radiographic film is manufactured to suit a variety of situations. It can be purchased at varying speeds and sizes. Different speeds are also related to sensitivity. Slower speed films are usually more sensitive than faster film.

9.9.4.2 Interpretation

Interpretation is essentially a matter of the inspector's experience. The primary reason is that the image on the film represents the radiation characteristics of the material, not its visual characteristics. Like ultrasonic inspection, there are varieties of different causes that may produce virtually the same indication on the radiograph. A second problem is that everything between the tube and the film is overlaid upon one another in the resulting image.

Discontinuity orientation also plays an important role. It should be oriented such that the major axis is parallel to the radiation beam. This provides the greatest difference in the density between the discontinuity and the surrounding area. Some very thin or small discontinuities are nearly undetectable because of the extremely small difference in the apparent density.

9.9.5 Radiographic Advantages and Disadvantages

The major advantage of radiographic inspection is the ability to present a view of the interior of the structure. The result is also a permanent record of the inspection. Little to no preparation is required to the structure surface compared to other methods of NDI.

There are a number of disadvantages to this method. The primary one is safety. The radiation safety concerns usually involve government regulation. Inspectors require training to interpret film. The equipment and safety precautions are very expensive compared to the other NDI methods.

The expected discontinuity must be properly oriented for detection. It must also show enough of a density difference to be detectable. For all these reasons, unless there is enough customer need to justify the expense, most NDI companies tend to avoid doing radiographic inspections.

9.10 Determining the Minimum Detectable Discontinuity

The basic process of determining the size of the smallest detectable discontinuity is the same regardless of the method of inspection selected. The structural engineer will supply the necessary information regarding the expected discontinuity. A certain amount of experimentation may be necessary to establish detection limits, and some testing of the final inspection will occur. At this point the aircraft inspection requirements may need to be altered to accommodate the capabilities of the detection method chosen or other ways sought to improve the NDI situation.

The result is a minimum detectable discontinuity, c_{det} , which is presented to the structural engineers. This will allow them to complete the inspection interval and requirements process. Many times this process can become iterative when the smallest detectable discontinuity, c_{det} , is larger than the desired critical discontinuity size, c_{crit} .

9.10.1 Required Information

The information collected from the structural engineer includes:

1. The location of the inspection. This will allow NDE to determine accessibility issues and problems that might be encountered using various methods.
2. The types of discontinuities to be detected. This will be the major influence on the inspection method selected.
3. The expected area of interest and orientation of the discontinuity. This information will allow NDE to focus on specific areas rather than expending great efforts to find the smallest possible discontinuity in any location.

9.10.2 Experimentation

With the given information from the previous section, an inspection method will be selected based on the experience of the NDE personnel. In Section 9.11, a set of general guidelines is provided on the selection of the inspection method for different discontinuities. The complexity of the proposed inspection will determine the next step in the process.

If the proposed inspection is relatively simple in nature, the inspection procedure and minimum detectable discontinuity size may be taken from standard industry parameters and the experience of the NDE personnel.

If the situation presents a more difficult inspection scenario, the NDE personnel will need to do some physical experimentation to establish the minimum detectable crack length, c_{det} . This will generally consist of creating a reference standard that matches the characteristics of the area of interest as closely as possible. A simulated discontinuity will be introduced in this standard at the location and orientation specified by the Structural Engineer. The size of the discontinuity will generally be the desired minimum size. The proposed inspection method will be optimized on the reference standard to detect the discontinuity presented.

If the discontinuity can't be detected, two options arise. The first is to change the proposed inspection method. Usually this is not done unless it is obvious that the wrong method was chosen. The other is to increase the size of the discontinuity and try to detect it again. The discontinuity will be gradually increased in size until detection is possible and can be demonstrated to an acceptable level of confidence of detection. This level of confidence is often specified as a ninety percent repeatable event.

9.10.3 Testing

Two concerns need to be checked during the testing phase of this process. The first mainly entails checking accessibility to the area of interest and ensuring the workability of the inspection method. The second concern is how the field conditions relate to the laboratory conditions used to determine the minimum detectable discontinuity. In the laboratory it is difficult to simulate the effects of field use in a reference standard. In the field the holes may be damaged, the skins scratched or gouged, the paint thick and uneven. These influences on the inspection need to be factored into the size of the minimum detectable discontinuity. In addition the expected technical ability of the field inspectors needs to be considered. Is the technique for inspectors at Level III with twenty years experience or should it be simple enough for a Level II with the minimum requirements to be certified?

Depending on the conditions cited in the previous paragraph, the size of the minimum detectable discontinuity would need to be increased to ensure confidence

of detection under field conditions. Section 9.12 will explore in more detail the major factors affecting the detection limits of the various methods.

9.11 Selection of an Inspection Method

Some basic guidelines can be used to initially select an inspection method. Several of the methods overlap in their detection abilities. Because of this and the complementary nature of the methods, the final selection of a NDI method should be made only after consulting properly qualified personnel.

9.11.1 Surface Cracks

In this particular situation, a surface crack is a crack open to the surface and located on the same surface to which the inspector has access. This is the inspection situation most often encountered by inspectors. The methods used most often are visual, eddy current, magnetic particle, and penetrant. Radiography and ultrasonic methods are usually reserved for situations where direct access to the crack location is not available. In many cases, a crack found with one method can be confirmed through the application of a second method. Examples of surface cracks include cracks extending beyond fastener heads and cracks in boltholes with direct access to the hole wall.

9.11.1.1 Visual Method

If the crack is large enough, the visual method may be satisfactory. Some questions need to be considered in this selection. Is the area accessible to the inspector? Will paint or other coatings mask a visual crack indication? Generally, visual inspection does not require personnel with NDI qualification.

9.11.1.2 Eddy Current Method

The eddy current method is usually the first choice of NDI methods. It provides a quick and accurate detection method which does not ordinarily require paint or coating removal. If the paint or coating is too thick, either it can be removed or the crack treated as a subsurface crack. Close proximity to geometry changes or dissimilar materials may cause problems with detection.

9.11.1.3 Magnetic Particle Method

Magnetic particle inspection is used only for magnetic materials such as steel. It can be used through paint with degraded results. It is normally done on unpainted surfaces for maximum effectiveness. Demagnetization is usually required following inspection. This method should not be used where other aircraft components will be affected by the magnetic fields generated.

9.11.1.4 Penetrant Method

Penetrant inspection can be used on most surfaces that are not so porous as to retain the penetrant under the surface. Generally, it is used on non-magnetic materials since magnetic particle inspection is faster and as efficient on magnetic materials. It can't be used on painted surfaces or areas where smeared metal or foreign material may fill in the crack. Inspection around joints or holes may present difficulties with the removal of the penetrant and application of developer.

9.11.1.5 Ultrasonic Method

Ultrasonic inspection is useful for detecting surface cracks which are not located with direct access to the surface. A shear technique may be used to find cracks in an adjacent area such as around the sides of a hole. A surface technique may be used to find surface cracks from an adjacent area, but is very sensitive to surface debris. An example of a surface technique is presented in Figure 9-16.

9.11.1.6 Radiographic Method

Radiographic inspection may be used when direct access is not available to the area of interest. Surface crack detection using radiographic techniques is not an effective method unless the expected crack meets the correct orientation and size requirements. If possible, experiments should be conducted to ensure that the crack could be detected.

9.11.2 Subsurface Cracks

Subsurface cracks can present some of the more challenging NDI situations. The term subsurface is most often defined as discontinuities located in areas without direct access to the inspection surface. It may or may not involve multiple layers of material between the crack and the surface where the inspection actually takes place. Examples include detection of cracks under rivet heads and cracks located on the surface opposite that from where inspection takes place. Interpretation skills are vital. Rejection may be entirely dependent on the interpretation of the instrument response. Eddy current and ultrasonic methods are the two most commonly used detection methods.

9.11.2.1 Eddy Current Method

The eddy current method is usually the first choice for inspection. This method will normally ignore laminar type indications such as would be presented by a multiple layered inspection situation. However, it also represents a compromise between the depth of penetration and the size of the expected crack. There is an exponentially increasing relationship between the probe-to-crack-surface distance and the size of the detectable crack. A material thickness will be reached for a

given frequency where detection is no longer possible. Detection of cracks in fastener holes can be done as a subsurface inspection with the fastener installed or as a surface inspection with the fastener removed.

9.11.2.2 Ultrasonic Method

The ultrasonic method is the other primary choice for detecting subsurface cracks. The size of the detectable discontinuity does not appreciably increase with increasing distance from the probe for a given frequency. However, there are two requirements that are the main barriers to its use. First, the need for a clear path for the sound pulses to reach the location of the expected crack. The second is the need for intimate contact between any layers that may be present. This generally requires a bonded structure. Sound may be unable to cross the interface between different layers of the structure. An example of a subsurface inspection situation using a shear technique is presented in Figure 9-16.

9.11.2.3 Visual Method

Visual inspection techniques can be used if access is available to the area for a boroscope. These are available in a variety of sizes and configurations. The primary consideration is whether a discontinuity on the surface to be inspected will be masked by paint, debris or sealant layers. Another is the degree of sophistication required of the instrument to accurately measure the size of indications found.

9.11.2.4 Magnetic Particle Method

The primary limitation for magnetic particle inspection is its use only on materials which can be magnetized. The ability to detect a crack decreases with depth. Thus, it should only be considered where the crack is located relatively close to the inspection surface.

9.11.2.5 Radiographic Method

Radiographic inspection may be used, but suffers from the same problems as in surface crack detection. Crack detection using radiographic techniques is not an effective method unless the expected crack meets the correct orientation and size requirements. Experiments should be conducted to ensure that the desired crack could be detected.

9.11.3 Corrosion

Corrosion detection is the most challenging NDI situation. Current methods detect the effects of corrosion rather than the corrosion itself. These indications are usually

stress corrosion cracks, pitting and general material thickness reduction. Therefore, all the major NDI methods are capable of detecting corrosion in one way or another.

9.11.3.1 Visual Method

Visual inspection is often made for the effects of corrosion. When visual effects are noticeable, the corrosion has reached an advanced stage. This requires that the selected structure be able to tolerate a relatively large amount of corrosion damage if visual inspection without paint removal is to take place. In any case, experience is necessary to recognize that the discontinuities found are indeed the result of corrosion.

9.11.3.2 Penetrant Method

Penetrant inspection is not normally used for corrosion detection, but will detect surface cracks resulting from stress corrosion. However, many times the surface cracks are too small for detection or masked by the general surface conditions. It will detect surface pitting, but only if the pits are deep and narrow enough to hold the penetrant during the removal step.

9.11.3.3 Magnetic Particle Method

Magnetic particle inspection falls into much the same category as penetrant inspection. It is not normally used, but will detect discontinuities such as cracks. However, many times the surface cracks are too small for detection or masked by the general surface conditions.

9.11.3.4 Eddy Current Method

Eddy current can be effectively used to detect surface or subsurface corrosion. Surface cracking is detectable as previously discussed. Pitting, depending on the concentration and size, may take the form of many extremely small crack-like indications or as a generally rough surface. Subsurface or far surface corrosion detection essentially becomes a thickness test. The guidelines concerning depth of penetration and increasing discontinuity size apply as discussed in the eddy current inspection section. Thus, the amount of pitting that can be detected is relatively large for thicker structures.

9.11.3.5 Ultrasonic Method

Ultrasonic inspection is used mainly for subsurface corrosion detection. Surface corrosion detection involves interpretation of signals similar to a rough surface condition. Detection of subsurface corrosion is essentially a thickness test. Pitting

becomes detectable as it causes variations in the material thickness. Internal corrosion may be detectable with pulse echo or through transmission techniques through scattering of the signal. However, relatively large amounts of corrosion will need to be present to produce a noticeable response. The relatively small size of the transducer limits the ability to check large areas.

9.11.3.6 Radiographic Method

Radiography is useful for areas of corrosion where there is a definite difference between the corrosion and the adjacent area. This is not a good method of detection for laminar type discontinuities to which a thin surface corrosion can be compared. It is also not ideal for detection of gradual changes in the composition of a part. It is necessary that the corrosion have a definite boundary to allow for accurate sizing by the inspector.

9.11.4 Disbonds and Honeycomb Discontinuities

Face sheet to honeycomb core disbonds are best located using a bond tester or an ultrasonic instrument. The bond tester will generally have better penetration of the honeycomb than the ultrasonic instrument due to the lower operating frequency. In most situations this will allow inspection of the bond between both face sheets from one surface of the part. Since bond testing returns limited information about the exact quality of the bond, further investigation using ultrasonic or radiographic techniques may be required to determine the exact nature of the indication. Tap tests are an effective inspection method for thin face sheets and where inspection is not required through to the opposite surface.

Bond testers will usually be the first choice. Inspection time is lower and interpretation easier than the ultrasonic method. These instruments are usually somewhat limited regarding thick or complex structures. Bond testers are somewhat more limited in composite applications due to the nature of the material. Experiments should be performed using the bond tester as the initial inspection method before switching to other methods.

High frequency ultrasonic methods are usually effective within limits. The primary problem encountered is the relationship between penetration and sensitivity. The frequency required allowing penetration of unfavorable bond lines may not be capable of detecting a small enough discontinuity. This is usually encountered when penetration is needed to the opposite outer surface of the part. This situation may require inspection from both sides of the part or switching to a through transmission method which also requires access to both sides of the part with the added complication of keeping transducers aligned.

Tap tests provide a quick and easy method to check bond quality using inspectors that do not require special NDI qualification. It is usually restricted to thin face

sheets and to situations where the test is not expected to detect problems with the opposite side bond line. Experiments should be conducted to ensure the change in sound quality between the bonded and disbanded area is readily apparent.

Radiography is usually the best method for determining the cause of indications within the core. Such discontinuities as a crushed core, separated cells, and water in the core are easily found on a radiograph. The other bond test methods will be able to detect these, but are generally unable to identify the specific cause of the indication.

9.11.5 Delamination

Delamination between layers of a laminate structure is usually detected with bond testing or ultrasonic methods. Bond testers are generally the first choice due to inspection speed and easier interpretation. Experiments should be conducted since the success of the bond test will depend on favorable conditions concerning layer thickness, stiffness, and the size of the expected delamination. High frequency ultrasonic methods are normally used where bond test inspection proves inadequate.

Tap tests provide a quick and easy method to check for delamination using inspectors that do not require special NDI qualification. It is usually restricted to thin face sheets and is highly dependent on the characteristics of the particular material. Experiments should be conducted to ensure the change in sound quality between the acceptable area and delaminated area is readily apparent.

Penetrant inspection is not used since the discontinuity must be open to the surface. Eddy current, magnetic particle, and radiographic methods are not normally used due to problems with detecting laminar discontinuities.

9.11.6 Foreign Objects

Foreign object detection is usually done with visual or radiographic methods. Mirrors or boroscopes can be used to assist the visual search. In areas that are inaccessible or those that can't be visually checked, radiography is normally used. Experience is a key in this situation. The different densities of different objects within the view may result in normal items such as rivets that appear to float attached to nothing on the radiograph. Knowledge of likely foreign object migration routes can greatly reduce the area to be covered by the inspection.

9.12 Detection Limits

Each method has detection limits that restrict the use of the method. They have physical, electrical and chemical limits that are usually still more sensitive than the practical limits established. The practical limits are based upon guidelines which

evaluate many factors such as the part being inspected, the sensitivity of the equipment, and the inspection environment itself. Each section will discuss general guidelines to the detection limitations encountered with each method. Section 9.13 discusses the general access requirements for each method.

9.12.1 Probability of Detection Plot

A plot of the ratio of discontinuities found to those present versus the discontinuity size is referred to as a probability of detection plot (POD). These plots can be used for a number of purposes including setting inspection intervals and discontinuity detection limits. Quite often empirical data and models are available from a number of government and private organizations. The following describes the general process toward developing these plots.

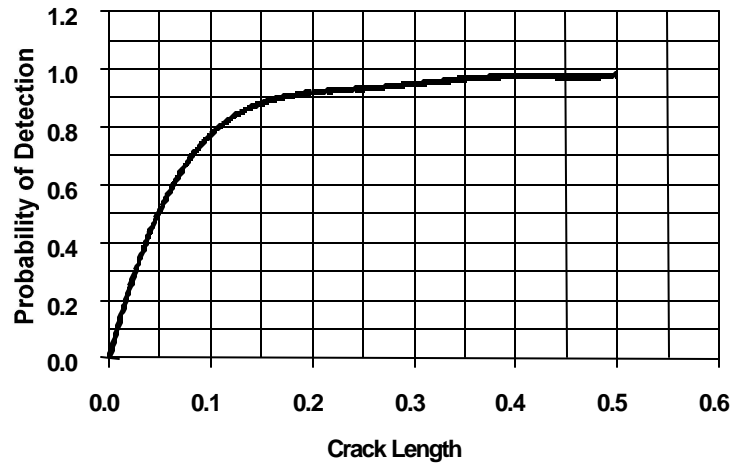
9.12.1.1 Development

The process to develop a POD for an inspection procedure consists of four basic steps. A large number of reference parts are constructed with discontinuities of various known sizes. These parts are then processed through the proposed inspection technique by the target inspectors. The results of the inspections are recorded.

An example of a generic POD plot is presented as Figure 9-20. For this example, the requirement is to be able to find the required minimum discontinuity size in at least ninety percent of the inspections. For this plot, a minimum crack length of about 0.17 inches is needed to achieve ninety percent probability of detection for this particular inspection.

FIGURE 9-20

GENERIC EXAMPLE OF POD PLOT



9.12.1.2 Influences and Limitations

There are a number of factors that influence the results recorded on the POD plot. The number of discontinuities used must be large enough to show the true distribution of discontinuities detected versus those missed. The distribution of discontinuity sizes used must be large enough to avoid extreme interpolation of the data line.

There are also a number of limitations that affect the use of the POD plot. The plot is part and material specific. For example, the crack detection plot for a certain alloy of steel inspected using a magnetic particle method is not necessarily the same plot when transferred to a different steel alloy. The plot is specific to the inspection conditions presented. For example, inspecting the reference part on a workbench may present different results from the same inspection done overhead on an aircraft. The plot is operator specific. The inspection results will vary based on the skill level of the inspectors. The plot is also procedure specific. For example, a plot representing one method of penetrant may not be transferable to the use of another type or brand of penetrant. Last, the plot is quality control specific. As an example, it will vary greatly between a test accomplished within quality control parameters and one conducted outside quality control parameters.

9.12.2 Visual Inspection

9.12.2.1 Equipment Influence

Magnifiers can greatly enhance visibility of discontinuities in the inspection process. They can also be instrumental in determining whether there is a crack or a scratch. Magnifiers do present accessibility problems that will be discussed in Section 9.13.

As presented earlier, the boroscope allows visual access to very remote areas of the aircraft. The two major influences are the distance from the inspection surface and the location of the boroscope. It is often very difficult with limited visual cues to determine the distance from the inspection surface. If the surface is farther away than the inspector believes, this may make discontinuities appear much smaller than their actual size. Similarly, if the boroscope is much closer than thought, the discontinuity becomes much larger than the actual size. The other problem is locating the inspection surface. If the area has a complex path to the inspection surface, it may prove difficult to locate the area of interest. It may take great concentration and skill to maneuver the flexible boroscope to the required location.

9.12.2.2 Part Influence

The major part influence is the surface condition. It must be cleaned to ensure that discontinuities are not hidden under dirt or debris. Another factor is the condition of paint or other coatings. Some of these are designed to stretch as part of their thermal cycle. In this situation, smaller discontinuities may not cause enough stress to affect the paint or other coatings in ways such as cracking or bubbling.

9.12.2.3 Environmental Influence

The physical environment will greatly influence detection. Lighting is the main factor. General lighting conditions alter the apparent contrast between the discontinuity and the surroundings. Shadows or glare can hide discontinuities. Lighting needs to be bright and even, but without glare. It may also be positioned to enhance shadows or reflections that may help locate discontinuities. There are situations where detection is largely a matter of interpretation. The inspector will see what his experience and prejudices dictate.

9.12.3 Penetrant Inspection

9.12.3.1 Equipment Influence

The three major influences are the penetrant, the developer, and the ultraviolet light. The penetrant must be kept under proper quality controls and used for inspection as intended. Some studies have claimed an increase of 100 times in the visibility of a crack using fluorescent penetrant versus a normal visual inspection. The developer

must be properly used. It must be thick enough to draw out the penetrant, but thin enough for the penetrant to get to the surface. The ultraviolet light should be of the proper wavelength to cause penetrant fluorescence and intense enough to make the fluorescence visible. Ultraviolet lights not within quality control parameters can significantly decrease the visibility of an otherwise detectable discontinuity.

9.12.3.2 Part Influence

Three of the major part influences are material blocking the discontinuity opening, proper cleaning, and material porosity. Any material that blocks the opening to the discontinuity will significantly decrease detection probabilities. The discontinuity must be open to the surface for penetration to occur. Chemical etching can be used to open the discontinuity. Care should be taken to ensure that etching does not adversely affect the part.

Proper cleaning is vital. Again, the defect has to be open to the surface for penetrant inspection. Mechanical cleaning methods should be avoided as practical. Material freed by the cleaning may be deposited inside the discontinuity. These methods also can create a visible indication because of roughing the surface.

Material porosity can increase the minimum detectable discontinuity. A porous surface will cause a speckled appearance to the inspection. This may mask indications. It may also hide very small indications since the inspector may interpret this as more porosity.

9.12.3.3 Environmental Influence

Penetrant inspection chemicals are generally designed to work within a specific temperature range. Fluorescence and viscosity may be adversely affected when used outside this range. When using aerosol cans, humidity and cold may result in damp or icy conditions on the inspection surface.

As discussed in Section 9.4, penetrant inspection materials may react with or adversely affect the material tested. Care must be exercised to ensure the correct penetrant is used. The inspection technique should also clearly identify any concerns or problems.

9.12.4 Magnetic Particle Inspection

9.12.4.1 Equipment Influence

The three major inspection influences by the equipment are the type of current applied, the method of particle application and amount of current. The type of current refers to alternating or direct current. Alternating current is best for detection of surface discontinuities and has very limited application toward subsurface ones.

Direct current is slightly less effective at surface discontinuity detection, but is vastly superior for subsurface application.

Particle application refers to the choice between the continuous and the residual methods. In the continuous method, the particles are applied when the magnetic field is at its most intense. In the residual method the particles are applied after the current is removed. This method allows inspection of large numbers of parts quickly as the magnetization and inspection are separate events. However, the magnetic characteristics of the part must be such that an adequate magnetic field is present after the current is removed.

There are general guidelines and formulas that provide a starting point for determining the amount of current needed to produce an indication. These are not specific to any particular type of metal, and operator experience will be the major factor. Enough of a magnetic field must be present to produce an indication. Too much current will produce a confusing background that may mask relevant indications. Quality indicators can be used to check for an adequate magnetic field.

Of course, the magnetic particles and ultraviolet lights are important. They should both be used within their quality control parameters. Particles without sufficient fluorescence capability or ultraviolet lights without sufficient output will significantly increase the size of the minimum detectable discontinuity. Magnetic particles that have already been magnetized before application will have little ability to migrate toward a discontinuity site.

9.12.4.2 Part Influence

Several part characteristics influence the inspection. The most important of these are the magnetic characteristics. The ability to be magnetized and to hold that magnetic field greatly influences the amount of current that must be applied. Sharp corners, radii, and other geometry features of the part will also affect inspection.

The characteristics of the discontinuity will influence detection. Magnetic particle inspection is not adequate for detection of laminar type discontinuities. It is optimized for detecting those with the major axis perpendicular to the direction of the magnetic field. It may take several inspections to adequately cover the part in the case of multiple defect directions.

9.12.4.3 Environmental Influence

Magnetic particle inspection should not be performed in a wet environment. This will have an adverse effect on particle flow and indication formation. A thorough clean up must occur after inspection. The particles and their carrier fluids may promote corrosion in certain alloys. If left to dry, particles and carrier fluids can present a general fluorescent background that may interfere with future inspections.

9.12.5 Eddy Current Inspection

9.12.5.1 Equipment Influence

The two major equipment influences are the probe and the parameters set for the inspection. The major probe influence is the probe diameter. This can be roughly equated with sensitivity. A general rule is that the expected discontinuity should disrupt about half the total coil field. This is to ensure the disruption produces an obvious response from the instrument. With the shielded probes used for aircraft inspection, the coil field diameter is roughly the diameter of the coil itself.

The most important parameter for the inspection is the frequency used. This affects both the sensitivity of the inspection and the depth of penetration. As a general rule, the higher the frequency, the higher the sensitivity to smaller discontinuities. This also increases sensitivity to other material characteristics that may comprise the signal. Higher frequencies also result in less depth of penetration under the surface. This relationship can be shown through

$$\delta = 1.98 \sqrt{\frac{\rho}{f\mu_r}} \quad \text{or} \quad f = \frac{3.92\rho}{\delta^2\mu_r}$$

where:

- δ = Standard depth of penetration (inches).
- ρ = Material resistivity (Ohms).
- f = Operating frequency (Hertz).
- μ_r = Relative permeability (1.0 for non-ferrous materials).

Again, this should be considered as a starting point. Experiments may be necessary to confirm detection since this determines the frequency necessary to reach the required depth, but indicates little about the exact size of a discontinuity that can be detected at this distance. It should be noted that increases in the magnetic characteristics (permeability) and the conductivity (reciprocal of the resistivity) of the material will also decrease the depth of penetration.

9.12.5.2 Part Influence

Many part characteristics can influence the size of the minimum detectable discontinuity. Scanning near part edges can present problems. Edges create a signal response similar to that of a crack indication. Scanning near edges requires proper technique to avoid confusion between relevant and non-relevant signals. The material thickness can be an influence. If the part is rather thin or changes thickness abruptly, the eddy current instrument may react. Scanning in a radius can present problems if proper techniques are not followed. Probe lift off can reduce sensitivity. This was defined as the distance from the probe to the part surface. Thick paints or

other coatings have the effect of reducing inspection sensitivity. Surface damage can cause significant problems. This is particularly important when scanning for subsurface discontinuities. Gouges or rough surfaces may mask relevant indications.

9.12.5.3 Environmental Influence

One of the chief environmental influences is the position of the inspection surface relative to inspector. Working overhead or in cramped conditions can add a significant fatigue factor to the inspection. An area without direct visual contact can also affect inspection as the inspector must feel the inspection and has few options to confirm or size any discontinuity found. Other errors such as scanning away from the area of interest and tilting the probe may result in this situation.

9.12.6 Ultrasonic Inspection

9.12.6.1 Equipment Influence

The piece of equipment that most influences the inspection is the transducer. It does this through the operating frequency and the crystal diameter. A general rule for crack detection is that the smallest possible detection size is approximately half the wavelength of the sound pulse. For example, a 2.25 MHz frequency in aluminum will result in a wavelength of approximately 0.11 inches. Therefore, the smallest detection size is about 0.05 inches. Naturally, other factors will increase this result. Another rule is that for disbonds or delaminations the discontinuity should be at least approximately half the diameter of the transducer. As a rule, raising the frequency increases the sensitivity, provides better resolution, but decreases the penetrating ability. Both the frequency and the diameter influence the beam divergence. However, at the distances found in most aircraft inspection, this is usually not a major problem.

9.12.6.2 Part Influence

The major part influences are the geometry, the surface roughness and internal attenuation. With respect to geometry, the primary concern is providing a clear path for the sound energy to reach the inspection site. Another concern is other features that may be in the immediate area of the inspection. Each of these may cause confusing signals, mask discontinuities from detection or make inspection impractical.

Surface roughness can affect the inspection in several ways. The primary two are high surface noise and entrapped air. A rough surface may cause some attenuation or reflection of the sound pulse. This will reduce the amount of energy reaching the part. In the case of reflection, it may mask discontinuities within the noise caused by

the condition. A rough surface may trap air bubbles in the couplant. A rough surface may also cause the transducer to come uncoupled with the part. All of these may be mistakenly interpreted as attenuation within the part or as a discontinuity.

Internal attenuation reduces the effectiveness of the inspection. The two primary causes are the material grain size and interfaces. The material grain may require that the frequency of the transducer be reduced to achieve the necessary penetration. Interfaces can be major attenuation factors. Some sealants or adhesives can have such high attenuation factors that they do not allow for the practical transfer of the sound energy to the far side of the interface. An example is attempting to penetrate into a wing spar through the skin with a layer of sealant between the two. Another is an inspection through a bond line made with a particularly porous adhesive material.

9.12.6.3 Environmental Influence

The primary environmental concern is the condition of the part surfaces. The surface where the transducer will be located needs to be free of loose material such as paint. A loose paint layer or other such material will block penetration of the sound pulse into the part. Surface gouges or other large discontinuities may cause interfering signals. This would be particularly true in an inspection of the far surface of a part. The inspector may have difficulties interpreting non-relevant surface indications in areas where visual confirmation is not possible.

9.12.7 Bond Inspection

9.12.7.1 Equipment Influence

For those based on eddy current or ultrasonic methods, the guidelines stated for that method also apply here. The usual difference is that larger diameter probes are used to reduce response to localized conditions.

For those using the tap methods, the primary influence is the inspector. The pace, force applied and the technique of the tapping can affect the quality of the response. For example, resting a hand on the inspection surface can act to dampen the surface response.

9.12.7.2 Part Influence

The use of the larger probe makes the inspection sensitive to part curvature. Scanning along curvatures leads to probe wobble and false instrument response. The primary cures for this are to use a smaller probe near curvatures or to switch to a method that allows smaller probes. Edges or areas with underlying structure can alter instrument response.

9.12.7.3 Environmental Influence

Environmental influences also follow the guidelines stated for the eddy current and ultrasonic methods. The primary concern is rough surfaces and loose coatings. Each may mask indications or create unacceptable background noise.

9.12.8 Radiographic Inspection

9.12.8.1 Equipment Influence

The control box settings used for the shot parameters can have a significant effect on the quality of the radiograph. The wrong combinations of voltage, current, and time may have the effect of decreasing the ability of the film to show smaller density differences. The primary counter to this problem is to use quality indicators. These are small plates that have holes which represent specific density differences within the part. The ability to discern the different holes can be used as an indication of the quality of the radiograph. Unfortunately, it is often impractical to determine the exact thickness of the material under test on a field aircraft inspection. Geometry may make the placement of quality indicators of little value.

The radiation beam expands as it moves farther from the tube similar to a flashlight beam. The area that can be imaged at one time is directly related to the distance from the tube to the inspection surface. However, radiation intensity is inversely related to distance. Thus, increasing the distance to increase the area of coverage also increases the time needed to expose the film.

Film selection affects the detection probability. The grain size of the silver bromide used in the film emulsion determines the size of the smallest object that can be imaged. Slower speed films tend to be made from smaller grains. This results in greater sensitivity. Faster films use larger grains to speed image development. This increases the size of the smallest detectable object relative to the slower films.

9.12.8.2 Part Influence

The general rule is that a good radiographic technique should be able to show a film density difference of two percent. This translates to a total change in material thickness of two percent. It says nothing about the length of the discontinuity. The other problem is the need for a two percent difference in the thickness regardless of the orientation of the discontinuity to the thickness. This can be considered the minimum that is generally practical to obtain.

For example, the radiographic inspections of a spar cap 0.250 inches thick for a crack. This suggests a minimum crack depth of 0.005 inches. Unfortunately, with the film on one side of the wing and the tube on the other, one must add two skins of 0.063 inch thickness for a total of 0.376 inches of material. Now, the crack depth

has risen to 0.008 inches deep which is now three percent of the spar cap thickness. If it is not possible to aim the tube to avoid the other spar cap, an additional 0.250 inches of material is added to total 0.626 inches. This presents a crack of 0.013 inches deep or five percent of the spar cap thickness. It would be up to the structural engineer to use crack modeling techniques to determine the typical lengths associated with these crack depths in the given material.

Unfortunately, both the general rule and the example represent an ideal condition. They assume a perfect vertically oriented crack and that all the materials have the same radiographic characteristics. Table 9-1 presents the effect of angling the crack relative to the radiation beam on the probability of detection for this idealized situation. The type of discontinuity will also affect detectability. Many laminar type discontinuities such as disbonds may not present a large enough change in film density to ensure detection. The preferred discontinuity is one that has its major axis located parallel to the radiation beam.

TABLE 9-1

CRACK ANGLE EFFECT ON DETECTION PROBABILITY

Beam to Crack Angle	Probability of Crack Detection
0°	96%
3°	89%
6°	82%
9°	75%
15°	48%
21°	30%
27°	23%
45°	4%

Different materials such as sealant and paint can significantly affect the radiographic results. Places where two drastically different materials overlay each other such as steel and aluminum may make detection of small discontinuities in the less dense material virtually impossible. Material grain size will also effect the film quality. Steel is more difficult to radiograph as compared to aluminum.

9.12.8.3 Environmental Influence

The primary environmental influence is the ability to place the film as close to the inspection surface as possible. Distance between the object and the film results in a distortion effect referred to as “geometric unsharpness.” The radiation beam expands as it moves farther from the tube. This is also true inside the part and beyond the part. Misalignment of the radiation beam may result in the part being skewed to the side. Each of these alters the dimensions of discontinuities found on the film. They may also mask others from view.

Radiographic inspection can't be accomplished through most types of fuel. It has the effect of scattering the radiation beam. This will produce an effect such as might be seen when looking at an object at the bottom of a swimming pool. When

radiography is to be used in areas where fuel is located, the tank should be defueled prior to inspection.

9.13 Accessibility

Each method has accessibility limits to the area of interest for the inspector. Depending upon the method used, the inspector will require a certain amount of room in the inspection area to accomplish these tasks. General guidelines are presented for each method in this section.

9.13.1 Visual Inspection

There is a wide range of accessibility demands depending on the technique used. For the most basic, the area must be large enough to maneuver a light and for the inspector's eyes to get within a few inches of the inspection surface. Adding magnification, the area must accommodate the light, the inspector, and the magnifier. Boroscopes require adequate room for the viewer and a hole large enough for the shaft.

9.13.2 Penetrant Inspection

As has been mentioned, penetrant inspection involves the inspector applying, removing, and visually inspecting the area of interest. This process requires that the inspector be able to physically reach and move in the inspection area to perform these tasks. The removal and development stages will require the use of aerosol cans in this area. The method also requires a clean-unpainted surface. This will require adequate access to allow proper paint removal and surface cleaning.

Penetrant inspection requires the use of ultraviolet lights throughout the procedure. This requires enough space so that the inspector can be able to see the inspection site and maneuver the light to within a foot of the surface. These lights can reach 350° F at the bulb surface and are usually not sealed from the atmosphere. This precludes the use of a penetrant inspection in areas where flammable liquids or vapors may be present.

9.13.3 Magnetic Particle Inspection

Portable magnetic particle inspection equipment is rather bulky and rigged with power cords. It is therefore practical for use in areas that are at least large enough for someone's shoulders to fit. In addition ultraviolet lights are needed for inspection. The same problems apply to these as did for the penetrant inspection. Aerosol cans are used for the magnetic particles and cleaning. Adequate ventilation is required for the safety of the inspector.

9.13.4 Eddy Current Inspection

The primary access requirement for this method is that the inspector be able to reach the area of interest. Depending on the probe configuration, a straight probe is usually less than a quarter inch diameter and extends two or three inches high. A right angle probe is usually an inch high and extends three or four inches to the side. As probe frequency decreases, the general trend is to also increase the diameter of the coil. Therefore, low frequency inspections will require more space than high frequency inspections.

While this would seem to allow inspection in rather tight areas, other factors need consideration. If the size of the discontinuity needs to be determined, the inspector must be able to reach the area with the probe and with a marker at the same time. This will also require the inspector to have visual contact with the area of interest.

9.13.5 Ultrasonic Inspection

The primary access requirements for this method are essentially the same as those for eddy current inspection. The inspector must be able to reach the area of interest. Most longitudinal transducers have a contact surface size of less than half an inch diameter. Extra room needs to be allowed to maneuver the probe in the area of interest. Since inspections will require some type of couplant, the inspector will be required to apply and remove it. Another factor might be the need for access to opposite sides of the part depending on the method of inspection desired.

While this would seem to allow inspection in rather tight areas, other factors need consideration. If the discontinuity size needs to be accurately determined, the inspector must be able to reach the area with the probe and with a marker at the same time. This will also require the inspector to have visual contact with the area of interest.

9.13.6 Bond Inspection

Accessibility for bond testing depends on the method being used. Methods based on eddy current or ultrasonic techniques have the same accessibility needs as described above. The probe size is usually larger, quarter to half inch, than would be used for something such as crack detection. The inspector will need adequate space to mark the limits of any discontinuities found.

Methods based on tap testing techniques require an open area. The inspector will need room to swing the tap hammer. A minimum of surfaces for the sound to echo from is desirable. This eliminates sound interference that may mask discontinuity indications.

9.13.7 Radiographic Inspection

The main accessibility concerns for radiography relate to film and tube placement. The film should be placed as close to the area of interest as possible and parallel to the surface being inspected. Enough space must be present to place the film. The tube is placed on the side opposite to the film and generally perpendicular to the surface being inspected. A rather small tube will occupy an area of at least a six-inches in diameter and two feet long. In addition, cooling and control cables will be connected to the tube. To achieve the necessary distance between the tube and film, tube placement in the interior of the aircraft is generally limited to larger areas such as the cabin or cockpit.

9.14 Creating a Field Inspection

The NDE process is not finished once the size of the detectable discontinuity, C_{det} , has been found. Once the final inspection interval and discontinuity size has been established, the NDI technique must be transformed for field use. Creating a field technique is the result and must be kept in mind during the entire development process.

9.14.1 Cost

The cost of the inspection must be considered. It is to the manufacturer's advantage to reduce the cost of maintaining the aircraft to the customer. NDI inspections can be one of the more costly items in a maintenance program. These are intended as general guides and not specific to a particular type of inspection.

The least expensive is the visual inspection. No equipment is usually involved, and little to no consumables are needed. In addition, there is usually no NDI qualification required of the inspector. Adding complex magnifiers or boroscopes will add to the cost.

The eddy current inspection ranks next. Ignoring the purchase price of equipment, it involves little time, and no consumables. The major advantage over the other surface discontinuity detection methods is the need for little to no part preparation. This method does require NDI certified personnel. Bond testers based on eddy current methods also fall into this rank. Of course, adding requirements for an instrument with a CRT, automatic bolt hole scanners or for special reference standards can add significantly to the cost.

Magnetic particle inspection is next. The equipment is rather inexpensive and the inspection is usually rather quick. However, paint removal, surface preparation and repaint, if required, involve some time and consumables. Clean up needs to be thorough to prevent corrosion problems and contamination of future inspections. Personnel require NDI certification.

Penetrant inspection is the next most expensive. While the equipment is rather inexpensive, it is one of the most time consuming methods. Paint removal, surface preparation and repaint involve some time and consumables. The inspection process contains several waiting periods for chemical dwells and can use many consumables. Clean up needs to be thorough to prevent reaction with other materials and contamination of future inspections. Inspectors require NDI certification.

Ultrasonic inspection is next. The equipment can be somewhat expensive. Special reference standards may be required which can add significantly to the cost of inspection. Personnel require NDI certification. For complex situations, the method is dependent on the interpretive skills of the inspector. Discontinuities may not be able to be confirmed without destructive tests. Inspection of large areas can be very time consuming. Bond testers based on ultrasonic techniques are less expensive and the inspection situations much less complicated.

Radiographic inspection is the most expensive of the inspection methods. The equipment is expensive. The personnel involved require medical monitoring, periodic training and are usually subject to government regulation. Generally this is the most time consuming method considering set up, tear down, and film development. An additional consideration is bystander safety. During the inspection, no other personnel will be allowed in the area surrounding the aircraft. Finally, the method is dependent on the interpretation skills of the inspector. Discontinuities are not usually confirmed without disassembly.

9.14.2 Reference Standards

The need for special standards can add significantly to the cost of an inspection. It is preferable that reference standards be of types that are in widespread field use. This will increase the number of facilities that are available to the aircraft operator at inspection time. Many inspection situations will require a specially constructed reference standard.

Visual, penetrant, radiographic and magnetic particle methods do not usually require a reference standard. In the case of penetrant, radiography and magnetic particle methods, quality control tests and quality indicators are used to ensure the quality of the inspection. Boroscope inspection may need photographs or a model to clarify what the inspector will see if the situation is complicated.

Eddy current, ultrasonic and bond test methods usually require some type of reference standard. The two options usually considered are to select an aircraft feature that produces a response similar to that required or to use a standard specific to the inspection. Using an aircraft feature eliminates the need for a special standard. However, the consistency of this feature from one aircraft to another must be considered. The instrument response from the feature would represent the

normal condition for the inspection. The discontinuity signal would then be described based on the normal condition signal. Usually, a standard specific to the inspection will be desired. Generally, these standards are not such that they may be built by the field inspectors. This insures consistency from one standard to another. Again, it is preferred to keep the complexity low in order to reduce construction time and cost. Discontinuities of the type to be detected and at the minimum size will be introduced at the expected location.

For the eddy current method, surface crack detection generally uses a surface or bolt hole reference standard that is widely available in the field. Subsurface inspections or a complex geometry will require a standard that specifically duplicates the inspection.

For the ultrasonic method, the majority of inspections will require a reference standard specific to the inspection situation. Several standards are widely available in the field. The usual situation is that some factor will dictate the use of a standard specific to the situation.

Bond testing will also required specially constructed standards. These should match the inspection situation as closely as possible. Depending on the size and tolerance of the expected discontinuity, this may be as simple as cutting a hole in the adhesive sheet before building up a honeycomb standard. Others may be more complex if the discontinuity to be detected is rather thin or small.

9.14.3 Method Availability

A further consideration in selecting an inspection method is the availability of the inspection method to the customer. Eddy current, penetrant and magnetic particle methods are usually readily available to the maintenance facility. Ultrasonic methods may be limited if there is a need for special transducers or reference standards. Radiographic inspection facilities may be limited in areas where the general work load does not justify the expense to the NDI facility to maintain this method.

10.0 SID Development

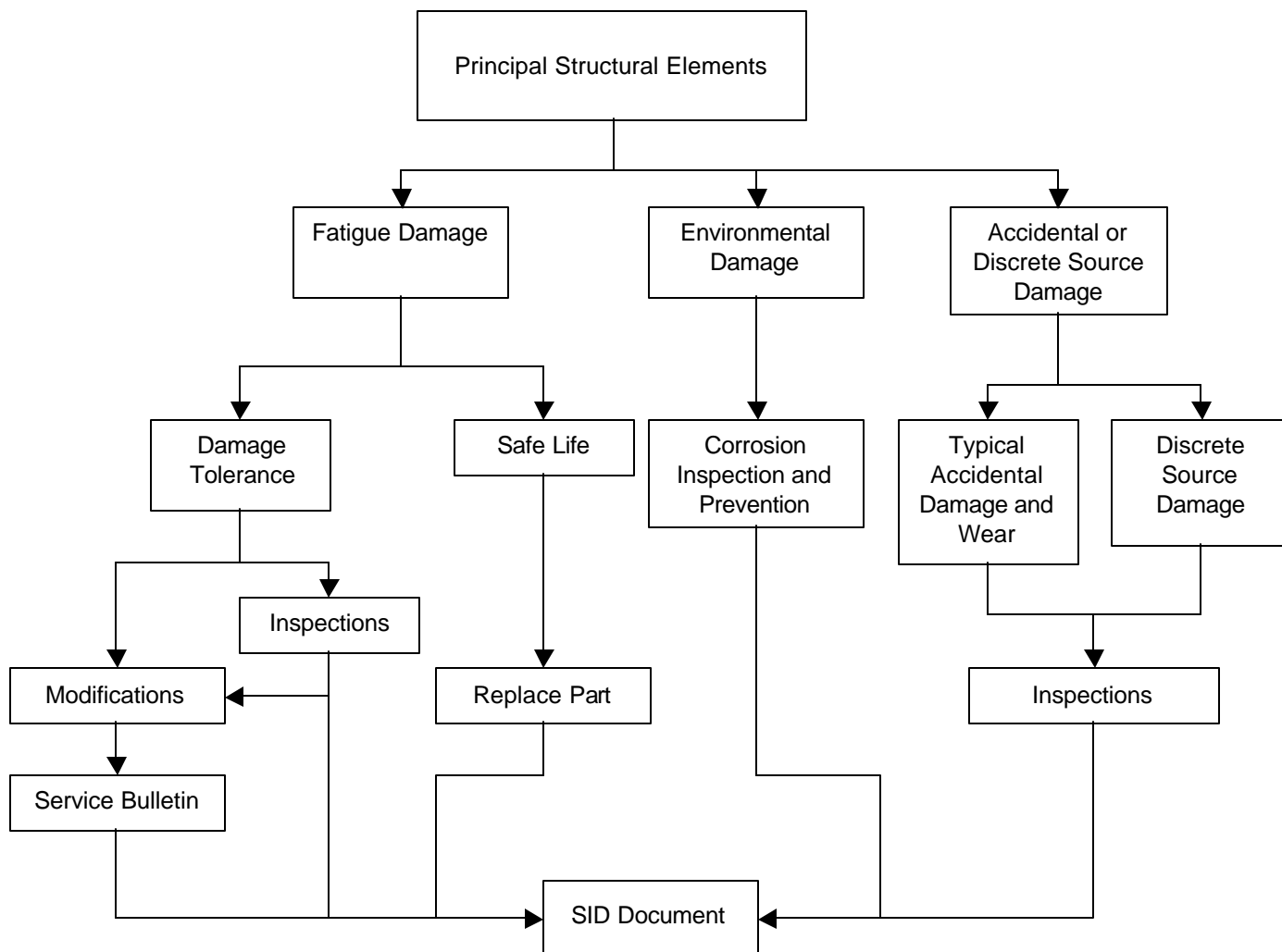
While Sections 3 through 9 provided guidelines for gathering data, performing the damage tolerance analyses and then setting appropriate inspection intervals, this section outlines the development of the SID itself, both in terms of determining appropriate action items, and the recommended formatting and documentation of the SID.

10.1 Developing a SID Document

This section outlines how the results of the analyses described in Sections 3 through 9 are used to determine the appropriate field action to be published in the SID document. A flowchart of the SID Document development process is presented in Figure 10-1.

FIGURE 10-1

SID DOCUMENT DEVELOPMENT FLOW CHART



10.1.1 Intent of SID Document

The SID is the document that defines the continued structural integrity program. The intent of the SID is to supplement the existing maintenance program. Therefore, before writing the SID document, a review of the existing maintenance program is required to determine the areas where the existing maintenance program is lacking as a result of the damage tolerance analysis. Also, if a CAP (Continued Airworthiness Program) or other inspection document has been written for the airplane, the contents of the CAP or other inspection document should also be reviewed. The SID at a minimum must include the damage tolerance based inspections and procedures needed for continued safe operation of the airplane. In addition, AC 91-MA "Continued Airworthiness of Older Small Transport and Commuter Airplanes; Establishment of Damage-Tolerance-Based Inspections and Procedures" recommends that the SID include the following:

- Special inspections to determine the condition of the airplane at the time of initial implementation of the continued structural integrity program.
- Descriptions of repairs and/or modifications needed to operate the airplane for the duration of effectivity specified in the continued structural integrity program.
- Listing of optional replacement components that may be installed to reduce, delay or eliminate specific damage tolerance based inspections and/or modifications.
- Modifications of the airplane to provide access to accomplish, or to reduce the need for the inspections of bullet 1 above, or to provide access to accomplish the necessary damage tolerance based inspections and procedures.
- A review of the repairs and modifications to assess their structural integrity and damage tolerance.

The structural integrity program must be adequately defined in the SID and presented in an effective manner. The SID document needs to contain field action items for:

- All structural components identified as PSEs based on the criteria discussed in Section 3.0. This includes all locations identified as the critical areas that were analyzed as well as those that were not analyzed due to similarity of structure. In addition to a directed NDI inspection (other than visual) of a specific component, a visual inspection of the entire component or area should also be incorporated into the SID.
- Structural components that were not classified as PSEs, but are critical to flight safety. Examples include control surface hinges, wing spoilers and speed

brakes. These items should be listed in the SID document if they are not appropriately addressed in the aircraft maintenance manual.

- If a CAP document (or other inspection document) exists for the airplane, the contents of the CAP, or other inspection document that apply to structural components, should be incorporated into the SID document if these components are not already addressed.

Any inspection intervals published in the SID must be given both in terms of usage (hours or landings) and calendar time. The calendar time limit is essential to detecting environmental damage, such as corrosion, which increases as a function of calendar time, not usage.

The completed SID needs to clearly state what aircraft (Model and Serial Number or Serial Number Range) it applies to. Furthermore, if STCs have been issued for a given aircraft, it is the responsibility of the holder of the STCs to perform damage tolerance evaluations of the STCs, and to determine the required inspection programs. In most cases the aircraft manufacturer (or SID writer) does not have knowledge of the STCs. The inspection programs for the STCs will also need to be included in the SID. Also, if multiple airplanes have received a specific modification or repair, then a damage tolerance evaluation of the modification/repair will need to be completed, and the resulting inspection requirements will need to be documented in the SID.

The SID is intended to be a dynamic document that should be revised when additional information resulting from the inspections or other new information becomes available. The SID should also provide a means to provide feedback from the operator to the aircraft manufacturer (or SID writer) about problems encountered in carrying out the inspections, modifications and repairs detailed in the SID.

The recommended program along with the criteria used and the basis for the criteria should be submitted to the FAA Aircraft Certification Office. Any revision to the SID criteria should also be submitted to the FAA for review and approval.

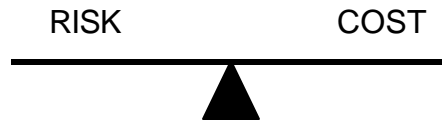
10.1.2 Considerations in Preparing the SID Document

The results from the damage tolerance analysis completed as described in Section 8.0 must be incorporated into the SID document. At this point economic factors must be considered. The risk to the airplane must be balanced against the cost of inspections/repair. Operators strive to spend the minimum amount of money to meet operational requirements at the minimum risk level. On the other hand structures engineers strive to eliminate all risk at any cost. Accomplishing the minimization of risk with the minimization of cost can be a very complex balancing act. Overemphasizing either side brings the optimal solution out of balance (Figure

10-2). The questions must be asked, 'Is it cheaper to modify the aircraft than inspect it?', and 'When should an aircraft be salvaged instead of repaired/rebuilt?'

FIGURE 10-2

BALANCING RISK VS. COST



From the analytical results, the best method of inspection needs to be determined as described in Section 9.0. The resulting initial and recurring inspection intervals should be reviewed to see if these intervals make economic sense. Inspections can be costly especially if analysis shows the inspections must be repeated frequently. If inspections do not make economic sense then other options need to be considered. In deciding on the appropriate field action for a given structural component the following issues need to be considered:

- 1) Is the area to be inspected easily accessible? If no, then consideration should be given to designing/modifying access covers and inspection plates to facilitate access to the area to be inspected.
- 2) If the inspection intervals are unacceptably short, or the area is completely uninspectable, then alternative solutions need to be explored. Examples are:
 - Adding straps or doublers (which are easily inspectable) to reduce the stress levels in the component, and making the strap/doubler more critical than the component itself (refer to Section 3.3.3.2 on "Multiple load path structure – not inspectable for less than load path failure"). New inspection requirements for the modified structure will need to be determined.
 - Replacing the component with a new part, and declaring it a safe-life part that will require replacement at the end of its published safe-life.
 - Replacing the component with a new component that has improved damage tolerance due to improved material or design details. The inspection interval would then be based on the damage tolerance analysis of the new part. Sometimes changing the alloy of the part will be enough to gain the desired results. However, care must be taken to avoid contact of dissimilar metals.

- Cold-working the fastener holes in the component. Cold-working generates permanent compressive stresses around the holes which retard crack growth and therefore extend the inspection intervals. Additional analysis to calculate new inspection intervals must be completed to include the effects of cold-working (Section 8.1). Before concluding that cold-working is a viable option, however, consideration must be given as to whether or not it is possible for a crack to start at the edge of the component and not grow through a fastener hole. In this situation the component could fail before the next inspection based on cold-working would occur. As a result, inspection intervals would have to be based on an edge crack and cold-working would not result in the desired extended inspection intervals.
- 3) If it is not feasible, both technically and economically, to modify/repair the component to reduce the number of recurring inspections, then the component needs to be replaced.
 - 4) If the WFD evaluation outlined in Section 8.7 shows that a PSE is susceptible to WFD damage, an inspection program will not be feasible. Alternatives, such as straps, doublers or component replacement need to be evaluated.
 - 5) If the necessary inspections, modifications, and repairs and/or replacements cannot be economically justified then the aircraft will no longer be able to operate under 14 CFR Part 121, 129 or 135 rules and should be retired from service.

Once a required modification, repair of component or replacement is decided upon, a service bulletin is the recommended way to implement the changes. If a service bulletin is issued as a field action item, it must be referenced in the SID.

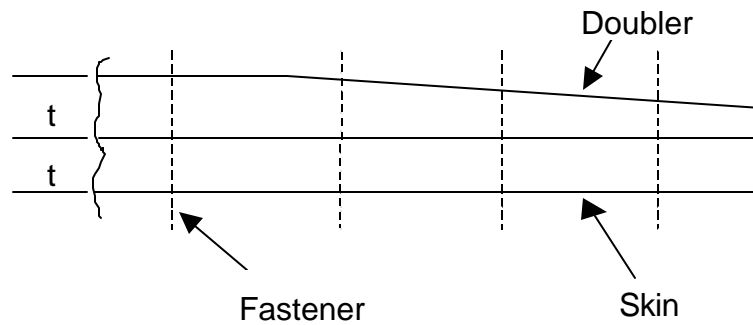
Any modifications or repairs that are made to components need to undergo a static strength as well as a damage tolerance analysis to determine the appropriate inspections. In the past, airframe repair has been based on static strength without consideration of fatigue. This led to a design with considerable static strength but considerable loss in fatigue quality as compared to the original structure. Some things that can be done to improve the damage tolerance aspects of the repair are:

- Taper the repair doubler (Figure 10-3). A repaired structure is sensitive to the doubler thickness and the magnitude of the end (first) fastener load. Several configurations should be analyzed to obtain the critical fastener load for a variety of skin and repair doublers as shown in Figure 10-4.
- Improve inspectability. Any repair doubler will decrease the inspectability of the component being repaired. This is especially true for fuselage skins in a pressurized cabin. Skin cracking at the first fastener will be hidden externally by the doubler (Figure 10-4a,d). The inspectability can be improved by placing the secondary doubler inside and the primary doubler outside as shown in Figure

10-4b,e. Adding “fingers” to the doubler as shown in Figure 10-4c,f, will improve the residual strength of the repair in the presence of MSD.

FIGURE 10-3

SKIN WITH A TAPERED DOUBLER

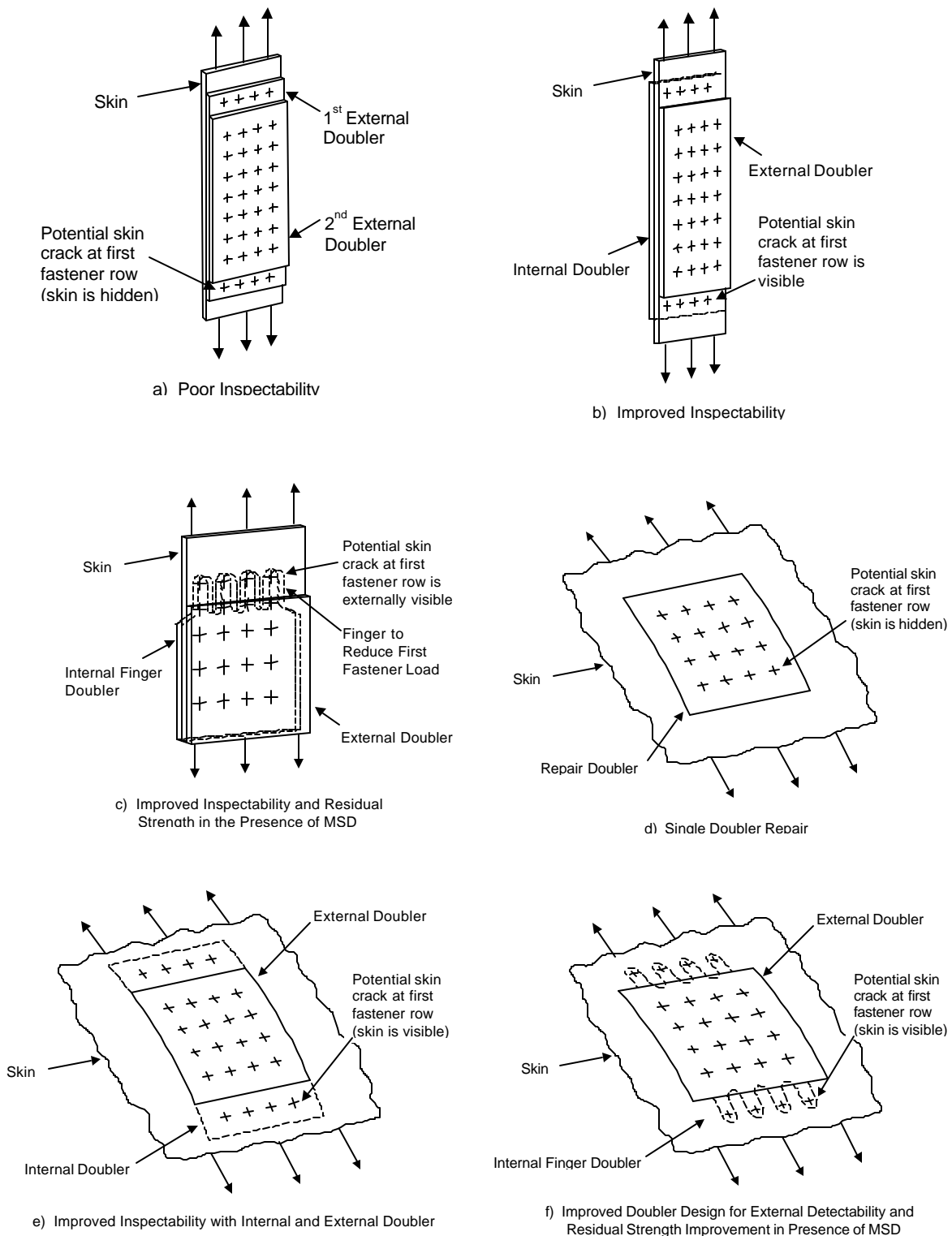


Structural degradation in aging aircraft occurs not only due to fatigue cracking, but also because of environmental effects, such as corrosion, stress corrosion cracking and corrosion fatigue and because of wear, accidental damage and discrete source damage. Therefore, the action items listed in the SID must also include:

- Items related to the corrosion protection plan for the aircraft (such as inspections and repairs/modifications for corrosion damage), and
- Field action items related to wear, accidental damage and discrete source damage (such as general inspections of safe-life parts like landing gears).

FIGURE 10-4

IMPROVEMENT OF FATIGUE LIFE AND INSPECTABILITY



10.2 SID Handbook Format

Reference 100, "Specification for Continuing Airworthiness Program (CAP)" describes in detail suggestions for the format requirements of a Continuing Airworthiness Program. The CAP was intended to be a supplement to the airplane's maintenance manual. It was developed in response to the FAA Advisory Circular 91-60, "The Continued Airworthiness of Older Airplanes", and Advisory Circular AC 91-56, "Supplemental Structural Inspection Program for Large Transport Category Airplanes." These circulars provide specific information regarding continued airworthiness requirements for the manufacturer and aircraft operator. The latest FAA Advisory Circular that deals with smaller aircraft is AC 91-MA: "Continued Airworthiness of Older Small Transport and Commuter Airplanes; Establishment of Damage-Tolerance-Based Inspections and Procedures." The CAP document closely adheres to the inspection program requirements and documentation defined in AC 91-56 and AC 91-MA.

Therefore the CAP format can easily be adapted for a Supplemental Inspection Document (SID). This format is recommended to develop an industry standard for Supplemental Inspection Documents. If a company format is used, the format and layout should follow the format outlined in this document as closely as is practical.

10.2.1 Physical Requirements

Section I of Reference 100, describes the physical requirements of a CAP document. These requirements should be used in developing the SID document. Some of the recommended physical format requirements are summarized below.

1. **Binder Type and Page Size** – The type of binder used needs to consider the fact that the document must be easily revised. Common page sizes should be used.
2. **Paper, Printing and Type Size** – White paper of sufficient weight should be used to eliminate bleed-through when printed on both sides. Use a method of printing that results in an image that is suitable for reproduction. The basic text should be 10 or 12 point type. Use 14-point uppercase bold for the word **WARNING** and 10-point uppercase bold for the **WARNING TEXT**. Use 12-point uppercase bold for the word **CAUTION** and 10-point uppercase for the **CAUTION TEXT**. Use 10-point uppercase bold for the word **NOTE** and 10-point mixed case for the note text. Captions should be distinctive in size or style or both. Type style is determined by the document producer.
3. **Page Identification** – Number the pages containing only one section in sequence. Section 1 should be numbered 1-1, 1-2, etc. while Section 2 will be numbered 2-1, 2-2, etc. The page number should be printed in the lower right corner of the page of odd pages and in the lower left corner of the page of even pages. The date of issue or revision should be printed in the lower left

corner of odd pages and in the lower right corner of even pages. Blank pages should be identified by printing “This page intentionally blank” or else identified by dual page numbering on the preceding page [for example, 3-3 (3-4 blank)].

4. **Copy Standards** – Text may be presented in one or two column format. Warning, cautions and notes may be highlighted. Both sides of the paper should be used. New sections should begin on the right hand page. The SID writer’s masthead, publication title, airplane model and date of issue or revision must appear on all pages.
5. **Identifying Revised Material** – Revisions should be identified by a vertical black line along the outside of the page opposite the portion of the printed material that was changed. Identify a revision to an illustration with a black vertical line in the left margin opposite the revised portion or use a “pointed hand” [✎]. The date of the revision should be placed on each revised page.

10.2.2 Contents

The Supplemental Inspection Document contains the following information:

- Title Page
- List of Effective Pages
- Record of Revisions
- Table of Contents
- Applicability
- Objectives
- Technical Document Reference
- List of Supplemental Inspections
- Supplemental Inspection Documents (in Chapter Number order)
- Inspection Methods and Requirements

Each item in the Supplemental Inspection Document is discussed in detail in the following sections.

10.2.2.1 Title Page

An example title page is shown in Figure 10-5. The title page contains the following information:

- The title, Supplemental Inspection Document, or the acronym SID [Item 1, Figure 10-5].
- The airplane model name or description of the components covered [Item 2, Figure 10-5].
- The SID writer’s or company logo [Item 3, Figure 10-5].

- The effective date and revision number and date if applicable [Item 4, Figure 10-5].
- The SID writer's or company address [Item 5, Figure 10-5].

Additional information, such as GAMA membership identification [Item 6, Figure 10-5], copyright notice [Item 7, Figure 10-5], etc. may be included. The format and the layout is to be determined by the SID producer, keeping in mind that it is desirable that the format and layout be similar to existing SID documents. The back of the Title Page should be left blank except for items such as the SID producer's masthead.

10.2.2.2 List of Effective Pages

- The List of Effective Pages is formatted to provide:
 - a) A Chapter/Section/Subject column [Item 1, Figure 10-6].
 - b) A page number column [Item 2, Figure 10-6].
 - c) A date column [Item 3, Figure 10-6].
- Revision instruction information (such as, "Insert Latest Revised Pages; Destroy Superseded or Deleted Pages") or revision history information, or both, may also be included.

10.2.2.3 Record of Revisions

The Record of Revisions is formatted to provide (see Figure 10-7):

- A Revision Number column [Item 1, Figure 10-7].
- A Date Inserted column [Item 2, Figure 10-7].
- A Date Removed column (optional) [Item 3, Figure 10-7].
- A Page Number column [Item 4, Figure 10-7].

10.2.2.4 Table of Contents

The Table of Contents is formatted to provide (see Figure 10-8):

- A Section Title column [Item 1, Figure 10-8].
- A Page Number column [Item 2, Figure 10-8].

10.2.2.5 Applicability

The Applicability Statement contains the following information, appropriately formatted:

- A list of models or components affected, in a column on the left side of the page [Item 1, Figure 10-9], and a list of corresponding serial/unit numbers (or other identifying information), in a corresponding column on the right side of the page [Item 2, Figure 10-9]. This information is specifically required by item 3a(1) in Appendix 1 of AC 91-MA.
- Special information, such as exclusions or additions, in note form [Item 3, Figure 10-9].
- An upper boundary for the application of the SID document must be established. The upper boundary may be in terms of flight hours, flight cycles, or calendar time. It may be set at any value chosen by the manufacturer that [Item 4, Figure 10-9]:
 1. Does not exceed the limit validated by analysis and approved by the FAA, or
 2. Does not exceed the time when repair or replacement of a critical PSE is due, and the action is considered uneconomical.

This information is specifically required by item 5 in Appendix 1 of AC 91-MA.

The listed model or components and listed serial/units are to be cumulative for all inspections in the Supplemental Inspection Document. This will allow the user to identify an affected airplane by examining one list rather than having to check each individual Supplemental Inspection for applicability. Figure 10-9 shows an example Applicability Statement.

10.2.2.6 Objectives

The Objectives section can contain information outlining the rationale utilized to select the Supplemental Inspections. The following outline highlights possible sections to include. Items which are specifically required by AC 91-MA are noted. Figures 10-10 through 10-21 show an example Objectives section.

- Discussion [Figure 10-10]
 - a) Introduction
 - b) History
 - c) Objective
- Principle Structural Elements [Figure 10-11]
 - a) Rationale Used to Select Principle Structural Elements

- b) Selection Criteria
- Durability – Fatigue and Damage Tolerance [Figures 10-12 thru 10-17]
 - a) Aircraft Usage [Section 3a(2) in Appendix 1 of AC 91-MA]
 - b) Stress Spectrum
 - c) Description of the Flight Profiles [Section 3a(2) and 3a(4) of Appendix 1 of AC 91-MA.]
 - d) Classifications for Types of Operations [See Figure 10-14]
 - e) Damage Tolerance and Fatigue Assessments [See Figure 10-16]
- Reporting – Communications [Figures 10-17 and 10-18]
 - a) Discrepancy Reporting [See Figure 10-21]
 - b) Discrepancy Form Disposition
 - c) Follow-Up Action
- Inspection Methods [Figure 10-18]
- Related Documents [Section 3a(3) and 3a(5) of Appendix 1 of AC 91-MA.] [Figure 10-19]
 - a) Existing Inspections, Modifications, and Repair Documents
 - b) Service Letters/Bulletins Affected by SID
- Applicability/Limitations [Figure 10-19]
- PSE Details [Figure 10-20]
 - a) PSE Data Sheets
 - b) Repair Information/Modifications

10.2.2.7 Technical Document Reference

The Technical Document Reference contains a listing of necessary service documents (e.g., service bulletins, service letters, service kits, etc.) and related information directly identified in a SID inspection [Figure 10-22]. Service documents listing existing inspections or component modifications as well as documents developed specifically for the SID should be referenced. A statement must be added stating that the operator must account for these service bulletins [Section 3a(3) and 3a(5) in Appendix 1 of AC 91-MA].

10.2.2.8 Listing of Supplemental Inspection Document Inspections

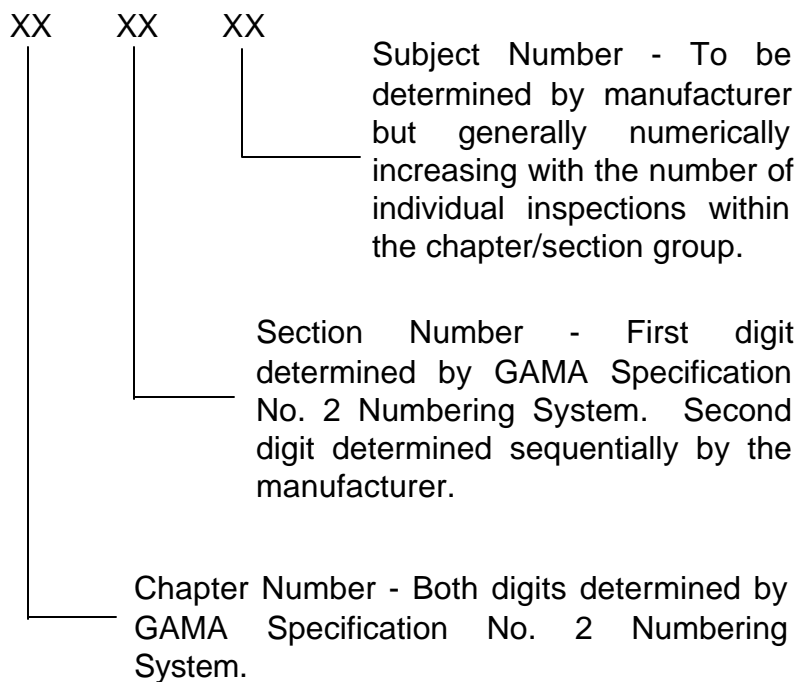
- The Listing of Supplemental Inspections contains all Supplemental Inspection Document inspections in the SID, in numerical order by SID inspection number [Item 1, Figure 10-23], with full title [Item 2, Figure 10-23], date [Item 3, Figure 10-23], effectivity [Item 4, Figure 10-23], and inspection compliance [Item 5, Figure 10-23] (initial and repeat inspection intervals).

- In the alternative, a block diagram, showing only Supplemental Inspection Document Inspection numbers and time blocks may be used (Figure 10-25).
- Inspection intervals published in the SID must be given both in terms of usage (hours or landings) and calendar time. A chart giving the relationship between time and usage as shown in Figure 10-24 is useful.
- Tables or charts should be presented to determine the usage type or severity type if more than one type of usage and severity were analyzed in Section 5. Section 5.0 defines the aircraft utilization guidelines for the aircraft under consideration. The utilization of the aircraft is important because manufacturers will set different inspection intervals for different usages of the airplanes. Figure 10-16 includes a decision flowchart as an example of this table or chart.

10.2.2.9 Supplemental Inspection Document Inspections

- Supplemental Inspection Document Inspections usually consist of at least two pages including at a minimum one text page and one illustration page. Figures 10-26 through 10-29 show examples of the inspection text and illustration pages.
- The Supplemental Inspection Document Inspection contains the following sections, in order, from the top of the page to the bottom (except as noted), in bold face type or underscored:
 - a) **SUPPLEMENTAL INSPECTION DOCUMENT INSPECTION NUMBER** - in the upper right corner of the image area on the text page(s) and, optionally, on the illustration page(s). The SID Inspection Number is also displayed at the bottom of the page and is the SID section number (see Note) [Item 1, Figure 10-28].

NOTE: The Supplemental Inspection Document Inspection number is determined as follows:



- b) TITLE - at the top of the text page, at the left margin [Item 2, Figure 10-28].

For example: Wing Lower Aft Auxiliary Spar Cap

- c) EFFECTIVITY - directly below the title; shows both model and serial/unit numbers as applicable [Item 3, Figure 10-28]. Exceptions and additions are also noted here (such as “except airplanes incorporating Service Kit Number 999”).
- d) INSPECTION COMPLIANCE - directly to the right of the effectivity and near the right margin [Item 4, Figure 10-28]. Instructions regarding “when” an inspection is required, and if repetitive, are located here. Also state if additional repetitive inspections are required based upon initial inspection results [Item 3b(9) & (10) in Appendix 1 of AC 91-MA].
- e) PURPOSE - directly below the Effectivity and Inspection Compliance sections, extending from the left to the right margins [Item 5, Figure 10-28]. Any service history discussion is also located here. A description of the part and the type of damage being considered should be listed [Item 3b(1)-(3) in Appendix 1 of AC 91-MA].

- f) INSPECTION INSTRUCTIONS - directly below the Purpose section and extending from the left to the right margins [Item 6, Figure 10-28]. The likely critical areas of damage should be described [Item 3b(4) in Appendix 1 of AC 91-MA].
- g) ACCESS/LOCATION - directly below the Inspection Instructions section at the left margin [Item 7, Figure 10-28]. Access and location instructions are provided here unless obvious.

For example: Remove wing attach fairings.

- h) SIGNIFICANT INSPECTION CONDITION (detectable crack size, wear limits, corrosion condition, etc.) - directly to the right of the Access/Location section near the right margin [Item 8, Figure 10-28]. Specifies, for a crack inspection, the minimum size crack expected to be discovered or, if no minimum is defined, a statement to this effect. Specifies, for other inspection conditions, the wear limits, corrosion pit depth, etc. [Item 3b(6) in Appendix 1 of AC 91-MA].
- i) INSPECTION PROCEDURE - located directly below the Access/Location section, extending from the left to the right margins [Item 9, Figure 10-28]. Sets forth the inspection procedure(s) to be utilized, such as magnetic particle, visual, eddy current, etc., and may reference another document or section for the actual procedure, such as a nondestructive testing (NDT) manual or NDT section of the SID [Item 3b(5) in Appendix 1 of AC 91-MA].
- j) REPAIR/MODIFICATION - located directly below the Inspection Procedure section, extending from the left to right margins [Item 10, Figure 10-28]. Sets forth repair or modification instructions and may refer to a standard repair in another document or a special repair or modification defined elsewhere, such as in a service kit, service bulletin, etc. [Item 3b(7), (11), & (12) in Appendix 1 of AC 91-MA].
- k) COMMENTS - located directly below the Repair/Modification section, extending from the left to right margins [Item 11, Figure 10-28]. Additional information or instructions, such as "Report any cracks found to this manufacturer", are contained here [Item 3b(8) in Appendix 1 of AC 91-MA].
- l) SECTION NUMBER, PAGE NUMBER AND PAGE DATE - as indicated in paragraph (a) [Item 12, Figure 10-28]. The

Supplemental Inspection Document Inspection number becomes the section number and defines its placement within the SID.

- m) RECOMMENDED OR REQUIRED RETIREMENT TIMES OF LIFE LIMITED PARTS (if established) - on right side of the page in an appropriate space. Use of the word CAUTION, with appropriate 10-point uppercase for the text, enclosed in a box, is recommended. Sets forth manufacturer recommended retirement times for parts or assemblies (using hours, cycles or another appropriate determinant) and FAA required retirement (removal from service) times for life limited parts or assemblies.

10.2.2.10 Inspection Methods and Requirements

- A General Requirements section describes the licensing and equipment requirements of the performing facility. It also states that the appropriate reporting forms for the applicable regulatory agency shall be used for compliance of the SID [Figure 10-30].
- Each type of non-destructive inspection (NDI) is then described in its own section. [Figure 10-31].
 - a) A general statement about the effectiveness, background, and uses of the particular NDI method is included.
 - b) The required equipment for the NDI method is listed and any additional materials are noted.
 - c) Any required abbreviations or safety warnings are spelled out.
- Inspection Methods and Requirements usually consist of two pieces: a text description of the inspection and any required illustrations for that inspection procedure. Figures 10-32 and 10-33 show an example Inspection Method procedure. Figure 10-34 shows the accompanying illustration of the Inspection Method.
- The Inspection Methods and Requirements text pages contain the following sections, in order, from the top of the page to the bottom (except as noted), in bold face type or underscored:
 - a) SUPPLEMENTAL INSPECTION DOCUMENT INSPECTION NUMBER - in the upper right corner of the image area on the text page(s) and, optionally, on the illustration page(s) [Item 1, Figure 10-32]. The SID Inspection Number is also displayed at the bottom of the page and is the SID section number. The

Supplemental Inspection Document Inspection number is determined as described in Section 10.2.2.9 paragraph (a).

- b) TITLE - at the top of the text page, at the left margin [Item 2, Figure 10-32].
- c) EFFECTIVITY - directly below the title; shows both model and serial/unit numbers as applicable [Item 3, Figure 10-32]. Exceptions and additions are also noted here.
- d) DESCRIPTION - directly below the effectivity and near the left margin [Item 4, Figure 10-32]. Describe what the inspection is intended to look for or find and where.
- e) PREPARATION - directly below the description section, extending from the left to the right margins [Item 5, Figure 10-32]. Any special paint removal or surface preparation is provided here.
- f) INSPECTION METHOD - directly below the preparation section [Item 6, Figure 10-32]. State what type of inspection is to be performed.
- g) CRACK SIZE - directly below the Inspection Method section [Item 7, Figure 10-32]. The minimum detectable crack size by the inspection method stated in the INSPECTION METHOD heading.
- h) EQUIPMENT - directly below the Crack Size section at the left extending all the way to the right margin [Item 8, Figure 10-32]. Specifies, for an inspection, the specific NDI equipment, part number, quantity, and use of that equipment in the inspection. The manufacturer, and their address, of each piece of equipment is provided for ease of purchase.
- i) INSPECTION INSTRUCTIONS - located directly below the Equipment section, extending from the left to the right margins [Item 1, Figure 10-33]. Sets forth the specific inspection instructions to be utilized. Calls out the surface preparation, penetrant application and removal (if applicable), inspection, interpretation, and reporting instructions.

10.3 Sample Supplemental Inspection Document

Examples of each of the chapters covered in Section 10.2.2 are shown here. These example figures are shown for a Supplemental Inspection Document for a fictitious aircraft and are only intended to illustrate the format detailed in the previous section.

FIGURE 10-5

EXAMPLE TITLE PAGE

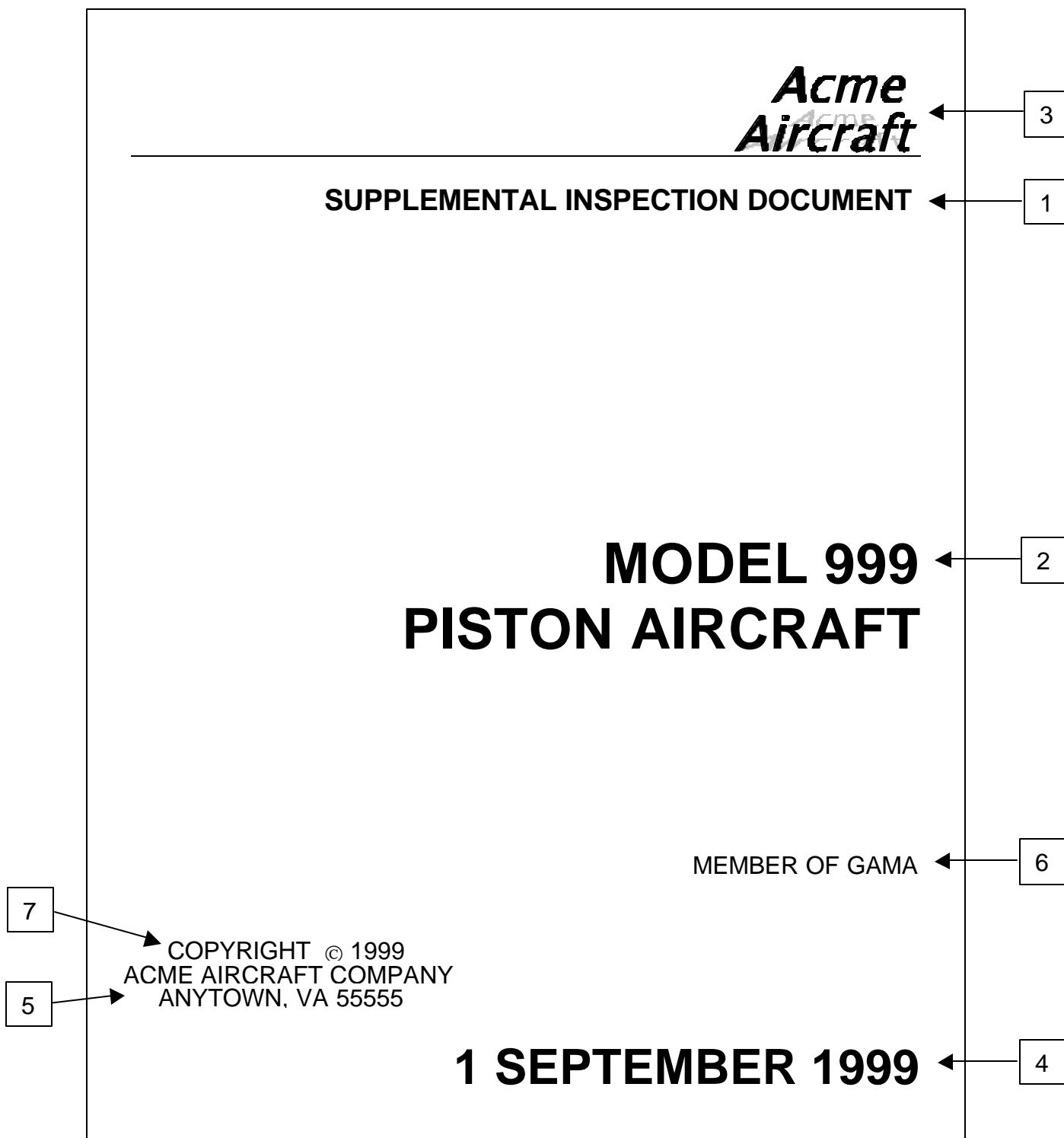


FIGURE 10-6

EXAMPLE LIST OF EFFECTIVE PAGES

ACME AIRCRAFT COMPANY MODEL 999 SUPPLEMENTAL INSPECTION DOCUMENT		
CHAPTER SECTION SUBJECT	PAGE	DATE
COVER	i	September 1999
TITLE PAGE	ii	September 1999
LIST OF EFFECTIVE PAGES	iii	September 1999
RECORD OF REVISIONS	iv	September 1999
TABLE OF CONTENTS	v	September 1999
	vi	September 1999
	vii	September 1999
APPLICABILITY	viii	September 1999
INTRODUCTION	ix	September 1999
	x	September 1999
	xi	September 1999
	xii	September 1999
	xiii	September 1999
	xiv	September 1999
	xv	September 1999
	xvi	September 1999
	xvii	September 1999
	xviii	September 1999
	xix	September 1999
	xx	September 1999
	xxi	September 1999
SECTION I		
SECTION II		
SECTION III		
SECTION IV		
TECHNICAL DOCUMENT REFERENCE	I-1	September 1999
LISTING OF SUPPLEMENTAL INSPECTION DOCUMENTS	II-1	September 1999
SUPPLEMENTAL DOCUMENT INSPECTIONS	III-1	September 1999
INSPECTION METHODS AND REQUIREMENTS	IV-1	September 1999

FIGURE 10-8

EXAMPLE TABLE OF CONTENTS

1	ACME AIRCRAFT COMPANY MODEL 999 SUPPLEMENTAL INSPECTION DOCUMENT	2
SECTION TITLE	TABLE OF CONTENTS	PAGE
	LIST OF EFFECTIVE PAGES.....	i
	RECORD OF REVISIONS	ii
	TABLE OF CONTENTS.....	iii
	APPLICABILITY.....	viii
	INTRODUCTION.....	ix
SECTION I	TECHNICAL DOCUMENT REFERENCE	I-1
	Service/Maintenance Manuals.....	I-1
	Service Bulletins.....	I-1
SECTION II	LISTING OF SUPPLEMENTAL INSPECTIONS.....	II-1
	Inspection Requirements Hours to Years Equivalence Figure.....	II-5
	Typical Spectrum Summary of Inspections Model 999-0001thru Model 999B-0787	II-6
	Severe Spectrum Summary of Inspections Model 999-0001thru Model 999B-0787	II-7
	Short Flight Spectrum Summary of Inspections Model 999-0001 thru Model 999B-0787	II-8
SECTION III	SUPPLEMENTAL INSPECTION DOCUMENTS.....	III-1
	27-10-05 Aileron Hinges and Fittings.....	III-1
	27-20-03 Rudder Structure	III-7
	32-20-01 Nose Gear Attachment and Wheel Well Structure.....	III-21
	53-10-02 Fuselage Left and Right Hand Longerons.....	III-35
	53-10-03 Horizontal Tail Rear Spar Angle Attachment.....	III-67
	54-10-03 Model 999 Engine Beams.....	III-85
	57-10-20 Wing Lower Aft Auxiliary Spar Cap.....	III-109
SECTION IV	INSPECTION METHODS AND REQUIREMENTS.....	IV-1
	General Requirements.....	IV-1
	General Eddy Current Inspection.....	IV-2
	27-10-05 Aileron Hinges and Fittings.....	IV-33
	57-10-20 Wing Lower Aft Auxiliary Spar Cap.....	IV-135

FIGURE 10-9

EXAMPLE APPLICABILITY STATEMENT

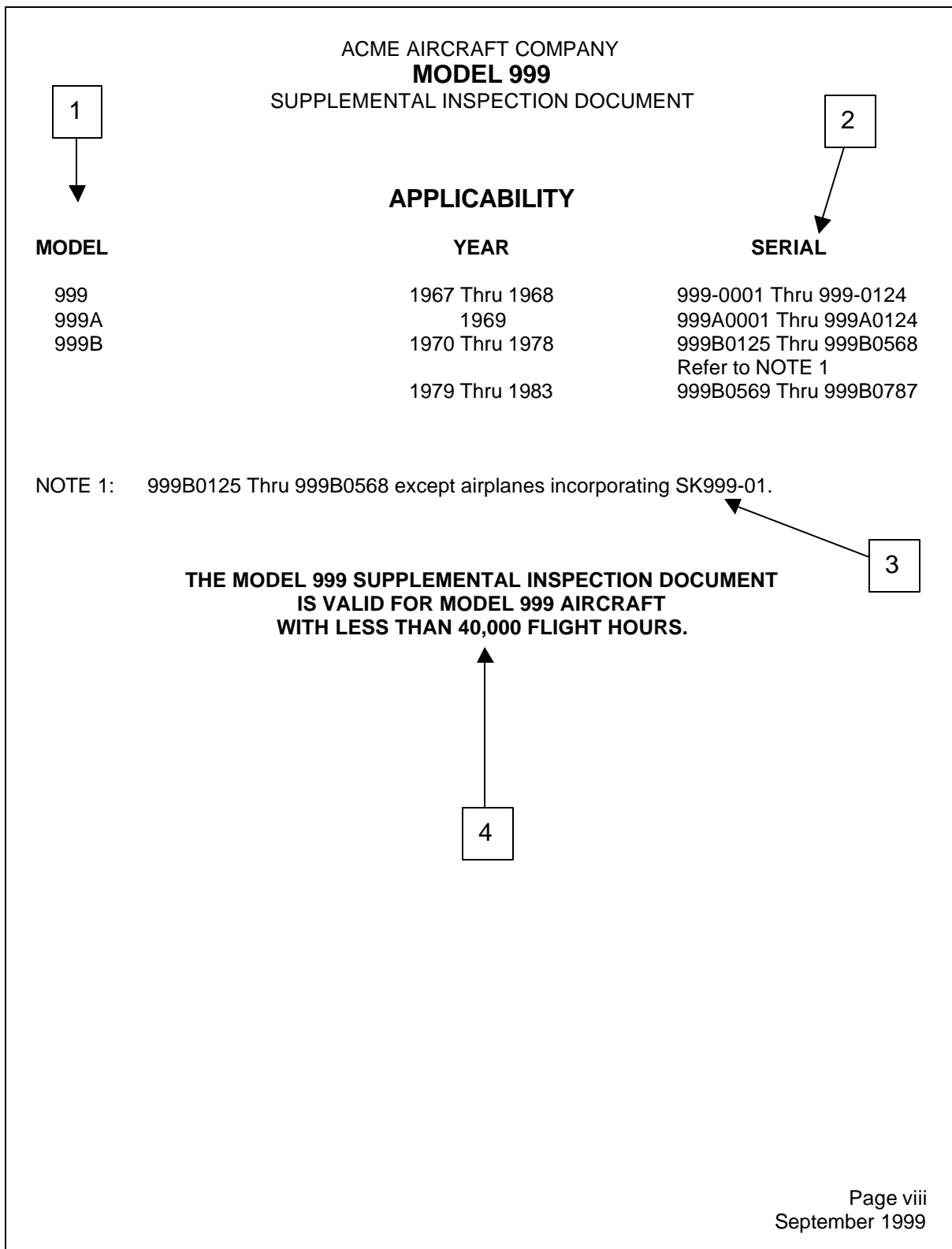


FIGURE 10-10

EXAMPLE PAGE 1 IN INTRODUCTION SECTION

ACME AIRCRAFT COMPANY
MODEL 999
SUPPLEMENTAL INSPECTION DOCUMENT

1-0. DISCUSSION

1-1. Introduction

The Supplemental Structural Inspection Program for the Acme Model 999 aircraft is based on Model 999 current aircraft usage and state-of-the-art analysis, testing and inspection methods. Analysis methods include durability, fatigue and damage tolerance assessments. A practical state-of-the-art inspection program is established for each Principle Structural Element (PSE), where:

A PSE is that structure whose failure, if it remained undetected, could lead to the loss of the aircraft. Selection of a PSE is influenced by the susceptibility of a structural area, part or element to fatigue, corrosion, stress corrosion, or accidental damage.

The inspection program consists of the current structural maintenance inspection plus supplemental inspections, if necessary, as required for continued airworthiness of the aircraft as they grow older. The current inspection program is considered to be adequate in detecting corrosion and accidental damage. The emphasis of the Supplemental Inspection Program is to detect fatigue damage whose probability increases with time.

The Supplemental Structural Inspection Program was developed through the combined efforts of Acme Aircraft Company, Model 999 operators, and the FAA.

1-2. History

The first Acme Model 999 was produced in 1967. The basic version of the Model 999 was produced through 1983 as the Model 999, 999A and 999B. Models 999 through 999B are, for the purposes of the supplemental inspection program, identical. Over 700 Model 999 through 999B airplanes were produced.

1-3. Objective

The objective of the Supplemental Structural Inspection Program is the detection of damage due to fatigue, overload or corrosion through the practical use of Non-Destructive Inspection (NDI). This SID addresses primary and secondary airframe components only. Powerplant, electrical items and primary and secondary systems are not addressed in this document.

To establish the basis for those items included the following assumptions have been made:

- A. The aircraft has been maintained in accordance with Acme recommendations or equivalent.
- B. Where the SID is directed to a specific part or component, it is implied that the inspection will include observation and evaluation of the surrounding area of parts and equipment. Any discrepancies found during this inspection outside of the scope of the SID should be reported to Acme through the existing condition reporting system so that changes can be made to the SID where necessary.

FIGURE 10-11

EXAMPLE PAGE 2 IN INTRODUCTION SECTION

ACME AIRCRAFT COMPANY
MODEL 999
SUPPLEMENTAL INSPECTION DOCUMENT

- C. Aircraft modified by Supplemental Type Certificate (STC) are not the responsibility of Acme. Any inspections called for in Acme manuals or the SID that have areas that have been modified by STC(s) shall automatically be referred to the STC holder(s) by the owner and/or maintenance organization for obtaining FAA approval guidelines.

2-0. PRINCIPLE STRUCTURAL ELEMENTS

2-1. Rationale Used to Select Principal Structural Elements

An aircraft component is classified as a Principal Structural Element (PSE) if the component contributes significantly to carrying flight and ground loads, and if failure of the component could result in catastrophic failure of the airframe. The monitoring of these PSE's is the main focus of this Supplemental Inspection Program.

2-2. Selection Criteria

The factors used in determining the PSE's in this document include:

- A. Service Experience: Three sources of information were used to determine service problems.
- 1) Service experience data was collected from current Model 999 owners. Surveys were conducted which asked the operators to describe any major structural repairs made to their airplanes.
 - 2) Acme Service Bulletins, issued to repair common service problems, were reviewed.
 - 3) FAA Service Difficulty Records covering a time period from the mid-1970's to December 1998 were reviewed.
- The data collected was also used to determine a component's susceptibility to corrosion or accidental damage, as well as its inspectability.
- B. Stress Analysis: Mathematical models were developed for the Model 999 through Model 999B airframe and airframe components. Models were developed for the wing and carry-thru, flaps, aileron, engine beam, fuselage, horizontal stabilizer, elevator, vertical stabilizer, rudder and nose and main landing gears. These models were reviewed to identify components that exhibit the potential for additional inspection requirements.
- C. Fatigue and Damage Tolerance Analysis: Fatigue and damage tolerance analyses were conducted for the critical areas of the PSE's. Details of these analyses are presented in Section 3.0.
- D. Testing: New static tests were conducted to verify the mathematical models which were developed. Test results from previously conducted static tests and fatigue cyclic tests were also reviewed to identify the critical areas of the PSE's.
- E. Inspection of Aircraft: A high-time aircraft was purchased from a customer for disassembly and inspection in 1988. The aircraft had over 20,000 flight hours and 60,000 landings. Locations where cracking was discovered during disassembly are included as inspection locations.

FIGURE 10-12

EXAMPLE PAGE 3 IN INTRODUCTION SECTION

ACME AIRCRAFT COMPANY
MODEL 999
SUPPLEMENTAL INSPECTION DOCUMENT

3-0. DURABILITY - FATIGUE & DAMAGE TOLERANCE

3-1. Aircraft Usage

Aircraft usage data for the SID program is based on the evaluation of the in-service utilization of the aircraft. This data was used to develop the representative fatigue loads spectra. Operational data for development of the Supplemental Inspection Program was obtained from two sources:

1. A survey of operators identified by the FAA which encompassed 14 operators and 85 airplanes. The airplanes included in the survey represent a usage of 1777 flights per week. This survey was conducted in January 1999.
2. A survey of three operators representing 4 airplanes was conducted by Acme in 1974.

The usage from each survey is shown in Figure 3-1.-1.

The usage for spectra determination is defined in terms of a mix of different flights representing typical average in-service utilization of the aircraft. This usage, in terms of different flights, reflects the typical in-service flight variation of flight length, takeoff gross weight, payload and fuel.

Each flight is defined in detail in terms of a flight profile. The profile identifies the gross weight, payload, fuel, altitude, speed, distance, etc., required to define the pertinent flight and ground parameters needed to develop the fatigue loads. The flight is then divided into operational segments, where each segment represents the average values of the parameters (speed, payload, fuel, etc.) that are used to calculate the loads spectrum.

FIGURE 10-13

EXAMPLE PAGE 4 IN INTRODUCTION SECTION

ACME AIRCRAFT COMPANY
MODEL 999
 SUPPLEMENTAL INSPECTION DOCUMENT

FIGURE 3-1.-1
FLIGHT LENGTH SUMMARY

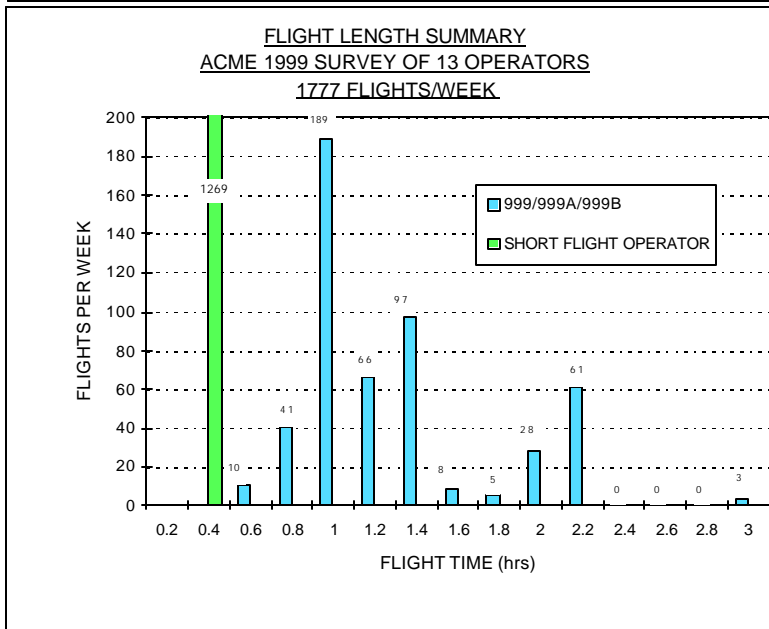
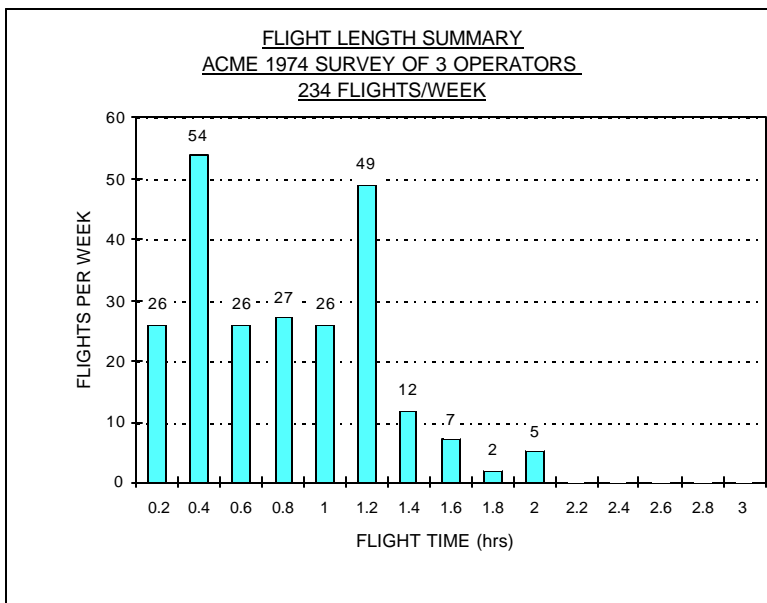


FIGURE 10-14

EXAMPLE PAGE 5 IN INTRODUCTION SECTION

ACME AIRCRAFT COMPANY
MODEL 999
SUPPLEMENTAL INSPECTION DOCUMENT

3-2. Stress Spectrum

A fatigue loads spectrum, in terms of gross area stress, was developed for each PSE to be analyzed based on the usage-flight profiles. The spectrum represents the following loading environments: flight loads (gust and maneuver), landing impact, balancing tail loads, thrust loads, ground loads (taxi, turning, landing, braking, pivoting, etc.), and ground-air-ground cycles. The resulting spectrum is a representative flight-by-flight, cycle-by-cycle random loading sequence that reflects the appropriate and significant airplane response characteristics.

After reviewing the aircraft usage data and the way in which the surveyed aircraft were flown, three sets of stress spectrum were developed, one for each flight profile, as described in Section 3-3.

3-3. Description of the Flight Profiles

The first profile is the Short Flight Profile and consists of one flight. Of the 2011 flights per week, 1269 of the flights were made by one operator flying a Model 999 using the same mission for each flight which is 25 minutes in length.

The second profile is the Severe Profile and consists of two individual flights. The flights are at low altitudes over mountainous terrain.

The third profile is the Typical Usage Profile which consists of six individual flights. These profiles were derived from the usage data collected from the survey, minus the Short Flight and Severe Flight operators. The six individual flights were defined to represent the overall flight distributions as shown in Figure 3-3.-1.

3-4. Classifications for Types of Operation

To determine the frequency of inspections, first determine the total number of hours and total number of landings on the airplane, then determine an average flight length over the life of the airplane:

$$\frac{\text{Number of Flight Hours}}{\text{Number of Flights}} = \text{Average Flight Length}$$

or

$$\frac{\text{Number of Flight Hours}}{\text{Number of Landings}} = \text{Average Flight Length}$$

whichever is less. If the average flight length is less than or equal to 40 minutes then the Short Flight Profile should be used for inspections.

FIGURE 10-15

EXAMPLE PAGE 6 IN INTRODUCTION SECTION

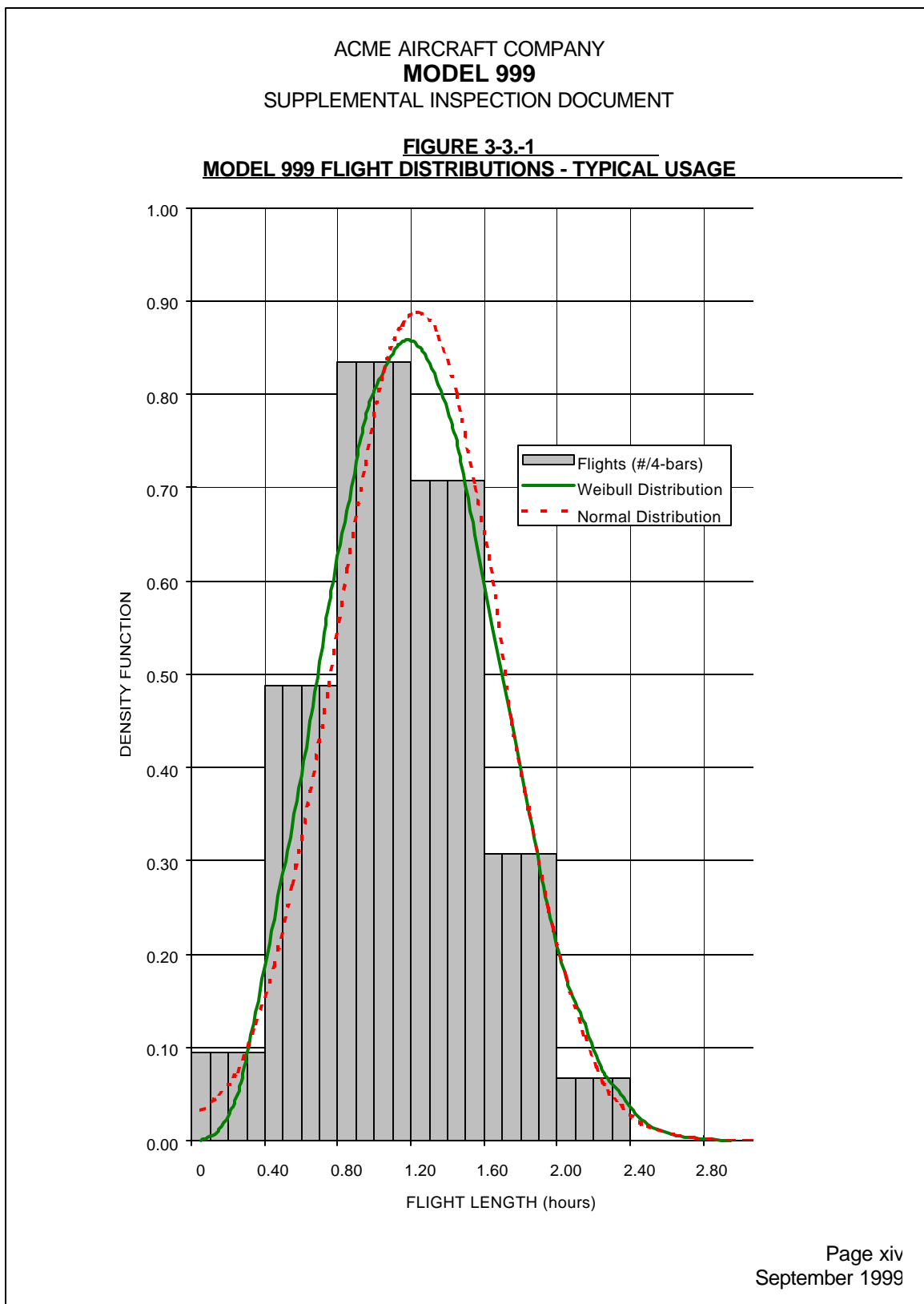


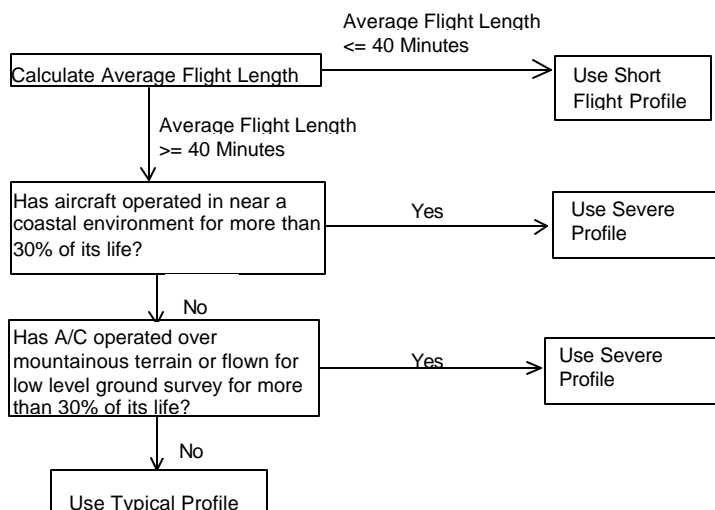
FIGURE 10-16

EXAMPLE PAGE 7 IN INTRODUCTION SECTION

**ACME AIRCRAFT COMPANY
 MODEL 999
 SUPPLEMENTAL INSPECTION DOCUMENT**

For aircraft with an average flight length greater than forty minutes, the severity of the operating environment needs to be determined. If the aircraft currently operates in severe environments or has in the past, the Severe Profile should be used. Examples of severe operations would include flying over mountainous terrain or near coastal areas or conducting low level ground surveys. For all other operating environments the Typical Usage Profile should be used. Figure 3-4.-1 illustrates the selection process.

**FIGURE 3-4.-1
 FLIGHT PROFILE DETERMINATION FOR MODEL 999**



3-5. Damage Tolerance Assessment

The damage tolerance assessment provides the basis for establishing inspection frequency requirements for each PSE. The evaluation includes a determination of the probable location and modes of damage and is based on analytical results, available test data and service experience. The evaluation includes the determination of the crack growth time history and residual strength. Linear elastic fracture mechanics are used to perform the damage tolerance analysis.

In the analysis, particular attention is paid to potential structural problem areas associated with aging aircraft. Examples include (a) large areas of structure working at the same stress level, which could develop widespread fatigue damage; (b) a number of small (less than detectable size) adjacent cracks suddenly joining into a long crack (e.g., as in a line of rivet holes); (c) redistribution of load from adjacent failing or failed parts causing accelerated damage of nearby parts (i.e., the "domino" effect); and (d) concurrent failure of multiple load path structure (e.g., crack arrest structure).

The crack growth for each PSE is calculated from the initial crack size a to crack length at instability/failure, a_{crit} , due to limit load. The crack growth history is represented (see Figure 3-5.-1) in terms of crack length versus time in flight hours.

FIGURE 10-17

EXAMPLE PAGE 8 IN INTRODUCTION SECTION

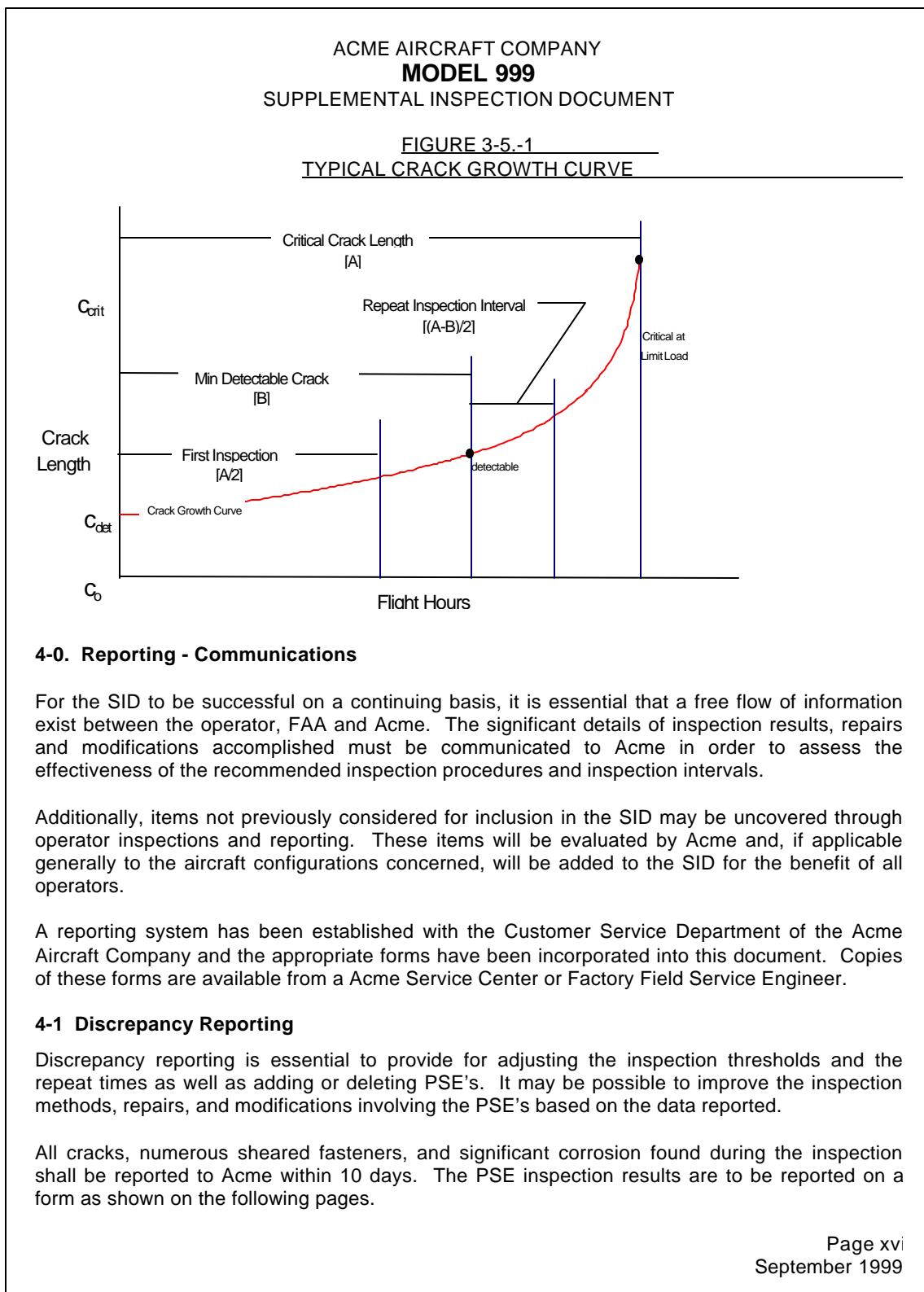


FIGURE 10-18

EXAMPLE PAGE 9 IN INTRODUCTION SECTION

ACME AIRCRAFT COMPANY
MODEL 999
SUPPLEMENTAL INSPECTION DOCUMENT

4-2 Discrepancy Form Disposition

Send all available data including forms, repairs, photographs, sketches, etc., to:

Acme Aircraft Company
Attn. SID Program
Technical Support Services
Dept. 123
P.O. Box 4567
Anytown, VA USA 55555
Fax: 555-123-4567

NOTE: This system does not supersede the normal channels of communication for items not covered by the SID.

4-3. Acme Follow-up Action

All SID reports will be reviewed to determine if any of the following actions should be taken:

1. Check the effect on structural or operational integrity.
2. Check other high-time aircraft to see if a Service Bulletin should be issued.
3. See if a reinforcement is required.
4. Revise the SID if required.

5-0. Inspection Methods

A very important part of the SID program is selecting and evaluating state-of-the-art non-destructive inspection (NDI) methods applicable to each PSE, and determining a minimum detectable crack length, c_{det} , for each NDI method. The minimum detectable crack length is used in conjunction with the critical crack length, c_{crit} , to define the life interval for the crack to grow from c_{det} to c_{crit} as: $(\text{Life @ } c_{crit} - \text{Life @ } c_{det})/2$. This interval is used to define the repeat inspection frequency for the SID program's required inspections. The initial inspection occurs at $\text{Life @ } c_{crit}/2$. For a given NDI method and PSE, c_{det} corresponds to a crack size with a 90% probability of detection. An example of initial and repeat inspection interval determination is shown in Figure 3-5.-1.

Potential NDI methods were selected and evaluated on the basis of crack orientation, location, c_{crit} , part thickness and accessibility. Inspection reliability depends on size of the inspection task, human factors (such as qualifications of the inspector), equipment reliability and physical access. Visual, radiographic, liquid penetrant, eddy current and magnetic particle methods are used. A complete description of each of these methods is presented in SECTION IV- INSPECTION METHODS AND REQUIREMENTS.

FIGURE 10-19

EXAMPLE PAGE 10 IN INTRODUCTION SECTION

ACME AIRCRAFT COMPANY
MODEL 999
SUPPLEMENTAL INSPECTION DOCUMENT

6-0. Related Documents

6-1. Existing Inspections, Modifications, and Repair Documents

Acme has a number of documents that are useful to maintaining continued airworthiness of aircraft:

1. Acme 999 Series Service/Maintenance Manuals.
2. Acme 999 Series Illustrated Parts Catalogs.
3. Acme Multi Engine Service Information and Service Bulletin Summaries.
4. Acme Service Newsletter and Newsletter Summaries.

For information regarding these documents, contact:

Acme Aircraft Company Acme Parts Distribution
Attn. SPA Dept.
P.O. Box 4567
Anytown, VA USA 55555
Fax 555-123-4567

Modifications accomplished under STC'S by other organizations are not addressed in this SID, see Section 7.0.

6-2. Service Letters/ Bulletins Affected by SID

As an aid to the operator, a listing of the Service Letters/Bulletins pertaining to the SIDs are listed in SECTION I - TECHNICAL DOCUMENT REFERENCE. For information concerning the technical data included in these Service Letters/Bulletins that apply to your aircraft, contact Acme Propeller Technical Information Services, Department 321. A Service Bulletin Listing Program provides a list of all Acme Service Bulletins and Service Newsletters, applicable to a particular airplane model and serial number is also available from Acme. This service is obtained by calling 555-123-9876/FAX 555-123-4567.

7-0. Applicability/Limitations

This SID is applicable to the Acme Models 999-0001 through 999B-0787.

The Acme 999 series aircraft have had many modifications that were accomplished under STC's by other organizations without Acme Engineering involvement. Because Acme does not have knowledge of the airworthiness of these STC's, this report cannot apply to those areas affected by such STC's and the holder should prepare a SID for his particular modification.

FIGURE 10-20

EXAMPLE PAGE 11 IN INTRODUCTION SECTION

ACME AIRCRAFT COMPANY
MODEL 999
SUPPLEMENTAL INSPECTION DOCUMENT

8-0. PSE Details

This section contains the significant details selected by the rationale process described in paragraph 2-0. These items are considered significant to maintain continued airworthiness of the Acme 999 series models. Service Bulletins pertaining to the PSEs are listed in SECTION I - TECHNICAL DOCUMENT REFERENCE.

A summary of the PSEs is presented in the SECTION II - LISTING OF SUPPLEMENTAL INSPECTIONS. This can be used as a check list by the operators. A summary of inspections by flight hours is also given.

8-1. PSE Data Sheets

A data sheet for each PSE is provided in SECTION III - SUPPLEMENTAL INSPECTION DOCUMENT INSPECTIONS. Each data sheet contains the following:

1. Supplemental Inspection Number.
2. Title.
3. Effectivity.
4. Inspection Compliance.
5. Initial Inspection Interval(s).
6. Repeat Inspection Interval(s).
7. Purpose.
8. Inspection Procedure.
9. Access/Location.
10. Detectable Crack Size.
11. Inspection Procedure.
12. Repair/Modification.
13. Comments.

NOTE: The entry N/A under item 10 (Detectable Crack Size) means that no cracks are allowed in the PSE. Where both hour and calendar time is listed in items 5 and 6, inspection shall occur at whichever comes first.

8-2. Repair Information/Modifications

Modifications and repairs may be made in accordance with the applicable Acme Service/Maintenance Manual, SID, or acceptable methods of alteration and repair. Any repair not covered by the recommendations in this SID program may be coordinated with Acme Technical Information Services at telephone 555-123-9876/FAX 555-123-1234.

FIGURE 10-21

EXAMPLE DISCREPANCY REPORT FORM (IN INTRODUCTION SECTION)

<p>ACME AIRCRAFT COMPANY MODEL 999 SUPPLEMENTAL INSPECTION DOCUMENT</p> <p>Discrepancy Report</p>		
SID NO:	AIRPLANE LOCATION:	S/N OF AIRPLANE:
INSPECTION CONDUCTED: Date	Airplane Total Hours	Cycles
	Component Total Hours	Cycles
SERVICE HISTORY:		
INSPECTION METHOD/LIMITS:		
ACCESS REQUIRED:		
REPAIR DESCRIPTION:		
COMMENTS:		
Enclose all available data including photos, sketches, etc. to:		
<p>Acme Aircraft Company Attn. SID Program Technical Support Services Dept. 123 P.O. Box 4567 Anytown, VA USA 55555 Fax 555-123-4567</p>		
		Page xx September 1999

FIGURE 10-22

EXAMPLE TECHNICAL DOCUMENT REFERENCE PAGE

ACME AIRCRAFT COMPANY
MODEL 999
 SUPPLEMENTAL INSPECTION DOCUMENT

SECTION I - TECHNICAL DOCUMENT REFERENCE

SERVICE/MAINTENANCE MANUALS

Aircraft	Number	Title
Model 999	X999-18-13	Service Manual
Model 999	X999-5-13	Maintenance Manual

To obtain a Service/Maintenance Manual

Acme Aircraft Company Acme Parts Distribution
 Attn. SPA Dept.
 P.O. Box 123
 Anytown, VA USA 55555
 Fax 555-123-4567

SERVICE BULLETINS

Number	Title	Date	Reference SID No.
ME70-01	Elevator Bellcrank Inspection	7-15-70	27-30-01
ME70-02	Emergency Exit Lever Installation	8-21-70	52-20-01
ME71-03	Elevator Torque Fitting Inspection	4-23-71	27-30-01
ME76-04	Nose Landing Gear Fork Bolts	8-02-76	32-10-00 32-10-01
ME80-05	Lower Front Wing Spar Modification	9-26-80	57-10-01
ME85-06	Front Carry Thru Rib Web Inspection	11-01-85	57-10-02
ME87-07	Engine Beam Fitting Inspection And Improvement	10-23-87	54-10-01
ME89-08	Nose Gear Trunnion Inspection/Replacement	1-31-89	32-30-05
ME90-09	Main Gear Side Brace Inspection And Repair	11-02-90	32-30-04
ME91-10	Horizontal Stabilizer Center Spar Inspection/Replacement	12-13-91	32-20-00
ME95-11	Aileron Inspection and Sealing	9-01-95	57-10-23

Section III assumes that the following Service Bulletins/Service Kits have been accomplished.

ME99-12	(Effectivity 999-0001 through 999B0287)
ME99-13	(Effectivity 999B0001 through 999B0787)
SK99-14	(Effectivity 999B0001 through 999B0787)

To obtain a Service Bulletin listed above, write to:

Acme Aircraft Company
 Dept. 123C
 P.O. Box 8989
 Anytown, VA USA 55555
 Fax 555-123-4567

Section I Page I-1
 September 1999

FIGURE 10-23

EXAMPLE LIST OF SUPPLEMENTAL INSPECTIONS

ACME AIRCRAFT COMPANY MODEL 999 SUPPLEMENTAL INSPECTION DOCUMENT						
SECTION II - LISTING OF SUPPLEMENTAL INSPECTIONS						
Supplemental Inspection Number	Inspection Compliance Title	Date	Effectivity	INITIAL	REPEAT	
27-10-05	Aileron Hinges and Fittings	Sep 1/99	999-0001 Thru 999B0787	15,000 Hrs	2,500 Hrs	
27-20-03	Rudder Structure	Sep 1/99	999-0001 Thru 999B0787	7,500 Hrs	2,500 Hrs	
32-20-00	Nose Gear Drag Brace	Sep 1/99	999B0001 Thru 999B0787	5,000 Hrs	500 Hrs	
32-20-01	Nose Gear Attachment and Wheel Well Structure	Sep 1/99	999-0001 Thru 999B0787	7,500 Hrs	2,500 Hrs	
53-10-02	Fuselage Left and Right Hand Longerons	Sep 1/99	999-0001 Thru 999B0787	15,000 Hrs	5,000 Hrs	
53-10-03	Horizontal Tail Rear Spar Angle Attachment	Sep 1/99	999-0001 Thru 999B0787	15,000 Hrs	5,000 Hrs	
54-10-03	Model 999B Engine Beams	Sep 1/99	999B0001 Thru 999B0787	15,000 Hrs	5,000 Hrs	
57-10-03	Wing Rib Improvement-Main Landing Gear Side Brace	Sep 1/99	999-0001 Thru 999B0787	10,000 Hrs	5,000 Hrs	
57-10-06	Lower Wing Rear Spar Cap at Splice, WS 97.87	Sep 1/99	999-0001 Thru 999B0787	Note 1	Note 1	
57-10-20	Wing Lower Aft Auxiliary Spar Cap	Sep 1/99	999B0001 Thru 999B0787	15,000 Hrs	5,000 Hrs	
57-10-21	Wing Rear Spar Lower Cap at Spar Splice	Sep 1/99	999B0001 Thru 999B0787	15,000 Hrs	5,000 Hrs	
57-10-22	Wing Lower Carry-Thru Rear Spar Cap, BL 49.50	Sep 1/99	999B0001 Thru 999B0787	15,000 Hrs	Note 1	

NOTE:
 1. See SID details for initial and repeat inspections times.

Section II Page II-1
 September 1999

FIGURE 10-24

EXAMPLE HOURS TO YEARS EQUIVALENCE

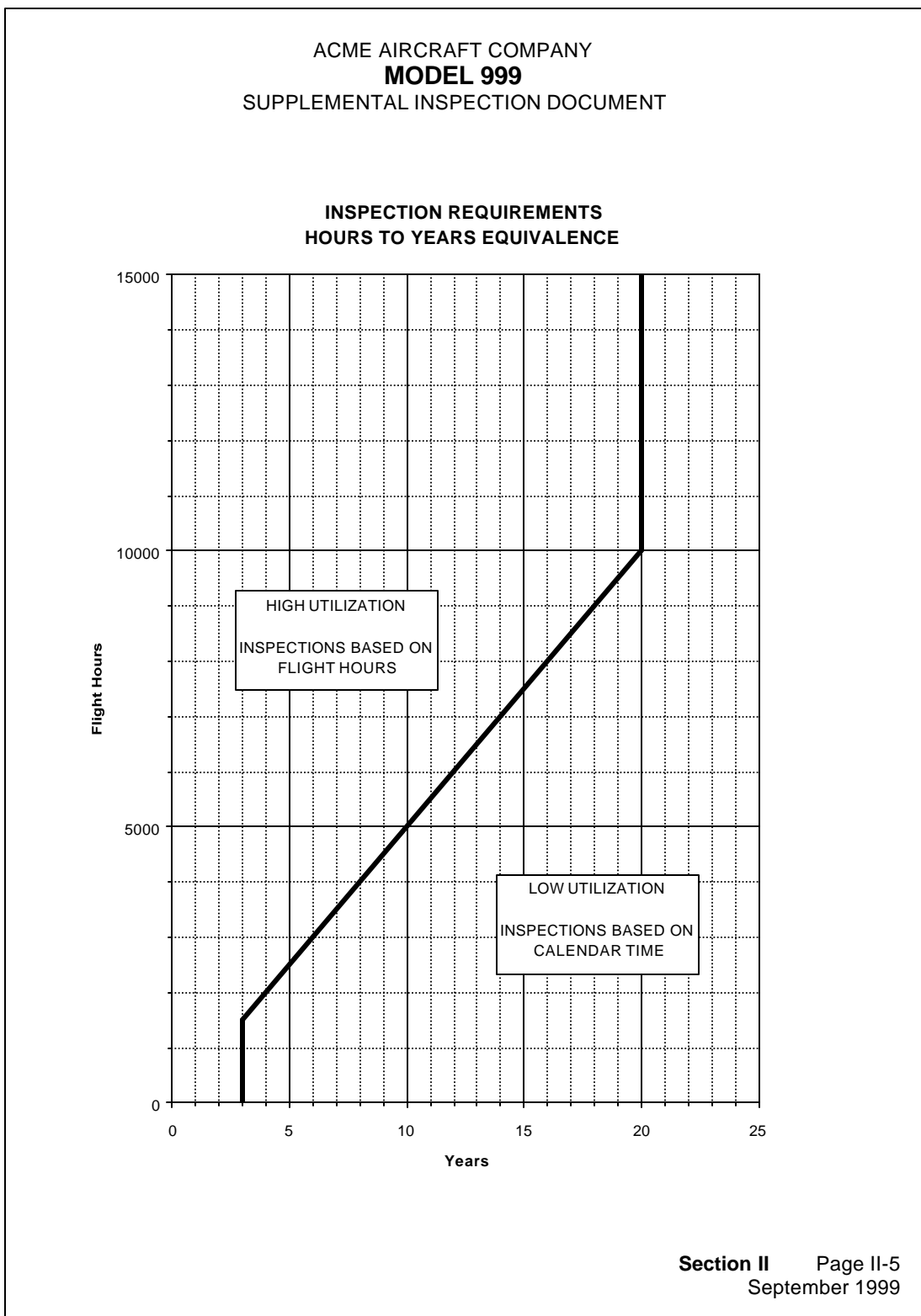


FIGURE 10-25

EXAMPLE LIST OF SUPPLEMENTAL INSPECTIONS (TABLE FORMAT)

ACME AIRCRAFT COMPANY
MODEL 999
 SUPPLEMENTAL INSPECTION DOCUMENT

Severe Spectrum - Summary of Inspections by Flight Hours
 Model 999-0001 Thru Model 999B0787
 Initial Inspection Intervals

Initial Inspection	Effectivity	SID Inspection #'s
5000 Hrs. or 10 Yrs.	999B0001 Thru 999B0787	32-20-00
7500 Hrs. or 15 Yrs.	999-0001 Thru 999B0787	27-20-03, 32-20-01
10000 Hrs. or 20 Yrs.	999-0001 Thru 999B0787	57-10-03
15000 Hrs. or 20 Yrs.	999-0001 Thru 999B0787	27-10-05, 53-10-02, 53-10-03
15000 Hrs. or 20 Yrs.	999B0001 Thru 999B0787	54-10-03, 57-10-20, 57-10-21, 57-10-22
Per SID	999-0001 Thru 999B0787	57-10-06

Repeat Inspection Intervals

Repeat Inspection	Effectivity	SID Inspection #'s
500 Hrs. or 3 Yrs.	999B0001 Thru 999B0787	32-20-00
2500 Hrs. or 5 Yrs.	999-0001 Thru 999B0787	27-10-05, 27-20-03, 32-20-01
5000 Hrs. or 10 Yrs.	999-0001 Thru 999B0787	53-10-02, 53-10-03, 57-10-03
5000 Hrs. or 10 Yrs.	999B0001 Thru 999B0787	54-10-03, 57-10-20, 57-10-21
Per SID	999-0001 Thru 999B0787	57-10-06
Per SID	999B0001 Thru 999B0787	57-10-22

FIGURE 10-26

EXAMPLE SUPPLEMENTAL INSPECTION TEXT PAGE (WITH REPAIR)

<p>ACME AIRCRAFT COMPANY MODEL 999 SUPPLEMENTAL INSPECTION DOCUMENT</p>			
TITLE		SUPPLEMENTAL INSPECTION NUMBER: 32-20-01	
Nose Gear Attachment and Wheel Well Structure			
EFFECTIVITY		INSPECTION COMPLIANCE	
999-0001 through 999B0787		Typical:	Initial 7,500 Hrs or 15 Yrs Repeat 2,500 Hrs or 5 Yrs
		Severe:	Initial 7,500 Hrs or 15 Yrs Repeat 2,500 Hrs or 5 Yrs
PURPOSE			
Inspect wheel well structure including nose gear attachment and drag brace attachment areas for cracks, loose rivets and corrosion.			
INSPECTION INSTRUCTIONS			
<ol style="list-style-type: none"> 1. Remove avionic equipment, oxygen bottles and other equipment per appropriate Service/Maintenance Manual to gain full access to wheel well structure. 2. Visually inspect wheel well structure including webs, stiffeners, braces, brackets and support channels for cracks, loose rivets, corrosion and deterioration. 3. Inspect local areas surrounding the nose gear attach points and drag brace attach points for cracks, loose rivets corrosion and deterioration. 4. Reinstall all equipment removed from nose area for access. 			
ACCESS/LOCATION		DETECTABLE CRACK SIZE	
Refer to inspection procedure above.		0.25 in	
INSPECTION METHOD			
Refer to inspection procedure above.			
REPAIR/MODIFICATION			
Repair using standard repair procedures in accordance with appropriate Service/Maintenance Manual and approved data if major in scope, or replace weakened parts. However, care must be taken not to over-stiffen the web areas. Some flexibility is required to ensure that the gear can travel to over-center position during extension and retraction without overloading the structure.			
COMMENTS			
The nose wheel well structure carries all landing and gear retraction loads into the nose structure. If the structure has deteriorated, gear failure upon landing could occur.			
		Section III – 32-20-01 Page 21 September 1999	

FIGURE 10-27

EXAMPLE SUPPLEMENTAL INSPECTION ILLUSTRATION PAGE
(WITH REPAIR)

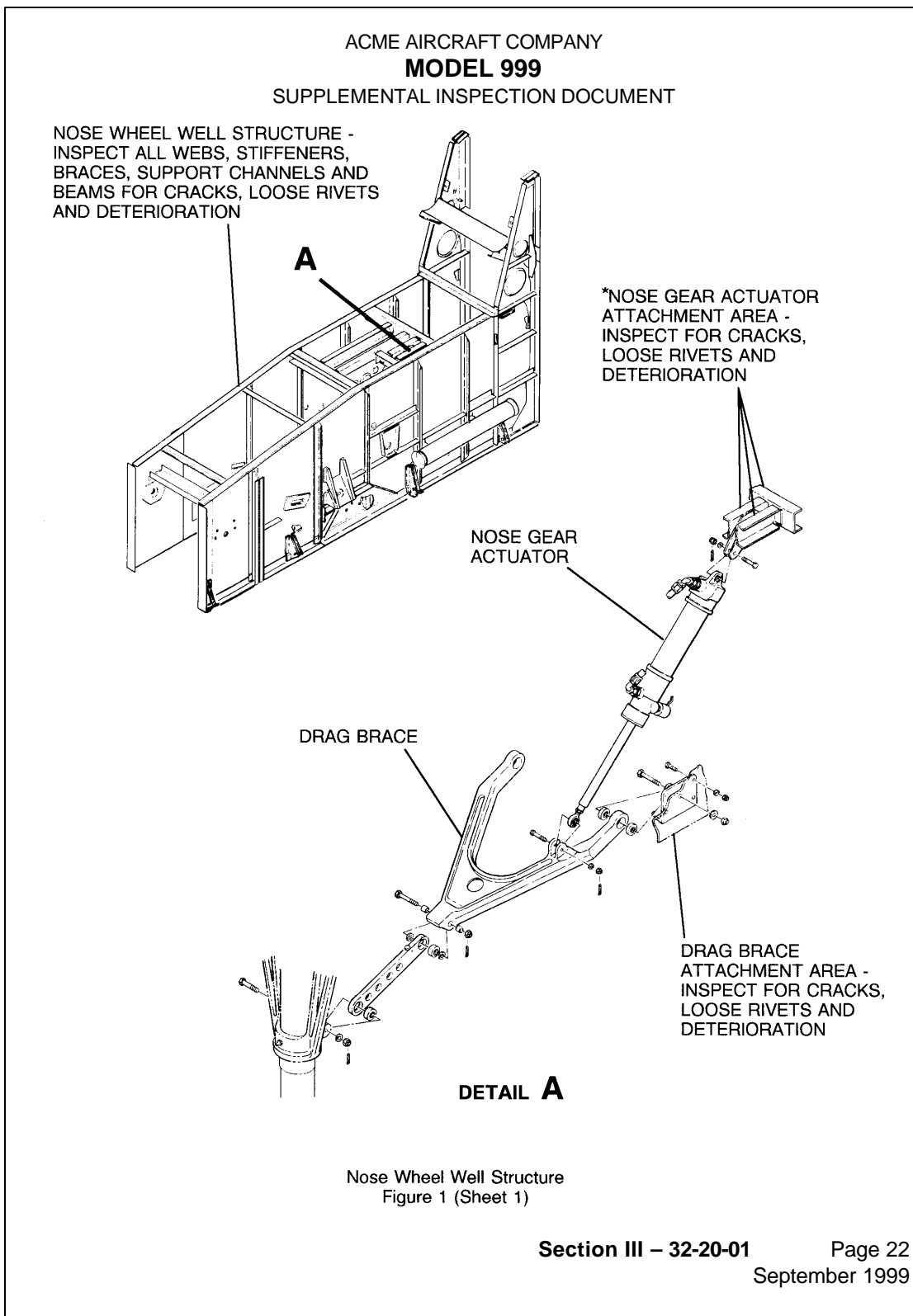


FIGURE 10-28

EXAMPLE SUPPLEMENTAL INSPECTION TEXT PAGE

ACME AIRCRAFT COMPANY MODEL 999 SUPPLEMENTAL INSPECTION DOCUMENT		1
TITLE	SUPPLEMENTAL INSPECTION NUMBER: 57-10-20	
Wing Lower Aft Auxiliary Spar Cap	2	
EFFECTIVITY	INSPECTION COMPLIANCE	
999B0001 through 999B0787	Typical:	Initial 15,000 Hrs or 20 Yrs Repeat 5,000 Hrs or 10 Yrs
3	Severe:	Initial 15,000 Hrs or 20 Yrs Repeat 5,000 Hrs or 10 Yrs
	Short Flight:	Initial 15,000 Hrs or 20 Yrs Repeat 5,000 Hrs or 10 Yrs
PURPOSE	5	
Detailed inspection of aft auxiliary spar for cracks due to fatigue, overload, and corrosion.		
INSPECTION INSTRUCTIONS	6	
1. Through the wheel well area, open the access panels in the rear auxiliary spar web. Refer to Figure 1.		
2. Visually inspect aft auxiliary spar structure for cracks, overload deformations, corrosion and loose fasteners.		
3. Refer to Section IV (NDI Inspection), Supplemental Inspection Number 57-10-20, for specific instructions.		
4. Install access panels in the rear auxiliary spar web.		
ACCESS/LOCATION	7	
Wing	DETECTABLE CRACK SIZE	
INSPECTION METHOD	8 0.080 in.	
Visual/Bolt Hole Eddy Current	9	
REPAIR/MODIFICATION	10	
COMMENTS	11	
If a crack is detected, contact the Customer Service Department of the Acme Aircraft Company.		
12		
Section III – 57-10-20		Page 109 September 1999
1		

FIGURE 10-29

EXAMPLE SUPPLEMENTAL INSPECTION ILLUSTRATION PAGE

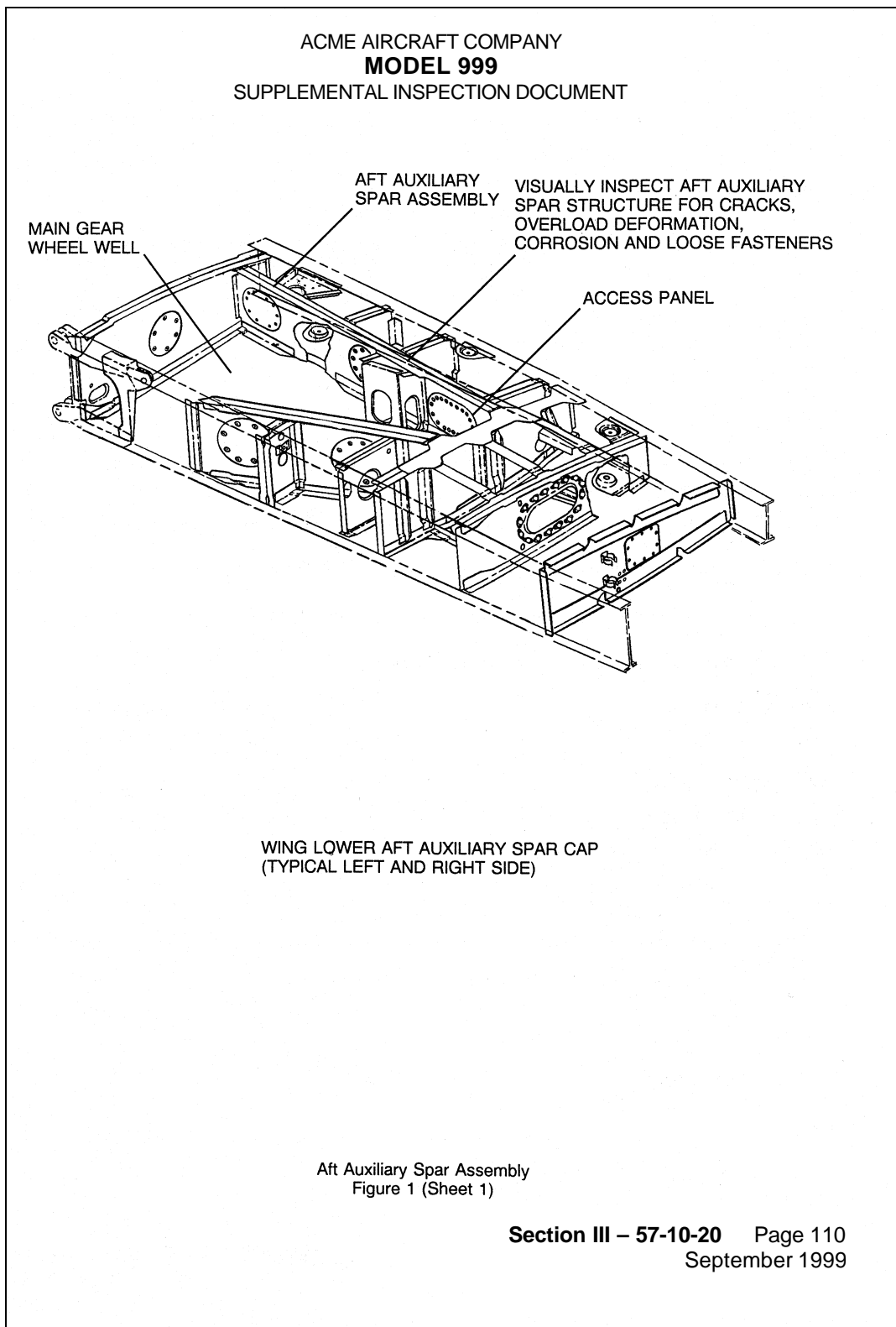


FIGURE 10-30

EXAMPLE NON-DESTRUCTIVE INSPECTION INTRODUCTION PAGE

ACME AIRCRAFT COMPANY
MODEL 999
SUPPLEMENTAL INSPECTION DOCUMENT

SECTION IV – INSPECTION METHODS AND REQUIREMENTS

GENERAL REQUIREMENTS

1. General
 - A. Facilities performing nondestructive inspection as defined in this Supplemental Inspection Document must hold a valid FAA Repair Station Certificate with a Specialized Service Rating in the applicable method of nondestructive inspection.
 - B. Facilities performing nondestructive inspection as defined in this SID, must own or have access to the appropriate test equipment capable of performing the inspection and reporting the test results as defined in this manual.
 - C. Personnel performing nondestructive inspection defined in this Supplemental Inspection Document shall be certified to a minimum of a Level II in the appropriate inspection method as defined by The American Society for Nondestructive Testing Recommended Practice Number SNT-TC-1A.
 - D. Organizations and personnel engaged in the application of nondestructive inspection and operating under the jurisdiction of a foreign government shall use the appropriate documents issued by the applicable regulatory agency in complying with the above requirements.

FIGURE 10-31

EXAMPLE NON-DESTRUCTIVE INSPECTION GENERAL PROCEDURE PAGE

ACME AIRCRAFT COMPANY
MODEL 999
SUPPLEMENTAL INSPECTION DOCUMENT
GENERAL EDDY CURRENT INSPECTION

1. General

- A. Eddy current inspection is effective for the detection of surface and near surface cracks in non-ferrous metals. The inspection is accomplished by inducing eddy currents into the part and observing electrical variations of the induced field. The character of the observed field change is displayed and interpreted to determine the nature of the indication. This method can be applied to airframe parts or assemblies where the inspection area is accessible to contact by the eddy current probe. An important use of eddy current inspection is for the detection of cracking caused by corrosion or stress in and around fastener holes. Bolt hole eddy current probes are effective in detecting fatigue cracks emanating from the wall of the fastener hole. Surface probes can detect cracks around the fastener hole area with the fasteners installed.
- B. Eddy current inspection equipment requires that good contact be made between the probe and the part being tested unless a specific procedure requires a certain amount of liftoff. The area to be inspected must be clean, dry, free of dirt, grease, oil, loose paint or any contaminates which would interfere with the eddy current inspection. Cleaning methods selected for a particular component shall be consistent with the contaminates to be removed and shall not be detrimental to the component or its intended function. All cleaning materials must be approved for use by the appropriate Acme Aircraft Maintenance Manual, Structural Repair Manual, or Component Maintenance Manual.
- C. Conduct the inspection at the required locations as referenced by the specific nondestructive inspection procedure. Scan the inspection area at width increments that do not exceed the width of the eddy current test coil. Wherever possible, the areas to be inspected using surface eddy current shall be scanned in two different directions. The scans shall be conducted at scan paths 90 degrees to each other. All areas that require bolt hole eddy current inspection shall be scanned for the entire depth of the hole. The bolt hole probe index rate shall not exceed the width of the eddy current test coil.
- D. If an indication is detected, carefully repeat the inspection in the opposite direction of probe movement to verify the indication. If the indication persists, carefully monitor the amount of probe movement or rotation required to cause the instrument to move off the maximum indication response.

2. Equipment

- A. In the development of the eddy current inspection techniques contained in this manual, the eddy current equipment listed in the individual procedure was utilized. Equivalent eddy current test equipment may be used providing the equipment is capable of achieving the required frequency range and test sensitivity. When substitute equipment is used, it may be necessary to make appropriate adjustments to the established techniques.

FIGURE 10-32

EXAMPLE NON-DESTRUCTIVE INSPECTION TEXT PAGE

	ACME AIRCRAFT COMPANY MODEL 999 SUPPLEMENTAL INSPECTION DOCUMENT													
2		1												
TITLE:	SUPPLEMENTAL INSPECTION NUMBER: 57-10-20													
	Wing Lower Aft Auxiliary Spar Cap													
EFFECTIVITY:	999B0001 through 999B0787	3												
DESCRIPTION:	Inspect for fatigue cracks in the wing lower aft auxiliary spar cap.	4												
PREPARATION:		5												
	<ol style="list-style-type: none"> 1. Remove all the fasteners on the lower auxiliary spar bottom flanges from the second fastener outboard of WS 91.19 to the third fastener inboard of WS 102.01. (Ten fasteners from each of the fwd and aft flanges.) Refer to 57-10-20 Figure 1. 2. Clean the inspection area with solvent to remove dirt, grease, oil and other substances that may interfere with the inspection. 													
INSPECTION METHOD:	Bolt Hole Eddy Current	6												
CRACK SIZE:	Minimum detectable crack size: 0.080 in.	7												
EQUIPMENT:		8												
	<p>The following equipment was used to develop this procedure; equivalent eddy current test equipment may be used providing the equipment is capable of achieving the required frequency range and test sensitivity.</p> <table border="0" style="width: 100%; border-collapse: collapse;"> <thead> <tr> <th style="text-align: left;">PART NUMBER</th> <th style="text-align: left;">QUANTITY</th> <th style="text-align: left;">DESCRIPTION</th> </tr> </thead> <tbody> <tr> <td>Model 19e^{II}</td> <td style="text-align: center;">1</td> <td>EDDY CURRENT INSTRUMENT NDI Instruments Inc. 987 N. Main Chicago, IL 54321</td> </tr> <tr> <td>ABC101BS 5/32" shielded absolute coil, 0.10" coil dia, 100-500 KHz.</td> <td style="text-align: center;">1</td> <td>EDDY CURRENT PROBE Bolt Hole Probe ABC Products 1254 61st Avenue Dallas, TX 65432</td> </tr> <tr> <td>ABC 89A</td> <td style="text-align: center;">1</td> <td>REFERENCE STANDARD ABC Products 1254 61st Avenue Dallas, TX 65432</td> </tr> </tbody> </table> <p>Reference Standard Notch Size Bolt hole Inspection: 45 Degree Corner Notch 0.050" x 0.050", 0.005" width.</p>		PART NUMBER	QUANTITY	DESCRIPTION	Model 19e ^{II}	1	EDDY CURRENT INSTRUMENT NDI Instruments Inc. 987 N. Main Chicago, IL 54321	ABC101BS 5/32" shielded absolute coil, 0.10" coil dia, 100-500 KHz.	1	EDDY CURRENT PROBE Bolt Hole Probe ABC Products 1254 61st Avenue Dallas, TX 65432	ABC 89A	1	REFERENCE STANDARD ABC Products 1254 61st Avenue Dallas, TX 65432
PART NUMBER	QUANTITY	DESCRIPTION												
Model 19e ^{II}	1	EDDY CURRENT INSTRUMENT NDI Instruments Inc. 987 N. Main Chicago, IL 54321												
ABC101BS 5/32" shielded absolute coil, 0.10" coil dia, 100-500 KHz.	1	EDDY CURRENT PROBE Bolt Hole Probe ABC Products 1254 61st Avenue Dallas, TX 65432												
ABC 89A	1	REFERENCE STANDARD ABC Products 1254 61st Avenue Dallas, TX 65432												
	Section IV – 57-10-20 Page 135 September 1999													

FIGURE 10-33

EXAMPLE NON-DESTRUCTIVE INSPECTION ADDITIONAL TEXT PAGE

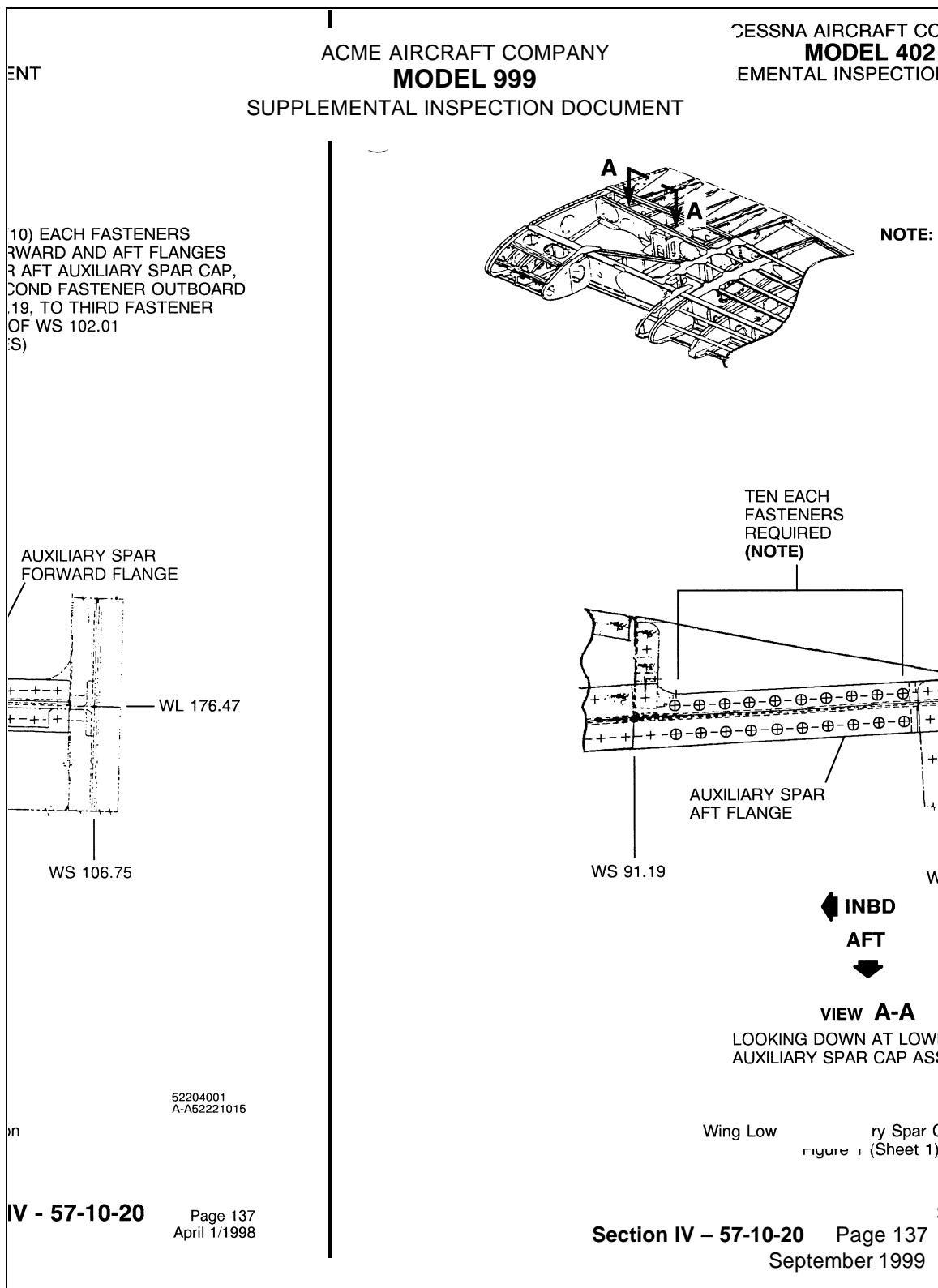
ACME AIRCRAFT COMPANY
MODEL 999
SUPPLEMENTAL INSPECTION DOCUMENT

INSPECTION INSTRUCTIONS ← 1

1. Connect the bolt hole probe (0.156" dia.) to the eddy current instrument and adjust the instrument frequency to 200 KHz.
2. Null the probe in the appropriate reference standard hole away from the calibration notch.
3. Adjust liftoff on impedance plane instrumentation so the deflection of the liftoff trace is horizontal and deflects from right to left as the probe is lifted from the part surface.
4. Adjust the instrument gain controls to obtain a signal amplitude response from the calibration notch that is a minimum of 2 major screen divisions.
5. Refer to 57-10-20 Figure 1. Inspect the inner circumference of each of the specified holes common to the wing lower aft auxiliary spar cap. Inspect the entire depth of each hole. Observe the phase and amplitude changes on the eddy current instrument.
6. If an indication is noted, carefully repeat the inspection in the opposite direction of probe rotation to verify the indication.
7. If no cracks are detected during this inspection, install CM3827AD5 rivets.
8. Cracks detected during this inspection shall be reported to Acme Customer Services Department along with the following information: Hole diameter; Location of hole; Hole Edge distance; Length and direction of crack.

FIGURE 10-34

EXAMPLE NON-DESTRUCTIVE INSPECTION ILLUSTRATION PAGE



11.0 References

- (1) DOT/FAA Contract DTFA03-98-C-00032, "Development of a Supplemental Inspection Document for Commuter Category Airplanes", September 22, 1998.
- (2) Pendley, B. J., Henslee, S. P., Manning, S. D., "Durability Methods Development, Vol. III – Structural Durability Survey: State-of-the-Art Assessment", AFFDL TR-79-3118, September 1979.
- (3) Gran, R. J., Orazio, F. D., Paris, P. C., Irwin, G. R., Hertzberg, R., "Investigation and Analysis Development of Early Life Aircraft Structural Failures", AFFDL TR-70-149, March 1971.
- (4) Swift, T., "Damage Tolerance Technology, A Course in Stress Analysis Oriented Fracture Mechanics, Phase I", dated March 30, 1998.
- (5) Niu, M. C. Y., "Airframe Stress Analysis and Sizing", Conmilit Press Ltd., 1997.
- (6) Department of Defense MIL-HDBK-5G, "Metallic Materials and Elements for Aerospace Vehicles Structures", dated November 1, 1994.
- (7) Skinn, D. A., Gallagher, J. P., Berens, A. P., Huber, P. D., Smith, J., "A Compilation of Fracture and Crack Growth Data for High Strength Alloys", Damage Tolerance Design Handbook, CINDAS/USAF CRDA Handbooks, December 1994.
- (8) "Aerospace Structural Metals Handbook", CINDAS/USAF CRDA, Purdue University, 1997 Edition.
- (9) Gallagher, J. P., Miedlar, P. C., Cross, C. W., Papp, M. L., "CRACKS 95 System", University of Dayton Research Institute, Dayton, OH, November 1995.
- (10) "ASM Metals Reference Book", 2nd Edition, American Society for Metals, 1983.
- (11) Forman, R. G., "Fatigue Crack Growth Computer Program - NASA/FLAGRO," JSC-22267, NASA/Lyndon B. Johnson Space Center, Houston, TX, August 1986, Revised 1999.
- (12) Chang, J. B. and Engle, R. M., "Improved Damage-Tolerance Analysis Methodology", Journal of Aircraft, Vol. 21, No. 9, AIAA 1984, pp. 722-730.

- (13) "Tension Testing of Metallic Materials", ASTM E8-98, Annual Book of ASTM Standards, Vol. 3.01, American Society for Testing and Materials, 1998.
- (14) "Standard Test Method for Young's Modulus, Tangent Modulus, and Chord Modulus", ASTM E111-97, Annual Book of ASTM Standards, Vol. 3.01, American Society for Testing and Materials, 1998.
- (15) "Standard Test Method for Plane-Strain Fracture Toughness of Metallic Materials", ASTM E399-90, Annual Book of ASTM Standards, Vol. 3.01, American Society for Testing and Materials, 1998.
- (16) "Standard Practice for R-Curve Determination", ASTM E561-94, Annual Book of ASTM Standards, Vol. 3.01, American Society for Testing and Materials, 1998.
- (17) Harter J. A., "AFGROW Users Guide and Technical Manual", AFRL-VA-WP-TR-1999-3016, February 1999.
- (18) Engineering Sciences Data Unit, "Fatigue-Fracture Mechanics", Volumes 1-4, ESDU International, London, UK.
- (19) "Standard Test Method for Measurement of Fatigue Crack Growth Rates", ASTM E647-95a, Annual Book of ASTM Standards, Vol. 3.01, American Society for Testing and Materials, 1998.
- (20) "Standard Practices for Force Verification of Testing Machines", ASTM E4-98, Annual Book of ASTM Standards, Vol. 3.01, American Society for Testing and Materials, 1998.
- (21) "Standard Practice for Verification of Constant Amplitude Dynamic Loads and Displacements in an Axial Load Fatigue Testing System", ASTM E467-90, Annual Book of ASTM Standards, Vol. 3.01, American Society for Testing and Materials, 1998.
- (22) Willenborg, J., Engle, R. M., and Wood, H. A., "A Crack Growth Retardation Model Using An Effective Stress Concept", Air Force TM 71-1-FBR, dated January 1971.
- (23) Gallagher, J. P., "A Generalized Development in Yield Zone Models", USAF TM FBR-74-28, dated January 1974.
- (24) Gallagher, J. P. and Hughes, T. F., "Influence of Yield Zone Strength on Overload Affected Fatigue Crack Growth Behavior in 4340 Steel", AFFDL-TR-74-27, dated July 1974.

- (25) Probst, E. P. and Hillberry, B. M., "Fatigue Crack Delay and Arrest Due to Single Peak Tensile Overloads", AIAA Paper No. 73-325, AIAA Dynamics Specialists Conference, Williamsburg, VA., March 1973.
- (26) "Standard Practice for Conducting Force Controlled Constant Amplitude Axial Fatigue Tests of Metallic Materials", ASTM E466-96, Annual Book of ASTM Standards, Vol. 3.01, American Society for Testing and Materials, 1998.
- (27) "Standard Practice for Presentation of Constant Amplitude Fatigue Test Results for Metallic Materials", ASTM E468-90, Annual Book of ASTM Standards, Vol. 3.01, American Society for Testing and Materials, 1998.
- (28) ASTM, STP 588, "Manual on Statistical Planning and Analysis", Little, R.E., American Society of Testing and Materials, 1975.
- (29) FAA Report ACE-100-01, "Fatigue Evaluation of Empennage, Forward Wing, and Winglets/Tip Fins on Part 23 Airplanes", dated February 15, 1994.
- (30) FAA Report AFS-120-73-2, "Fatigue Evaluation of Wing and Associated Structure on Small Airplanes", dated May 1973.
- (31) FAA Report DOT/FAA/CT-91/20, "General Aviation Aircraft-Normal Acceleration Data Analysis and Collection Project", dated February 1993.
- (32) NASA TM-84660, "Tabulations of Recorded Gust and Maneuver Accelerations and Derived Gust Velocities for Airplanes in the NASA VGH General Aviation Program", dated 1983.
- (33) MIL-A-8866B (USAF), "Airplane Strength and Rigidity Reliability Requirements, Repeated Loads and Fatigue", 22 August 1975.
- (34) Jewel, J. W., Jr., "Progress Report on the NASA V-G/VGH General Aviation Program", NASA Aircraft Safety and Operating Problems, Volume I, NASA SP-270, 1971, pp. 347-390.
- (35) Engineering Sciences Data Unit, "Average Gust Frequencies, Subsonic Transport Aircraft", ESDU 69023, The Royal Aeronautical Society.
- (36) MIL-A-87221 (USAF), "Military Specification, Aircraft Structures, General Specifications For", 28 February 1985.
- (37) Engineering Sciences Data Unit, "Frequencies of Vertical and Lateral Load Factors Resulting from Ground Maneuvers of Aircraft", ESDU 75008, The Royal Aeronautical Society.

- (38) FAA Report DOT/FAA/CT-93/69.II, "Damage Tolerance Assessment Handbook Volume II: Airframe Damage Tolerance Evaluation", dated October 1993.
- (39) MIL-A-8866A (USAF), "Airplane Strength and Rigidity Reliability Requirements, Repeated Loads and Fatigue", 31 March 1971.
- (40) TN-505, "Strain Gage Selection Criteria, Procedures, Recommendations," Technical Notes and Tips from Measurements Group Inc., Micro-Measurement Division, Raleigh, NC.
- (41) TN-502, "Optimizing Strain Gage Excitation Levels," Technical Notes and Tips from Measurements Group Inc., Micro-Measurement Division, Raleigh, NC.
- (42) TT-603, "The Proper Use of Bondable Terminals in Strain Gage Applications," Technical Notes and Tips from Measurements Group Inc., Micro-Measurement Division, Raleigh, NC.
- (43) TT-604, "Lead Wire Attachment Techniques for Obtaining Maximum Fatigue Life of Strain Gages," Technical Notes and Tips from Measurements Group Inc., Micro-Measurement Division, Raleigh, NC.
- (44) TN-514, "Shunt Calibration of Strain Gage Instrumentation," Technical Notes and Tips from Measurements Group Inc., Micro-Measurement Division, Raleigh, NC.
- (45) TN-504, "Temperature Induced Apparent Strain and Gage Factor Variation in Strain Gages," Technical Notes and Tips from Measurements Group Inc., Micro-Measurement Division, Raleigh, NC.
- (46) Gardenhire, L.W., AGARD Flight Test Instrumentation Series, Volume 1, "Basic Principles of Flight Test Instrumentation Engineering, Section 6 – Sampling and Filtering."
- (47) TN-507, "Errors Due to Wheatstone Bridge Nonlinearly," Technical Notes and Tips from Measurements Group Inc., Micro-Measurement Division, Raleigh, NC.
- (48) "Microsoft Excel Function Reference Guide, V.4.0", Microsoft Excel software documentation, dated 1992.
- (49) "Standard Practice for Cycle Counting in Fatigue Analysis", ASTM E1049-85, Annual Book of ASTM Standards, Vol. 3.01, American Society for Testing and Materials, 1998.
- (50) United States Air Force, AFGS-87221A, "General Specification For Aircraft Structures", dated June 8, 1990.

- (51) Tada, H., Paris, P. C., and Irwin, G. R., "The Stress Analysis of Cracks Handbook", Del Research Corporation, Hellertown, PA, 1973.
- (52) Rooke, D. P., and Cartwright, D. J., "Compendium of Stress Intensity Factors", H.M., Stationary Office, London, 1975.
- (53) Sih, G. C., "Handbook of Stress Intensity Factors", Lehigh University, Bethlehem, PA, 1973.
- (54) Murakami, Y., (ed.), "Stress Intensity Factors Handbook", Pergamon Press, New York, 1987.
- (55) Elber, W., "The Significance of Fatigue Crack Closure", in "Damage Tolerance in Aircraft Structures," ASTM STP 486, American Society for Testing and Materials, Philadelphia, PA, 1971.
- (56) Gallagher, J. P., Miedlar, P. C., "CRACKS 98 System", University of Dayton Research Institute, Dayton, OH, 1999.
- (57) Elber, W., "Equivalent Constant Amplitude Concept for Crack Growth Under Spectrum Loading," in "Fatigue Crack Growth Under Spectrum Loads", ASTM STP 595, American Society for Testing and Materials, Philadelphia, PA, 1976.
- (58) Newman, J. C., Jr., "A Crack Closure Model for Predicting Fatigue Crack Growth Under Aircraft Spectrum Loading", in "Methods and Models for Predicting Fatigue Crack Growth Under Random Loading", ASTM STP 748, 1981.
- (59) "Stress Check," available from Engineering Software Research & Development, Inc., St. Louis, MO.
- (60) Swenson, D., and James, M, "FRANC2D/L: A Crack Propagation Simulator for Plane Layered Structures," version 1.4, 1997.
- (61) "BEASY", available from Computational Mechanics, Inc., Billerica, MA.
- (62) Glinka, G., and Shen, G., "Universal Features of Weight Functions for Cracks in Mode I", Engineering Fracture Mechanics, Vol. 40, pp. 1135-1146, 1991.
- (63) Shen, G., and Glinka, G., "Weight Functions for a Surface Semi-Elliptical Crack in a Finite Thickness Plate", Theoretical and Applied Fracture Mechanics, Vol. 15, pp. 247-255, 1991.
- (64) Shen, G., and Glinka, G., "Determination of Weight Functions from Reference Stress Intensity Factors", Theoretical and Applied Fracture Mechanics, Vol. 15, pp. 237-245, 1991.

- (65) Moftakhar, A., and Glinka, G., "Calculation of Stress Intensity Factors by Efficient Integration of Weight Functions", Engineering Fracture Mechanics, Vol. 40, pp. 749-756, 1992.
- (66) Zheng, X. J., Glinka, G., and Dubey, R. N., "Stress Intensity Factors and Weight Functions for a Corner Crack in a Finite Thickness Plate", Engineering Fracture Mechanics, Vol. 51, pp. 49-61, 1996.
- (67) Kiciac, A., Glinka, G., and Eman, M., "Weight Functions and Stress Intensity Factors for Corner Quarter-Elliptical Crack in Finite Thickness Plate Subjected to In-plane Loading", Engineering Fracture Mechanics, Vol. 60, No. 2, pp. 221-238, 1998.
- (68) Swift T., "The Effects of Fastener Flexibility and Stiffener Geometry on the Stress Intensity in Stiffened Cracked Sheet", Douglas Paper 6211, presented to Conference on Prospects of Fracture Mechanics, Delft, Netherlands, June 24, 1974.
- (69) Swift T., "Fracture Analysis of Adhesively Bonded Cracked Panels", Transactions of the ASME, Volume 100, January 1978, Paper No. 77-WA/Mat-2.
- (70) Swift T., "Damage Tolerance Analysis of Redundant Structures", Douglas Paper 6673, presented to Fracture Mechanics Design Methodology AGARD-NATO Lecture Series, Delft, Netherlands, October, 1978.
- (71) Swift T., "Fracture Analysis of Stiffened Structure", Damage Tolerance of Metallic Structures: Analysis Methods and Application, ASTM STP 842, J. B. Chang and J. L. Rudd, Eds., American Society for Testing and Materials, 1984, pp. 69-107.
- (72) Tate, M. B., and Rosenfeld, S. J., "Preliminary Investigation of the Loads Carried by Individual Bolts in Bolted Joints", NACA TN 1051, May 1946.
- (73) Kuhn, P., "Notch Effects on Fatigue and Static Strength", Proceedings of International Conference on Aeronautical Fatigue, Rome, Italy, 1963.
- (74) Chen, D., and Schijve, J., "Bulging of Fatigue Cracks in a Pressurized Aircraft Fuselage", Report LR-644, Delft University of Technology, Delft, The Netherlands, May 1991.
- (75) Riks, E., "Bulging Cracks in Pressurized Fuselages: A Numerical Study", NLR MP-8705-U, National Aerospace Laboratory, The Netherlands, 1987.
- (76) Bakuckas, J. G., Jr., Nguyen, P. V., Bigelow, C. A., Broek, D., "Bulging Factors for Predicting Residual Strength of Fuselage Panels", Proceedings of International Conference on Aeronautical Fatigue, Edinburgh, Scotland, June 1997.

- (77) Swift, T., "Unarrested Fast Fracture", Presented to International Workshop on Structural Integrity of Aging Airplanes, Atlanta, Georgia, 31 March-April 1992.
- (78) Swift, T., "Damage Tolerance Capability", Fatigue of Aircraft Materials, Delft University Press, 1992.
- (79) Pilkey, W. D., "Peterson's Stress Concentration Factors", 2nd Edition, John Wiley & Sons, New York, 1997.
- (80) Heywood, R. B., "Designing Against Fatigue of Metals", Reinhold Press, 1962.
- (81) Niu, M. C. Y., "Airframe Structural Design", Conmilite Press Ltd., 1988.
- (82) Swift, T., "Widespread Fatigue Damage Monitoring-Issues and Concerns," Proceedings from 5th International Conference on Structural Airworthiness of New and Aging Aircraft, June 16-18, 1993.
- (83) Maclin, J., "Performance of Fuselage Pressure Structure", Proceedings of 1991 International Conference on Aging Aircraft and Structural Airworthiness, NADSA CP-3160.
- (84) Lincoln, J., "Risk Assessments of Aging Aircraft", Presented at the First DoD, FAA, NASA Aging Aircraft Conference, Ogden, Utah, July 1997.
- (85) NRC Report Publication NMAB-488-2, Aging of U.S. Air Force Aircraft, National Academy Press, 2101 Constitution Avenue, N.W., Box 285, Washington, D.C. 20055.
- (86) "Structural Fatigue Evaluation for Aging Airplanes", Final Report of the Airworthiness Assurance Working Group - Industry Committee on Widespread Fatigue Damage, R. Wickens, Chairman, October 1993.
- (87) General Dynamics Convair Division, "Programmed Instruction Books: Nondestructive Testing Eddy Current", American Society for Nondestructive Testing, Columbus, Ohio, 1980.
- (88) General Dynamics Convair Division, "Programmed Instruction Books: Nondestructive Testing Magnetic Particle", American Society for Nondestructive Testing, Columbus, Ohio, 1977.
- (89) General Dynamics Convair Division, "Programmed Instruction Books: Nondestructive Testing Ultrasonic", American Society for Nondestructive Testing, Columbus, Ohio, 1981.

- (90) General Dynamics Convair Division, "Programmed Instruction Books: Nondestructive Testing Liquid Penetrant", American Society for Nondestructive Testing, Columbus, Ohio, 1977.
- (91) General Dynamics Convair Division, "Programmed Instruction Books: Nondestructive Testing Radiography", American Society for Nondestructive Testing, Columbus, Ohio, 1983.
- (92) Hagemaiier, D., Bates, B., and Christina, D., "Optically Aided Visual Inspection of Aircraft Structure", Materials Evaluation, December 1988, American Society for Nondestructive Testing, Columbus, Ohio.
- (93) McIntire, P., ed., "Nondestructive Testing Handbook - Second Edition Volume 6: Magnetic Particle Testing", American Society for Nondestructive Testing, Columbus, Ohio, 1989.
- (94) McIntire, P., ed., "Nondestructive Testing Handbook - Second Edition Volume 4: Electromagnetic Testing", American Society for Nondestructive Testing, Columbus, Ohio, 1986.
- (95) McIntire, P., ed., "Nondestructive Testing Handbook - Second Edition Volume 7: Ultrasonic Testing", American Society for Nondestructive Testing, Columbus, Ohio, 1991.
- (96) McMaster, R., ed., "Nondestructive Testing Handbook - Second Edition Volume 2: Liquid Penetrant Tests", American Society for Nondestructive Testing, Columbus, Ohio, 1982.
- (97) Rummel, W. D., "Probability of Detection As a Quantitative Measure of Nondestructive Testing End-To-End Process Capabilities", Materials Evaluation, January 1998, American Society for Nondestructive Testing, Columbus, Ohio.
- (98) United States Air Force, Technical Order T.O. 33B-1-1, "Nondestructive Inspection Methods", United States Department of Defense, Kelly Air Force Base, Texas, March 1990.
- (99) Rummel, W. D., et al., "Nondestructive Evaluation (NDE) Capabilities Data Book", NTIAC: DB-95-02, Contract DLA900-90-D-0123.
- (100) "Specification for Continuing Airworthiness Program", GAMA Specification No. 7, March 1991.

Appendix A: Flight Profile Length Determination

A.1 Calculation of Weibull Parameters

An example using a Microsoft Excel spreadsheet best illustrates how to perform a Weibull statistical analysis on operator usage data. Table A-1 presents the results of an example survey. For this example, special usage aircraft are not included in the data.

TABLE A-1
EXAMPLE FLIGHT DISTRIBUTION DATA

Raw Data Returned from Survey		Segmented Data for Histogram	
Flight Time (Hrs)	Occurrences	Flight Time (Hrs)	Occurrences
0.10	2		
0.20	1	0.2	4
0.30	0		
0.40	1		
0.50	4		
0.60	4		
0.65	1	0.6	12
0.70	2		
0.75	1		
0.80	4		
1.00	1	1.0	11
1.10	4		
1.20	2		
1.25	3		
1.40	3	1.4	9
1.55	3		
1.70	2		
1.80	3	1.8	6
2.00	1		
2.10	1		
2.20	2	2.2	4
2.30	1		
2.50	1	2.6	2
2.70	1		
3.00	0		
3.40	1	3.4	1
3.80	0		
4.20	0	5.0	1
5.00	1		
		Sum of Occurrences = 50	

The first step after completing the usage survey is to divide the data into groups representing six to fifteen time intervals as shown in Table A-1 (right column). This will reduce the data to a manageable number of groups. This data can be plotted on a histogram as shown in Figure A-1. The next step is to calculate the actual probability of each of the groups of flights occurring as shown in Table A-2.

FIGURE A-1

TYPICAL FLIGHT DISTRIBUTION HISTOGRAM

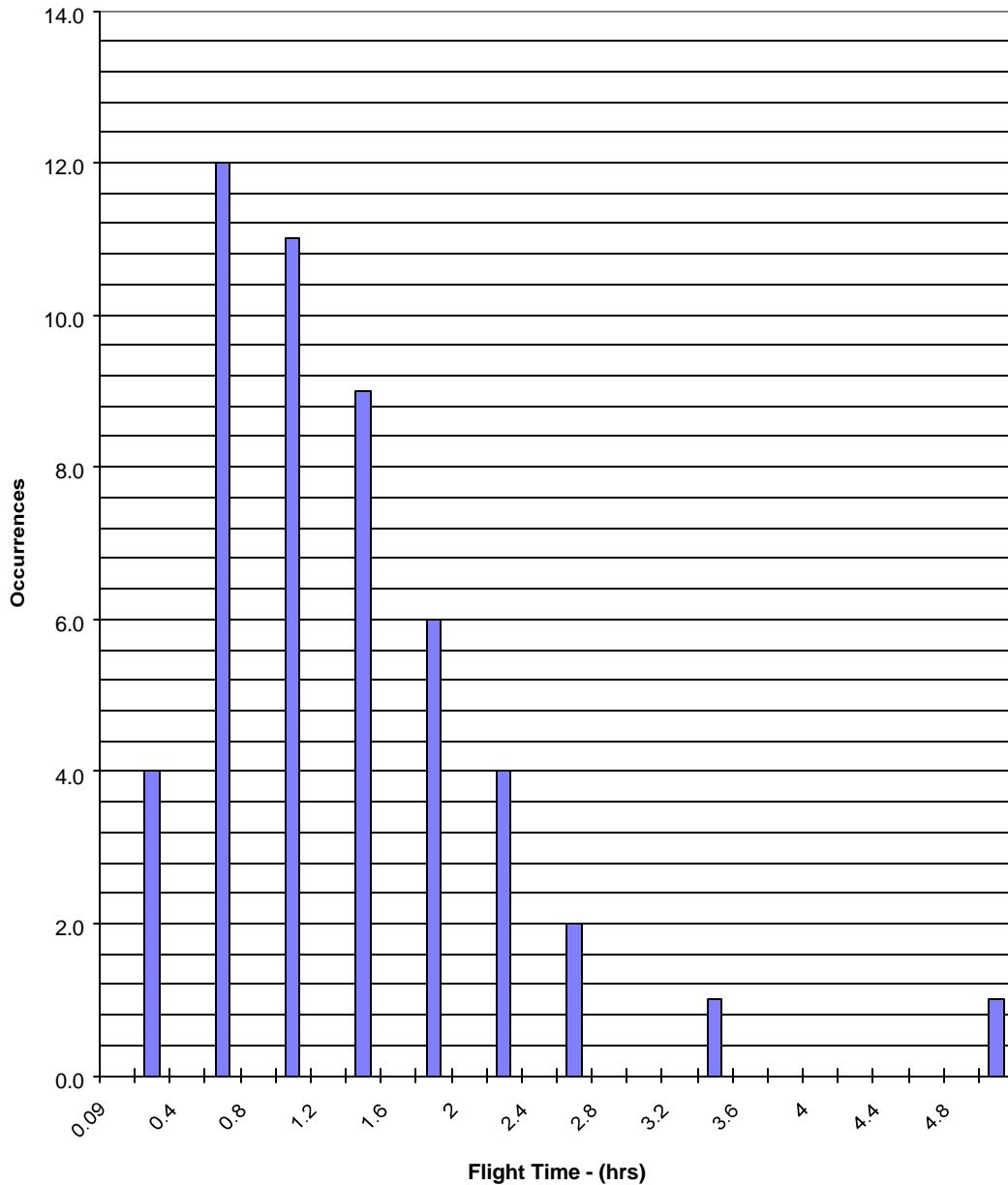



TABLE A-2

PROBABILITY OF OCCURRENCE CALCULATION

Flight Time (hrs)	Occurrences	Probability of Occurrence
0.2	4	0.080
0.6	12	0.240
1.0	11	0.220
1.4	9	0.180
1.8	6	0.120
2.2	4	0.080
2.6	2	0.040
3.4	1	0.020
5.0	1	0.020
Sum of Occurrences =	50	

$$\text{Prob. of Occ.} = \frac{\text{Occurrences}}{\text{Sum of Occurrences}}$$


To calculate the Weibull density function, the parameters η , the characteristic life and β , the shape parameter must be determined. An iterative procedure using Excel's "solver" function can be used to determine the best shape parameter and characteristic life. The Flight Occurrence Probability, which is the integration of the Weibull Probability Density Function between 0 and t, is calculated as the first step in solving for the Weibull parameters. The Flight Occurrence Probability is defined as:

$$F(t) = 1 - e^{-\left[\frac{t}{\eta}\right]^\beta}$$

Table A-3 shows the calculation of the Flight Occurrence Probability in the Excel spreadsheet. To solve this equation, initial values of β and η are assumed. For the characteristic life, η , the average flight length (in hours) of all the usage data is selected (1.30 hours for this example). The initial shape parameter, β , chosen is 1.25.

The probability of a flight time between times t_1 and t_2 is the occurrence probability of a flight of length t_2 less the occurrence probability of a flight of length t_1 :

$$F(\Delta t) = F(t_2) - F(t_1)$$

TABLE A-3

CALCULATION OF FLIGHT OCCURRENCE PROBABILITY

Flight Time (hrs)	Occurrences	Probability of Occurrence	Flight Occurrence Probability (F(t _i))
0.2	4	0.080	0.092
0.6	12	0.240	0.317
1.0	11	0.220	0.515
1.4	9	0.180	0.668
1.8	6	0.120	0.779
2.2	4	0.080	0.856
2.6	2	0.040	0.908
3.4	1	0.020	0.965
5.0	1	0.020	0.996
Sum of Occurrences =	50		

Shape Parameter, $\beta = 1.25$
 Characteristic Life, $\eta = 1.30$

$$F(t) = 1 - e^{-\left(\frac{t}{\eta}\right)^\beta}$$

The time increment, Δt , contains the number of flights greater than time t_1 , but less than time t_2 . So the occurrence probability is the percentage of flight times that occur between time t_1 and time t_2 . This is the same value as the actual probability that was calculated from usage data in Table A-2. Table A-4 shows the calculation of $F(\Delta t)$.

TABLE A-4

CALCULATION OF F(ΔT)

Flight Time (hrs)	Occurrences	Probability of Occurrence	Flight Occurrence Probability (F(t _i))	F ^Δ (t)
0.2	4	0.080	0.092	0.092
0.6	12	0.240	0.317	0.225
1.0	11	0.220	0.515	0.197
1.4	9	0.180	0.668	0.153
1.8	6	0.120	0.779	0.111
2.2	4	0.080	0.856	0.077
2.6	2	0.040	0.908	0.052
3.4	1	0.020	0.965	0.056
5.0	1	0.020	0.996	0.031
Sum of Occurrences =	50			

Shape Parameter, $\beta = 1.25$
 Characteristic Life, $\eta = 1.30$

where:

$$F\Delta(t) = F(t_2) - F(t_1) = \text{Flight Occ. Prob. } (F(t_2)) - \text{Flight Occ. Prob. } (F(t_1))$$

In order to calculate the correct Weibull parameters, the Excel solver tool should be used to vary β and η until the sum of the squares of the differences between the actual probability and the occurrence probability is minimized. This is a least squares error fit. Table A-5 shows this calculation before starting the solver in the example.

TABLE A-5
CALCULATION OF LEAST SQUARES ERROR

Flight Time (hrs)	Occurrences	Probability of Occurrence	Flight Occurrence Probability (F(t _i))	F ^Δ (t)	Least Squares Error
0.2	4	0.080	0.092	0.092	0.000148666
0.6	12	0.240	0.317	0.225	0.000218043
1.0	11	0.220	0.515	0.197	0.000512369
1.4	9	0.180	0.668	0.153	0.000741538
1.8	6	0.120	0.779	0.111	0.000080345
2.2	4	0.080	0.856	0.077	0.000006972
2.6	2	0.040	0.908	0.052	0.000148686
3.4	1	0.020	0.965	0.056	0.001322884
5.0	1	0.020	0.996	0.031	0.000120865
Sum of Occurrences =	50			Sum of Least Squares =	0.003300368

Shape Parameter, $\beta = 1.25$
 Characteristic Life, $\eta = 1.30$

where:

$$\text{Least Squares Error} = [(F(t_2) - F(t_1)) - (\text{Probability of Occurrence})]^2$$

The Microsoft Excel solver window is shown in Figure A-2. To solve the Weibull analysis for the best possible β and η , the sum of the least squares is to be minimized by varying the β and η values.

FIGURE A-2

MICROSOFT EXCEL SOLVER WINDOW

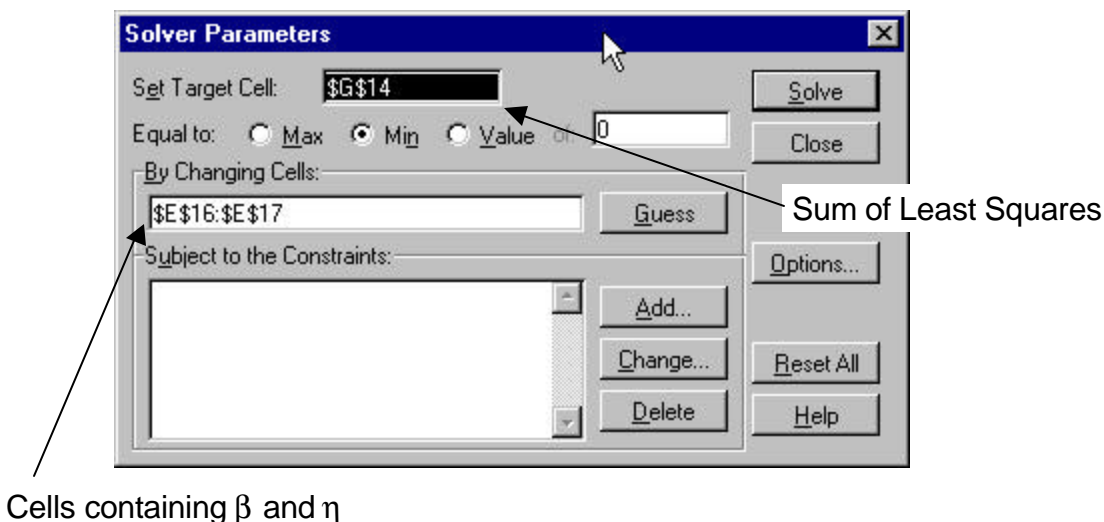


Table A-6 shows the example table after the solver was run. The β and η values have been iterated until the sum of the least squares was minimized. Table A-6 shows that the actual probability and the calculated probability are now very close. The solver should be run with a different set of starting β and η values to verify the β and η values match those that were first calculated. It is possible for the β and η values to find a local valley in the convergence curve and therefore not the correct values.

TABLE A-6

CALCULATION OF β AND η VALUES BY ITERATION

Flight Time (hrs)	Occurrences	Probability of Occurrence	Flight Occurrence Probability ($F(t_i)$)	$F^{\Delta}(t)$	Least Squares Error
0.2	4	0.080	0.069	0.069	0.000116740
0.6	12	0.240	0.287	0.217	0.000515045
1.0	11	0.220	0.500	0.214	0.000038367
1.4	9	0.180	0.672	0.172	0.000067631
1.8	6	0.120	0.796	0.124	0.000014682
2.2	4	0.080	0.879	0.083	0.000007437
2.6	2	0.040	0.931	0.052	0.000145266
3.4	1	0.020	0.980	0.049	0.000840601
5.0	1	0.020	0.999	0.019	0.000000816
Sum of Occurrences =	50			Sum of Least Squares =	0.001746586

Shape Parameter, $\beta = 1.410153$
 Characteristic Life, $\eta = 1.296000$

A.2 Flight Length Distribution

The mean flight time between t_1 and t_2 represents the flight time for any given profile and is defined as:

$$\text{Mean} = \frac{\int_{t_1}^{t_2} t \cdot p(t) dt}{\text{Area}} + \Gamma$$

where Γ = the minimum life (typically a minimum of 0.09 hours)
 $p(t)$ = Weibull Probability Density Function
 Area = $F(t_2) - F(t_1)$

To solve for the mean flight time of each flight profile, the t_1 and t_2 time increments for each profile are used. The mean flight time equation needs to be integrated between time t_2 and time t_1 . Also, the occurrence probability of each profile occurring between time t_2 and time t_1 , ($F(t_2) - F(t_1)$) can be calculated with time increments. Table A-7 shows the Microsoft Excel spreadsheet of the example problem that calculates the mean flight time of each flight profile and the occurrence probability of each profile.

TABLE A-7

CALCULATION OF MEAN PROFILE TIME AND OCCURRENCE PROBABILITY

Flight Profile	t_1 (hours)	t_2 (hours)	Weibull Probability Density Function	Flight Occurrence Probability ($F(t_i)$)	$F(t_2)-F(t_1)$	Mean Flight Time (hours)
1	0.09		0.3560	0.023		
		0.3	0.5258	0.119	0.119	0.250
2	0.3		0.5258	0.119		
		0.79	0.5400	0.392	0.273	0.636
3	0.79		0.5400	0.392		
		1.21	0.4268	0.597	0.205	1.080
4	1.21		0.4268	0.597		
		1.79	0.2567	0.793	0.197	1.562
5	1.79		0.2567	0.793		
		2.41	0.1275	0.909	0.116	2.150
6	2.41		0.1275	0.909		
		4.59	0.0048	0.997	0.088	3.101

The final step in determining flight profile utilization is to create a summary table that specifies the percentage of total flights and total hours each profile makes up. This data is used to calculate flight profile segment data used in stress equation calculations. Table A-8 shows an example of a flight profile utilization table.

TABLE A-8

FLIGHT PROFILE UTILIZATION TABLE EXAMPLE

Flight Profile	Flight Description	t ₁ (hours)	t ₂ (hours)	Mean Flight Time (hours)	F(t ₂)-F(t ₁)	% Total of Flights	% Total of Flight Hours
1	Checkout	0.09	0.30	0.250	0.119	11.9%	2.4%
2	Short Range	0.30	0.79	0.636	0.273	27.3%	13.8%
3	Medium Range	0.79	1.21	1.080	0.205	20.5%	17.6%
4	Medium Range	1.21	1.79	1.562	0.197	19.7%	24.5%
5	Long Range	1.79	2.41	2.150	0.116	11.6%	19.8%
6	Long Range	2.41	4.59	3.101	0.088	8.8%	21.8%
					Σ = 1.00	Σ = 100%	Σ = 100%

Average Flight Length = 1.26 hours

In this table, the F(t₂) - F(t₁) is the probability of occurrence of that flight profile. This number multiplied by 100 gives the % Total of Flights column. This value represents the percentage of flights for each particular profile that would occur. The % Total of Flight Hours is calculated from:

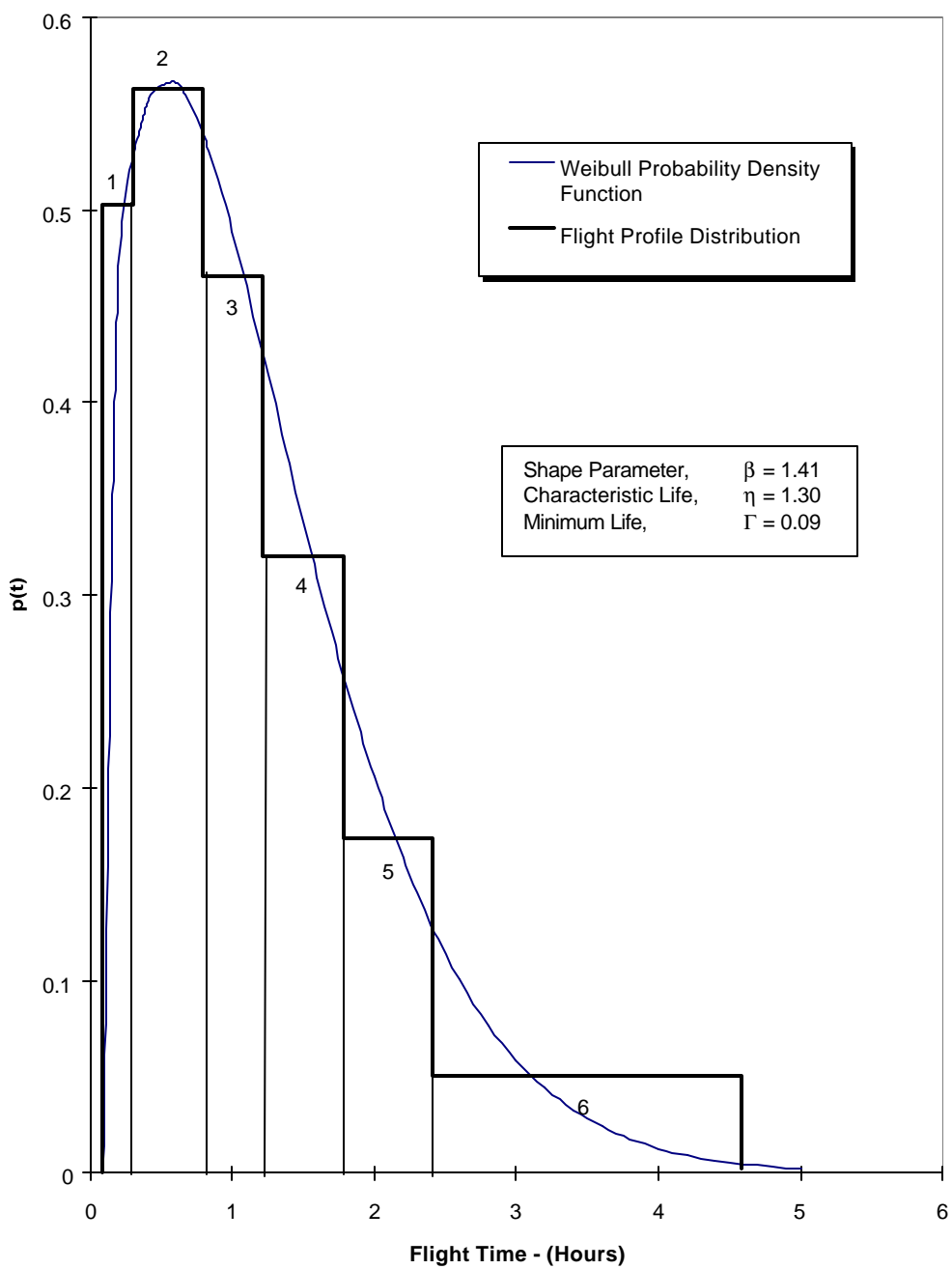
$$\% \text{ Total of Flight Hours} = \frac{(\% \text{ Total of Flights} \times \text{Mean Flight Time})}{\sum (\% \text{ Total of Flights} \times \text{Mean Flight Time})}$$

The average flight length of all of the flight profiles is calculated from (this value should be close to the Characteristic Life, η used in the Weibull equations):

$$\text{Average Flight Length} = \frac{\sum (\% \text{ Total of Flights} \times \text{Mean Flight Time})}{100}$$

After determining each flight profile's mean flight time and probability of occurrence, the flight distribution should be plotted with the Weibull Probability Density function to verify if the data fits a Weibull statistical distribution. Figure A-3 shows this comparison.

FIGURE A-3
FLIGHT LENGTH DISTRIBUTION



Appendix B: Flight Profile Data Calculations

This appendix presents a systematic procedure for calculating flight profile data. The data presented here can be used in hand calculations or in the construction of a computer program. Table B-1 presents an example of a flight profile table. The ramp weight for this example airplane is 6,185 lbs with 875 lbs of fuel and 23.21% cg location (Fuselage Station 153.50).

TABLE B-1

EXAMPLE FLIGHT PROFILE TABLE

<u>Flight Load Segment</u>	<u>Start-End Altitude</u>	<u>Total Fuel (lb)</u>	<u>GRWT (lb)</u>	<u>Segment Time-min</u>	<u>KEAS</u>	<u>Mach</u>	<u>ALT (ft)</u>	<u>%CG</u>	<u>Diff. Press (psi)</u>	<u>Thrust (lb)</u>
Taxi/Takeoff Roll		860	6170	N/A	0	0	0	23.21	0	0
Climb	0-5000 ft	834	6144	6.04	120	0.19	2500	23.22	0	874
Climb	5000-8300 ft	816	6126	4.45	120	0.205	6650	23.23	0	801
Cruise	8300-8300 ft	773	6083	26.60	146	0.257	8300	23.24	0	517
Cruise	8300-8300 ft	701	6011	26.60	146	0.257	8300	23.27	0	514
Cruise	8300-8300 ft	629	5939	26.60	146	0.257	8300	23.30	0	514
Descent	8300-2000 ft	574	5884	12.60	170	0.282	5150	23.33	0	451
Approach	2000-0 ft	543	5853	2.97	102	0.158	1000	23.34	0	76
Maneuver - 15° Flap		543	5853	N/A	102	0.158	1000	23.34	0	76
Maneuver - 45° Flap		543	5853	N/A	102	0.158	1000	23.34	0	76
Landing Impact		531	5841	N/A	0	0	0	23.34	0	0
Landing Roll/Taxi to Ramp		516	5826	N/A	0	0	0	23.44	0	0

The steps required to calculate the data in the profile table are:

1. Determine the amount of fuel used during the taxi/takeoff roll segment. This value is usually presented in the Pilots Operating Handbook (POH) or Flight Manual. The average of the initial fuel and the fuel remaining at the end of the takeoff roll is used to calculate the profile segment parameters.
2. Calculate the average remaining fuel weight, gross weight, and cg position for the taxi/takeoff roll segment. One half of the total weight of fuel burned during

the taxi/takeoff roll is subtracted from the starting aircraft gross weight to get the average taxi/takeoff roll gross weight. To calculate the average aircraft cg location during taxi/takeoff roll the following formula was used (fuel weight cg is usually found in the POH):

$$\text{GRWT} \times \text{Aircraft cg} = \text{ZFW} \times \text{ZFW Aircraft cg} + \text{FW} \times \text{Fuel Weight cg}$$

$$6,170 \text{ lb} \times \text{Aircraft cg} = (5,310 \text{ lb}) \times (153.13 \text{ in}) + (860 \text{ lb}) \times (155.84 \text{ in})$$

$$6,170 \text{ lb} \times \text{Aircraft cg} = (813,120 \text{ in-lb}) + (134,022 \text{ in-lb})$$

$$6,170 \text{ lb} \times \text{Aircraft cg} = 947,142 \text{ in-lb}$$

$$\text{Aircraft cg} = 947,142 \text{ in-lb} / 6,170 \text{ lb}$$

$$\text{Aircraft cg} = 153.51 \text{ in}$$

The mean aerodynamic chord (MAC) can be found in the POH. For this example, the MAC is 61.99 in. and starts at FS 139.12. Therefore the %cg for this example is:

$$\%cg = [(\text{Aircraft cg FS} - \text{MAC Leading edge FS}) / \text{MAC}] \times 100$$

$$\%cg = [(153.51 \text{ in} - 139.12 \text{ in}) / 61.99 \text{ in}] \times 100$$

$$\%cg = [14.39 \text{ in} / 61.99 \text{ in}] \times 100$$

$$\%cg = 23.21$$

Figure B-1 illustrates the MAC concept.

3. To determine climb segment parameters, the time and fuel to climb to cruising altitude is required. These values can be determined from a "Time, Fuel, and Distance to Climb" chart that is usually found in the POH. Figure B-2 shows an example of this kind of chart. By knowing the cruise altitude and the aircraft gross weight at the beginning of the climb, the total time and fuel to climb to the cruise altitude can be determined. If the climb portion of the profile has been split into more than one segment, this chart can be used to determine the incremental times and fuel burn for each segment.
4. Calculate the average gross weight for each climb segment by subtracting out the weight of fuel burned.
5. Calculate the average %cg for the climb segments using the equation in Step 2.

FIGURE B-1

MEAN AERODYNAMIC CHORD CONCEPT

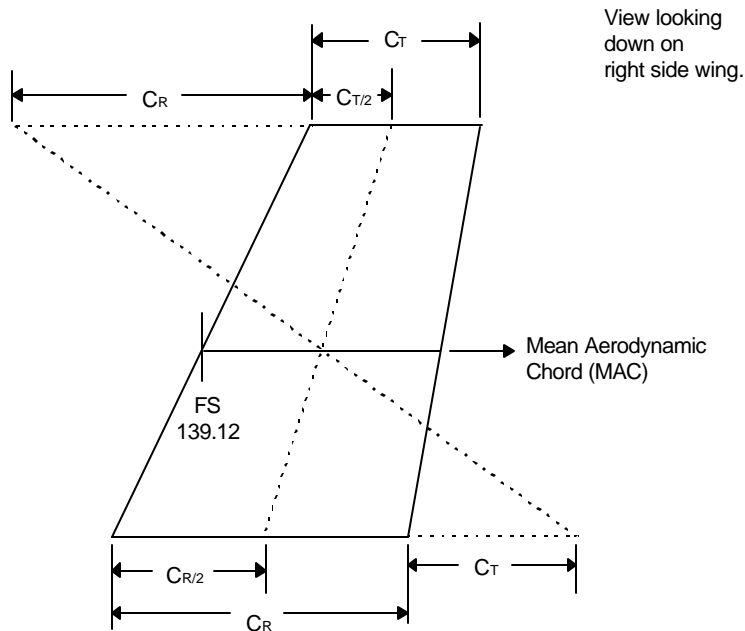
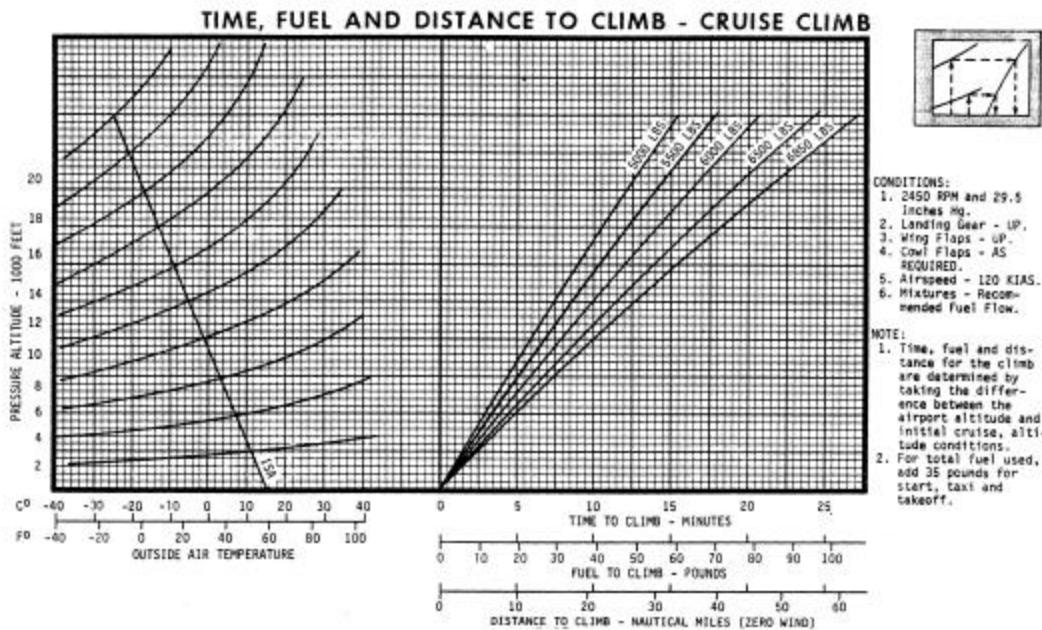


FIGURE B-2

TIME, FUEL, AND DISTANCE TO CLIMB EXAMPLE CHART



6. Determine climb speed. The climb speed is usually defined in the “Time, Fuel, and Distance to Climb” chart or in the POH. Mach number can then be calculated for each climb segment. Since airspeed is defined as equivalent airspeed in Table B-1, it needs to be converted to true airspeed before the Mach number can be calculated.

$$V_{\text{True}} = V_{\text{Equiv}} \sqrt{\frac{\rho_{\text{Sea Level}}}{\rho_{\text{At Altitude}}}}$$

Then:

$$\text{Mach} = \frac{V_{\text{True}}}{V_{\text{Speed of sound at altitude}}}$$

where both ρ and the speed of sound can be found in standard atmosphere tables.

7. Before calculating the cruise parameters, the time and fuel to descend are calculated. Go to the POH “Time, Fuel, and Distance to Descend” chart. Using the cruise altitude, the time and fuel to descend can be determined. Figure B-3 shows an example of this chart.
8. To determine the time spent in the cruise portion of the profile, subtract both the time to climb and time to descend from cruise altitude from the total flight time of the profile. This remaining time is the total amount of time spent cruising.
9. Calculate cruise parameters. In the POH “Cruise Performance” tables, cruise speeds and fuel burn rates can be found. Using the time spent cruising, the total amount of fuel burned during cruise can be calculated. The average cruise segment gross weight can be calculated after the average fuel weight remaining is determined. Finally, the cg location can be calculated as shown previously in Step 2. Repeat this step for each cruise segment.
10. Calculate descent parameters with the values already determined in Step 7. For each descent and approach segment, Steps 4-6 should be repeated using descent values.
11. Repeat approach segment parameters for both approach flap maneuver and landing flap maneuver segments.
12. Calculate weight and cg location for the landing impact segment. Use the end of the approach segment weights rather than an average weight because landing impact is an instantaneous event.

13. Calculate the average landing roll/taxi fuel and gross weights and cg location. Subtract half of the landing roll/taxi fuel weight used from the landing impact segment weights.

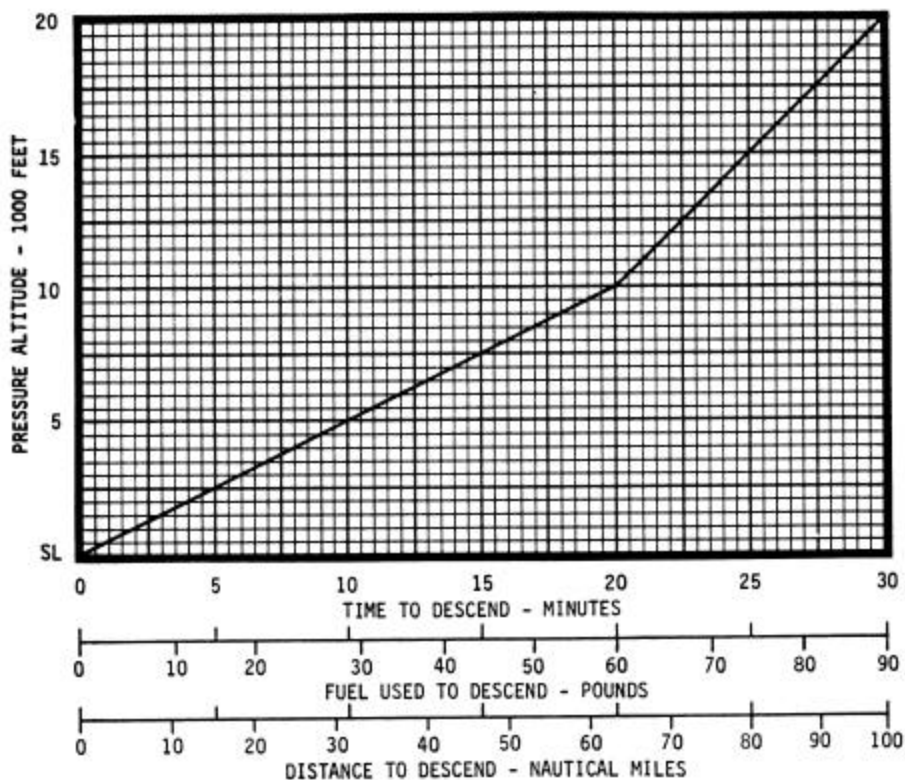
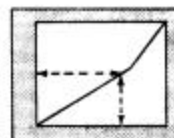
FIGURE B-3

TIME, FUEL, AND DISTANCE TO DESCEND EXAMPLE CHART

TIME, FUEL AND DISTANCE TO DESCEND

CONDITIONS:

1. Power - AS REQUIRED.
2. Above 10,000 Feet, Descend at 1000 Feet Per Minute.
3. Below 10,000 Feet, Descend at 500 Feet Per Minute.
4. Landing Gear - UP.
5. Wing Flaps - UP.
6. Airspeed - 180 KIAS.
7. Cowl Flaps - CLOSED.



In summary, a flight profile parameter table like Table B-1 should be constructed for each profile defined in Section 5.1. The previously mentioned steps should be used to create a table for each profile. The following items should be remembered when defining the flight profiles:

- Change in fuel weight is the first parameter calculated. Find the fuel burned in the POH charts or in burn rate tables also in the POH. The remaining fuel weight presented in the table is the average over that segment (except for the landing impact event).
- The change in gross weight is the same as the change in fuel weight.
- %cg is calculated for each segment using that segment's average gross weight, average fuel weight, and the zero fuel weight (which is constant) of the aircraft. The cg location of the zero fuel weight will be constant throughout the flight but the fuel weight cg location will constantly be changing. The Weights and Balance section of the Pilot Operating Handbook (POH) or Flight Manual usually will give aid in calculating this location.
- Airspeeds for each segment should be defined in the POH or Flight Manual.
- Mach number can be calculated with the segment airspeed and standard atmosphere tables.
- Cabin pressurization is zero for this example, but in pressurized aircraft, the pressurization schedule for each altitude should be called out in the POH.
- Thrust should be calculated (converted from power for piston engine aircraft) for each flight segment if thrust influences any of the PSEs (and therefore is included in the stress equation - Section 7.0). If the maximum and minimum thrust cycle is the only thrust values used, these can be found in the POH under engine performance. For piston engine aircraft, thrust values are calculated as follows:

$$\text{Thrust} = \frac{(\text{Throttle \%}) \times \eta_p \times \text{BHP} \times 550}{V_{\text{True}}}$$

Where: Throttle % = Throttle setting (75% = 0.75)

η_p = Propeller efficiency

BHP = Rated Shaft Brake Horsepower (in Hp, found in POH)

550 = Conversion factor from horsepower to ft-lb/sec

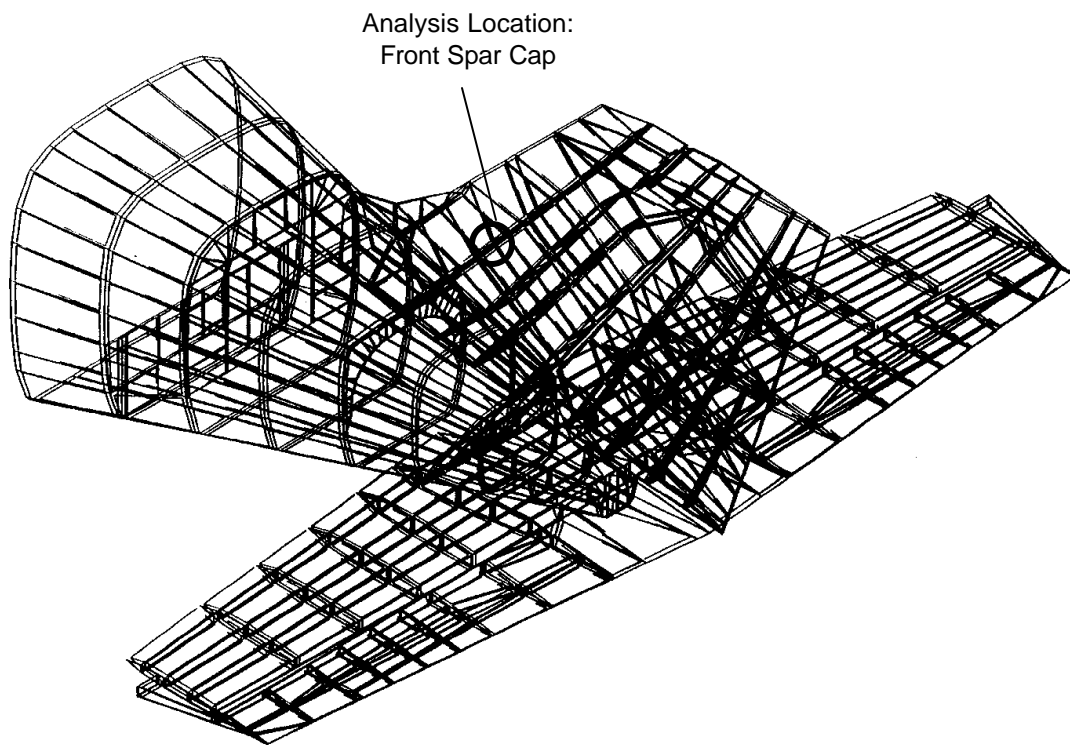
V_{true} = Airspeed in ft/sec (Multiply knots by 1.689 to get ft/sec)

Appendix C: Empennage Spectrum Determination

This Appendix presents a step-by-step example of a vertical tail spectrum development for a fictitious twin engine aircraft, the Acme Model 999. For this example a location on the front spar cap of the vertical tail is chosen. Figure C-1 shows the empennage finite element model and the analysis location used for this example.

FIGURE C-1

EMPENNAGE FINITE ELEMENT MODEL AND ANALYSIS LOCATION



The required steps in determining an empennage spectrum are:

1. Define Usage (Section C.1)
2. Identify Load Spectrum Type (Section C.2)
3. Develop Load Spectrum (Section C.3)
4. Develop Stress Spectrum for Analysis Location (Section C.4)

C.1 Define Usage

The aircraft usage is defined by the mission profile and mission mix data which was defined using the procedures given in Section 5.0 and Appendices A and B. The profile data used in this example is presented in Table C-1.

TABLE C-1
EXAMPLE FLIGHT PROFILE TABLE

<u>Flight Load Segment</u>	<u>Start-End Altitude</u>	<u>Total Fuel (lb)</u>	<u>GRWT (lb)</u>	<u>Segment Time-min</u>	<u>KEAS</u>	<u>Mach</u>	<u>ALT (ft)</u>	<u>%CG</u>	<u>Diff. Press (psi)</u>	<u>Thrust (lb)</u>
Taxi/Takeoff Roll		860	6170	N/A	0	0	0	23.21	0	0
Climb	0-5000 ft	834	6144	6.04	120	0.19	2500	23.22	0	874
Climb	5000-8300 ft	816	6126	4.45	120	0.205	6650	23.23	0	801
Cruise	8300-8300 ft	773	6083	26.60	146	0.257	8300	23.24	0	517
Cruise	8300-8300 ft	701	6011	26.60	146	0.257	8300	23.27	0	514
Cruise	8300-8300 ft	629	5939	26.60	146	0.257	8300	23.30	0	514
Descent	8300-2000 ft	574	5884	12.60	170	0.282	5150	23.33	0	451
Approach	2000-0 ft	543	5853	2.97	102	0.158	1000	23.34	0	76
Maneuver - 15° Flap		543	5853	N/A	102	0.158	1000	23.34	0	76
Maneuver - 45° Flap		543	5853	N/A	102	0.158	1000	23.34	0	76
Landing Impact		531	5841	N/A	0	0	0	23.34	0	0
Landing Roll/Taxi to Ramp		516	5826	N/A	0	0	0	23.44	0	0

C.2 Identify Load Spectrum Type

In this step the type of load spectrum is identified based on profile information. Reference 30 has maneuver and gust exceedance data for different types of usage for twin-engine aircraft. The three different spectrum types are:

1. Special Usage: 0 – 5000 feet AGL
 Gust & Maneuver – Figure 4 from Reference 30
2. General Usage: 5001 – 10000 feet AGL
 Gust – Figure 2 from Reference 30
 Maneuver – Figure 7 from Reference 30
3. Pressurized Usage: > 10000 feet AGL
 Gust – Figure 5 from Reference 30
 Maneuver – Figure 7 from Reference 30

For the vertical tail of the Acme Model 999 aircraft the gust spectrum data from Figure 2 of Reference 30 is used. Since the Acme Model 999 horizontal tail is directly attached to the tailcone (see Figure C-1), neither maneuver or vertical gust loads need to be considered in the spectrum development. Reference 29 provides analysis procedures for other empennage configurations. The maneuver loads are accounted for through the use of a factor of two (2) on the gust exceedances.

The data from Figure 2 of Reference 30 shows vertical gust exceedances per nautical mile as a function of acceleration ratio. The vertical gust exceedance data is shown in Table C-2.

TABLE C-2
VERTICAL GUST EXCEEDANCE DATA
 (Taken from Figure 2 of Reference 30)

Negative Gust		Positive Gust	
a_n/a_{nLLF}	Exceedances/nm	a_n/a_{nLLF}	Exceedances/nm
-0.905	2.000E-06	1.135	2.000E-06
-0.775	1.000E-05	1.000	5.000E-06
-0.745	1.500E-05	0.900	1.000E-05
-0.705	2.500E-05	0.840	1.500E-05
-0.655	4.500E-05	0.768	2.500E-05
-0.600	9.000E-05	0.700	4.500E-05
-0.570	1.500E-04	0.620	9.000E-05
-0.530	2.500E-04	0.568	1.500E-04
-0.500	3.500E-04	0.525	2.500E-04
-0.465	6.000E-04	0.500	3.500E-04
-0.435	1.000E-03	0.460	6.000E-04
-0.404	1.500E-03	0.425	1.000E-03
-0.360	3.000E-03	0.400	1.500E-03
-0.320	6.000E-03	0.360	3.000E-03
-0.300	9.000E-03	0.320	6.000E-03
-0.255	2.000E-02	0.300	9.000E-03
-0.215	4.500E-02	0.260	2.000E-02
-0.200	6.000E-02	0.220	4.500E-02
-0.105	5.000E-01	0.210	6.000E-02
-0.045	1.500E+00	0.105	5.000E-01

C.3 Develop Load Spectrum

In order to use exceedance data from Table C-2 for lateral gust loading on the vertical tail it must first be converted to gust velocity (U_{de}) exceedance data. The first step is to convert from acceleration ratio (a_n / a_{nLLF}) to normal acceleration a_n .

The limit load factor, a_{nLLF} , is calculated based on the following equation:

$$a_{nLLF} = \frac{K U V_c m}{498 (W/S)}$$

Where: $K = \frac{1}{2} (W/S)^{1/4}$ for $(W/S) < 16 \text{ lbs/ft}^2$

$$K = 1.33 - \frac{2.67}{(W/S)^{3/4}}$$
 for $(W/S) > 16 \text{ lbs/ft}^2$

$U = 30 \text{ ft/sec EAS}$, nominal gust velocity

$V_c =$ airplane design cruise speed in KEAS

$m =$ wing lift curve slope, C_l per radian

$W/S =$ wing loading at take-off gross weight in lbs/ft^2

$W =$ Aircraft take-off gross weight in lbs

$S =$ Reference wing area in ft^2

For the Acme Model 999 the following values were used:

$$V_c = 150 \text{ KEAS}$$

$$m = 3.7$$

$$W = 6850 \text{ lbs}$$

$$S = 230 \text{ ft}^2$$

The resulting limit load factor is $a_{nLLF} = 1.258$

Note: 1) The above equation for limit load factor was used in FAR 23.341 prior to Amendment 23-7. Since it was used in the reduction of the data in the exceedance curves in Reference 30, it is appropriate to use it for this analysis.

2) m may be determined approximately as $m = 6A/(2+A)$, where A is the wing aspect ratio.

Load spectra are generally expressed in terms of cycles/flight or cycles/1000 flights. For this example, the load spectrum is desired in the form of exceedances/1000 flights. Therefore the exceedances need to be converted from exceedance per nautical mile to exceedances/1000 flights. This is accomplished by multiplying the exceedance per nautical mile by the cruise speed in knots (EAS) times 1000 (1000 flights) and dividing by the flight length. The profile used for this example (shown in Table C-1) has a cruise speed of 146 KEAS and a flight length of 1.76 hours. Applying the cruise speed to all profile segments for the exceedance calculations adds some conservatism to the load spectrum development.

After the conversion to exceedances/1000 flights the positive and negative accelerations are paired to form the cycles of the load spectrum. The maximum and minimum accelerations that have the same exceedance levels are paired together to form a complete acceleration cycle. It is now also possible to determine the number of occurrences for each of the defined load cycles. The number of occurrences/1000 flights is simply the difference between the exceedances/1000 flights between two adjoining acceleration cycles. The resulting table of normal acceleration cycles (a_n Max and a_n Min) for a given exceedance or occurrence level is shown in Table C-3.

The gust loads on the vertical tail are based on lateral gust velocity. Hence it is necessary to convert the vertical accelerations to vertical gust velocities. The gust velocity exceedances are assumed to be isotropic, i.e., the gusts occur with the same exceedances in all directions. Therefore, the vertical gust exceedances that are obtained from the vertical acceleration exceedances can be directly used as lateral gust exceedances. The conversion from vertical acceleration to vertical gust velocity is accomplished using the following equation.

$$\frac{U_{de}}{a_n} = \frac{498}{K_g V a} \left(\frac{W}{S} \right)$$

Where: U_{de} = Vertical gust velocity in ft/s

a_n = Vertical acceleration

V = Airplane speed in KEAS

a = Slope of airplane normal force coefficient curve (C_{NA}) per radian

W/S = Wing loading in lbs/ft²

W = Aircraft weight in lbs

S = Wing reference area in ft²

$$K_g = \frac{0.88 u_g}{5.3 + u_g} = \text{gust alleviation factor}$$

$$u_g = \frac{2 \left(\frac{W}{S} \right)}{\rho \bar{c} g} = \text{airplane mass ratio}$$

ρ = Density of air at altitude in slugs/ft³

\bar{c} = Mean geometric chord in feet

g = Acceleration due to gravity, 32.2 ft/s²

TABLE C-3

VERTICAL GUST CYCLE ACCELERATION EXCEEDANCES AND OCCURRENCES

a_n Max	a_n Min	Exceedances per 1000 flights	Occurrences per 1000 flights
0.0642	-0.0566	1.244E+05	8.2955E+04
0.1321	-0.1321	4.148E+04	3.6500E+04
0.2642	-0.2516	4.977E+03	1.2443E+03
0.2768	-0.2705	3.733E+03	2.0739E+03
0.3271	-0.3208	1.659E+03	9.1250E+02
0.3774	-0.3774	7.466E+02	2.4886E+02
0.4026	-0.4026	4.977E+02	2.4886E+02
0.4529	-0.4529	2.489E+02	1.2443E+02
0.5032	-0.5082	1.244E+02	4.1477E+01
0.5347	-0.5472	8.295E+01	3.3182E+01
0.5787	-0.5850	4.977E+01	2.0739E+01
0.6290	-0.6290	2.903E+01	8.2955E+00
0.6605	-0.6667	2.074E+01	8.2955E+00
0.7145	-0.7171	1.244E+01	4.9773E+00
0.7800	-0.7548	7.466E+00	3.7330E+00
0.8806	-0.8240	3.733E+00	1.6591E+00
0.9661	-0.8869	2.074E+00	8.2955E-01
1.0567	-0.9372	1.244E+00	4.1477E-01
1.1322	-0.9750	8.295E-01	6.6364E-01
1.4278	-1.1385	1.659E-01	1.6591E-01

Note that the conversion from vertical acceleration to gust velocity, U_{de}/a_n , involves the airspeed, density and aircraft weight. Therefore, the conversion will differ for each segment of the profile shown in Table C-1, and a separate gust velocity cycle exceedance/occurrence table will need to be constructed for each profile segment. For this example the gust velocity cycle exceedance/occurrence table is developed for the second cruise segment shown in Table C-1. For this segment the parameters used for the conversion for the Acme Model 999 are taken from Table C-1 and are shown below.

$$V = 146 \text{ KEAS}$$

$$a = 3.3$$

$$W = 6011 \text{ lbs}$$

$$S = 230 \text{ ft}^2$$

$$\rho = 1.851 \times 10^{-3} \text{ slugs/ft}^3 \text{ (obtained from standard atmosphere table)}$$

$$\bar{c} = 4.5 \text{ feet}$$

This results in a conversion factor of gust velocity per unit of vertical acceleration, $U_{de}/a_n = 33.4522$ seconds. The vertical acceleration cycle exceedance/occurrence table shown in Table C-3 can now be converted to a gust velocity cycle exceedance/occurrence table by multiplying the $a_{n \text{ Max}}$ and $a_{n \text{ Min}}$ accelerations by the conversion factor (U_{de}/a_n), as shown in Table C-4.

Since the gust velocities are assumed to be isotropic, the gust velocity cycles are directly used to determine the vertical tail load. The vertical tail load per gust velocity, L_{vt}/U_{de} , conversion factor is obtained from the equation shown below.

$$\frac{L_{vt}}{U_{de}} = \frac{K_{gt} V a_{vt} S_{vt}}{498}$$

Where: L_{vt} = Vertical tail load in lbs

U_{de} = Vertical gust velocity in ft/s

V = Airplane speed in KEAS

a_{vt} = Lift curve slope of vertical tail (C_{NA}) per radian

S_{vt} = Vertical tail area in ft^2

$$K_{gt} = \frac{0.88 u_{gt}}{5.3 + u_{gt}} = \text{Gust alleviation factor}$$

$$u_{gt} = \frac{2W}{\rho \bar{c}_t g a_{vt} S_{vt}} \left(\frac{K}{l_t} \right)^2 = \text{Lateral mass ratio}$$

ρ = Density of air at altitude in slugs/ft³

\bar{c}_t = Mean geometric chord of vertical tail in feet

g = Acceleration due to gravity, 32.2 ft/s²

W = Aircraft weight in lbs

K = Radius of gyration in yaw in feet

l_t = Distance from aircraft center of gravity to lift center of vertical tail surface in feet

TABLE C-4

GUST VELOCITY CYCLE EXCEEDANCE/OCCURRENCE TABLE

U _{de} Max (ft/s)	U _{de} Min (ft/s)	Exceedances per 1000 flights	Occurrences per 1000 flights
2.1462	-1.8937	1.244E+05	8.2955E+04
4.4187	-4.4187	4.148E+04	3.6500E+04
8.8374	-8.4166	4.977E+03	1.2443E+03
9.2582	-9.0478	3.733E+03	2.0739E+03
10.9415	-10.7311	1.659E+03	9.1250E+02
12.6249	-12.6249	7.466E+02	2.4886E+02
13.4665	-13.4665	4.977E+02	2.4886E+02
15.1498	-15.1498	2.489E+02	1.2443E+02
16.8331	-17.0015	1.244E+02	4.1477E+01
17.8852	-18.3060	8.295E+01	3.3182E+01
19.3581	-19.5685	4.977E+01	2.0739E+01
21.0414	-21.0414	2.903E+01	8.2955E+00
22.0935	-22.3039	2.074E+01	8.2955E+00
23.9031	-23.9872	1.244E+01	4.9773E+00
26.0914	-25.2497	7.466E+00	3.7330E+00
29.4580	-27.5643	3.733E+00	1.6591E+00
32.3196	-29.6684	2.074E+00	8.2955E-01
35.3496	-31.3517	1.244E+00	4.1477E-01
37.8746	-32.6142	8.295E-01	6.6364E-01
47.7641	-38.0850	1.659E-01	1.6591E-01

As was the case for the conversion from vertical acceleration to gust velocity, the conversion from gust velocity to vertical tail load varies between profile segments. The vertical tail load cycle exceedance/occurrence table needs to be developed separately for each profile segment. For this example the second cruise segment for the profile shown in Table C-1 is used again. The following parameters for the Acme Model 999 aircraft, and data from Table C-1 were used.

$$V = 146 \text{ KEAS}$$

$$a_{vt} = 4.8$$

$$S_{vt} = 45 \text{ ft}^2$$

$$\rho = 1.851 \times 10^{-3} \text{ slugs/ft}^3 \text{ (obtained from standard atmosphere table)}$$

$$\bar{c}_t = 6.5 \text{ ft}$$

$$W = 6011 \text{ lbs}$$

$$K = 9.35 \text{ ft}$$

$$l_t = 25 \text{ ft}$$

This results in a conversion factor $L_{vt}/U_{de} = 44.096 \text{ lbs/ft/s}$ to be applied to the gust velocities ($U_{de \text{ Max}}, U_{de \text{ Min}}$) in Table C-4. Because there is no simple way to account for maneuver loads on the vertical tail, the vertical tail exceedances/occurrences due to gust are multiplied by a factor of two (2) to account for the maneuver loads. Table C-5 shows the vertical tail load cycle exceedance/occurrence table, which was obtained by multiplying the gust velocities in Table C-4 by the conversion factor, L_{vt}/U_{de} , and the exceedances/occurrences by a factor of two (2) to account for the maneuver loads.

C.4 Develop Stress Spectrum for Analysis Location

The load cycle exceedance/occurrence table is used to determine the stress spectrum for the analysis location of interest. The stress spectrum is obtained through the use of transfer factors. The transfer factors are developed using finite element models. Unit load conditions are applied and the stresses at the analysis locations are determined. For each analysis location the transfer factor in terms of stress per unit load for each load condition is determined. If multiple load conditions are present at an analysis location, the load exceedances for each load condition is determined separately, and the final stress spectrum is obtained by superposition of the individual load exceedances multiplied by their respective load transfer factors.

For the analysis location on the front spar cap of the vertical tail of the Acme Model 999 shown in Figure C-1 a lateral load of 1000 pounds produces a stress of 6.708 ksi. Therefore, the transfer factor is 6.708 ksi/1000 lb. load. By multiplying the load data (Table C-5) by the transfer factor for the analysis location the stress cycle occurrence table is readily constructed. Linear interpolation is commonly used to obtain the stress cycles (σ_{Max} , σ_{Min}) for integral occurrences. The resulting stress spectrum presented in the form of number of occurrences for a given stress cycle ($\sigma_{Max} - \sigma_{Min}$) is shown in Table C-6. Note that the stress spectrum in Table C-6 is only for the second cruise segment of the profile given in Table C-1. To obtain the stress spectrum for the entire flight, the stress spectra for each of the profile segments need to be developed.

TABLE C-5

VERTICAL TAIL LOAD CYCLE EXCEEDANCES/OCCURRENCES

L_{vt} Max (Lbs)	L_{vt} Min (Lbs)	Exceedances per 1000 flights	Occurrences per 1000 flights
94.6	-83.5	2.489E+05	1.6591E+05
194.8	-194.8	8.295E+04	7.3000E+04
389.7	-371.1	9.955E+03	2.4886E+03
408.3	-399.0	7.466E+03	4.1477E+03
482.5	-473.2	3.318E+03	1.8250E+03
556.7	-556.7	1.493E+03	4.9773E+02
593.8	-593.8	9.955E+02	4.9773E+02
668.0	-668.0	4.977E+02	2.4886E+02
742.3	-749.7	2.489E+02	8.2955E+01
788.7	-807.2	1.659E+02	6.6364E+01
853.6	-862.9	9.955E+01	4.1477E+01
927.8	-927.8	5.807E+01	1.6591E+01
974.2	-983.5	4.148E+01	1.6591E+01
1054.0	-1057.7	2.489E+01	9.9545E+00
1150.5	-1113.4	1.493E+01	7.4659E+00
1299.0	-1215.5	7.466E+00	3.3182E+00
1425.2	-1308.3	4.148E+00	1.6591E+00
1558.8	-1382.5	2.489E+00	8.2955E-01
1670.1	-1438.2	1.659E+00	1.3273E+00
2106.2	-1679.4	3.318E-01	3.3182E-01

TABLE C-6

SECOND CRUISE SEGMENT STRESS SPECTRUM FOR VERTICAL TAIL
 FRONT SPAR CAP ON ACME MODEL 999 AIRCRAFT

σ_{Max} (psi)	σ_{Min} (psi)	Occurrences per 1000 flights
1111.65	-1089.97	100,000
2474.86	-2371.66	10,000
3545.98	-3522.41	1,000
3983.40	-3983.40	500
4928.05	-4972.73	100
5579.89	-5660.42	50
7070.20	-7095.10	10
8309.77	-7875.80	5
9386.03	-8647.87	2
10272.50	-9171.59	1
14810.46	-11642.7	0.1